

University of Alberta

**Sedimentology and Neoichnology of a Mixed-Energy
Estuary, Tillamook Bay, Oregon, United States**

by

Rares Bistran

A thesis submitted to the Faculty of Graduate Studies and Research
in partial fulfillment of the requirements for the degree of

Master of Science

Department of Earth and Atmospheric Sciences

© Rares Bistran
Spring 2014
Edmonton, Alberta

Abstract

Studies of modern, marginal marine sedimentary environments are widely used in paleoenvironmental interpretations, due to the high amount of sedimentological and neoichnological insight they can provide. Limited studies have been conducted on the distribution of facies in mixed-energy estuaries, which, when incorporated with observations from tide- and wave-dominated estuaries, can provide a better understanding of the range of controls on sediment and trace distribution within interpreted estuary settings observed in the rock record. This study focuses on the sedimentological and neoichnological facies observed within the inner estuary, middle estuary, and outer estuary settings of the mixed-energy Tillamook Bay Estuary, Oregon. Field research and data collection consists of detailed surface and subsurface observations aided by sediment cores. The sedimentological and neoichnological facies model presented contributes to the knowledge of proximal to distal facies models of estuary settings, ranging from the innermost fluvial-tidal transition zone to the outermost estuary, tidal sand bar-dominated zone.

Acknowledgements

First and foremost, I would like to thank my parents, Anastasia and Vali, and my sister Diana, for their full support throughout the years. You're the best family I could ask for, thank you for everything! Cheryl, thank you for all your assistance and support during the past few years, I am so proud to have you in my life. You are truly one of the hardest working people I know; the hardest working person in the world would have to compete with you. Thank you also Debbie and Rob for your kindness and support during the past few years.

Thank you to my supervisors Murray Gingras and John-Paul Zonneveld, for taking me on as a grad student. Mur and JP, thank you for giving me all the time and room to think, during my much slower-than-average writing process. Thank you both for your lessons, enthusiasm and laughs shared in the field and otherwise. I may not be the proud author of a book on vibratorer maintenance, but I promise you, no more locked up vibracore motors! My thanks also to George Pemberton for being part of my defense committee on such short notice. George, thank you for your encouragement over the years, and for setting the path for so many of us. Thank you Octavian Catuneanu for also being part of my defense committee, it is much appreciated.

Dave Herbers, thanks for being an excellent field assistant, and for all the hard work you put in, even when drifting away on the tidal current with no boat control whatsoever. Thanks for sharing jokes in the field and keeping it all real. My thanks for fieldwork support also go out to Cheryl, Eric, Greg, and Jesse. No amount of fieldwork could have been conducted without all of your help.

Ryan King, thank you for taking me along as a field assistant to Ferron. Those were some of the best fieldwork times I have experienced as a geology student. All the thousands of photos, countless backpacks full of rock samples, logging outcrops in the scorching desert sun (after all, the sun is burning in the Ferron!), and hikes in the canyons, were all worth it. Thanks for introducing me to so many great people along the way, for giving me the opportunity to see some great geology and places, and for understanding my weird sense of humour and laughing along. I enjoyed every minute of it. Thanks for being a great friend and mentor.

Many friends have made my time at the U of A memorable. The countless things that I am grateful for from all of you are too long to list here. My thanks go to: Andreas Enggist, Ali Imer, Miguel Cuba Espinoza, Mary Borrero, Guadalupe Maldonado, Xianmin Hu, Nelson Bernal, Osbaldo Zamora Vega, Yi Zhao, Anatoly Melnik, and Tibor Lengyel.

Thanks you to all members of the Ichnology Research Group, past and current. My thanks especially go out to Camilo Polo Camacho, Luke McHugh, Tiffany Playter, Ryan King, Andrew Lawfield, Greg Baniak, and Curtis Lettley. It has always been fun discussing different topics with all of you. Thank you also to Brad, Scott, Alina, Gord, Reed, Joel, and Carolyn. I know I am missing some of you, but please be sure I am thankful for all of your help.

Dr. Fred Clark, thank you for the academic support as well as your friendship over the years. I hope that there will be many more opportunities to discuss and share rare Stevie Ray, John Mayer, and Doyle Bramhall recordings, among many others, with you. It has always been a pleasant break from my studies. Thank you.

Music references, albeit trite, are something I also feel the need to include. On that note, I would like to thank a countless list of musicians for their music over the years, which has both kept me "sane" and resulted in my distraction during all the solos. If master theses had soundtracks, I hope that mine would include the catalogues of greats such as: Billy Preston, Gary Clark Jr., Roger Waters, Frank Ocean, the Three Kings, Steve Vai, and many others that would fill this page. Thanks for the great music.

My thanks go out to Ruby Fry Matson, of the Tillamook County Pioneer Museum. Thank you for giving me permission to use historical photos of Tillamook Bay in my thesis. Thank you Don Best for giving me permission to use your stunning aerial photos; they have been of great help. Lidia Zabcic, thank you for allowing me to use some of your aerial photos and one of your figures, it is greatly appreciated. Dr. Stefan Bachu, thank you for your support during the final stages of my thesis and continual mentorship.

Finally, I would like to thank all the staff of the Department of Earth and Atmospheric Sciences. Thank you Igor Jakab for your computer support and endless jokes. Mark Labbe, you have always been very helpful with any technical support, couldn't have done it without you. Thank you Dave Chesterman, Andrew Locock, Shyra Craig, and René Gobeil for help on many occasions.

TABLE OF CONTENTS

	Page
CHAPTER 1 – INTRODUCTION	1
BACKGROUND INFORMATION	1
<i>Previous Work</i>	3
<i>Purpose of Study</i>	3
STUDY AREA	6
<i>Geologic Setting</i>	17
METHODOLOGY	22
BIBLIOGRAPHY	34
CHAPTER 2 – SEDIMENTOLOGY AND NEOICHOLOGY OF INTERTIDAL FACIES, TILLAMOOK BAY ESTUARY, OREGON, UNITED STATES	37
INTRODUCTION	37
DESCRIPTIONS, RESULTS, AND INTERPRETATIONS	37
Inner Estuary Characteristics	37
Zone 1: Fluvial – Tidal Transition Descriptions and Results	37
<i>Sedimentological and Neoichnological Features</i>	37
Zone 1 Fluvial – Tidal Transition Vibracore Facies Descriptions	41
<i>Zone 1 Facies 1 (Z1F1) – Coarse to very coarse muddy sand</i>	41
<i>Zone 1 Facies 2 (Z1F2) – Massive mud</i>	48
<i>Zone 1 Facies 3 (Z1F3) – Massive fine to medium grained sand</i>	48
Zone 1: Fluvial – Tidal Transition Interpretations	49
Zone 2: Bayhead Delta and Shore-Attached Tidal Flats Descriptions and Results	52
<i>Sedimentological and Neoichnological Features of Zone Sub-environments</i>	52
<i>Salt marsh-adjacent bayhead delta flats</i>	53
<i>Bayhead delta free-meandering channel point bars and adjacent sand flats</i>	69
<i>Marginal sand and muddy sand flats</i>	78
Zone 2 Bayhead Delta and Shore-Attached Tidal Flats Vibracore Facies Descriptions	87
<i>Zone 2 Facies 1 (Z2F1) –Clay with Interlaminated to interbedded sand</i>	87
<i>Zone 2 Facies 2 (Z2F2) –Massive to planar laminated muddy sand and silt</i>	93
<i>Zone 2 Facies 3 (Z2F3) –Low angle planar laminated and rippled sand</i>	93

<i>Zone 2 Facies 4 (Z2F4) –Massive fine to coarse sand</i>	93
Zone 2: Bayhead Delta and Shore-Attached Tidal Flats Interpretations	94
<i>Salt marsh-adjacent bayhead delta flats</i>	96
<i>Bayhead delta free-meandering channel point bars and adjacent sand flats</i>	99
<i>Marginal sand and muddy sand flats</i>	101
Zone 3: Isolated Tidal Sand Bar Descriptions and Results	102
<i>Sedimentological and Neoichnological Features of Zone Sub-environments</i>	102
<i>Channel-flanked, transverse-rippled deposits</i>	102
<i>Rippled muddy sand deposits</i>	112
<i>Algae-stabilized muddy sand deposits</i>	123
Zone 3 Isolated Tidal Sand Bar Vibracore Facies Descriptions	128
<i>Zone 3 Facies 1 (Z3F1) – Massive to planar laminated clay and silt</i>	138
<i>Zone 3 Facies 2 (Z3F2) – Mud-dominated HS and/or HIS</i>	138
<i>Zone 3 Facies 3 (Z3F3) – Sand-dominated HS and/or HIS</i>	141
<i>Zone 3 Facies 4 (Z3F4) – Muddy sand</i>	142
<i>Zone 3 Facies 5 (Z3F5) – Laminated organic rich sand</i>	142
<i>Zone 3 Facies 6 (Z3F6) – Massive sand</i>	142
<i>Zone 3 Facies 7 (Z3F7) – Planar to rippled sand</i>	143
Zone 3: Isolated Tidal Sand Bar Interpretations	144
<i>Channel-flanked, transverse-rippled deposits</i>	150
<i>Rippled muddy sand deposits</i>	151
<i>Algae-stabilized muddy sand deposits</i>	151
Zone 4: Mud and Muddy Sand Flats Descriptions and Results	152
<i>Sedimentological and Neoichnological Features</i>	152
Zone 4 Mud and Muddy Sand Flats Vibracore Facies Descriptions	154
<i>Zone 4 Facies 1 (Z4F1) – Massive to planar-and/or low-angle-laminated mud</i>	154
<i>Zone 4 Facies 2 (Z4F2) – Muddy sand</i>	159
<i>Zone 4 Facies 3 (Z4F3) – Massive Sand</i>	159
<i>Zone 4 Facies 4 (Z4F4) – Laminated Sand</i>	159
Zone 4: Mud and Muddy Sand Flats Interpretations	160
Middle Estuary Characteristics	162
Zone 5: Marginal Tidal Flats Descriptions and Results	162
<i>Sedimentological and Neoichnological Features of Zone Sub-environments</i>	162
<i>Tidal sand flat</i>	162
<i>Areally-restricted firmground</i>	169
Zone 5 Marginal Tidal Flats Vibracore Facies Descriptions	169
<i>Zone 5 Facies 1 (Z5F1) –Massive to rippled silt</i>	171
<i>Zone 5 Facies 2 (Z5F2) –Massive sand</i>	171
Zone 5: Marginal Tidal Flats Interpretations	171
Outer Estuary Characteristics	180
Zone 6: Isolated Tidal Sand Bar Descriptions and Results	180
<i>Sedimentological and Neoichnological Features of Zone Sub-environments</i>	180
<i>Rippled sand deposits</i>	180

<i>Medium-relief dunes</i>	184
<i>Algae-covered muddy sand deposits</i>	194
Zone 6 Isolated Tidal Sand Bar Vibracore Facies Descriptions	199
<i>Zone 6 Facies 1 (Z6F1) –Burrowed massive sand</i>	199
<i>Zone 6 Facies 2 (Z6F2) –Massive sand</i>	205
<i>Zone 6 Facies 3 (Z6F3) –Laminated sand</i>	205
<i>Zone 6 Facies 4 (Z6F4) –Planar-bedded sand</i>	205
<i>Zone 6 Facies 5 (Z6F5) –Low-angle bedded sand</i>	210
<i>Zone 6 Facies 6 (Z6F6) –High-angle x-bedded sand</i>	210
Zone 6: Isolated Tidal Sand Bar Interpretations	210
DISCUSSION	214
Sedimentary Facies Model and Controls on Sedimentation	214
Neochronological Facies Model	229
Modern Estuary Comparison	239
Reservoir Characterization Analogue	247
BIBLIOGRAPHY	250
CHAPTER 3 – CONCLUSIONS	256
Future work and model improvements	261
BIBLIOGRAPHY	264
APPENDICES:	
Appendix A: Supplementary Figures	266
Appendix B: Sediment Logs	303
Appendix C: Microbially-Induced Sedimentary Structures (MISS): Examples from Intertidal Flats of Tillamook Bay Estuary, Oregon	331

List of Tables

	Page
Chapter 1	
Table 1-1: List of invertebrate organisms and aquatic plants observed in intertidal deposits of Tillamook Bay Estuary	32
Chapter 2	
Table 2-1: Summary of Facies Characteristics for Fluvial - Tidal Transition (Zone 1)	47
Table 2-2: Summary of Facies Characteristics for Bayhead Delta and Shore-Attached Tidal Flats (Zone 2)	91
Table 2-3: Summary of Facies Characteristics for Isolated Tidal Sand Bar (Zone 3)	135
Table 2-4: Summary of Facies Characteristics for Mud and Muddy Sand Flats (Zone 4)	157
Table 2-5: Summary of Facies Characteristics for Marginal Tidal Flats (Zone 5)	174
Table 2-6: Summary of Facies Characteristics for Isolated Tidal Sand Bar (Zone 6)	207
Appendix C	
Table C-1. Total Organic Carbon (TOC) percent values from sediment containing wrinkle marks.	340

List of Figures

	Page
Chapter 1	
Figure 1-1. Map showing the location of zones examined in the study.	5
Figure 1-2. Part I. Location of Tillamook Bay, Oregon, United States.	7
Figure 1-2. Part II. Land features surrounding Tillamook Bay, Oregon.	8
Figure 1-3. Historical photographs of the Bayocean Peninsula storm breach. View1	11
Figure 1-4. Historical photographs of the Bayocean Peninsula storm breach. View 2	12
Figure 1-5. Historical photographs documenting the erosion of Bayocean Peninsula.	13
Figure 1-6. Historical photographs of the Tillamook Fires.	16
Figure 1-7. Geologic map of Tillamook Bay and surrounding area.	18
Figure 1-8. Vibracoring method and equipment.	24
Figure 1-9. Locations of cores retrieved in this study.	25
Figure 1-10. High tide salinity variations.	30
Figure 1-11. Low tide salinity variations.	31
Chapter 2	
Figure 2-1. Grain size and TOC distribution in the fluvial-tidal transition zone.	38
Figure 2-2. Channels of the fluvial-tidal transition zone.	39
Figure 2-3. Salt marsh stratification.	42
Figure 2-4. Geomorphology at the mouth of the Tillamook River.	44
Figure 2-5. Core example from the inner estuary Zone 1.	46
Figure 2-6. Schematic vertical succession from the fluvial-tidal transition zone.	50
Figure 2-7. Sub-environments of Zone 2.	54
Figure 2-8. Grain size and TOC distribution in shore-attached tidal flats and the mouth of the Kilchis River.	55

Figure 2-9. Overview of Zone 2 salt marsh-adjacent bayhead delta flats sub-environment.	56
Figure 2-10. Surface texture and traces of the salt marsh-adjacent bayhead delta flats sub-environment, Zone 2.	58
Figure 2-11. Overview and surface texture of the salt marsh-adjacent bayhead delta flats, Zone 2.	60
Figure 2-12. Overview and surface texture of the salt marsh-adjacent bayhead delta flats, Zone 2, continued.	63
Figure 2-13. Overview and surface texture of the salt marsh-adjacent bayhead delta flats, Zone 2, continued 2.	64
Figure 2-14. Tidal creek within the salt marsh-adjacent bayhead delta flat sub-environment, Zone 2.	67
Figure 2-15. Sub-surface sedimentary features and traces of the salt marsh-adjacent bayhead delta flat sub-environment, Zone 2.	68
Figure 2-16. Sedimentary features and traces of the bayhead delta free-meandering channel point bars and adjacent sand flats sub-environment, Zone 2.	71
Figure 2-17. Sedimentary features and traces of the bayhead delta free-meandering channel point bars and adjacent sand flats sub-environment, Zone 2, continued.	73
Figure 2-18. Burrow mounds of <i>Neotrypaea californiensis</i> in the bayhead delta free-meandering channel point bars and adjacent sand flats sub-environment, Zone 2.	76
Figure 2-19. Sedimentary features and traces of the marginal sand and muddy sand flats sub-environment, Zone 2.	79
Figure 2-20. Surficial sedimentary features of the marginal sand and muddy sand flats sub-environment, Zone 2.	80
Figure 2-21. Traces observed in the sub-surface of the marginal sand and muddy sand flats sub-environment, Zone 2.	83
Figure 2-22. Traces observed in the sub-surface of the marginal sand and muddy sand flats sub-environment, Zone 2, continued.	85
Figure 2-23. Sediment logs of Zone 2.	88
Figure 2-24. Core examples from the inner estuary bayhead delta.	89
Figure 2-25. Schematic vertical succession from the bayhead delta.	95
Figure 2-26. Sub-environments of Zone 3.	103
Figure 2-27. Grain size and TOC distribution in the inner estuary tidal bar.	104

Figure 2-28. Sedimentary features and traces of the channel-flanked, transverse-rippled deposits sub-environment, Zone 3.	105
Figure 2-29. Fecal pellets and incipient biogenic flasers of the channel-flanked, transverse-rippled deposits sub-environment, Zone 3.	106
Figure 2-30. Inclined heterolithic stratification, sand bar edge, channel-flanked, transverse-rippled deposits sub-environment, Zone 3.	107
Figure 2-31. Sub-surface trace features in sand, channel-flanked, transverse-rippled deposits sub-environment, Zone 3.	108
Figure 2-32. Burrowed, muddy sediment at the sand bar edge, channel-flanked, transverse-rippled deposits sub-environment, Zone 3.	113
Figure 2-33. Burrowed layers of the inclined heterolithic stratification, sand bar edge, channel-flanked, transverse-rippled deposits sub-environment, Zone 3.	114
Figure 2-34. Burrowed layers of the inclined heterolithic stratification, sand bar edge, channel-flanked, transverse-rippled deposits sub-environment, Zone 3, continued.	116
Figure 2-35. Sub-surface sedimentary features and traces, rippled muddy sand deposits sub-environment, Zone 3.	118
Figure 2-36. Sub-surface sedimentary features and traces as observed in a boxcore from the rippled muddy sand deposits sub-environment, Zone 3.	120
Figure 2-37. Sub-surface sedimentary features and traces, rippled muddy sand deposits sub-environment, Zone 3, continued.	121
Figure 2-38. Surface sedimentary features, algae-stabilized muddy sand deposits sub-environment, Zone 3.	124
Figure 2-39. Surface sedimentary features and traces, algae-stabilized muddy sand deposits sub-environment, Zone 3.	125
Figure 2-40. Sub-surface trace features in muddy sand, algae-stabilized muddy sand deposits sub-environment, Zone 3.	127
Figure 2-41. Part I. Vibracore examples from the inner estuary tidal bar, Zone 3.	129
Figure 2-41. Part II. Vibracore examples from the inner estuary tidal bar, Zone 3.	130
Figure 2-42. Parts I, II, and III (next three pages). Sediment logs of the inner estuary sand bar, Zone 3.	131
Figure 2-42. Parts I. Sediment logs of the inner estuary Zone 3	132
Figure 2-42. Parts II. Sediment logs of the inner estuary Zone 3	133
Figure 2-42. Parts III. Sediment logs of the inner estuary Zone 3	134
Figure 2-43. Cores examples from the inner estuary Zone 3.	139

Figure 2-44, Part 1. Schematic vertical succession from the proximal end of an inner estuary tidal sand bar.	145
Figure 2-44, Part 2. Schematic vertical succession from the central part of an inner estuary tidal sand bar.	146
Figure 2-44, Part 3. Schematic vertical succession from the distal end of an inner estuary tidal sand bar.	148
Figure 2-45. Sediment logs of vibracores from the muddy, shore-attached tidal flats.	153
Figure 2-46. Vibracore examples from Zone 4.	155
Figure 2-47. Typical sediment core from the inner estuary Zone 4.	156
Figure 2-48. Schematic vertical succession from a muddy tidal flat succession.	161
Figure 2-49. Grain size and TOC distribution, western margin of Tillamook Bay.	163
Figure 2-50. Sedimentary features of the shore-attached tidal flats, western margin, Zone 5.	165
Figure 2-51. Wave refraction and formation of high-wavelength dunes, Zone 5.	167
Figure 2-52. Various views of a firmground sample.	170
Figure 2-53. Sediment logs from the sand-dominated, western part of Tillamook Bay.	172
Figure 2-54. Typical sediment core from the middle estuary Zone 5.	173
Figure 2-55. Schematic vertical succession from a sandy tidal flat succession.	176
Figure 2-56. Sub-environments of Zone 6.	181
Figure 2-57. Surface sedimentary features, rippled sand deposits sub-environment, Zone 6.	182
Figure 2-58. Dune and ripple features of the medium-relief dunes sub-environment, Zone 6.	185
Figure 2-59. Complex dune morphologies, medium-relief dunes sub-environment, Zone 6.	186
Figure 2-60. Transverse dunes, medium-relief dunes sub-environment, Zone 6.	188
Figure 2-61. Rippled sediment deposits at the base of dune fronts.	189
Figure 2-62. Complex dune morphologies, medium-relief dunes sub-environment, Zone 6.	191
Figure 2-63. X-radiograph of cross-bedded dune sediments, Zone 6.	193

Figure 2-64. Trace features of medium-relief dunes sub-environment, Zone 6.	195
Figure 2-65. Trace features of medium-relief dunes sub-environment, Zone 6, continued.	196
Figure 2-66. Part I. Vibracore examples from Zone 6.	200
Figure 2-66. Part II. Vibracore examples from Zone 6.	201
Figure 2-67. Parts I and II (next two pages). Sediment logs of the outer estuary, Zone 6.	202
Figure 2-67. Part I. Sediment logs of Zone 6.	203
Figure 2-67. Part II. Sediment logs of Zone 6.	204
Figure 2-68. Typical sediment core from the outer estuary Zone 6.	206
Figure 2-69. Schematic vertical succession from an outer estuary tidal sand bar.	212
Figure 2-70. Sediment grain size and source distribution, Tillamook Bay.	215
Figure 2-71. Salinity stratification during the dry season.	217
Figure 2-72. Salinity stratification during the wet season.	219
Figure 2-73. Summary of inferred and observed physical, sedimentary, and biological factors.	221
Figure 2-74, Part I. Sedimentation changes between the years 1971-2011.	223
Figure 2-74, Part II. Sedimentation changes between the years 1971-2011.	224
Figure 2-75. Schematic dip-oriented cross-section of Tillamook Bay.	230
Figure 2-76. Schematic three-dimensional and vertical succession facies model.	232
Figure 2-77. Ichnological and sedimentological facies model of Tillamook Bay Estuary.	233
Figure 2-78. Relationship of Tillamook Bay Estuary to the Bombetoka Bay Estuary, Madagascar.	240
Figure 2-79. Marine to marginal marine ichnofacies.	245
Figure 2-80. Interpreted reservoir potential of various sedimentary features and environments observed at Tillamook Bay.	248
 Chapter 3	
Figure 3-1. Tillamook Bay Estuary Characteristics.	257

Appendix A

Figure A-1. Intertidal Color Infrared Aerial Mosaic of Tillamook Bay Estuary.	267
Figure A-2. Historical photos of Bayocean Peninsula.	268
Figure A-3. Sediment and trace views, salt marsh-adjacent flats, Zone 2.	269
Figure A-4. Creek morphology, sedimentary structures and traces at channel margin, Zone 2.	271
Figure A-5. Pebble-rich layers, Zone 2.	273
Figure A-6. Sub-surface sedimentary features and traces, channel-margin sediments, Zone 2.	274
Figure A-7. Sub-surface sedimentary features and traces, muddy sand channel margin, Zone 2.	276
Figure A-8. Surface texture and tidal creek facies, Zone 2.	278
Figure A-9. Traces in pebble-rich sand, sub-environment 2, Zone 2.	279
Figure A-10. Miscellaneous sedimentary structures, Zone 2.	281
Figure A-11. Sedimentary features indicative of changing flow conditions.	282
Figure A-12. Low-relief dune, Zone 2.	283
Figure A-13. Parting lineations, Zone 2.	285
Figure A-14. Eel grass-generated drag marks, Zone 2.	286
Figure A-15. Low-relief dune features, Zone 2.	287
Figure A-16. Low-relief dune features, Zone 2 (general view).	289
Figure A-17. Sub-surface sedimentary features observed in tidal creek facies, Zone 3.	291
Figure A-18. X-ray image of boxcored tidal creek sediments, Zone 3.	293
Figure A-19. Sub-surface trace features in muddy sand and organic rich mud, Zone 3.	294
Figure A-20. Sub-surface trace features in muddy sand, Zone 3.	295
Figure A-21. Sedimentary features and traces observed in muddy central bar sediments, Zone 3.	297
Figure A-22. Surface texture and traces, distal Zone 3.	299

Figure A-23. Dune features of the outer estuary sand bar, Zone 6.	301
Figure A-24. Summary of sediment character.	302
Appendix B	
Figure B-1. Core #1, Core #2	304
Figure B-2. Core #3, Core #4	305
Figure B-3. Core #5	306
Figure B-4. Core #6	307
Figure B-5. Core #7	308
Figure B-6. Core #8	309
Figure B-7. Core #9	310
Figure B-8. Core #10 (1/2)	311
Figure B-8 continued. Core #10 (2/2)	312
Figure B-9. Core #11	313
Figure B-10. Core #12	314
Figure B-11. Core #13	315
Figure B-12. Core #14	316
Figure B-13. Core #15	317
Figure B-14. Core #16	318
Figure B-15. Core #17	319
Figure B-16. Core #18	320
Figure B-17. Core #19	321
Figure B-18. Core #20	322
Figure B-19. Core #21	323
Figure B-20. Core #22, Core #23	324
Figure B-21. Core #24	325
Figure B-22. Core #25, Core #26	326

Figure B-23. Core #27, Core #28	327
Figure B-24. Core #29	328
Figure B-25. Core #30, Core #31	329
Figure B-26. Core #32	330
Appendix C	
Figure C-1. Study locations of microbially-induced sedimentary structures.	333
Figure C-2. Algal mats and wrinkle marks, western margin of Tillamook Bay.	335
Figure C-3. Wrinkle marks on rippled sediment, western margin of Tillamook Bay.	337
Figure C-4. Wrinkle mark morphology.	339
Figure C-5. View of the microbial mat, southern part of Tillamook Bay.	342
Figure C-6. Various views of burrow morphologies from a burrowed microbial mat.	344
Figure C-7. Sedimentary features under the modern microbial mat surface.	347
Figure C-8. Sedimentary and biogenic structures present under a microbial mat.	348
Figure C-9. Part I. Sedimentary structures and layering under a microbial mat.	349
Figure C-9. Part II. Sedimentary structures and layering under a microbial mat.	350
Figure C-10. Eroded and preferentially-burrowed microbial mat.	360

List of Symbols

General symbols



Camera aperture symbol, indicating location of a photo



Wood fragments



Inferred / inexact layer contact

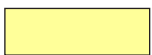


Certain layer contact

Figure drawings-specific symbols



Clay / organic-rich layer



Sand layer
(does not indicate grain size)



Muddy sand layer
(does not indicate grain size)



Sand layer with pebble / gravel content



Pebbles and gravel



Firmground layer
(plan view)

Sediment log-specific symbols



Organic laminae / matter



Clay laminae



Ripples (current or combined-flow)



Oscillatory ripples



Planar laminae



Planar bedding



Low-angle parallel laminae



Low-angle wavy parallel laminae



Low-angle bedding



High-angle bedding



Wavy parallel bedding



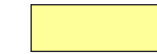
Wavy parallel laminae



Mud layer



Silt layer

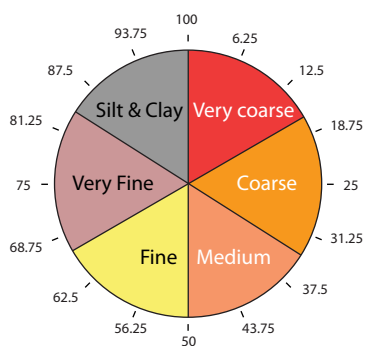


Sand layer



Muddy sand layer

Grain size relative percent distribution



Percent values

S-1

Sample number



Grain size pie chart

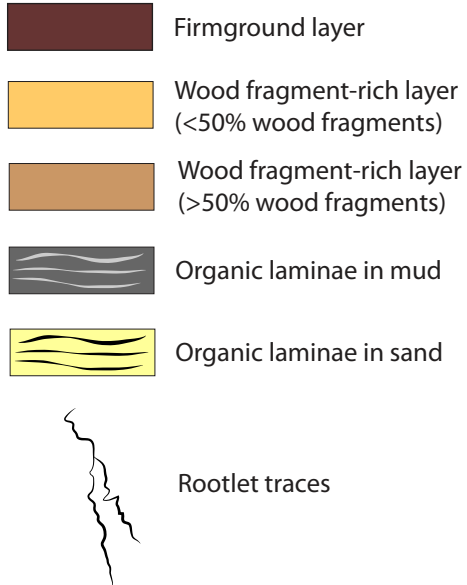
2.23

TOC percent

List of Symbols (continued)

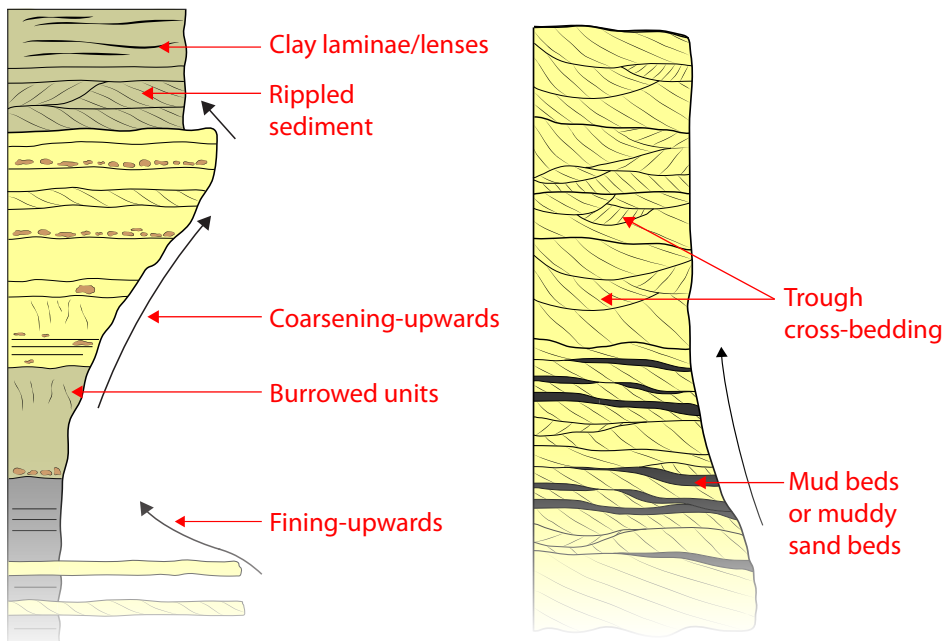
Core Facies Model (Fig. 2-77)*

*The list below does not include all symbols used in Figure 2-77, as they are explained in other sections of the symbols legend















Schematic Vertical Profiles*

*The figure below does not describe all symbols used in the interpreted vertical profiles, as they are explained in other sections of the symbols legend

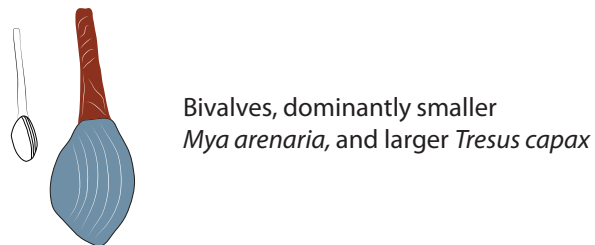
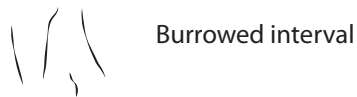
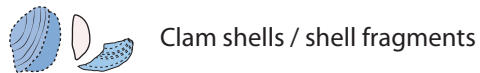
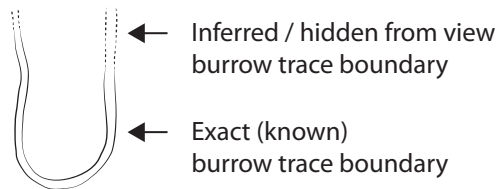


List of Symbols (continued)

Trace Fossil Modern Equivalent Abbreviations

 <i>Arenicolites</i>	 <i>Psilonichnus</i>
 <i>Cylindrichnus</i>	 <i>Siphonichnus</i>
 Cryptic bioturbation	 <i>Skolithos</i>
 <i>Palaeophycos</i>	 <i>Teichichnus</i>
 <i>Polykladichnus</i>	 <i>Thalassinoides</i>
 <i>Planolites</i>	 Rootlet trace

Biogenic activity-related symbols



CHAPTER 1 – INTRODUCTION

BACKGROUND INFORMATION

Tidal bars and tidal flats that form in easily-accessible modern depositional environments, such as estuaries, are ideal analogues to similar ancient depositional environments. Their use in paleoenvironmental interpretations can be applied, from an economic point of view, to hydrocarbon reservoirs. Many ancient environments host large reserves of hydrocarbons (e.g. Oficina Formation, Orinoco Oil Belt, Venezuela), and their efficient exploration relies on accurate and improved predictions of the distribution of reservoir-quality facies. The complex interplay between various physical factors (such as sedimentation rate, total current energy, and seasonal fluvial discharge fluctuations) greatly influences the distribution of estuarine sedimentary packages, which become highly variable through time. Physical factors also influence the distribution of epibenthic and endobenthic organisms within an estuary, affecting species distribution, diversity, concentration, organism size, and living behaviour. The presence of such organisms is most commonly recorded by burrows, which, in modern environments, take the form of their trace fossil equivalents.

The mixed-energy Tillamook Bay Estuary, located on the coast of Oregon, United States, experiences significant wave and tidal influences, as well as large seasonal fluctuations in sediment discharge. As a result, rapid lateral and vertical changes are observed in the distribution of sediment within the estuary. Those changes most notably occur in the inner estuary zone, where the interplay between fresh, fluvial water and saline, tidally-sourced seawater is the greatest. In sedimentary deposits of tidal flats and tidal bars of the inner estuary, heterolithic stratification and inclined heterolithic stratification (Thomas et al., 1987) – are commonly observed. Very rapid changes in sediment calibre and character are observed in the bayhead delta region, as

well as in shore-attached tidal flats and isolated tidal bars. Burrows and their trace fossil equivalents, resulting from the burrowing activity of numerous organisms, are widely distributed throughout the various estuarine sub-environments. The lowest concentration of burrows is observed in the bayhead delta region, where the highest sedimentation rates and sediment grain sizes are observed. The highest concentration of burrows, on the other hand, is observed in the middle of tidal bars, which are extensively covered by eelgrass and dominated by finer grained sediment.

For the purposes of this study, Tillamook Bay is referred to as an estuary, where an estuary is defined as “an inlet of the sea, reaching into the river valley as far as the upper limit of tidal rise, usually divisible into three sectors: a) a marine or lower estuary, in free connection with the open sea; b) a middle estuary, subject to strong salt and freshwater mixing; and c) an upper or fluvial estuary, characterized by freshwater but subject to daily tidal activity” (Dionne, 1963). The term “estuary” is derived from the Latin term *aestuarium*, originally referring to marshes and inlets, in addition to also having a strong linkage to the Latin word for tide - *aestus estus* (Gingras et al., 2012). The term “estuarine”, implies conditions between the extremes of fully marine seawater (35 ppt) and fully fresh fluvial water (0 ppt). In this thesis, the term “bay” is used purely from a geomorphological standpoint, to show the effects of a restricted bay setting on estuarine physical parameters (e.g. tidal prism, bathymetry of tidal channels, salinity changes, current energies etc.). The term, therefore, refers to the restricted setting of Tillamook Bay, and does not in any way refer to sedimentological or neoichnological characteristics of bay, or lagoon-type environments. Any other factors observed (e.g. sedimentology and neoichnology) are described and mentioned in the context of an estuarine depositional environment.

Previous Work

Most studies regarding Tillamook Bay have focused on engineering approaches to better manage flood events associated with increased sedimentation rates within the estuary. These include multiple hydrological and geographic information system characterization studies of the rivers draining into Tillamook Bay (e.g. Benoit, 1996; Melancon, 1999; Sullivan et al., 2001). Other studies are ecological studies of tidal marsh deposits (Seliskar and Gallagher, 1983), eelgrass distribution (Strittholt, and Frost, 1996), benthic macrofauna (Ferraro and Cole, 2012), and biological restoration (Hevlin, 1988).

Several excellent studies have addressed sedimentation within Tillamook Bay, as well as the erosion of Bayocean Spit (Terich and Komar, 1973; Glenn, 1978; McManus et al., 1998; Styllas, 2001; Komar et al., 2004). Terrestrial-ocean climate linkages, have also been studied through characterization of bulk sediment provenance of fluvial sediments in marginal marine settings, including Tillamook Bay (VanLaningham, 2007).

Early geologic maps include brief descriptions of the area surrounding Tillamook Bay (Warren et al., 1945; Peck, 1961), though much earlier studies mention the geology of units in the Tillamook Bay area (Diller, 1896). More recent studies include those on the geology of the Tillamook Highlands (Wells et al, 1995), on the Cascadia subduction zone and related studies covering the Tillamook Bay fault (e.g. Goldinger et al., 1992), and an extensive study of the geology of the Tillamook embayment (Parker, 1990).

Purpose of Study

The objectives of this thesis are to describe and interpret the distribution of the heterolithic sedimentary deposits observed at Tillamook Bay, as well as the distribution of burrowing organisms and the traces they leave behind. These, in turn, are used in a broader interpretation of the main influences on

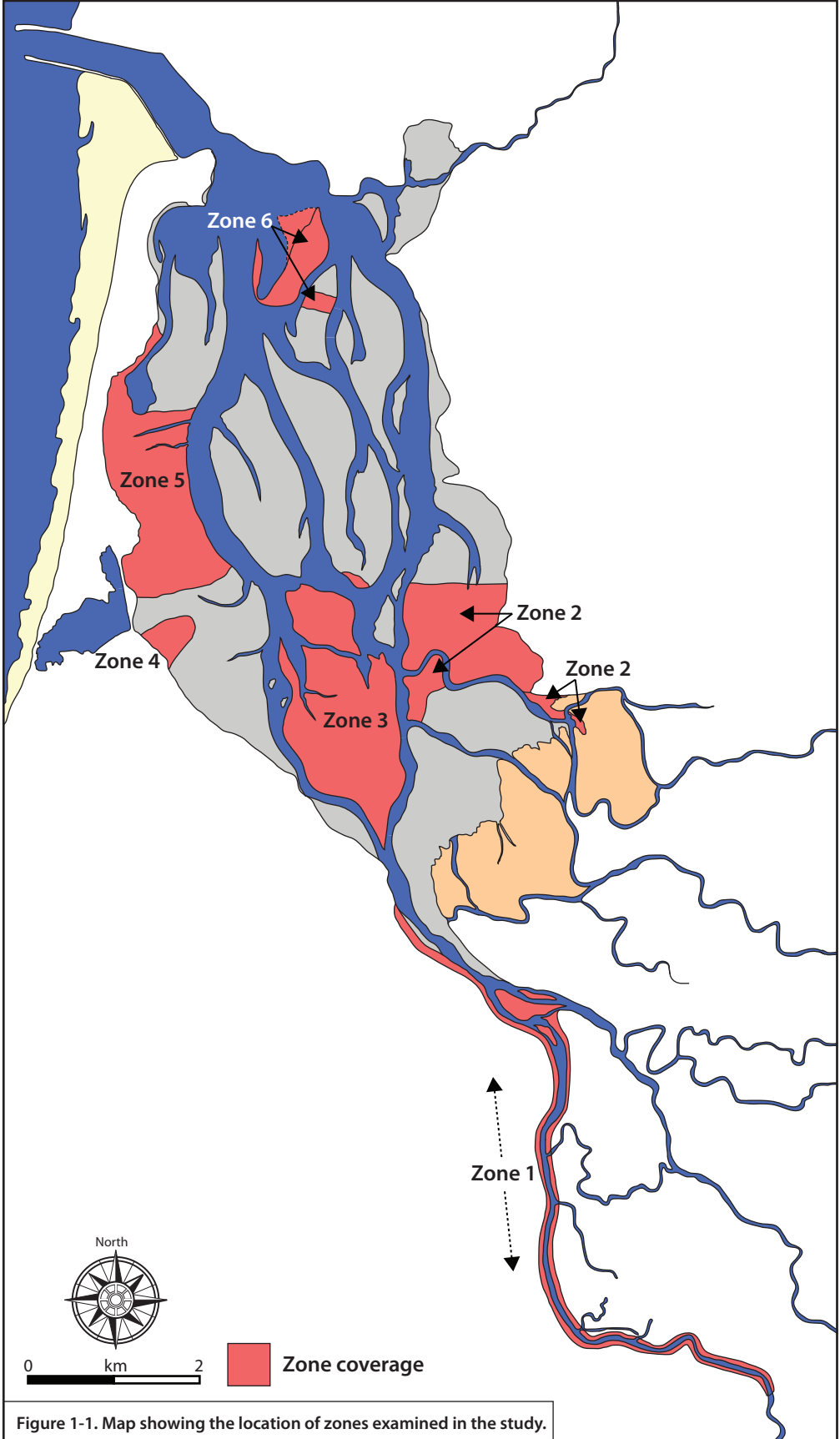
the formation of such sedimentary environments and the deposits and incipient traces observed therein.

In this study, a total of six zones are studied (Fig. 1-1). The zones are defined based on areas examined, and from which data was collected, as well as on geomorphologic features - such as the bay shore and tidal channels - they outline (Fig 1-1). Their boundaries are subjective, and are used to simply indicate zones that were studied, versus zones that were not studied. Zones 2, 3, 5, and 6 are subdivided into sub-environments, due to the high variability in sedimentary and biogenic structures observed.

Chapter one provides an introduction to the general knowledge surrounding the Tillamook Bay estuary. The first part of the chapter is outlined in the form of a literature review, summarizing the most important information regarding the geological and sedimentation history of the past approximately 10,000-11,700 years, when the drowning of rivers due to a rise in sea level began the filling-in of sediment that formed Tillamook Bay. The second part of the chapter outlines the methodology used in the study, both in and off the field.

Chapter two contains detailed results and observations of the neoichnology and sedimentology of various sub-environments studied at Tillamook Bay. Interpretations are then made regarding each sub-environment, and a discussion addressing a sedimentological and neoichnological model, along with reservoir characterization applicability, concludes the chapter.

Chapter three provides a summary of the results and observations outlined in this study, and concludes the main points of discussion. Additionally, the appendices section includes supplementary figures, detailed sediment logs, and a study focusing on microbially-induced sedimentary structures observed at Tillamook Bay. The latter addresses wrinkle marks and microbial mats, interpreted to have formed due to cyanobacterial activity. Their application to sedimentological interpretations is addressed.



STUDY AREA

Bordered by the Pacific Ocean, and located approximately 100 km west of the city of Portland (Fig. 1-2 A,B), Tillamook Bay is the second largest estuary along the Oregon coastline. It is approximately 10 km long in a northwest-southeast direction and 3.4 km wide, averaging approximately 2 meters water depth at high tide, over a 34 km² area (Komar et al., 2004). The mean tidal range is approximately 1.7 to 2.3 meters and makes Tillamook Bay a microtidal to mesotidal estuary. Approximately 50 to 60 per cent of the estuary is exposed as intertidal sand and mud flats during low tide. Five major rivers, comprising a watershed of 1,546 km², deliver sediment to Tillamook Bay. Four of the rivers (Tillamook, Trask, Wilson, and Kilchis Rivers) enter the bay from the southeast and deliver the vast majority of mud and sand deposited within it. A fifth river, the Miami River, enters the bay near the northeast end, carrying sediment into the bay to a much lesser extent than each of the other four rivers.

Tillamook Bay experiences a range of salinities, depending on the season and respective rainfall amounts. Salinity measurements recorded at various depths and locations within Tillamook Bay reveal that the bay is well-stratified during the rainy, fall and winter seasons (approx. October to February), due to high amounts of freshwater runoff from the Coast Range Mountains, and well-mixed during the drier, spring and summer seasons (approx. March to September) when freshwater runoff is greatly reduced (Burt and McAllister, 1958). Salinity fluctuations are smallest at the outer estuary, and range from 32 ppt to 25 ppt, whereas a much larger range of 2 ppt to 20 ppt occurs in the inner estuary, close to the river mouths. The salinity variation between estuarine zones depends on the limit of the flood tidal reach (and therefore seawater) upstream into the estuary. The extremes of the salinity range are dictated by the interaction between spring and neap tidal cycles and, as mentioned earlier, by summer (dry) and winter (wet) seasons. In drowned valley estuaries, the estuarine basin is usually not drained at ebb tide, and

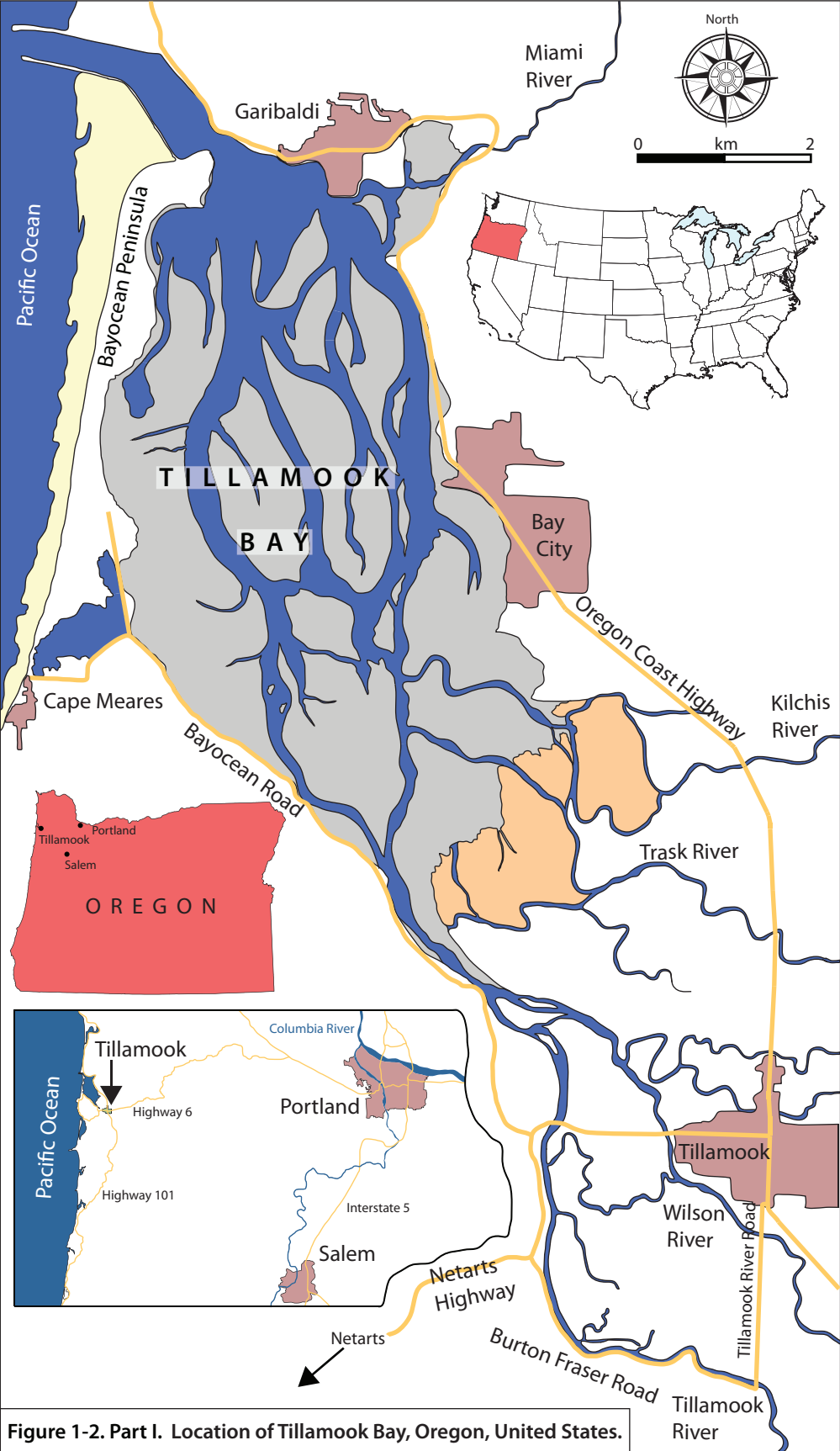


Figure 1-2. Part I. Location of Tillamook Bay, Oregon, United States.

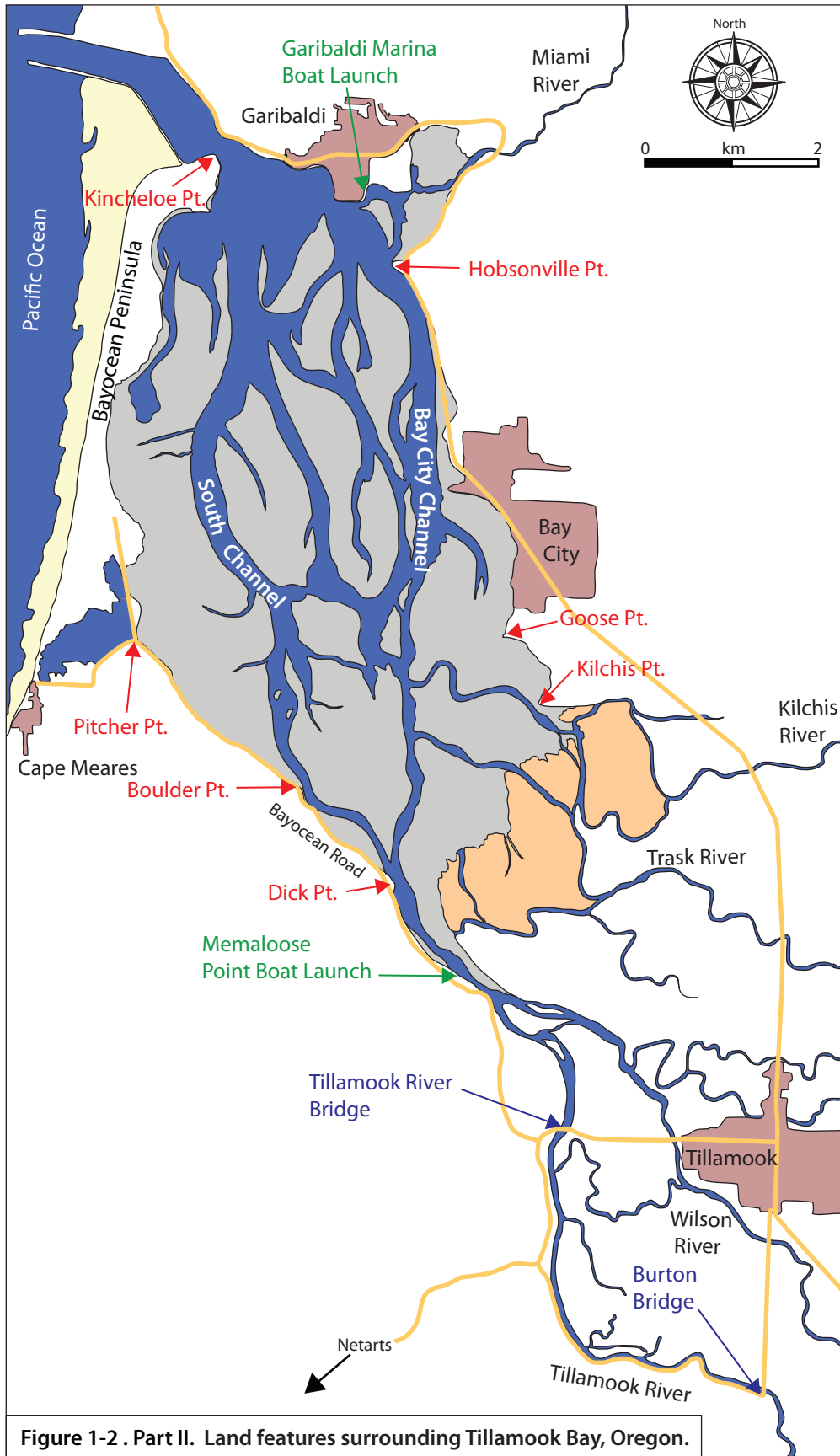


Figure 1-2 . Part II. Land features surrounding Tillamook Bay, Oregon.

therefore experiences a relatively steep salinity gradient, as opposed to smaller estuaries which completely drain on every tide, resulting in more drastic salinity ranges (Green, 1968). In the deep channels, less dense freshwater flows over denser seawater that penetrates as a mid-stream tongue during flood tides. The increased current speeds located mid-channel (in a vertical sense) result in the bulging of isohalines upstream during flood tide and downstream during the ebb tide (Green, 1968).

Due to a large surface area, but shallow water depth, the circulation of fluvial water and seawater is three-dimensional, with fluvial water entering the bay in the southeast corner and flowing close and largely parallel to the eastern margin towards the bay mouth in the northwest corner. Seawater enters the bay through the inlet and flows – under the influence of tidal currents – through a channel closer to the western margin. Sand bars separate the two flows, but still allow the mixing of the waters via the smaller tidal channels and creeks that dominate the central part of the bay (Pearson et al., 1996). This three-dimensional pattern of water transport has an effect on the sedimentation patterns observed within the bay (Komar et al., 2004).

The accumulation of clays at the river mouths often results from the flocculation of suspended fine minerals upon their interaction with saline water in the estuary, with the distribution of the clays dependent on the interaction between river flow and tidal action (Green, 1968). The majority of the clays in Tillamook Bay are deposited in the fluvial channels, upstream of the river mouths. This is indicative of the landward reach of the tides, and the mixing of freshwater and saline waters. The maximum tidal reach in fluvial channels of the Tillamook River entering the bay is approximately 10.2 kilometers (Jones et al., 2012). The tidal reach in the channels of the Trask, Wilson, Kilchis, and Miami River, are 7, 5, 2.7, and 1.3 kilometers, respectively (Jones et al., 2012).

Tillamook Bay connects to the Pacific Ocean through an inlet that is controlled by a north and south jetty, completed in 1917 and 1979, respectively, to facilitate navigation in the channel. Prior to the construction of

the south jetty, sand dredging took place between the city of Garibaldi and the inlet in order to maintain the channel; since the completion of the south jetty, however, the inlet channel has been maintained by the erosive action of the large tidal prism and strong tidal currents (Komar et al., 2004). The volume of the tidal prism (calculated between mean high tide and mean low tide) has been reported as approximately 58,000 acre-feet, or 7.15×10^7 cubic meters of water (U.S. Army Corps of Engineers, 1953), though another, lower estimate also exists, at approximately 4.6×10^7 cubic meters (Komar et al., 2004). With respect to other Oregon estuaries, the tidal prism of Tillamook Bay is regarded as large, due to the large surface area of the bay (Komar et al., 2004).

Before the construction of the jetties, strong flood currents carried beach sand bayward through the inlet, depositing it inside the northern and western part of the bay. However, the amount of sand transported into the bay was significantly reduced after the construction of the jetties (Komar et al., 2004). Due to the presence of the north jetty, longshore drift sand was trapped and deposited at the inlet shoal, causing the tip of the spit to grow (Komar et al., 2004). Thinning of the spit due to erosion took place in three main spots, known as the Southern, Jackson, and Natatorium Gaps, all of which were located at the south end of the spit (U.S. Army Corps of Engineers, 1953). Powerful storm waves, combined with a larger than usual high tide, breached the spit in November 1952 and deposited beach sand inside the bay. Over the next few years, the breach gap widened (Fig. 1-3, 1-4, 1-5). A survey conducted between January 13 and February 16, 1953, mentions the presence of two ridges, both composed of sand and gravel, extending bayward (Fig. 1-3, 1-4). The northwesterly directed ridge was approximately 1.2 kilometers long, and narrowed at the base, with a height of about 4.5 meter above lower low water (U.S. Army Corps of Engineers, 1953). The southeasterly directed ridge, much shorter at about 450 meters, but with a broader base, reached a maximum height of about 3 meters (U.S. Army Corps of Engineers, 1953). Approximately midway between these two ridges, a "low-lying sand and gravel island" was

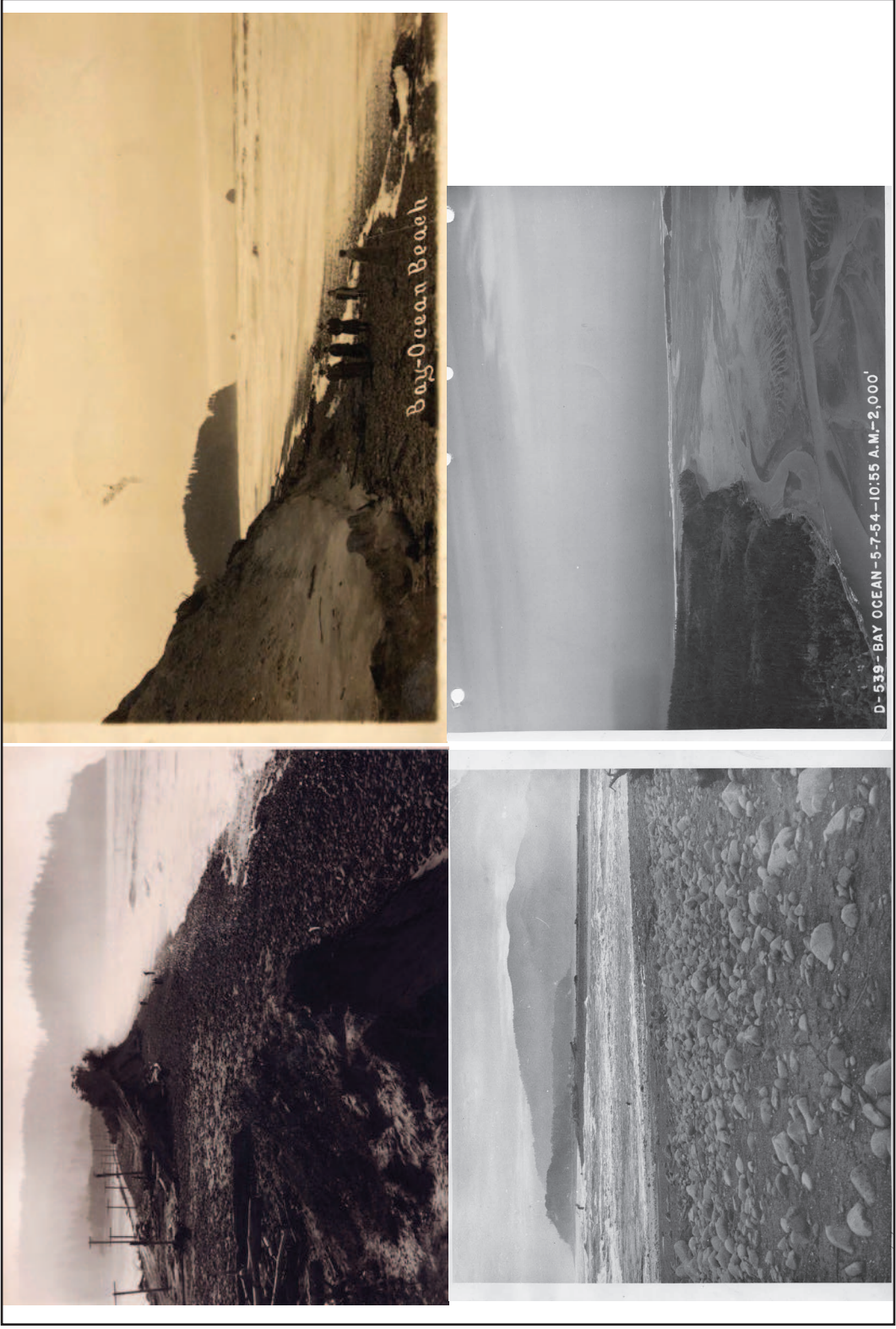


Figure 1-3. Historical photographs of the Bayocean Peninsula storm breach (View #1) .Top photo: aerial view to the southwest, towards Pacific Ocean and Cape Meares (center, left). **Bottom photo:** oblique, aerial view looking north along the spit. Storm breach and tidal inlet seen in the center of the photo. White sand ridges curving into the bay likely correspond to those mentioned by the U.S. Army Corps of Engineers (1953). Both photographs taken on July 5, 1954. Courtesy of Tillamook County Pioneer Museum, used by permission.



Figure 1-4. Historical photographs of the Bayocean Peninsula storm breach (View #2). Both photos: aerial views to the southeast. Tillamook River mouth can be seen in the background. Note presence of the sand ridge curving into the bay, and attached to the main part of the spit. Photos courtesy of Tillamook County Pioneer Museum, used by permission.

Figure 1-5. Historical photographs documenting the erosion of Bayocean Peninsula.
Top left photo: view to the south, showing the erosion of Quaternary dunes on Bayocean Peninsula; the shoreline and Pacific Ocean can be seen to the right of the dunes.
Top right photo: dune erosion on the Pacific Ocean side of the peninsula. View to the south; note Cape Meares in the center of the photo, and group of people in the bottom center for scale. **Bottom left photo:** view to the north, showing the strong ocean waves (likely seen at high tide) crashing inside the inlet formed during the 1952 storm breach. Photograph taken directly south of the inlet. Note the gravel-sized sediment in the foreground, and the vegetated Quaternary dunes in the background, and in front of the highlands. **Bottom right photo:** aerial view of the inner estuary of Tillamook Bay, with the breach zone on the peninsula seen in the center of the photograph. All photos courtesy of Tillamook County Pioneer Museum, used by permission.



located, with two main sediment washes that resulted from the breach, located north and south of this island (U.S. Army Corps of Engineers, 1953). The amount of beach sand that entered the bay through the breach has been estimated at 1.5×10^6 cubic meters (Komar et al., 2004).

Human influence has had drastic effects on the landscape surrounding Tillamook Bay, as well as the sedimentation rates within the bay. From the standpoint of bay sedimentation, logging practices have had the greatest effect, mainly due to the fact that they were combined with large fires that promoted widespread erosion. During the last two centuries, extensive logging of the watersheds, as well as the major forest fires, known as the Tillamook Burns, which took place between the years 1933 and 1951 (Fig. 1-6), have resulted in increased sediment input from the five major rivers draining into the bay. The first forest fire of the Tillamook Burns was also the largest, having burnt approximately 240,000 acres of forest, or approximately half of the total combined area of the Tillamook Bay watersheds (Komar et al, 2004). The main channel, running in a north-south direction between the north end near Garibaldi and the south end near Tillamook, was largely used for towing log rafts from the booming grounds at the river mouths in the southeastern part of the bay. Logs were transported to a mill center located at Garibaldi (U.S. Army Corps of Engineers, 1953).

Historically, the first known explorer to arrive in Tillamook Bay was the British naval officer John Meares, in 1788. On an unsuccessful voyage to locate the Columbia River, Meares traveled south and discovered Tillamook Bay, which he initially named Quicksand Bay. A band of Salish Indians was living on the shores of the bay, and although Meares did come into contact with them, it was not until twenty years later when Lewis and Clark arrived at Tillamook Bay that they referred to the same native Indians in their travel journals as the "Kilamox" and "Killamuck" natives. Over time, those names, along with John Meares' "Quicksand Bay", evolved into "Tillamook" and Tillamook Bay, respectively (Pinyerd, 2000).



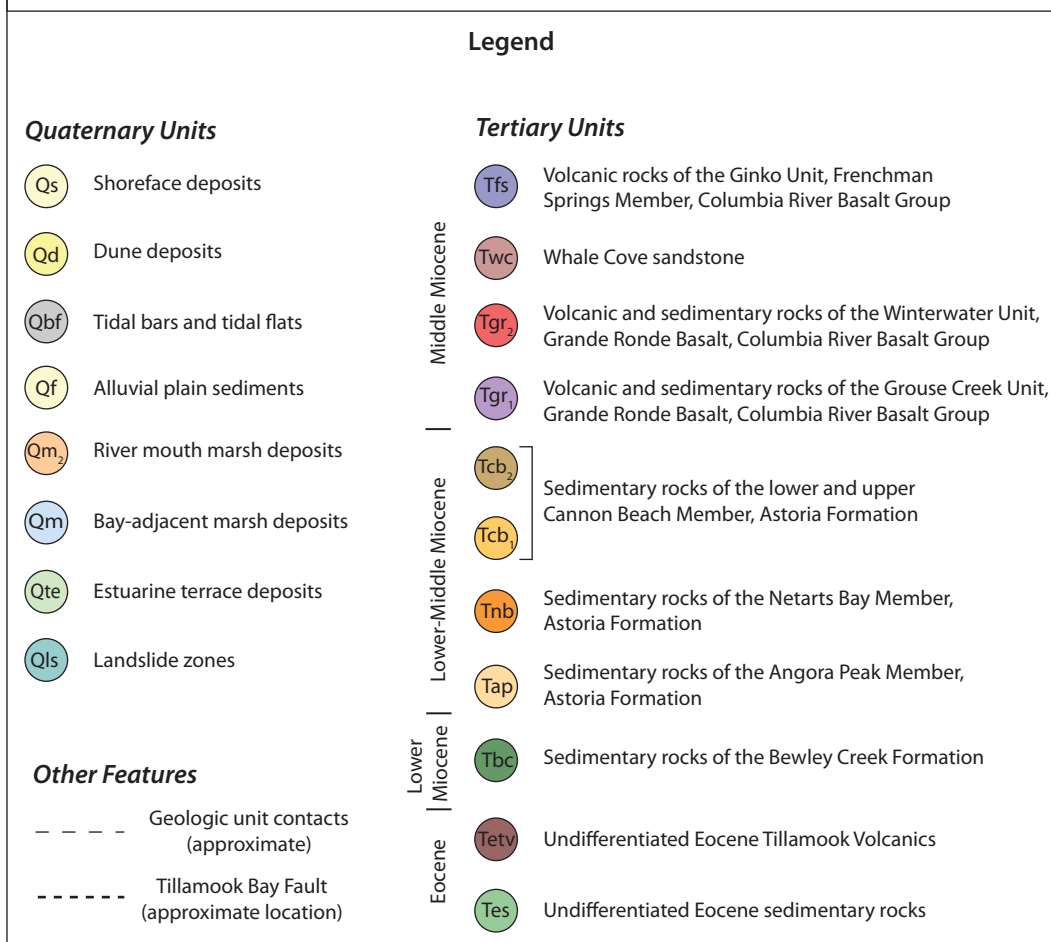
Figure 1-6. Historical photographs of the Tillamook Fires. Top photo: Scouting for spot fires during the 1951 Trask Fire. **Bottom photo:** Scene of the 1951 Tillamook Burn, taken along Highway 6. Photos courtesy of Tillamook County Pioneer Museum, used by permission.

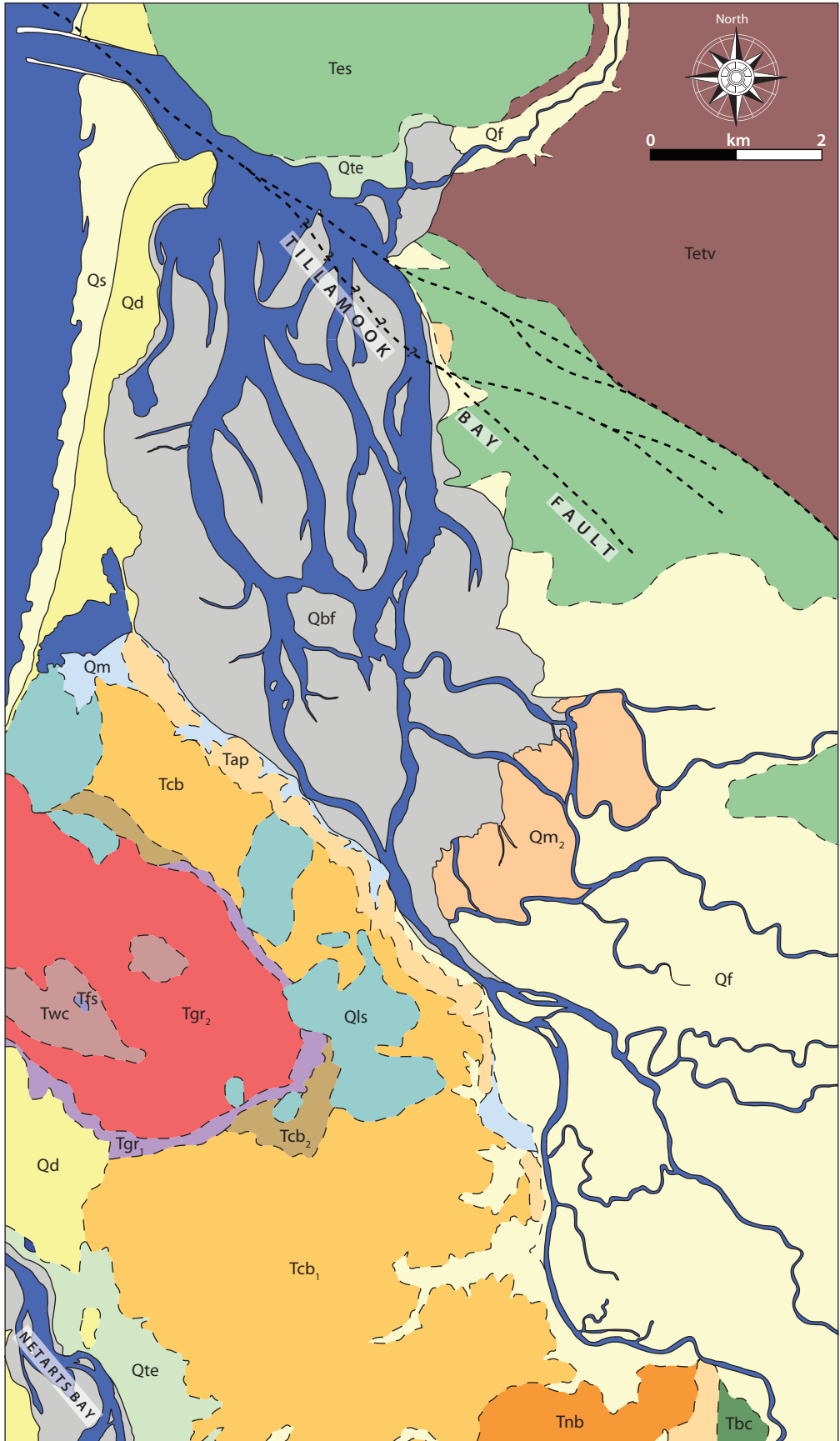
Geologic Setting

Rocks eroded from the Coast Range Mountains that are subsequently brought into the Tillamook Bay drainage basin consist of Tertiary Period marine sedimentary rocks and volcanic rocks. The oldest rocks, of the Eocene Epoch, are the Siletz River Volcanics, which consist of lava flows, both massive and in the form of submarine pillow flows, as well as basalt sills (Komar et al., 2004). These volcanic rocks are the main source of sand transported into Tillamook Bay, whereas the siltstones and mudstones of the Coast Range are the source of the fine-grained sediment (Komar et al., 2004). In the immediate vicinity of the bay, and surrounding it from three sides, are volcanic and sedimentary rocks of the Eocene to Middle Miocene Epochs (Fig. 1-7). Undifferentiated sedimentary rocks and the Tillamook Volcanics form the geology of the highs northeast of the strike-slip Tillamook Bay fault. The rest of the geological units, of the Miocene Epoch, compose the area southwest of the bay, known as the Tillamook embayment (Parker, 1990).

The Cascadia earthquake that occurred on January 26, 1700 in the Cascadia subduction zone off the coast of western United States and Canada, is regarded as one of the world's largest earthquakes on record (NRCAN, 2013). It resulted in a tsunami event, where the consequences of such an erosive event can be seen in the form of a buried beach retreat scarp in the spit of Nehalem Bay, north of Tillamook Bay (Williams, 2008). If cores can be retrieved down to the Pleistocene bedrock in Tillamook Bay (and other bays in the area), evidence of recurrent tsunamis may be observed, as there is geological evidence to suggest that 13 powerful earthquakes have occurred in the last 6000 years on the Cascadia subduction zone (NRCAN, 2013), during the rise in sea level and subsequent flooding of river valleys on the western coast of North America. It is possible that many of these large powerful earthquakes may have resulted in subsidence of bays and estuaries, and therefore an increase in accommodation space combined with an overall rise in sea level. There is evidence that the

Figure 1-7. Geologic map of Tillamook Bay and surrounding area. Overview of the various Tertiary and Quaternary geologic units, and their approximate locations. Map drafted and compiled after three sources: Parker (1990), for the geologic units located in the south-western part of the map (i.e. south-west of the network of rivers and southern shoreline of the bay); Peck (1961) and Wells et al. (1994), for the remaining geologic units in the western and northern part of the map, as well as Bayocean Peninsula; and Wells et al. (1994), for the location of the Tillamook Bay Fault. Note that due to differing map projections between the three sources, and the transfer of information on the current map, the contacts between units are not exact, and are therefore shown as dashed lines.





1700 Cascadia earthquake caused coastal subsidence and drowning of supratidal marshlands and forests that were subsequently buried during ensuing sedimentation episodes (NRCAN, 2013; Williams, 2008).

Sedimentologically, mud accumulates primarily in the southeast bayhead delta part of the bay, while the majority of fine-grained sediments (silt and clay) carried along by the rivers are typically flushed through the bay and transported to the ocean (Komar et al., 2004). Sand-sized grains, however, are the dominant sediment accumulation source in the bay (Komar et al., 2004). In 94 surface sediment samples and 9 sediment cores (with a depth range of 1.5 ± 0.25 m, and one core of 0.5 m depth), river-derived sediments are found primarily in the eastern half of the bay; the western part of the bay contains dominantly beach-derived sand (Komar et al., 2004). Coarser sand, transported into the bay by the rivers, is reworked by estuarine currents and dispersed farthest from the river mouths, at the north part of the bay (Styllas, 2001). The spatial arrangement of the coarse grain fractions is similar to the arrangement of the beach-derived sediments that enter the bay (Styllas, 2001).

The percentage of river-derived rock fragments versus beach-derived quartz and feldspar grains are 40 and 60 percent, respectively, assuming an even distribution of the minor amounts of heavy mineral deposits (Komar et al., 2004). The inclusion of fine-grained sediments in the sediment budget changes the percentage of river-derived sediment to 50%, with the beach sediment making up the other 50%. Geochemical analysis also supports the conclusion of the relative distribution of river-derived versus beach-derived sediment. It shows that beach-derived sediment was more important during the past few hundred years than it is in the present day, with as much as 75 % of the sediment accumulation being beach-derived (Komar et al. 2004). An increase in sedimentation between 1867 and 1954 (estimated at about 70 cm/century) is likely due to the higher sediment yields from the rivers in the deforestation areas (Komar et al. 2004). High quantities of sand deposited during the past few hundred years resulted due to the effects of subsidence and tsunami-

related sand deposition, associated with the Cascadia Earthquake of 1700 that resulted in a 1 m subsidence (Peterson et al, 2000), and a tsunami that likely may have washed over the narrower, southern part of the spit at lower elevation, carrying both beach and dune sand bayward (Komar et al., 2004). Sudden deepening of the bay may have had drastic effects on sedimentation rates and sedimentation patterns, permitting frequent breaching of the spit during major storms. Such episodic sedimentation events are believed to be responsible for the high amounts of beach-derived sediment deposited in the bay during the past few hundred years. Bay deepening may have also resulted in the regression of rivers and the accumulation of river-derived sands in the fluvial channels, as opposed to the bay area itself (Komar et al., 2004), resulting in higher percentages of beach-derived sand to be recorded in the bay during the past few hundred years.

Average sediment accumulation rates over the past 500 years are estimated at 20-40 cm/century (Komar et al. 2004). In a separate study, it was observed that between approximately 7000 and 8000 years before present (B.P.), sedimentation rates were on the order of 200 cm/century, and since then have been on average approximately 20-30 cm/century, being lower partly due to fluctuations in sea-level (Glenn, 1978). Recent bathymetric surveys have supported previous findings, with short-term estimates ranging from 50 cm/century to 70 cm/century, between 1867 and 1995, and between 1867 and 1954, respectively (Bernert and Sullivan, 1998).

METHODOLOGY

Inner estuarine and outer estuarine deposits were chosen in this study, in order to be able to compare and establish depositional indicators on a proximal to distal basis. Due to accessibility constraints and fieldwork time constraints, sand bars of the central middle estuary were not described or analyzed. Detailed observations of the surface sedimentary structures and

incipient trace fossils were recorded. Photography was conducted using a digital single lens reflex (DSLR) Canon Rebel T2i camera (equipped with an 18-55 mm, f2.8 lens) and a waterproof Olympus Stylus Tough camera. Incipient trace fossils and sediment character were often observed by digging shallow trenches and retrieving blocks of sediment from approximately the top 30 centimeters of sediment. Shore-attached tidal flats, such as those in the vicinity of Kilchis Point and Goose Point (Fig. 1.2, Part II), and on the western side of the bay, were accessed by foot. The sand bars of the inner and outer estuary were accessed by inflatable boat via the Memaloose Boat Launch and the Garibaldi Marina, respectively (Fig. 1.2, Part II). Memaloose Boat Launch was also used in accessing the fluvial-tidal transition zone upstream of the mouth of the Tillamook River.

Data were collected in the form of cores – vibracores, PVC cores and boxcores –, surface sediment samples, benthic organism samples, and salinity measurements. Surface sediment and core sediment samples were analyzed for grain size variation and total organic carbon (TOC) content. Each of the aforementioned methods is explained in greater detail in the following paragraphs. It should also be noted that fieldwork was mainly conducted during the relatively dry summer months. As such, due to reduced fluvial discharge and concentrations of suspended sediment, the observed surface sediments were sand-dominated. This plays a role in the observations, because mud deposition occurs primarily during the wet, winter months, as will be explained in the interpretations. Therefore, sedimentary structures observed and described are dominantly related to sand deposits on tidal flats and tidal bars. Similarly, burrow openings and burrow morphologies were observed in sediments close to the surface. High amounts of rainfall during low tide periods of the winter months would result in the closing of, and 'erasing' of many burrows, likely forcing organisms deeper into the substrate, in order to avoid a reduced salinity. With this in mind, it is important to note that biogenic structures described, as well as their distributions, are likely seasonally

controlled due to salinity and sedimentation fluctuations, and observations may differ during the winter months.

Vibracores - The method used to collect sediment cores from the inner and outer estuary is known as vibracoring (Fig. 1-8), and it employs a cement shaker that transmits high-frequency vibrations to a pipe clamp through a flexible hose and a steel head. A total of thirty-two sediment cores were retrieved as part of this study (Fig. 1-9). The steel head used in the vibracoring process in this study had a diameter of one inch. As learnt during fieldwork, a larger diameter (i.e. 2.5 – 3 inch) steel head would have been more suitable for deeper core retrievals. A pipe clamp with two attached parallel, hollow cylindrical bodies is used to connect the flexible hose to the pipe. The large cylindrical body, 3 inches in inside diameter, fits around the top of the pipe; similarly, the smaller cylindrical body of the clamp fits around the steel head.

Twenty-seven pipes used in the vibracoring process were made of aluminum, and five pipes were made of steel. The pipes had the following dimensions: 3 inch outside diameter, 3.1 millimeters thick (i.e wall thickness), and 3.3 meters long, although shorter, 1.5 m long pipes were also used. The relatively thick wall was chosen over a thinner wall (which would 'cut' into the sediments more easily) due to the tendency of thin-walled aluminum pipes to bend when retrieving them. The aluminum pipes are also lighter than steel pipes, and when vibracoring away from a boat or shoreline, it is more efficient to use lighter pipes in order to transport them back once they are filled with sediment. Thin-walled steel pipes usually work best for deeper pipe penetrations, the added weight of the pipe, along with the sharper pipe ends, aiding in the vibracoring process.

Vibrations transmitted to the pipe through the steel head advance the pipe into the sediment, ideally until the pipe clamp is right above the sediment surface and most of the pipe length has entered the sediment. However, this is not always the case, and core recovery varies widely. Multiple factors affect the

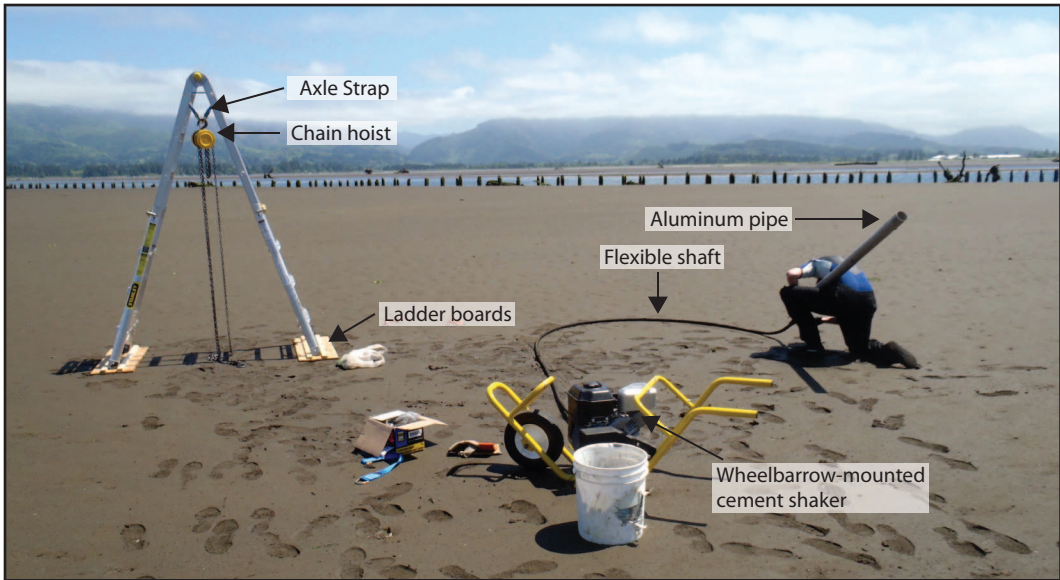
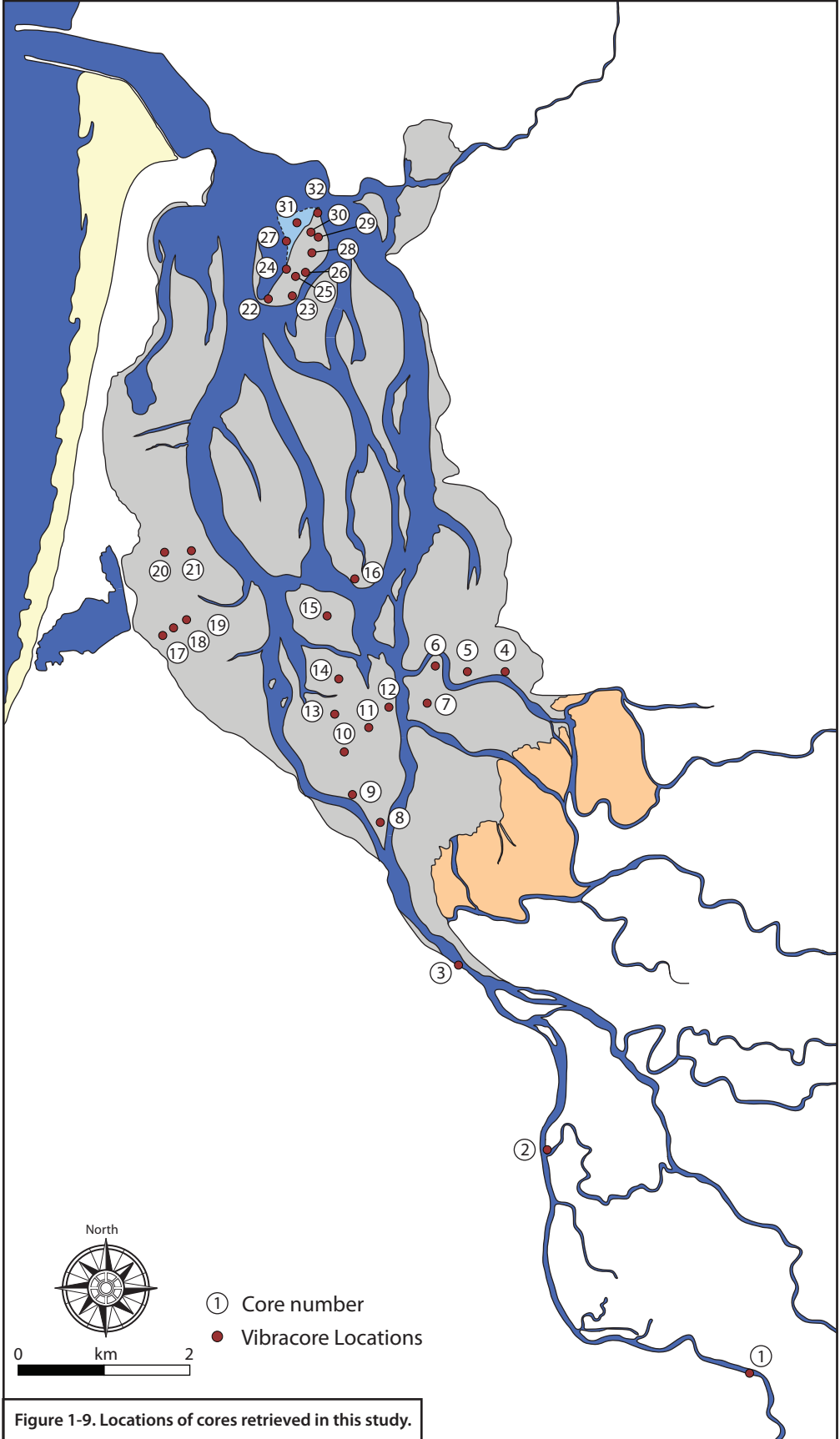


Figure 1-8. Vibracoring method and equipment. Top and center photos: Dave attaching an aluminum pipe to the pipe clamp. Once that step is complete, the pipe is raised into place over the sediment. The motor of the wheelbarrow-mounted cement shaker, once started, transmits high-frequency vibrations through the flexible hose, through the pipe clamp, and to the pipe itself. This process advances the pipe into the sediment. To retrieve the pipe, the ladder is placed over it; a chain is then wrapped around the exposed top of the pipe, and its ends are attached to the hook on the chain hoist, used to pull the pipe out of the sediment. Bottom photo: vibracoring in shallow water.



depth of penetration of the pipe. These factors certainly vary from place to place, and are listed here purely from observations of the vibracoring process in Tillamook Bay sediments. Some of those factors are:

1. Sediment sorting: very well sorted sediment tends to be more restricted to movement due to pipe vibrations, therefore making it more difficult for the pipe to advance. Similarly, very poorly sorted sediment results in little available pore space between sand grains, and therefore also restricts the movement of the sediment due to pipe vibrations.
2. Grain size: relatively small grain sizes (ranging from fine to medium grained sand) tend to allow for better advancement of the pipe into the sediment. Sediments dominated by water-rich clays, or very coarse-grained sand and pebbles (i.e. grains larger than the pipe wall thickness), restrict the movement of sediment around the pipe and therefore indirectly restrict the depth of penetration.
3. Water saturation: this factor can have both a positive or negative effect on pipe penetration. In fine-grained, well-sorted sediment, high water saturation tends to make the sediments more cohesive, due to the presence of water surface tension on a large surface area around individual grains. This can restrict or enhance pipe penetration, depending on the relative sand/clay ratio in a vertical section. In coarser-grained sediment, high water saturation has a positive effect on pipe penetration by making the sediment more fluid and increasing its ability to move due to pipe vibrations.

Core retrieval is done with the aid of a chain hoist, by attaching it to an axle strap hung from the top of a ladder. A one metre long steel chain is then wrapped around the exposed top of the pipe, with the chain ends attached to a chain hoist hook, allowing for the core retrieval. After retrieval, the ends of the pipes are capped using rubber caps, and transported back to the university at the end of the field season for analysis. In a university storage unit, pipes are cut and split longitudinally to expose the sediment cores. Using a thin-bladed

knife, the surface of cores is carefully smoothed out in order to obtain a flat and even surface area. One half of each core is x-rayed using a Soyee veterinary-use x-ray machine. The other half of each core is photographed and described in sediment logs. Descriptions generally consist of grain size, bed thickness and bed contacts. Sedimentary structures, where present, are noted and described. However, stratification in vibracores is often difficult to interpret, and as Lucchi (1995) notes, due to slight sediment contrasts and the soft, prediagenetic state of the sediment, bedding and sedimentary structures are often difficult to recognize. Adding to this is the fact that cores were transported from Oregon to Alberta, and as such, some element of sediment movement likely occurred, especially in beds with low clay content (clay sediments retain more water, and make the sediment more cohesive, thereby preventing movement inside the pipe).

Total Organic Carbon (TOC) - Numerous authors have published papers to report methods for the determination of total organic carbon (TOC) based on temperature of combustion, duration of combustion, mineral and inorganic carbonate content of the sample, among other factors. It is generally accepted that a maximum temperature of 550°C can be used in the determination of TOC, without burning off the inorganic carbonates. Analysis of sediment samples for total organic carbon (TOC) is initiated by drying each sample at 110°C for 24 hours, to remove interstitial water. The dried sediment is then transferred to a mortar, and disaggregated using a pestle, to dislodge any clumps of sediment that result during the drying process. Once disaggregated, a small size of sediment (50 - 100 g) is transferred to ceramic crucibles. The crucibles and sediment are weighed on a scale, and weights recorded in a notebook. Once weighed, the crucibles and sediment are placed in a high-temperature oven at 550°C, over a period of 6 hours. After heating at 550°C, the crucible weights are recorded once more.

Grain size analysis - The remaining portion of dried, disaggregated sediment was used for grain size analysis. This was performed on surface and core samples in three ways, using techniques outlined by Folk (1980) and Tucker (1988):

1. Sieving of samples to determine grain sizes present,
2. Graphical representation of unique frequency plots and cumulative frequency distribution curves, and
3. Statistical method analysis.

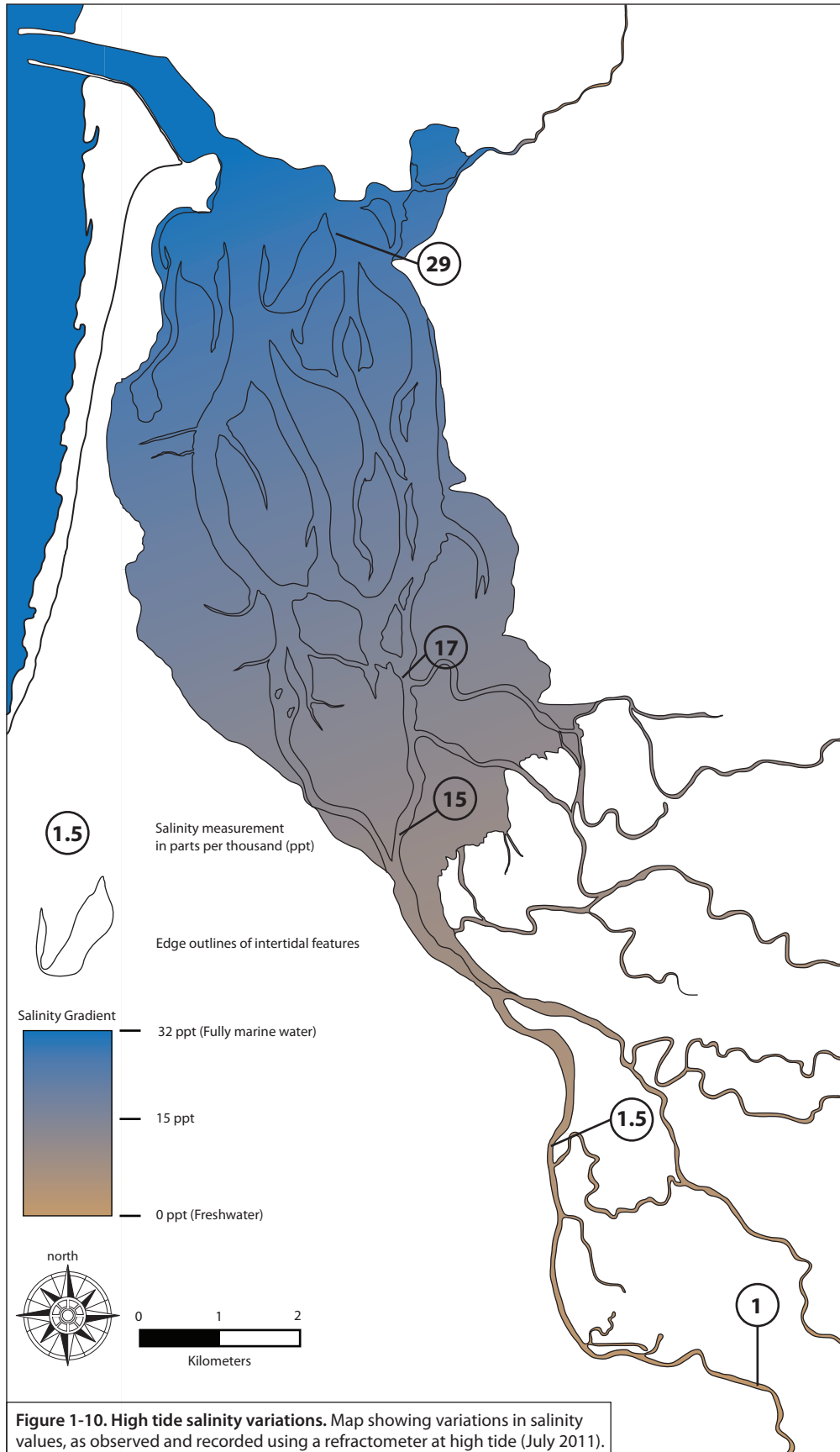
Each method is outlined below:

1. Sieving is performed on sediment samples of weights varying between 40 and 100 grams. Samples are placed in a sieve set containing sieves with mesh sizes based on the Udden-Wentworth scale, with a terminal pan at the bottom of the set. The smallest sieve size used is 63 microns (limit of sand grains). The sieve set is placed on a mechanical sieve shaker for a period of 15 minutes. Once the sieving process is completed, the sediment from each sieve is transferred onto a sheet of paper, and once again transferred into a small aluminum tray on a scale. Weights of the sample for each grain size are measured and recorded.
2. Graphical representation of data is performed by plotting each unique grain size percentage on a bar chart, to determine the most frequent grain size. Cumulative grain size percent is also plotted on a cumulative frequency distribution curve. From this curve, the grain size (in phi units) corresponding to percent values 5, 16, 50, 84, and 95 is recorded.
3. Using the methodology outlined by Folk (1980), the sorting, skewness, and kurtosis, is determined for individual zones containing multiple grain size analysis data.

Salinity measurements – salinity in the estuary waters is measured using a light refractometer, and ranges from approximately 1 parts per thousand (ppt) to

approximately 29 ppt, though the location of saline and fresh water is observed to vary between the low and high tides (Fig. 1-10; Fig 1-11).

Benthic Organism Sampling - Neoichnological observations were recorded in the field; methods used for the observation of benthic organisms and related burrow morphologies and behaviours include boxcoring, cores retrieved via clam guns, and sediment samples dug with a shovel into the intertidal exposed flats. Samples are photographed, and the burrow morphologies and abundances noted. Where possible, benthic organisms are sampled and preserved in ethanol-filled jars. Concentrations of burrows were described using descriptive terminology (i.e. absent, common, moderate, abundant). Bioturbation indices (BI) are also occasionally assessed, ranging from 0-6, as described by Reineck (1963) and modified by Taylor and Goldring (1993). The most common invertebrate organisms observed at Tillamook Bay, and sampled as part of this study, are listed in Table 1-1.



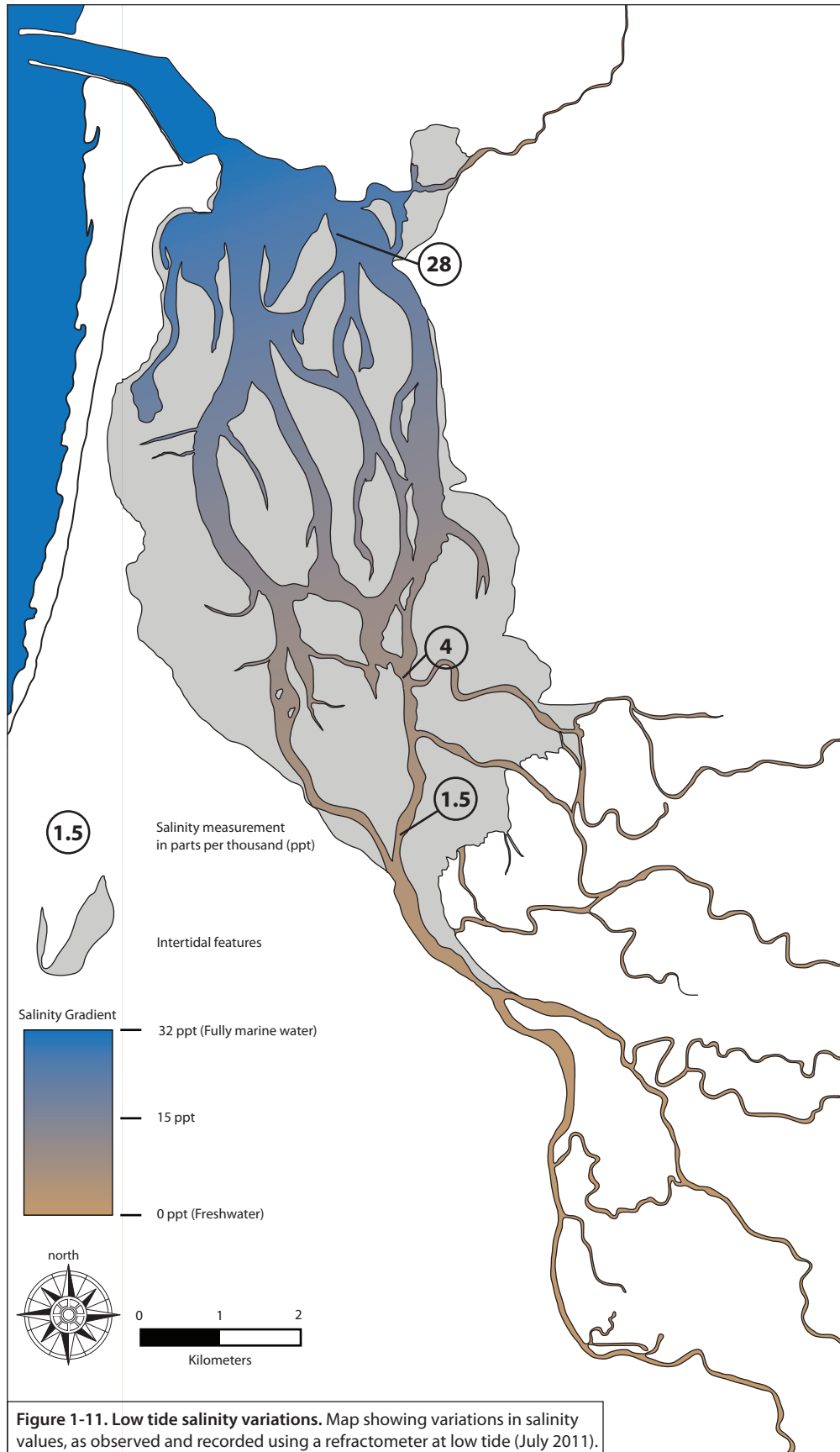


Figure 1-11. Low tide salinity variations. Map showing variations in salinity values, as observed and recorded using a refractometer at low tide (July 2011).

Table 1-1. List of invertebrate organisms and aquatic plants observed in intertidal deposits of Tillamook Bay Estuary. List of the most commonly observed tracemakers at Tillamook Bay. The total number of species documented from Tillamook Bay, and mentioned in available literature, is much higher. This study focused on the main tracemakers and their distribution.

List of invertebrate organisms and aquatic plants observed in intertidal deposits of Tillamook Bay Estuary				
Phylum	Invertebrate / Plant	Common Name	Behavior	Incipient Traces
Mollusca	<i>Clinocardium nuttallii</i>	Basket, heart cockle	Selective suspension feeder (filter feeder)	<i>Siphonichnus</i> , <i>Skolithos</i>
	<i>Macoma balthica</i>	Baltic macoma / clam	Interface feeder, filter feeder	<i>Siphonichnus</i> , <i>Skolithos</i>
	<i>Macoma secta</i>	White sand macoma	Suspension feeder, deposit feeder?	<i>Siphonichnus</i> , <i>Skolithos</i>
	<i>Mya arenaria</i>	Soft shell clam	Selective suspension feeder (filter feeder)	<i>Siphonichnus</i> , <i>Skolithos</i>
	<i>Nuttallia obscurata</i> <i>Tresus capax</i>	Purple varnish clam Pacific gaper / horseneck clam	Non-selective suspension feeder Selective and non-selective suspension feeder	<i>Siphonichnus</i> , <i>Skolithos</i> <i>Siphonichnus</i> , <i>Skolithos</i>
Annelida	<i>Abarenicola pacifica</i>	Lugworm	Deposit feeder	<i>Arenicolites</i>
	<i>Nephtys</i> sp.	Sand worm	Filter feeder, deposit feeder, active predator	<i>Palaeophycus</i> , <i>Planolites</i> , <i>Polykladichnus</i> , <i>Skolithos</i> cryptic bioturbation
	<i>Nereis</i> sp.	Varies depending on species	Carnivore, selective and non-selective suspension feeder, deposit feeder, interface feeder	<i>Palaeophycus</i> , <i>Planolites</i> , <i>Polykladichnus</i> , <i>Skolithos</i>
	<i>Notomastus</i> sp.	Threadworm	Deposit feeder	<i>Skolithos</i>
Arthropoda	<i>Hemigrapsus oregonensis</i>	Hairy shore crab	Predator, scavenger	<i>Psilonichnus</i>
	<i>Neotrypaea californiensis</i>	Sand / ghost shrimp	Deposit feeder	<i>Thalassinoides</i>
	<i>Pagurus hirsutiusculus</i>	Hairy hermit crab	Predator	Surface tracks
	<i>Traskorchestia traskiana</i> <i>Upogebia pugettensis</i>	Beach hopper Mud shrimp	Deposit feeder (?) Suspension feeder	<i>Skolithos</i> <i>Thalassinoides</i>
Nemertea	<i>Paranemertes peregrina</i>	Purple / wandering ribbon worm, wandering nemertean, restless worm, purple-backed ribbon worm	Predator	Unknown Not observed
Chlorophyta	<i>Kornmannia leptoderma</i>	Epiphytic sea lettuce	N/A	Rootlets
Anthrophyta	<i>Zostera marina</i>	Eelgrass	N/A	Rootlets

BIBLIOGRAPHY

- Benoit, G.M.** (1996) An interactive metadata catalog for the Tillamook Bay national estuary Project Geographic Information System. Master of Science Thesis, College of Oceanic and Atmospheric Sciences, Oregon State University, p. 92.
- Bernert, J.A.** and **Sullivan, T.J.** (1998) Bathymetric analysis of Tillamook Bay: comparison among bathymetric databases collected in 1867, 1957 and 1995. E&S Environmental Chemistry, Inc., Corvallis, Oregon, p. 24.
- Burt, W.V.** and **McAllister, B.** (1958) Hydrography of Oregon estuaries. Data Report No. 3, School of Science, Oregon State College, Corvallis, Oregon, p. 18.
- Diller, J.S.** (1896) A geological reconnaissance in Northwestern Oregon. U.S. Geological Survey, Report 17, Government Printing Office, Washington, D.C., p. 117. Accessed September 12, 2013, via <www.archive.org>.
- Dionne, J.C.** (1963) Towards a more adequate definition of the St. Lawrence estuary. *Zeitschrift für Geomorphologie*, v. 7, no. 1, p. 36-44.
- Ferraro, S.P.** and **Cole, F.A.** (2012) Ecological periodic tables for benthic macrofaunal usage of estuarine habitats: Insights from a case study in Tillamook Bay, Oregon, USA. *Estuarine, Coastal and Shelf Science*, v. 102-103, p. 70-83.
- Folk, R.L.** (1980) *Petrology of Sedimentary Rocks*. Hemphill Publishing Company, Austin, Texas, p.182.
- Gingras, M.K.** and **MacEachern, J.A.** (2012) Tidal ichnology of shallow-water clastic settings. In Davis Jr., R.A. and Dalrymple, R.W., eds. *Principles of Tidal Sedimentology*. Springer, p. 57-77.
- Glenn, J.L.** (1978) Sediment sources and Holocene sedimentation history in Tillamook Bay, Oregon: Data and Preliminary Interpretations. Open-file report 78-680: United States Department of the Interior Geological Survey, Denver, Colorado.
- Goldfinger, C., Kulm, L.D., Yeats, R.S., Appelgate, B., MacKay, M.E.** and **Moore, G.F.** (1992) Transverse structural trends along the Oregon convergent margin: Implications for Cascadia earthquake potential and crustal rotations. *Geology*, v. 20, p. 141-144.
- Green, J.** (1868) *The biology of estuarine animals*. University of Washington, p.401.
- Hevlin, W.A.** (1988) Restoration of Tillamook Bay: project planning. A marine resource management project report: Marine Resource Management Program, Oregon State University, p. 61.
- Jones, K.L., Keith, M.K., O'Connor, J.E., Mangano, J.F.,** and **Wallick, J.R.** (2012) Preliminary assessment of channel stability and bed-material transport in the Tillamook Bay tributaries and Nehalem river basin, northwestern Oregon. U.S. Department of the Interior, U.S. Geological Survey, Open-File Report 2012-1187, p. 121.
- Komar, P.D., McManus, J.** and **Styllas, M.** (2004) Sediment accumulation in Tillamook Bay, Oregon: natural processes versus human impacts. *The Journal of Geology*, v. 112, p. 455-469.

- Lucchi, F.R.** (1995) *Sedimentographica: A Photographic Atlas of Sedimentary Structures*. Columbia University Press, p. 280.
- Melancon, P.A.** (1999) A GIS based watershed analysis system for Tillamook Bay, Oregon. Master of Science in Engineering Thesis, Center for Research in Water Resources, The University of Texas at Austin, p. 376.
- McManus, J., Komar, P.D., Bostrom, G., Colbert D. and Marra, J.J.** (1998) Sediment sources and the history of accumulation in Tillamook Bay, Oregon. The Tillamook Bay National estuary Project, Sedimentation Study, p. 62.
- NRCAN** (2013) The M9 Cascadia Megathrust Earthquake of January 26, 1700: Natural Resources Canada, Government of Canada, April 26, 2013. Accessed May 27, 2013. <www.earthquakescanada.nrcan.gc.ca>.
- Parker, M.J.** (1990) The Oligocene and Miocene Geology of the Tillamook Embayment, Tillamook County, Northwest Oregon. Master of Science Thesis, Oregon State University, p. 515.
- Pearson, P, Baptista, A.M. and Alves, M.** (1996) Tillamook Bay circulation. Center for coastal and land-margin research, Oregon Graduate Institute.
- Peck, D.L.** (1961) Geologic map of Oregon west of the 121st Meridian. U.S. Geological Survey, Miscellaneous Geologic Investigations Map I-325. Accessed via the National geologic Map Database, <ngmdb.usgs.gov>, Accessed September 15, 2013.
- Peterson, C.D, Doyle, D.L. and Barnett, E.T.** (2000) Coastal flooding and beach retreat from coseismic subsidence in the central Cascadia margin, USA. *Environmental and Engineering Geoscience*, v. 6, no. 3, p. 255-269.
- Pinyerd, D.A.** (2000) The Preservation of Pre-World War Two Coast Guard Architecture in Oregon. M.Sc. Thesis, Interdisciplinary Studies Program, Historic Preservation: University of Oregon.
- Reineck, H.-E.** (1963) Sedimentgefüge im Bereich der südlichen Nordsee. *Abhandlungen der Senckenbergische Naturforschende Gesellschaft*, 505.
- Seliskar, D.M. and Gallagher, J.L.** (1983) The ecology of tidal marshes of the Pacific Northwest Coast: a community profile. Fish and Wildlife Service, U.S. Department of the Interior, p. 65.
- Strittholt, J.R. and Frost, P.A.** (1996) Determining abundance and distribution of eelgrass (*Zostera* spp.) in Tillamook Bay estuary, Oregon, using multispectral airborne imagery. Prepared for Tillamook Bay National Estuary Project, Garibaldi, Oregon, p. 19.
- Styllas, M.N.** (2001) Sediment accumulation and human impacts in Tillamook bay, Oregon. Master of Science Thesis. Oregon State University, p. 132.
- Sullivan, T.J., Bischoff, J.M., Kai, S.U., Raymond, R.B., White, S. and Binder, S.K.** (2001) Wilson river watershed assessment: final report. E&S Environmental Chemistry Inc., Corvallis, Oregon, p. 207.

- Taylor, A.M., and Goldring, R.** (1993) Description and analysis of bioturbation and ichnofabric. *Journal of the Geological Society of London*, v. 150, p. 141-148.
- Terich, T.A. and Komar, P.D.** (1973) Development and erosion history of Bayocean Spit, Tillamook, Oregon. School of Oceanography, Oregon State University, Corvallis, Oregon, p.145.
- Thomas, R.G., Smith, D.G., Wood, J.M., Visser, J., Calverley-Range, E.A. and Koster, E.H.** (1987) Inclined heterolithic Stratification – Terminology, Description, Interpretation and Significance. *Sedimentary Geology*, v. 53, p. 123-179.
- Tucker, M.** (1988) *Techniques in Sedimentology*. Oxford, England, Blackwell Scientific Publications, p. 394.
- U.S. Army Corps of Engineers** (1953) Review report on Tillamook Bay and Bar, Oregon. Office of the District Engineer, Portland, Oregon, p. 70.
- VanLaningham, S.** (2007) The fluvial response to glacial-interglacial climate change in the Pacific Northwest, USA. Doctor of Philosophy Thesis, Oregon State University, p. 213.
- Warren, W.C., Norbistrath, H. and Grivetti, R.M.** (1945) Geology of northwestern Oregon west of Willamette River and north of latitude 45 degrees and 15 minutes. U.S. Geological Survey, Oil and Gas Investigations Map OM-42. Accessed via the National Geologic Map Database, <ngmdb.usgs.gov>, Accessed September 15, 2013.
- Wells, R.E., Parke D.S. Jr, Macleod, N.S., Kelly, M.M., Parker, M.J., Fenton, J.S. and Felger, T.J.** (1995) Geologic map of the Tillamook Highlands, northwest Oregon Coast Range: A Digital Database: U.S. Geological Survey Open-File Report 95-670.
- Williams, S.S.** (2008) Report on 2007 fieldwork of the Beeswax wreck project, Nehalem Bay, Tillamook County, Oregon. Beeswax Wreck Project Group, Olympia, Washington, p. 65.

CHAPTER 2 – SEDIMENTOLOGY AND NEOICHOLOGY OF INTERTIDAL FACIES, TILLAMOOK BAY ESTUARY, OREGON, UNITED STATES

INTRODUCTION

Chapter 2 includes the descriptions and results, interpretations, and discussion surrounding the sedimentology and neoichnology of tidal sand bars and tidal flats of the Tillamook Bay estuary. The results are presented starting from the innermost estuary area of Tillamook Bay, and end with the outermost estuary area. For simplicity, the areas of the bay studied are divided into zones one through six (Fig. 1-1). Interpretations directly follow the descriptions and results section of each zone, with a final discussion at the end of the chapter highlighting a sedimentological facies model and a discussion of controls on sedimentation; a neoichnological model; and a reservoir characterization analogue.

DESCRIPTIONS, RESULTS, AND INTERPRETATIONS

Inner Estuary Characteristics

Zone 1: Fluvial – Tidal Transition Descriptions and Results

Sedimentological and Neoichnological Features

The fluvial – tidal transition zone (Fig. 2-1) covers an area that begins in the vicinity of the salt marshes, and extends as far as 10.2 kilometers upstream (Jones et al., 2012), at the limit of tide advancement in the straight to moderately sinuous fluvial-tidal channels. Highly vegetated banks, including large evergreen trees that extend to the steep-angled bank edges (Fig. 2-2

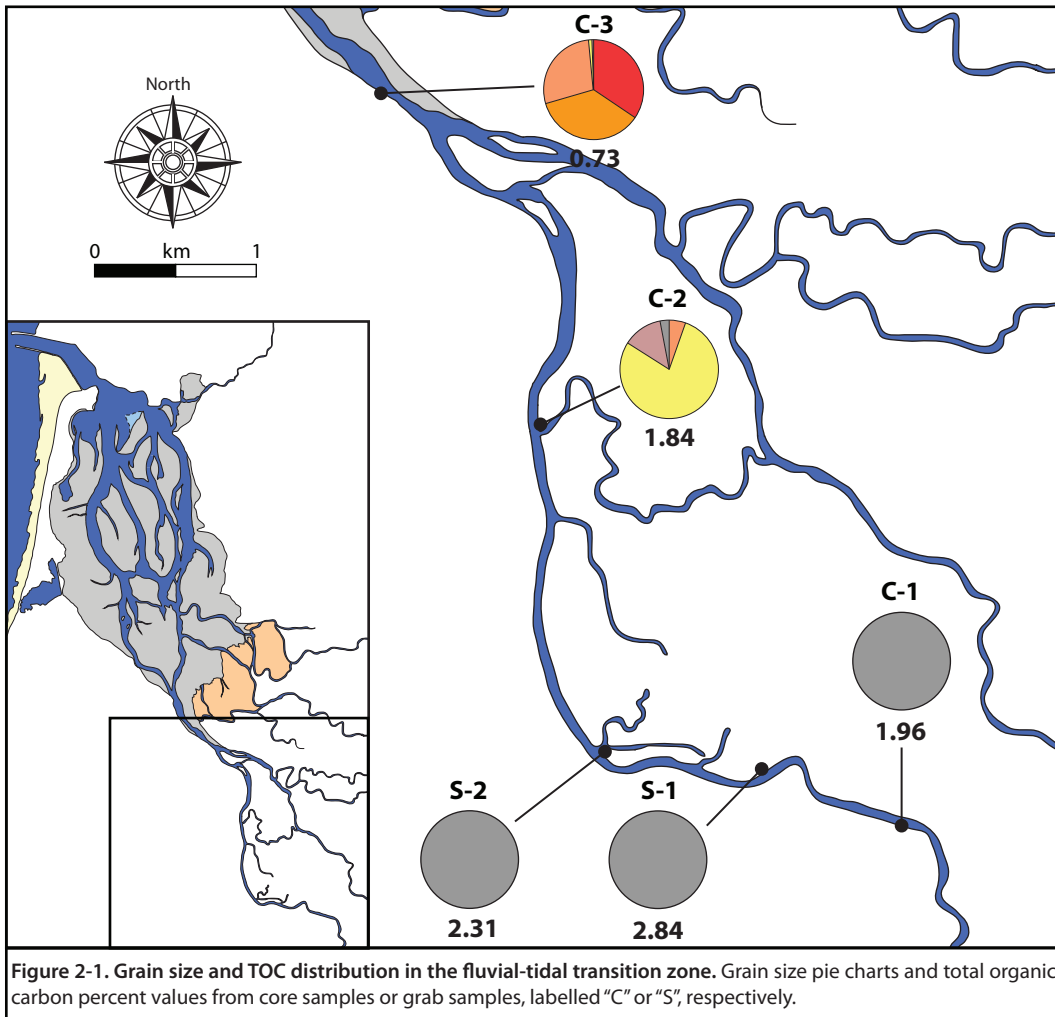


Figure 2-2. Channels of the fluvial-tidal transition zone. Views in (A),(B), and (C) are of mud-dominated, vegetation-stabilized, tidally-influenced fluvial channels; location shown in (A) is furthest upstream. (D) Sandy portion of a grassy fluvial point bar, slightly downstream of the transition from muddy to sandy portion of the channels.



A,B,C,D) dominate the environment of this zone. These stable banks inhibit short-term point bar lateral migration and are dominantly muddy. Locally, very coarse sand and gravel lenses are observed within the mud deposits of the fluvial-tidal channels, representing an estimated 5-10% of the total sediment volume.

In the vicinity of the Tillamook River Bridge (Fig. 1-2; part II), a gradual transition from mud-dominated facies to sandy facies is observed. A small exposed part of a point bar, adjacent to vegetated banks and farmland, appears sand dominated, and contains abundant traces of rootlets. No burrowing organisms are observed in the fluvial-tidal transition zone, where the maximum salinity measured during the dry season ranges between 1 ppt and 1.5 ppt at high tide (Fig. 1-10).

Layered salt marsh deposits (Fig. 2-3 A,A') are observed in the lower reaches of the fluvial-tidal transition zone. The salt marsh near the mouth of the Tillamook River is indicated in the aerial photo of Figure 2-4 (A,B,C). A sediment core retrieved 2.5 km downstream of the Tillamook River Bridge, near the Tillamook River mouth, acts as a good reference core as it reveals medium to coarse-grained sand, interlayered with mud (Fig. 2-4 A).

Zone 1 Fluvial – Tidal Transition Vibracore Facies Descriptions

A total of three cores were recovered from Zone 1, with each recovered core ranging from 55 cm – 65 cm in length. Three facies are identified from the Fluvial – Tidal Transition (Zone 1) according to distinct sedimentological and neoichnological characteristics. These facies are summarized in Table 2-1, with supplementary references to vibracore logs located in Appendix B.

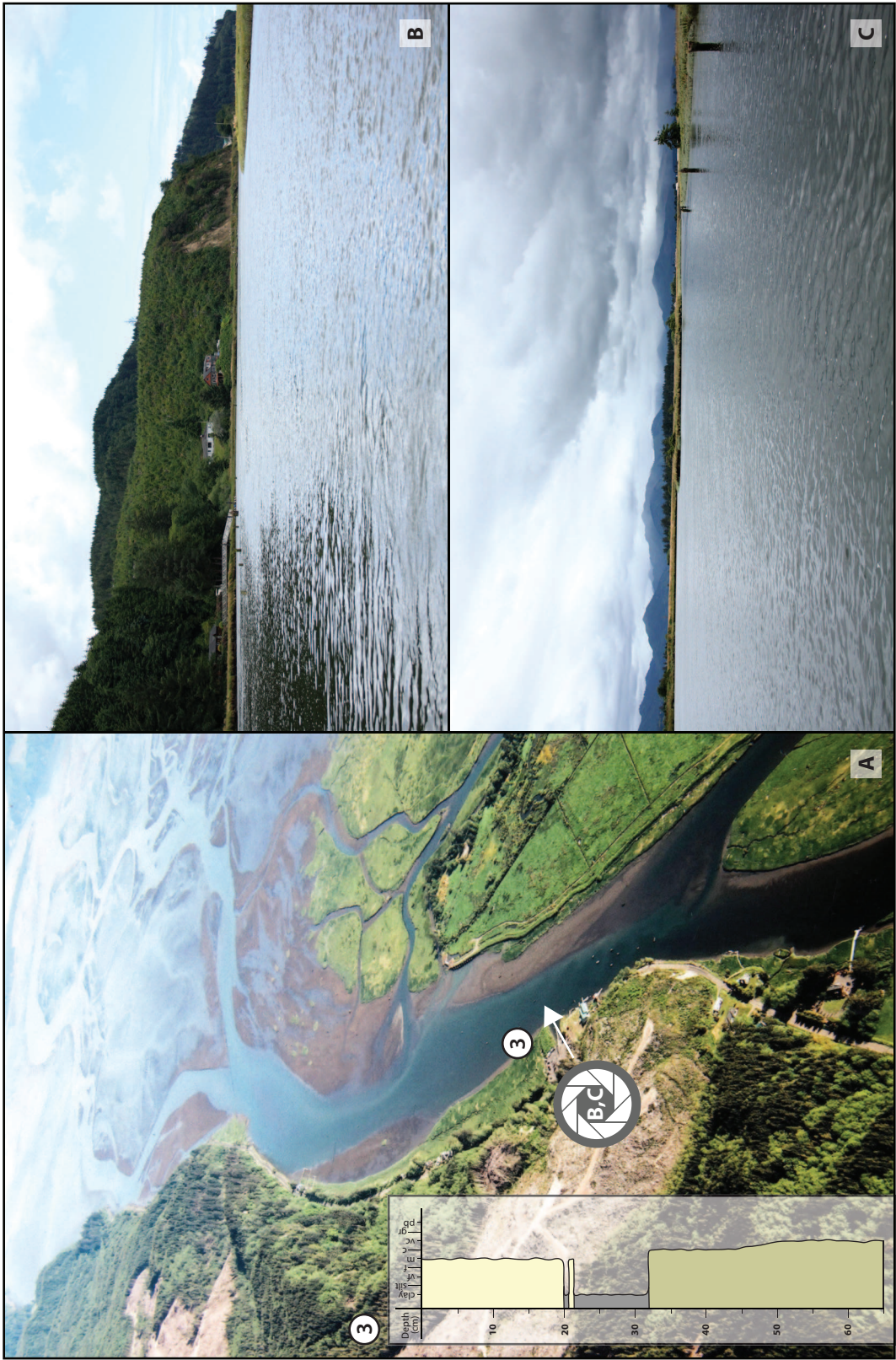
Zone 1 Facies 1 (Z1F1) – Coarse to very coarse muddy sand

Facies 1 is found within the most distal (bayward) vibracores taken within the fluvial-tidal channels (Fig. 2-4 A; Fig. 2-5; Table 2-1). The thickness of

Figure 2-3. Salt marsh stratification. (A and A') View of salt marsh near the Tillamook River mouth. Colors schematically drawn in (A') show distinct layering of salt marsh, (they do not indicate lithologies, or different layer characteristics).



Figure 2-4. Geomorphology at the mouth of the Tillamook River. (A) Aerial view of the mouth of the Tillamook River; photo courtesy of Don Best, Best Impressions Picture Co., used by permission. Location of core 3, along with the sediment log for this core, is shown in (A). (B): view downstream, to the north-west; (C): view upstream, to the south-east.



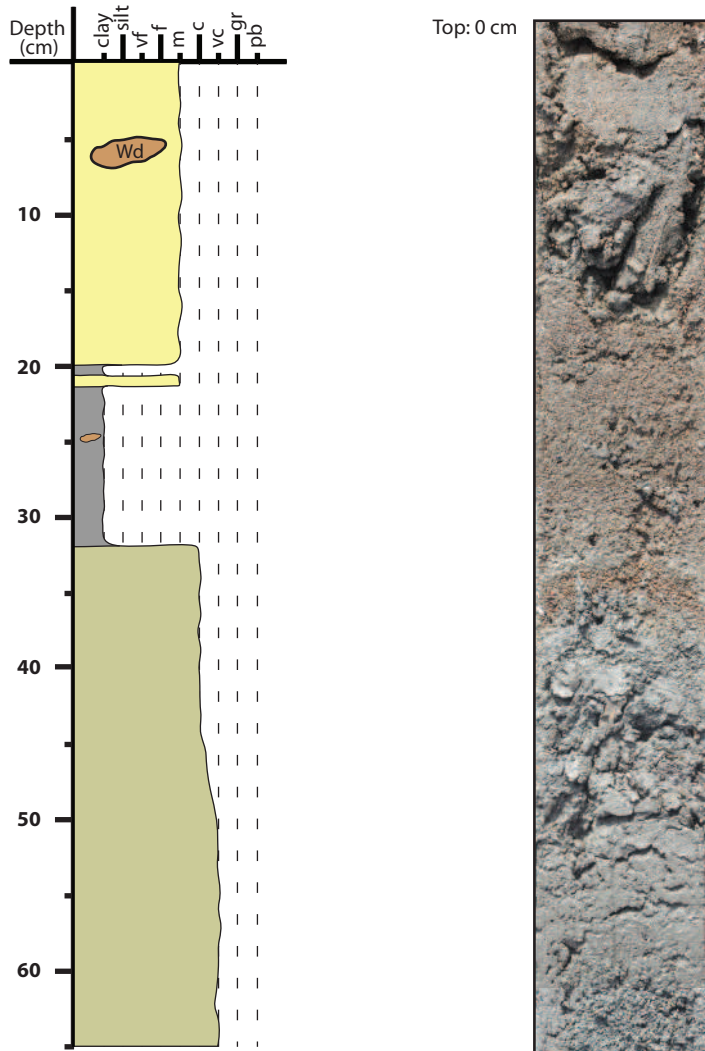


Figure 2-5. Core example from the inner estuary Zone 1. In the distal part of the fluvial-tidal transition, interbedded muddy sand, mud, and sand layers are observed. No bioturbation is observed. Pebbles and occasional gravel are observed in the very coarse-grained sands, as well as within the mud layers (as is the case in the proximal, muddy part of Zone 1).

Base: 65 cm

Facies Association	Facies	Facies Contacts	Sedimentary Characteristics	Neochronological Characteristics	Interpretation
Fluvial - Tidal Transition Facies Association (FA1)	Facies 1 (Z1F1) Coarse to very coarse muddy sand Appendix B Core Figure Reference(s): B-2	Upper contact of Facies 1, when present, is sharp with the overlying unit commonly consisting of Facies 2 and occasionally Facies 3, or may also occur as thick interbeds within overlying facies.	Massive appearing light grey to brown muddy sand with accessory amounts of pebble to granule sized grains, especially within the lowermost part of the facies. Thickness varies from absent in the most proximal areas to at least 30 cm thick in the most distal areas.	Bioturbation absent.	Distal sand-dominated channel base
	Facies 2 (Z1F2) Massive mud Appendix B Core Figure Reference(s): B-1; B-2	Facies 2 may appear as interlaminae or interbeds within Facies 1 or 3. At some locales Facies 2 may be the only facies present in core and therefore no contacts are observed.	Massive light grey mud characterizes the facies with accessory sporadic wood clasts present. Where typically present this facies can consist of the entire core sequence and be up to at least 55 cm thick, especially in the most proximal areas. In the most distal fluvial-tidal channels this facies is present instead as interlaminae or interbeds up to 15 cm thick.	Bioturbation absent.	Proximal mud-dominated channel
	Facies 3 (Z1F3) Massive fine to medium grained sand Appendix B Core Figure Reference(s): B-1; B-2	If present, Facies 3 sharply contacts underlying Facies 2 or is interlaminated or interbedded with Facies 2. At some locales Facies 3 may be the only facies observed thus no contacts are observed.	Mainly massive appearing, brown colored, fine to dominantly medium grained sand. Faint planar laminae or bedding may be present. Sediment may display a loamy texture and have sporadic wood clasts. Thickness varies from absent through interlaminae and interbeds to sequences at least 20 cm - 60 cm thick.	Bioturbation absent.	Distal sand-dominated middle channel to channel edge

Table 2-1: Summary of Facies Characteristics for Fluvial - Tidal Transition (Zone 1)

Facies 1 varies from absent in the most proximal areas to at least 30cm thick in the most distal areas. This facies is characterized by massive appearing light grey to brown muddy sand and accessorially contains up to 5% pebble to granule sized grains, especially within the lowermost part of the facies. Bioturbation is absent from this facies. The upper contact of Facies 1, when present, is sharp with the overlying unit commonly consisting of Facies 2 and occasionally Facies 3. This facies may appear as thicker interbeds with either Facies 2 and/or 3 displaying an overall fining upwards trend.

Zone 1 Facies 2 (Z1F2) – Massive mud

Facies 2 is the most prevalent facies found throughout the fluvial-tidal transition zone and is typically found in all channel deposits, but is absent from bank deposits of Core 2 (Fig. 2-4 A; Fig. 2-5; Table 2-1). Where typically present this facies can consist of the entire core sequence and be up to at least 55 cm thick, especially in the most proximal areas. In the most distal fluvial-tidal channels this facies is present instead as interlaminae or interbeds up to 15 cm thick. Massive light grey mud characterizes Facies 2 with accessory sporadic wood clasts present. Bioturbation is absent from Facies 2. Facies 2, when present, has sharp contacts with underlying Facies 1 and overlying Facies 3. Occasionally Facies 2 may appear as interlaminae or interbeds within Facies 1 or 3. At some locales Facies 2 may be the only facies present in core and therefore no contacts are observed.

Zone 1 Facies 3 (Z1F3) – Massive fine to medium grained sand

Facies 3 is found along channel banks or within the upper few centimeters of distal fluvial-tidal channel sediment (Fig. 2-4 A; Fig. 2-5; Table 2-1). The thickness of Facies 3 varies, it can be absent or occur as interlaminae or interbeds through to sequences that are at least 60 cm thick. Mainly massive appearing, brown colored, fine to dominantly medium grained sand characterizes this facies. Faint planar laminae or bedding may be present at

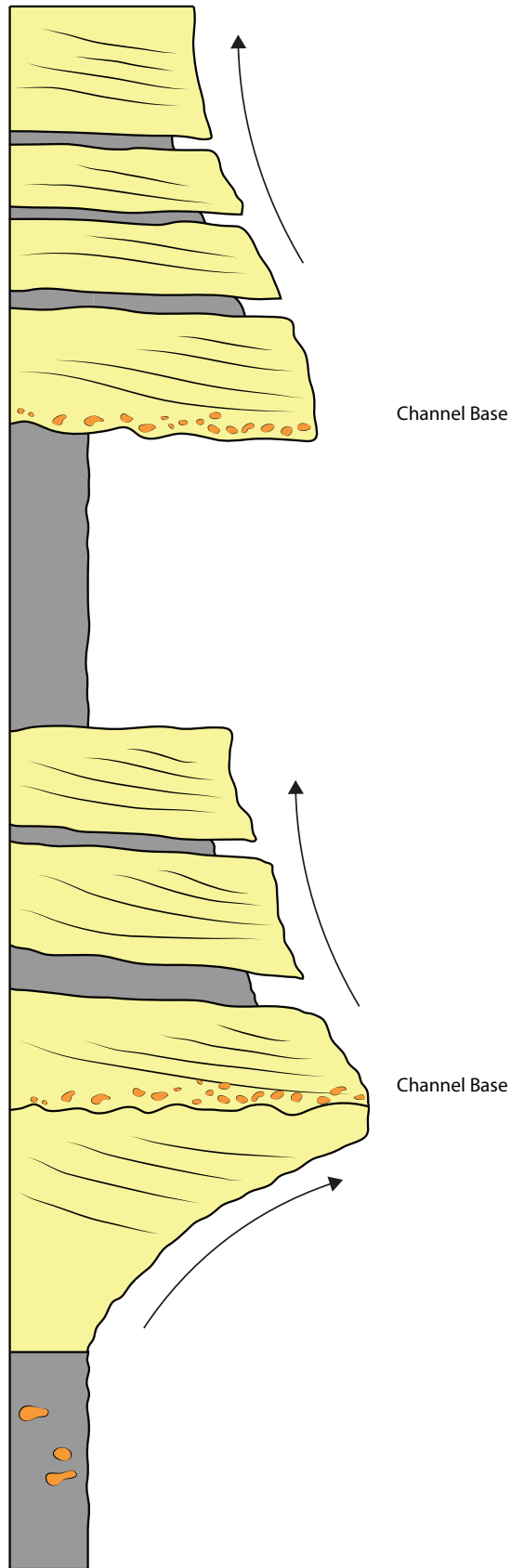
some locales. The sediment of Facies 3 may display a loamy texture and have sporadic wood clasts. As with the previous 2 facies, bioturbation is also absent from Facies 3. Facies 3, when present, experiences a sharp contact with underlying Facies 2 or is interlaminated or interbedded with Facies 2. At some locales Facies 3 may be the only facies present in core and therefore no contacts are observed.

Zone 1: Fluvial – Tidal Transition Interpretations

The three facies described for the Fluvial Tidal Transition (Zone 1) are interpreted as: Facies 1 (Z1F1: Distal sand-dominated channel base); Facies 2 (Z1F2: Proximal mud-dominated channel); and Facies 3 (Z1F3: Distal sand-dominated middle channel to channel edge). These interpreted facies comprise the Fluvial-Tidal Transition Facies Association (FA1) (Table 2-1). An interpreted idealized vertical succession from the fluvial-tidal transition zone would ideally consist of a full sequence of Facies 2 (Z1F2) to Facies 1 (Z1F1) through to Facies 3 (Z1F3) and finally back to Facies 2 (Z1F2) (Fig. 2-6).

Proximal fluvial-tidal deposits are characterized by massive mud-dominated channels, with most mud deposition occurring during the dry season, when fluvial discharge is at a low, and the turbidity maximum advances furthest upstream. Distal fluvial-tidal deposits are characterized by fining-upward, interbedded sand and mud channel deposits. Neither proximal nor distal deposits show any bioturbation. It is likely that the harsh brackish-water conditions (maximum recorded salinity 1-1.5 ppt), in association with variable and harsh physical conditions, likely results in a stressed environment where conditions are not favourable for long term colonization for most organisms (Dalrymple and Choi, 2007; Gingras et al., 1999). Pebble and gravel content is observed within channel bases, as well as within the mud channels. The source of the pebble and gravel content is likely the fluvial channels occupying the valleys upstream of the fluvial-tidal transition zone.

Figure 2-6. Schematic vertical succession from the fluvial-tidal transition zone. Vertical profile of fluvial-tidal channel deposits, as interpreted from core and surface observations from Tillamook Bay. Proximal fluvial-tidal deposits are characterized by massive mud-dominated channels, with most mud deposition occurring during the dry season, when fluvial discharge is at a low, and the turbidity maximum advances furthest upstream. Distal fluvial-tidal deposits are characterized by fining-upward, interbedded sand and mud channel deposits. Neither proximal nor distal deposits show any bioturbation. Pebble and gravel content is observed within channel bases, as well as within the mud channels. The source of the pebble and gravel content is likely the fluvial channels occupying the valleys upstream of the fluvial-tidal transition zone.



The mud-dominated fluvial-tidal transition zone of the inner estuary experiences tidal fluctuations of a lower magnitude than the rest of the inner estuary. Mud-dominated deposits are exposed at low tide along the banks. High vegetation density increases the cohesiveness of the mud deposits, and therefore the stability of the banks, which in turn inhibit short-term point bar lateral migration. Due to the interaction between fluvial freshwater and marine saline water, the fluvial-tidal transition zone is a mixing zone. In the low-discharge summer months, this zone of mixing occurs farther upstream than in the winter months, when much higher freshwater discharge takes place and the zone of mixing shifts downstream into the estuary. As a result the salinity node, or turbidity maximum, (the point where salinities begin to mix and suspended sediment concentration is highest) changes location between the fluvial-tidal transition zone and the inner estuary bay head delta region (Dalrymple and Choi, 2007; Doxaran et al., 2009; Chaumillon et al. 2013).

If the salinity node is located upstream, in the fluvial-tidal transition zone, during the dry season then flocculation and deposition of clay will occur in this region (Middleton, 1980; Chaumillon et al. 2013). This explains the mud-dominated character of the fluvial-tidal channels. Gravel found sparsely within the channel deposits may be due to bedload transport of sediment during the wet, winter months, when fluvial energy is increased. Alternatively, increased flow velocity during winter flood events may lead to erosion of mud layers that overly basal channel deposits leaving only exposed coarser grained deposits that are later buried, rather rapidly, by either massive channel sand or mud depending on corresponding energy levels and location of the turbidity maximum (Chaumillon et al., 2013).

The mud-dominated channels observed in proximal cores may correspond to the mud-rich, proximal facies, clay-flocculation zone (Musial et al., 2012). Mud-clast breccias are interpreted to have been deposited in tidally-influenced point bars, and are commonly found overlain by variably

heterolithic sand, such as those observed in the modern Garonne River of the Gironde Estuary (Musial et al., 2012).

The mud-dominated point bars and bayhead point bars at Tillamook Bay are not analyzed in enough detail to assess channel bottom sedimentary characteristics in the transition zone between the clay-rich (proximal) and sand-rich (distal) area of the inner estuary. More detailed studies should be conducted to determine the effect, if any, of tidal currents on the possible incorporation of muddy sediments in channel-fill deposits, as observed in the case of the Garonne River (Musial et al., 2012). However, given the significantly smaller scale of fluvial-tidal channels (compared to those of the Garonne River), as well as a smaller tidal range, energies required for the formation of such deposits may be enhanced by relative high fluvial discharge and high fluvial energies, as opposed to strong, high-energy tidal currents.

Zone 2: Bayhead Delta and Shore-Attached Tidal Flats

Descriptions and Results

Sedimentological and Neoichnological Features of Zone Sub-environments

The proximal part of bayhead delta region of the inner estuary is not a main focus of the study. However, because of the interesting character of the facies observed, and because of their high lateral variability over relatively short distances, it is important to record observations of the sedimentological and neoichnological changes. This proves useful in the overall interpretation of the inner estuary depositional model, as discussed in a later section.

The Kilchis River is straight to moderately sinuous, but because of the stable salt marsh deposits and vegetated bay margin, it is confined to its channel and experiences negligible migration near its mouth. It is not until the river reaches Kilchis point (Fig. 1-2, Part II), that it ceases to be confined and discharges into the bay. Downstream of Kilchis Point, the bayhead delta

contains point bar deposits, as well as shore-attached intertidal sand-flats (Fig. 2-7 A,B). Sediment samples, for grain size and total organic carbon (TOC) analysis, were collected from sub-environments 2 and 3, namely the bayhead delta free-meandering channel point bars and adjacent flats, and the marginal sand and muddy sand flats, respectively (Fig. 2-7 A). The main grain size present in Zone 2 is medium grained sand, along with coarse and very coarse sand near Kilchis Point (Fig. 2-8). A high variation of sedimentary structures, ranging from parting lineations, to sand sheets and linguoidal rippled flats, are observed in Zone 2, and are described in more detail in the next sections.

Salt marsh-adjacent bayhead delta flats

Sedimentology –

Strong fluvial and tidal currents occur at the mouth of the main Kilchis River channel, where larger proportions of sandy sediments accumulate. The salt marsh to the south and east of Kilchis Point, on the other hand, baffles water currents and reduces total energies, thus creating sheltered areas where mud and muddy sand sediments accumulate (Fig. 2-9 A,B,C; Figure 2-10 A). A gradual transition from salt marsh- adjacent mud sediments to muddy sand sediments is observed in the most proximal part of the bayhead delta. Further downstream, on a scale of 150-200 meters, the sediments grade into moderately sorted, medium to coarse grained rippled sand flats. Straight-crested and linguoidal combined-flow ripples are commonly observed. Pebble-to gravel-sized deposits are sporadically distributed within these sand flats.

Sand sheets (Fig. 2-11 A,B,C,D) are locally observed on the coarse-grained flats. The sheets range in length from 20 metres to approximately 70 metres, and have constant widths (within each sheet) ranging from approximately 7 metres to 12 metres. Sheet orientation is perpendicular to the dominant wind direction and parallel to sub-parallel to the linguoidal combined-flow ripple crests (Fig. 2-11 A,B,C,D).



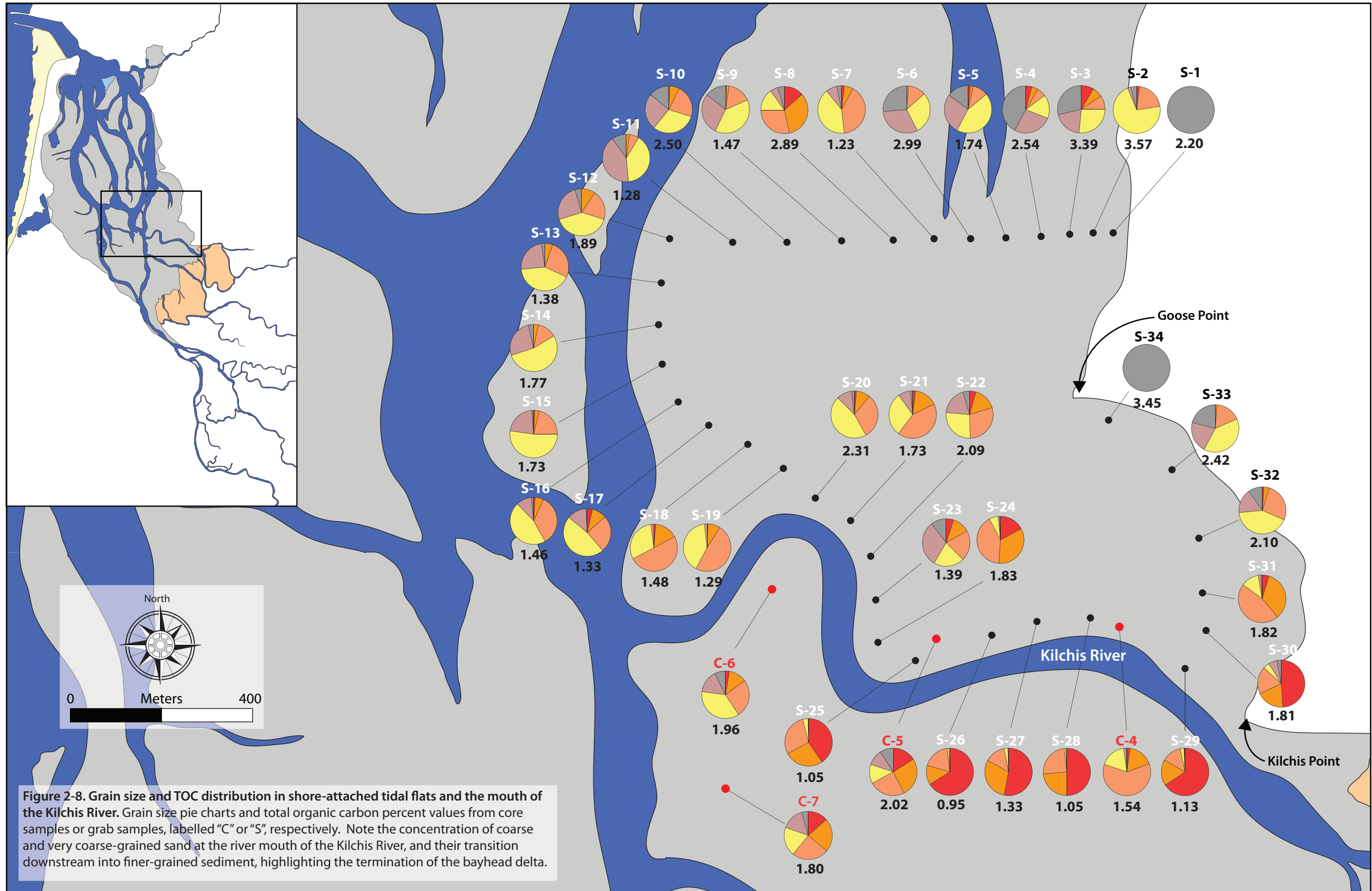


Figure 2-8. Grain size and TOC distribution in shore-attached tidal flats and the mouth of the Kilchis River. Grain size pie charts and total organic carbon percent values from core samples or grab samples, labelled "C" or "S", respectively. Note the concentration of coarse and very coarse-grained sand at the river mouth of the Kilchis River, and their transition downstream into finer-grained sediment, highlighting the termination of the bayhead delta.

Figure 2-9. Overview of Zone 2 salt marsh-adjacent bayhead delta flats sub-environment. (A) area sheltered from high-energy river currents behind salt marsh deposits; view to the south-east. (B) confluence between a sandy fluvial creek (left), and the Kilchis River (right); view to the west. (C) view of the left bank of the slough (flowing into the Kilchis River) and transitioning from salt marsh deposits to bayhead delta flats.

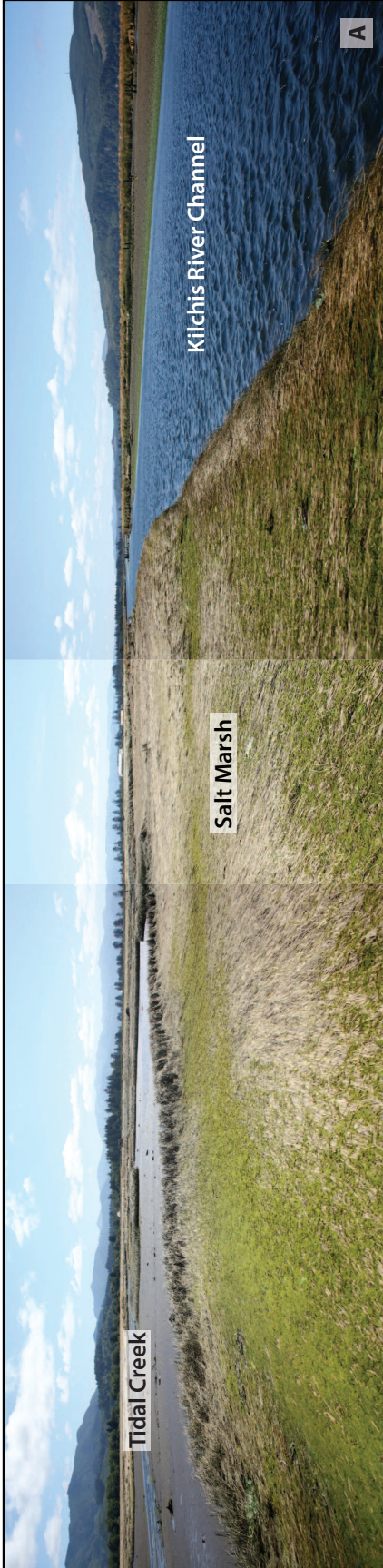


Figure 2-10. Surface texture and traces of the salt marsh-adjacent bayhead delta flats sub-environment, Zone 2. (A) Mud-dominated sheltered deposits **(B, C, D)** Cross-sectional views of the top 10-20 centimetres, showing mud-lined, vertical to sub-vertical to Y-shaped burrows of dominantly *Nereis* sp. worms, with occasional *Macoma balthica* and *Nephtys* sp. traces.

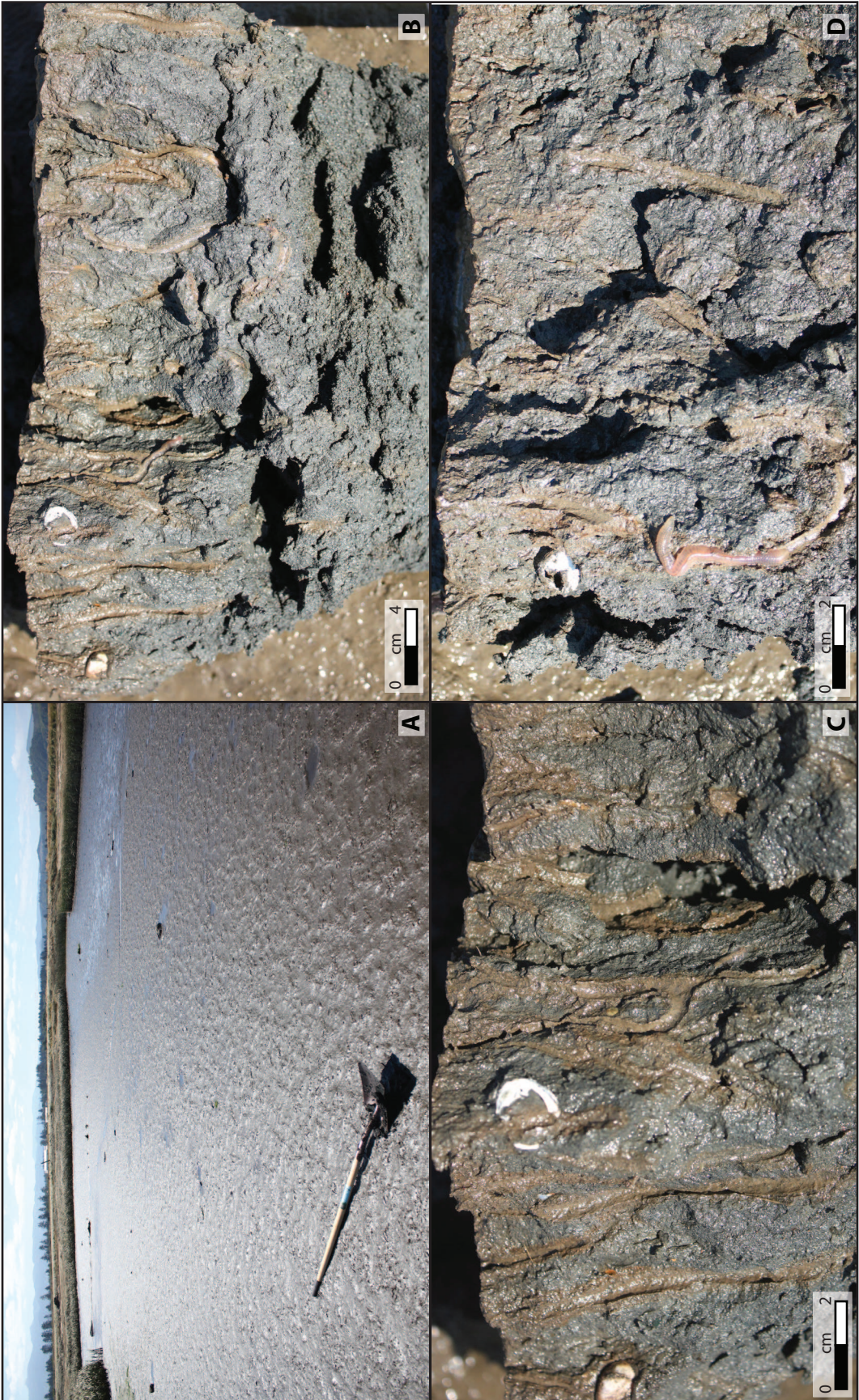


Figure 2-11. Overview and surface texture of the salt marsh-adjacent bayhead delta flats sub-environment, Zone 2. (A) Map view of the sand sheets observed in sub-environment. **(B)** General view of one sand sheet, showing its extension south toward the Kilchis River (seen in the background). **(C)** Close up view of the transition between rippled sediment - containing wind-blown sand in the ripple troughs - and the edge of the sand sheet; wind direction is from left to right. **(D)** View, from the sheet, looking up-wind towards the extensive rippled sediments containing wind-blown sand in troughs.



Adjacent to the main channel, as higher tidal and fluvial current velocities are reached, 6 to 7 meter long gravel ridges are observed (Fig. 2-12 A,B,C). The gravel ridges are approximately 5 centimeters above the surrounding gravel flat, at their highest point on the crests, which run parallel to the channel margin. Moving in a bayward direction, the pebble to gravel flat and gravel ridges rapidly transition into an area containing better sorted, rippled medium- to coarse-grained sand at the channel edges (Fig. 2-13 A,B,C,D). Tidal creek sediments are observed on the surface of the sand flat, and often contain horseshoe scours associated with large wood fragments (Fig. 2-14). Small wavelength and small amplitude, unidirectional current ripples, along with rill marks, are also observed within tidal creek sediment deposits. In the area of medium- to coarse-grained sand, layer thicknesses range from about 2 to 4 cm in the uppermost layer, which is muddy coarse sand. An alternation of muddy sand (top layers), cleaner sand (middle layers) and muddy sand (bottom layers) is observed to be consistent in the beds adjacent to the channel edge (Fig. 2-15 A,A'). Alternations of coarse sand layers and pebble-rich coarse sand layers are also observed. These layers dip in one general direction, at angles ranging from 3° near the surface, to 13° in underlying layers. Their direction of dip is perpendicular to the river flow, and parallel to the point-bar axis. The sharp boundaries between each layer appear to be rippled or erosional, due to their undulatory nature.

Neoichnology –

Mud deposits contain an abundance of 0.3 - 0.5 cm in diameter vertical, sub-vertical, Y-shaped, and U-shaped burrows. In muddy areas, bioturbation is abundant. All burrows are observed to extend to approximately 12 - 15 cm depth. The vertical, sub-vertical, and U-shaped burrows are observed to be made by the *Nereis* sp. worm (Fig. 2-10 B,C,D), whereas Y-shaped burrows are commonly produced by *Macoma balthica*.

Figure 2-12. Overview and surface texture of the salt marsh-adjacent bayhead delta flats sub-environment, Zone 2 (continued). (A) Location of very coarse sand and gravel flats within the sub-environment. (B) Ridge feature next to a tidal channel along the sub-environment. (C) Close up view of ridge feature shown in (B). Shovel for scale is 120 cm long.



Figure 2-13. Overview and surface texture of the salt marsh-adjacent bayhead delta flats sub-environment, Zone 2 (continued 2). (A) Ebb-oriented straight to sinuous crested ripples along the margin of a tidal channel. Shovel for scale is 120 cm long. (B) Close up view of ebb-oriented ripples shown in (A). Note coarser debris in troughs. (C) Alternate view looking along strike of the ebb-oriented ripples. Coarser debris is more noticeable in ripple troughs. Ruler for scale is extended to 42 cm. (D) Transition between rippled sand near the channel, and gravel flat located farther away from the channel, and observed in the background. Ruler for scale is 42 cm long oriented along strike of ripples.





Figure 2-14. Tidal creek within the salt marsh-adjacent bayhead delta flat sub-environment , Zone 2. Incision of a small tidal creek within muddy sand of the salt marsh-adjacent bayhead delta flat sub-environment. Note development of small point bar (right side of creek in photograph) and small cut bank (left side of creek in photograph). Tidal creek branches in the foreground of the photograph due to woody debris and algal binding of sediment. Note the open burrows in the muddy sediments at the right of the photo, as well as in the upper left part of the photo.

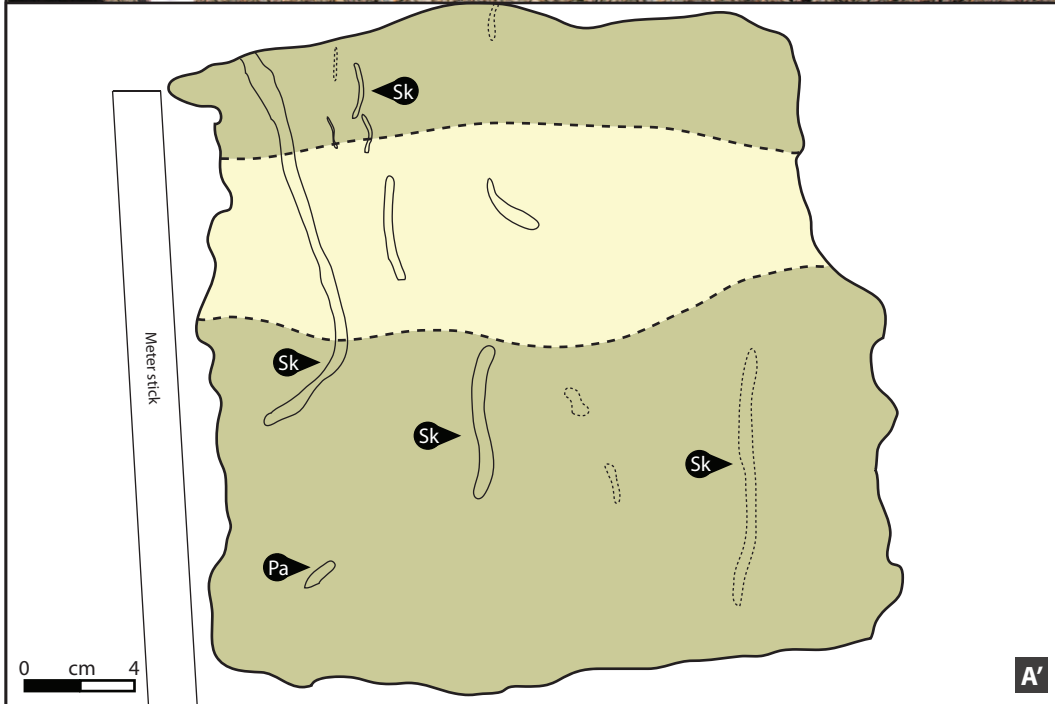


Figure 2-15. Sub-surface sedimentary features and traces of the salt marsh-adjacent bayhead delta flat sub-environment, Zone 2. (A and A') Cross-sectional view of muddy sand (darker beige-green colored layer in A') and sand layers (lighter beige colored layer in A'), with *Skolithos*-like (Sk) to *Palaeophycus*-like (Pa) burrows. Note that the burrows are commonly unlined to slightly lined in the coarser sandy layers grading into more heavily lined burrows with an oxidized (orange colored) lining or halo in the muddy sand layers.

Bioturbation intensity decreases in the area of gradual transition from muddy to muddy sand deposits. Burrow diameters in the muddy sand deposits are essentially identical to trace diameters in the mud deposits, with diameters between 0.2 – 0.6 cm. In the muddy sand deposits, bioturbation is sporadic to common. In areas adjacent to tidal creek sediments, within algae-stabilized muddy medium-grained sand deposits, a high concentration of small, approximately 0.5 cm in diameter, open-to-surface vertical burrows, is observed (Fig. 2-14).

Bioturbation along the channel edge is absent to sparse, occurring dominantly in the muddy sand layers when it is observed. Traces are mud-lined (Fig. 2-15), when they occur both in the muddy sand and in the cleaner sand layers. They appear short – 1 to 4 cm in length – and have diameters of about 3 to 7 mm. In the case of longer, 6 to 14 cm long, vertical traces, they cut across the layer boundaries into the cleaner sand, and may penetrate to the underlying muddy sand layers. The only tracemaker observed within channel edge is the *Nereis* worm. Bioturbation along the confluence of the Kilchis River and adjacent tidal creek was not seen and is likely either absent or very sporadically distributed.

Bayhead delta free-meandering channel point bars and adjacent sand flats

Sedimentology –

At the Kilchis Point location (Fig. 2-7), on the eastern margin of Tillamook Bay, the Kilchis River discharges into the bay and takes on a free-meandering character in an unconstrained environment. This contrasts to the salt-marsh adjacent bayhead delta sub-environment, in which it is confined due to stabilized salt marsh deposits and vegetated channel margins. As described in the previous section, any channel migration is negligible due to bank stabilization.

In the areas most proximal to the Kilchis River mouth, medium to coarse grained, light to dark brown sand dominates with an average total organic carbon (TOC) value of 1.45%. The bay mouth contains common to abundant wood clasts of varying sizes, from millimeter scale to meter-scale drift logs, especially in the sheltered sand tidal flat, located north of Kilchis Point and directly adjacent to the bay margin. Transverse to slightly sinuous, asymmetrical combined-flow ripples are extensive in this region (Fig. 2-16 A,B,C,C'). Close to the channel edge, poorly sorted, medium and coarse grained sands are highly water-saturated at low tide. Central to western portions of the sub-environment, following the margin of the river channel, are more poorly sorted than the eastern, shore-adjacent portion. Coarse- and very coarse-grained sand, along with common pebble and occasional gravel content make up the sediment character along the bank of the tidal flat / channel margin (Fig. 2-17 A,B,C,C'). Interbedded muddy sand and pebble- and gravel-rich sand layers occur at the margin of the river channel. Pebble and gravel sized clasts are spread over the tidal flat surface, and are also concentrated in the sand-dominated layers, where mud content is negligible. Ripples are absent from this channel bank area of the sub-environment, though small drainage creeks incise into the tidal flat and flow towards the main river channel. Other sedimentary structures observed are parting lineations, occurring within the pebble- and gravel-rich coarse sand flats, and commonly transitioning rapidly into low-relief dune sediments. The low-relief dunes, observed locally, contain superimposed linguoidal ripples on their stoss sides.

In the more distal sand flats away from the main channel, medium- and fine-grained sand dominates, with low amounts of clay content. Transverse, asymmetrical, ebb-oriented combined-flow ripples continue to be the dominant sedimentary structure observed. Horseshoe scours formed around large wood fragments are commonly observed. Coarse and very coarse-grained sand is observed to accumulate locally in the troughs of asymmetrical ripples. Total organic carbon (TOC) content, measured closer to the channel, is

Figure 2-16. Sedimentary features and traces of the bayhead delta free-meandering channel point bars and adjacent sand flats sub-environment, Zone 2. (A) Straight to sinuous, dominantly wave generated ripples are observed on the tidal flat surface. **(B)** Close up of ripples observed in **A**. Note slightly coarser grains in ripple troughs. **(C and C')** Photo **(C)** and drawing **(C')** of interbedded sand (beige color in **C'**) and pebble (orange color in **C'**) sub-surface layers. Pebble sized clasts also occur sporadically within sand layers. Note inclined nature of middle sand and pebble layers. A distinct *Arenicolites*-like trace is observed, with sporadic and indistinct, possibly *Skolithos*-like, traces also observed.

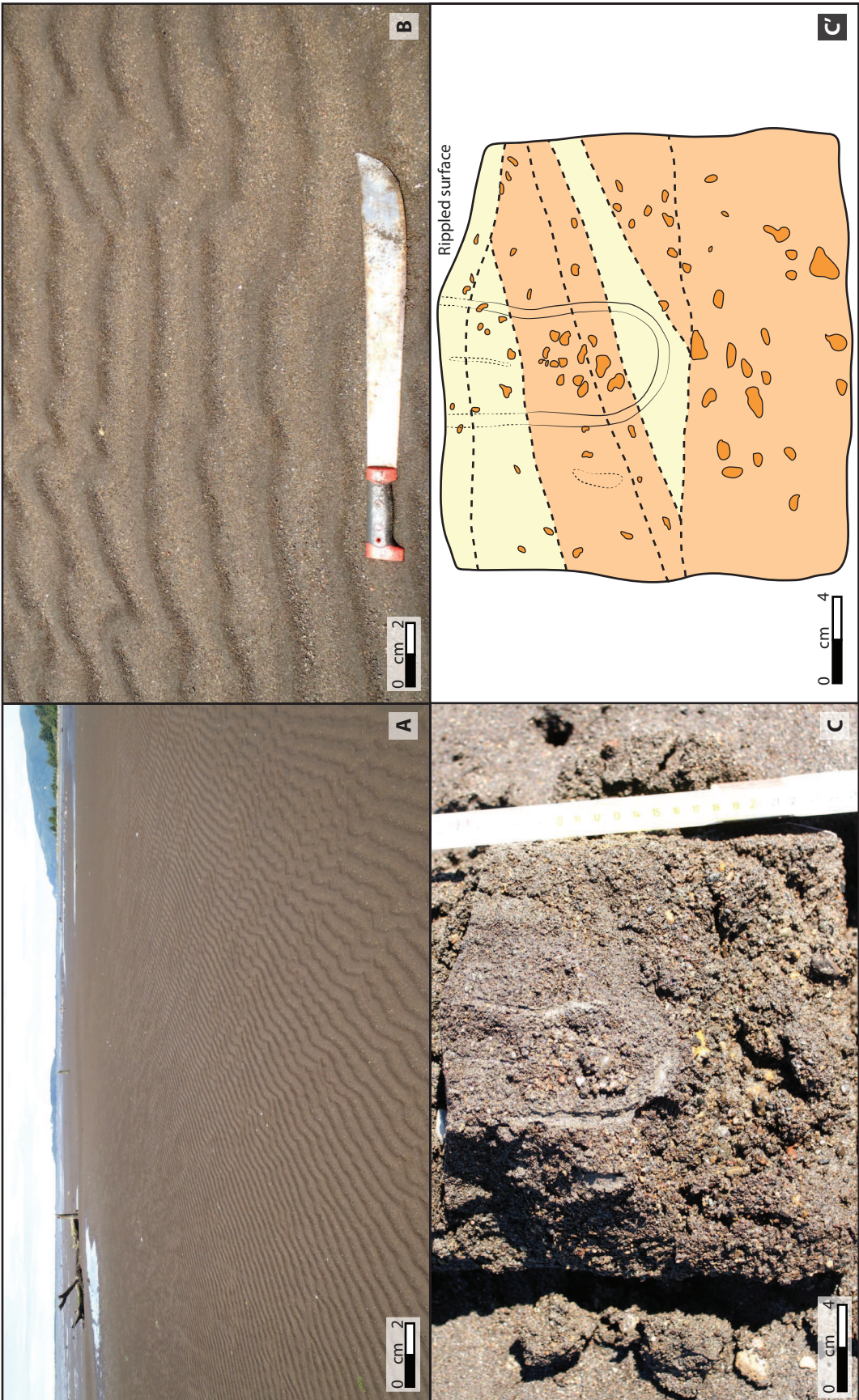
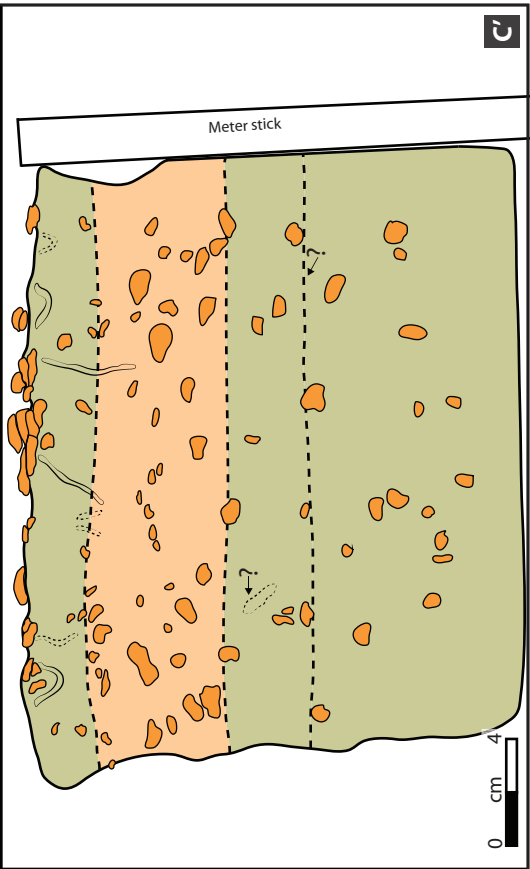


Figure 2-17. Sedimentary features and traces of the bayhead delta free-meandering channel point bars and adjacent sand flats sub-environment, Zone 2 (continued). (A) Dominantly planar surface of tidal flat composed of muddy sand to muddy pebbles. Ruler for scale next to shovel is 22 cm long. **(B)** Planar view of surface displaying muddy pebbles. Ruler for scale is 24 cm long. **(C and C')** Cross-sectional view of muddy sand (darker beige-green colored layer in C') and pebble (orange colored layer in C') sub-surface layers. Pebble sized clasts also occur sporadically within muddy sand layer. Small burrows that are *Skolithos*-like and *Arenicolites*-like in appearance occur within the upper muddy sand layer.



on average 1.5%. Drag casts are also commonly observed, and are either created by driftwood or algae of various sizes. In at least one case, drag casts created by algae are observed to form across ripples at an oblique angle.

Neoichnology –

Bioturbation is sparse and occurs in the form of vertical *Skolithos*-like burrows (possibly made by *Nereis* sp. worms, though the actual tracemaker was not observed), and *Thalassinoides*-like burrows of the sand shrimp *Neotrypaea californiensis*. Additionally, a lower concentration of *Mya arenaria* (and resulting *Siphonichnus*- and *Skolithos*-like traces) was observed, contributing to an overall low biodiversity. The high water table during low tide reduces the depth to which trenches can be dug before the sediment caves in. As a result, the maximum depth of the *Skolithos*-like and *Thalassinoides*-like burrows was not observed, with only the top 15-20 centimeters “preserved” during trenching. However, in light of the high water saturation of the sediment, the vast majority of burrows maintained their structure and did not collapse upon inspection; burrows were observed to be unlined. At the rippled sediment surface, relatively small (compared to other burrows slightly downstream in this same sub-environment) relief sand volcanoes are observed around the burrows, with fecal pellets commonly located around the burrow openings and in the adjacent ripple troughs (Fig. 2-18 A,B,C).

At the channel edge, mud-lined, open-to-surface, U-shaped *Arenicolites*-like traces are observed, with diameters of 0.5-0.7 centimeters, and an overall length of 20-25 centimeters (Fig. 2-16 C,C'). These burrows are comparatively sparse and in lower numbers than the vertical burrows observed at the same location.

Approximately 100 meters downstream from Kilchis Point, common to abundant *Thalassinoides*-like burrows of the sand shrimp *Neotrypaea californiensis* cover large portions of the sand tidal flat and channel margin. Sediment character is still persistently medium to coarse grained.

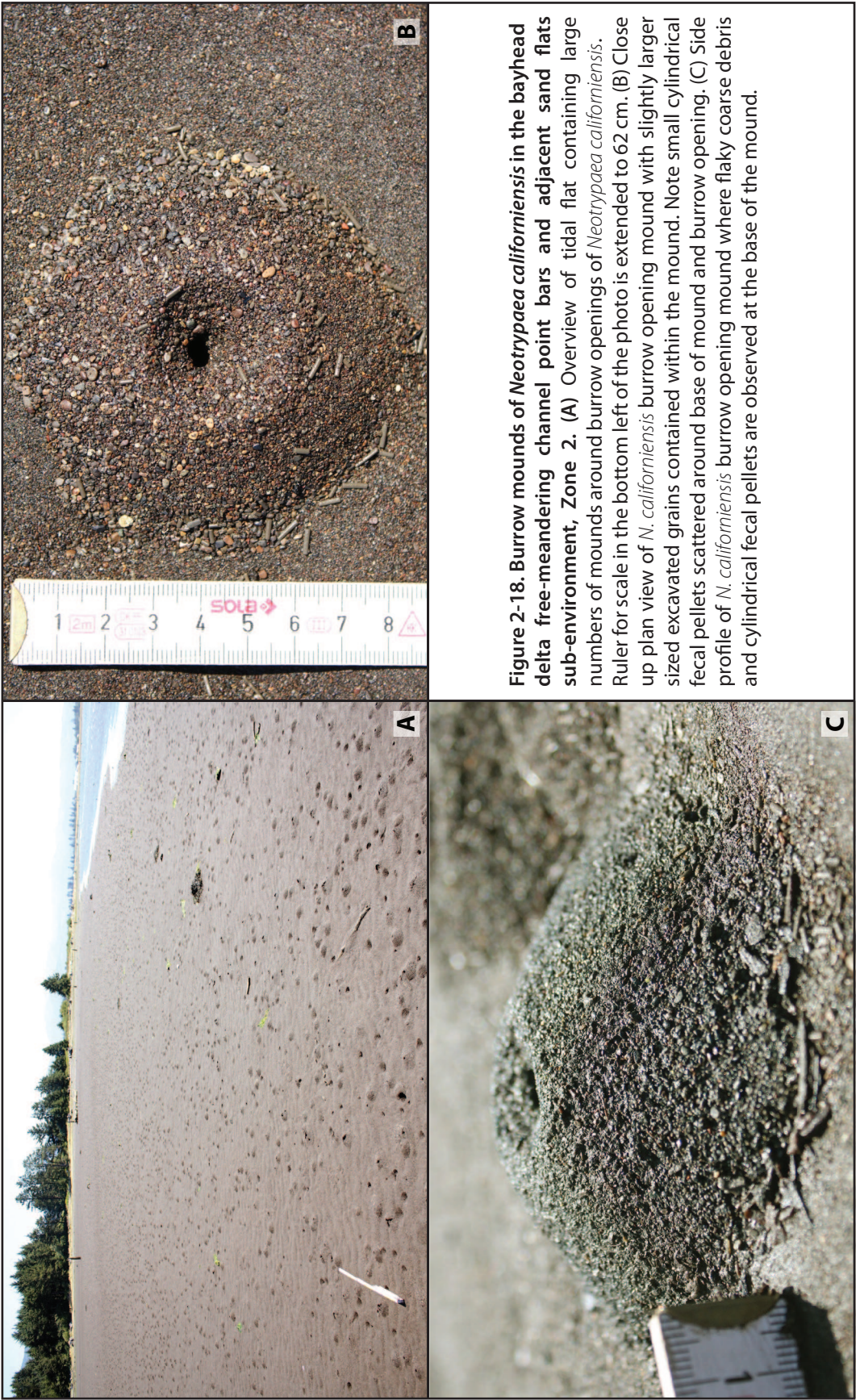


Figure 2-18. Burrow mounds of *Neotrypaea californiensis* in the bayhead delta free-meandering channel point bars and adjacent sand flats sub-environment, Zone 2. (A) Overview of tidal flat containing large numbers of mounds around burrow openings of *Neotrypaea californiensis*. Ruler for scale in the bottom left of the photo is extended to 62 cm. (B) Close up plan view of *N. californiensis* burrow opening mound with slightly larger sized excavated grains contained within the mound. Note small cylindrical fecal pellets scattered around base of mound and burrow opening. (C) Side profile of *N. californiensis* burrow opening mound where flaky coarse debris and cylindrical fecal pellets are observed at the base of the mound.

Asymmetrical, transverse combined-flow ripples are widely distributed over the area, but become masked by the comparatively larger-relief and highly-concentrated surface sand volcanoes associated with the burrows of the sand shrimp. Fecal pellets – 4-5 mm in length and 1 mm in diameter – are abundant and occur in high quantities within ripple troughs, and around the circular base of sand volcanoes.

Traces in the areas of poorly sorted medium and coarse grained sand along channel bank margins become diminutive and occur primarily in the form of small, U-shaped burrows and small, vertical burrows. Average burrow diameter (in both U-shaped and vertical burrows) is 3-5 mm, with small burrow lengths of 1-4 centimeters (Fig. 2-17 C,C'). Burrows are observed to occur in the muddy sand layers that also have lower pebble and gravel content.

Bioturbation is overall sparse to common in the extensive, medium and fine-grained, rippled sand flat zone away from the channel margin, with burrows of the soft-shell clam *Mya arenaria* being the most common. *Piscichnus*-like traces are also observed, and are likely created by fish feeding on the sediment surface.

Bioturbation was not observed in the outermost, distal bayhead delta zone containing low-relief dunes and parting lineation features. Contrasting to the sinuous combined-flow ripples occurring locally in front of dunes, the dune top surfaces contain superimposed linguoidal combined-flow ripples, along with sparse, *Siphonichnus*-like burrows and *Skolithos*-like burrows of the soft shell clam *Mya arenaria*. Sea-gull tracks, of the birds feeding on soft-shell clams, are also sparsely observed.

Marginal sand and muddy sand flats

Sedimentology –

This sub-environment has the highest concentration of clay (essentially almost fully clay in some parts), compared to the other sub-environments of Zone 2. It is located in a sheltered embayment directly adjacent to the gravelly shores of the eastern bay margin, and consists of highly bioturbated mud and muddy sand flats, separated locally from the bay margin by a shallow tidal creek. At the surface, the flats appear relatively flat, with low-relief mounds and pools widely distributed on the surface (Fig. 2-19 A). Overall this sub-environment is dominated by muddy, fine to very fine-grained sand flats.

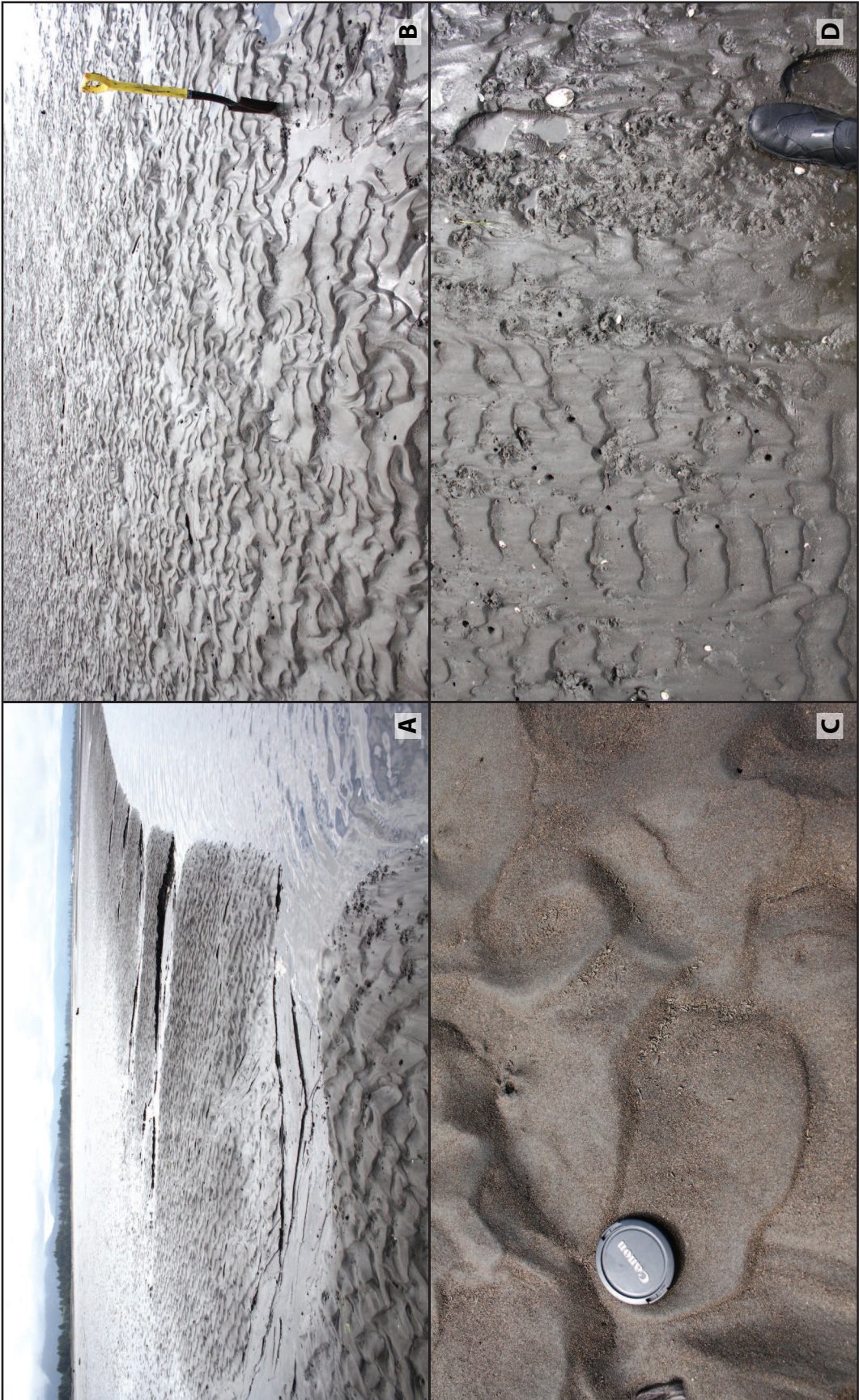
Transverse, asymmetrical combined-flow ripples and linguoidal combined-flow ripples are the most commonly observed sedimentary features of this sub-environment (Fig. 2-20 A,B,C,D). Tidal creeks commonly incise and drain these tidal flats. Elongate, transverse current ripples are observed as they actively migrate on the creek bed during the ebb tide. Shell fragments, as well as abundant fecal pellets and small, millimetre-scale wood fragments, are also observed to be transported downstream, dominantly collecting in the troughs of current ripples on the creek bed. Algae mounds are common to abundant near the tidal creeks and form mounds of muddy sediment at their base.

Transitioning towards the bay margin, silt and clay content gradually increases, as does gravel content. Gravel makes up the shore of the bay margin north of Goose point, as well as between Goose Point and Kilchis Point (Fig. 1-2; Part II). The muddy sediments of the tidal flat onlap over the gravel layer, which extends bayward from the shore at a shallow angle. Muddy sediments, high in organic and total organic carbon (TOC), can be found throughout the deposits of this sub-environment; the TOC percentage increases closer to the bay margin, to an average of 2.92%, where abundant algae grow (Fig. 2-8) .

Directly on the bay shore, a thin, 3-4 cm layer of woody, organic material is observed; directly underneath it, a compact clay layer, red-orange in



Figure 2-20. Surficial sedimentary features of the marginal sand and muddy sand flats sub-environment, Zone 2.(A) Overview of channel-margin tidal flats of sub-environment (B) Sinuous to linguoid ripples on tidal flat surface. Shovel for scale is ~1 m in length. (C) Sinuous to linguoid ripples with faint *Neotrypaea californiensis* burrow opening and scattered *N. californiensis* cylindrical fecal pellets in ripple troughs. Lens cap for scale is ~6.5 cm in diameter. (D) Sinuous to linguoid crested current generated ripples disturbed by *N. californiensis* burrow openings. Foot for scale is ~10 cm across.



color, and possibly iron-stained, is observed to extend into a relatively small area of approximately 20-25 square meters.

Neoichnology –

Burrows vary from vertical, sub-vertical, to U- and Y-shaped, and possibly J-shaped on the muddy sand flats (Fig. 2-19 B,C; Fig. 2-21 A,A',B,B'). They are observed to be made commonly by *Mya arenaria*, *Macoma balthica*, and *Nereis* sp. worms. Incipient traces from this area are *Skolithos*-like, *Arenicolites*-like, *Siphonichnus*-like, *Planolites*-like and *Palaeophycus*-like in appearance. Burrows range in diameter from less than 0.5 centimeter to approximately 1 centimeter, and vary widely in length from 0.5 centimeters to 20-25 centimetres below the surface. They are commonly mud-lined.

Burrows produced by the soft-shell clam *Mya arenaria* are most commonly observed within the very fine- to fine-grained sand flats. *Nereis* sp. burrows and *Macoma balthica* burrows are also observed, while the mud shrimp *Upogebia pugettensis* is observed in smaller numbers. Observed burrows have vertical to sub-vertical morphologies, with occasional burrows either connected to the same burrow system, or cross-cutting one another (Fig. 2-22 A,B,C,C'). *Skolithos*-like traces, as well as Y-shaped burrows of the *Macoma balthica* clam are common. Small, U-shaped, *Arenicolites*-like burrows are sparse.

Fecal pellets are common throughout the sub-environment, particularly near tidal creeks. Bioturbation intensity increases away from the channel margin, with trace diversity also increasing. The burrowing mud shrimp, *Upogebia pugettensis*, is locally observed in tidal creeks, or directly adjacent to them. The burrow morphology, however, is not reported, due to the high water saturation close to the creek boundary.

Figure 2-21. Traces observed in the sub-surface of the marginal sand and muddy sand flats sub-environment, Zone 2. (A and A') Cross sectional photo (A) and drawing (A') of muddy sand displaying *Skolithos*-like (Sk), *Arenicolites*-like (Ar), *Palaeophycus*-like (Pa) and *Thalassinoides*-like (Th) burrows. **(B and B')** Cross sectional photo (B) and drawing (B') of muddy sand displaying *Skolithos*-like (Sk), *Arenicolites*-like (Ar), *Palaeophycus*-like (Pa), *Polykladichnus*-like (Pk), *Thalassinoides*-like (Th), and *Siphonichnus*-like (Si) burrows.

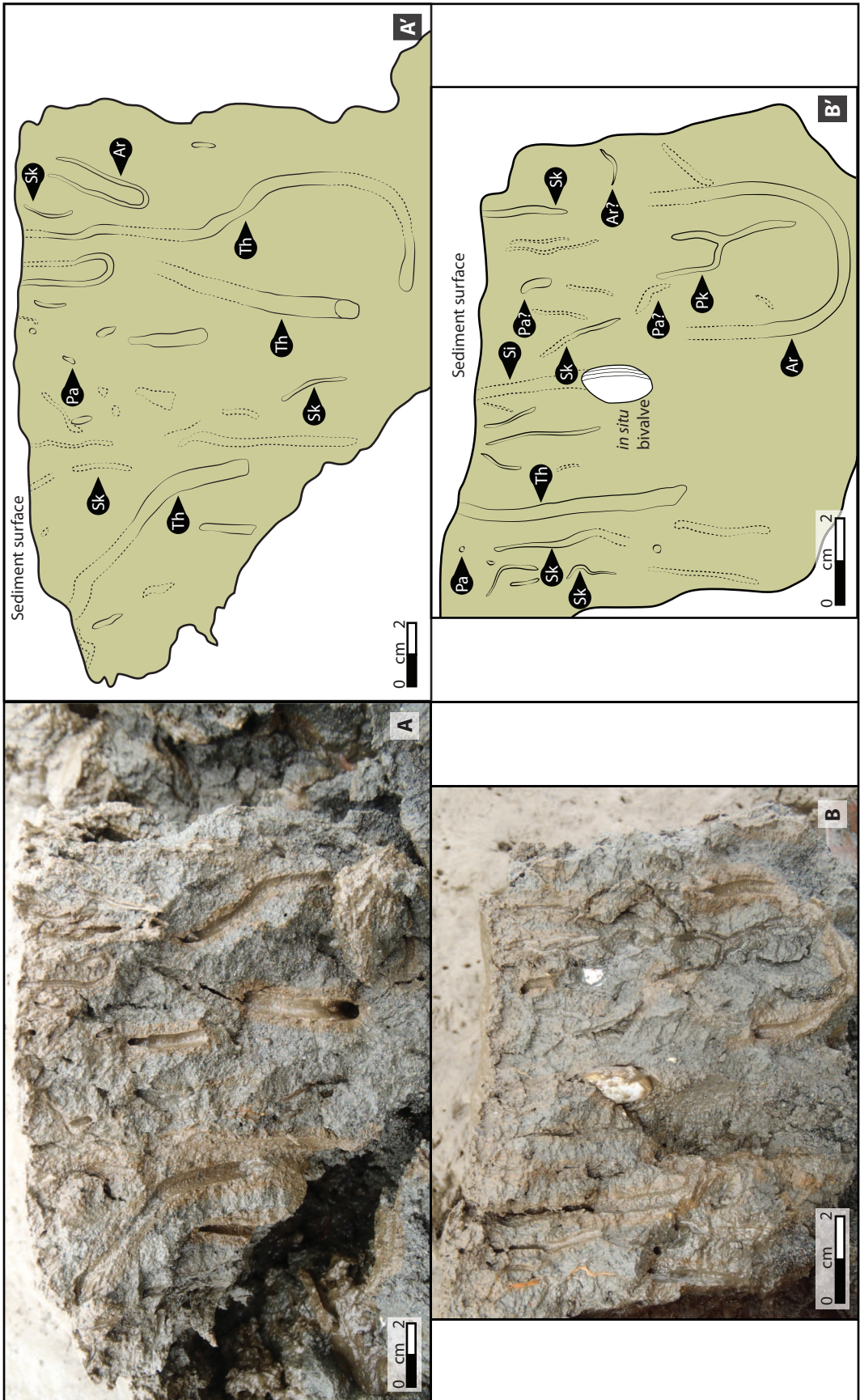
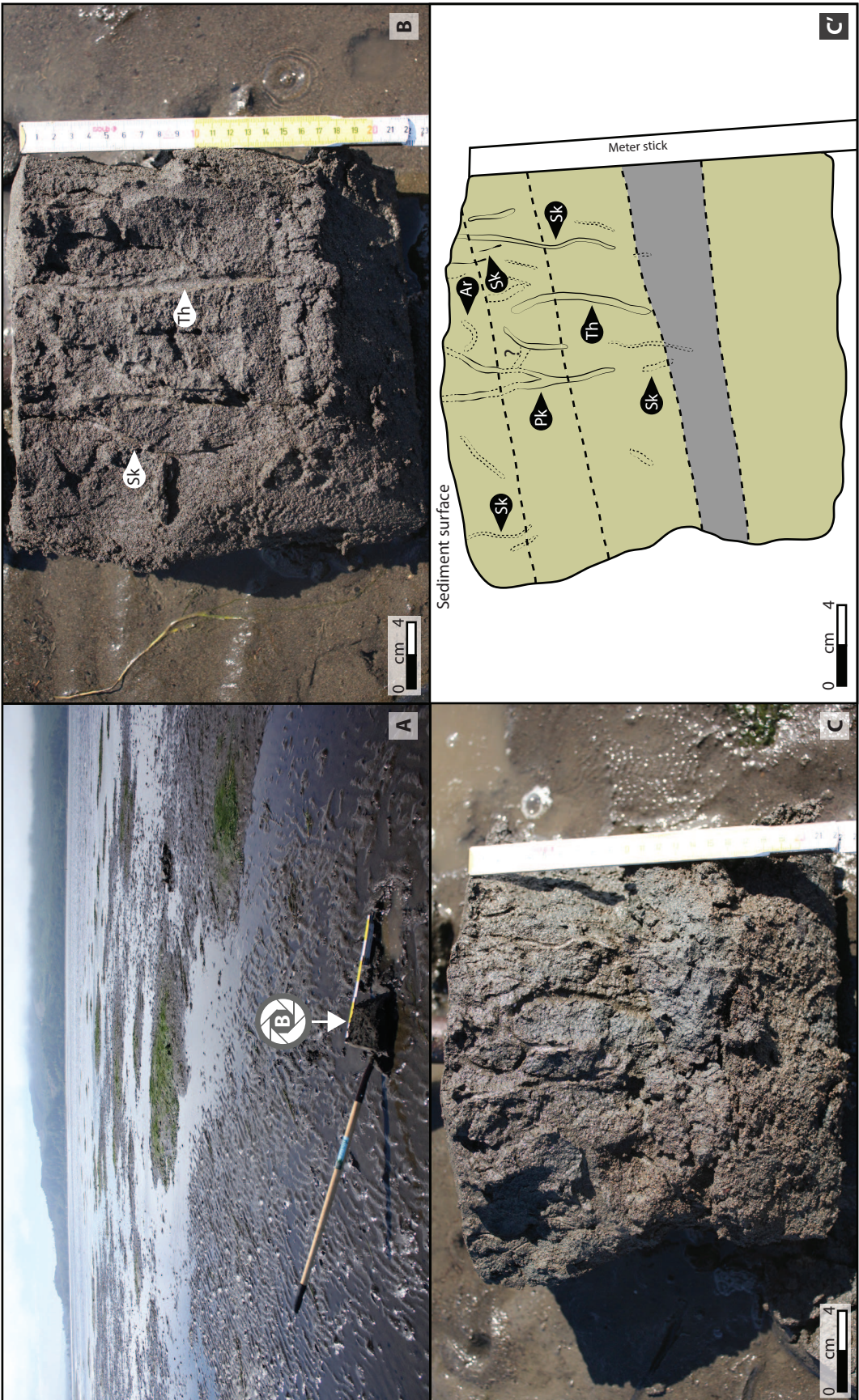


Figure 2-22. Traces observed in the sub-surface of the marginal sand and muddy sand flats sub-environment, Zone 2 (continued). (A) View of excavated area with dominantly wave generated ripples are common surface features with sporadic patches of macro-algae stabilizing slightly higher mounds. Ruler in photo is extended to 62 cm. (B) Close up view of excavated *Skolithos*-like (Sk) and *Thalassinoides*-like (Th) burrows. (C and C') Cross-sectional photo (C) and drawing (C') of muddy sand (darker beige-green colored layers in C') with a mud rich layer (grey colored layer in C'). *Skolithos*-like (Sk), *Arenicolites*-like (Ar), *Polykladichnus*-like (Pk) and *Thalassinoides*-like (Th) burrows mainly observed in the upper-most muddy sand layer.



Zone 2 Bayhead Delta and Shore-Attached Tidal Flats

Vibracore Facies Descriptions

Vibracores of the inner estuary Bayhead Delta and Shore-Attached Tidal Flats (Zone 2) were retrieved mainly in the area of the bayhead delta, downstream of the Kilchis River mouth. A total of four cores ranging from 95 cm to 120 cm long were recovered from Zone 2. Deeper cores were difficult to retrieve with the equipment available, complicated by poorly sorted sediment and medium to high concentrations of wood debris within the sediment. Cores 4 and 5 were recovered along cutbank sides, and core 6 was recovered on the aggrading point bar side of a free-meandering river channel. Core 7 was recovered from an area dominated by tidal flat morphology at the time fieldwork was completed. Four facies are identified from the Bayhead Delta and Shore-Attached Tidal Flats (Zone 2) according to distinct sedimentological and neoichnological characteristics. These facies are summarized in Table 2-2, with supplementary references to vibracore logs located in Appendix B.

Zone 2 Facies 1 (Z2F1) –Clay with Interlaminated to interbedded sand

Facies 1 is observed at free-meandering point bar and cut-bank locales, usually as the deepest facies observed in cored intervals (Fig. 2-23; Fig 2-24; Table 2-2). This facies, when present, is usually 5 cm to 20 cm thick with sand interlaminae or interbeds that are typically 0.5 cm to 2 cm thick. Facies 1 is predominantly massive grey colored clay with interspersed muddy to clean coarse grained sand. There does not appear to be any discernable sedimentary structures in this facies. Bioturbation is also rare to absent. The only trace observed within Facies 1 is a 1 cm diameter *Thalassinoides*-like burrow in clay that is infilled via coarse grained sand from an overlying interlamina. Facies 1, when present, is the lowermost facies observed in core, thus no lower contact is discernable. There is a relatively abrupt transition from Facies 1 into either Facies 2 or Facies 4 above.

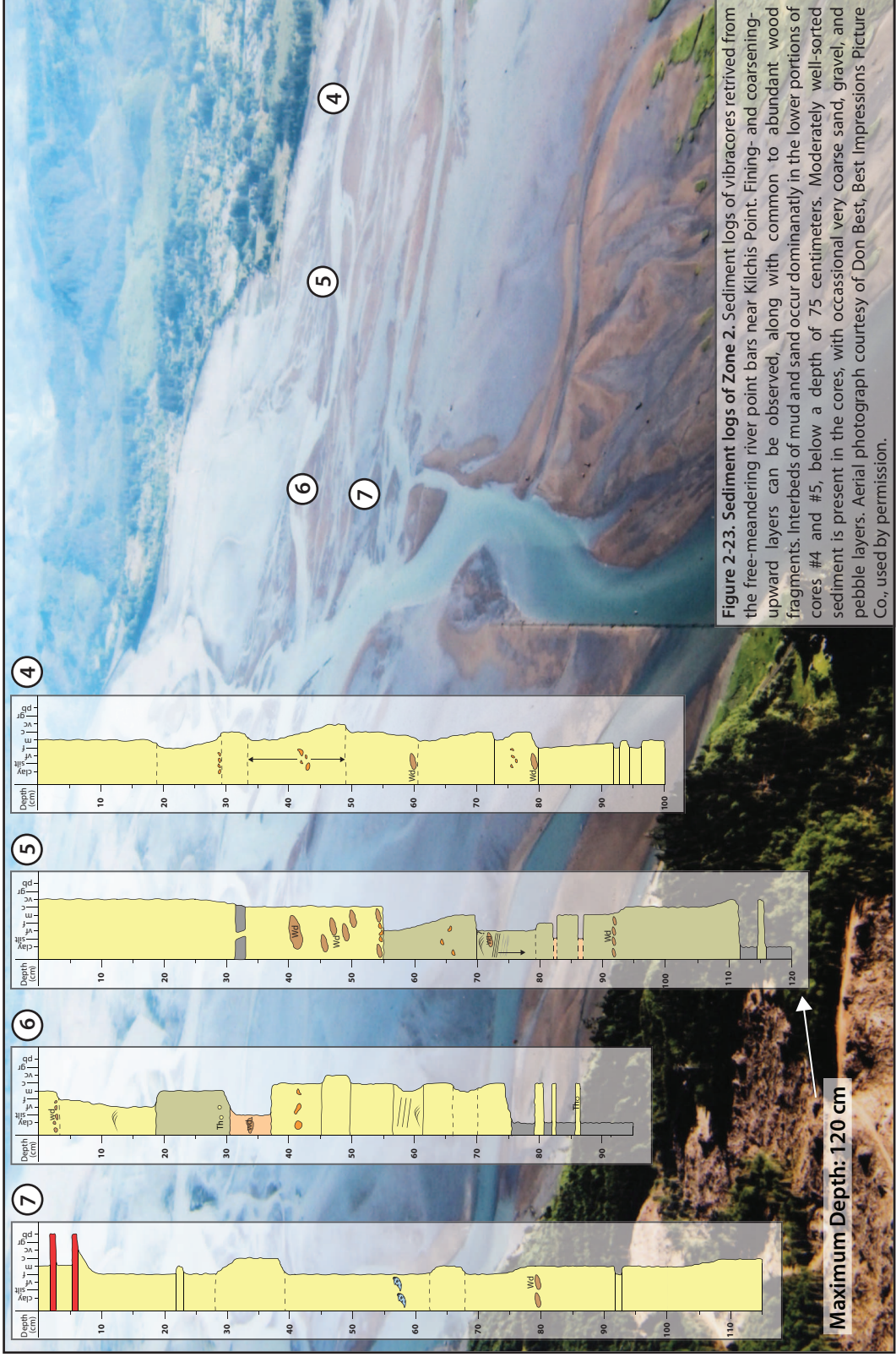
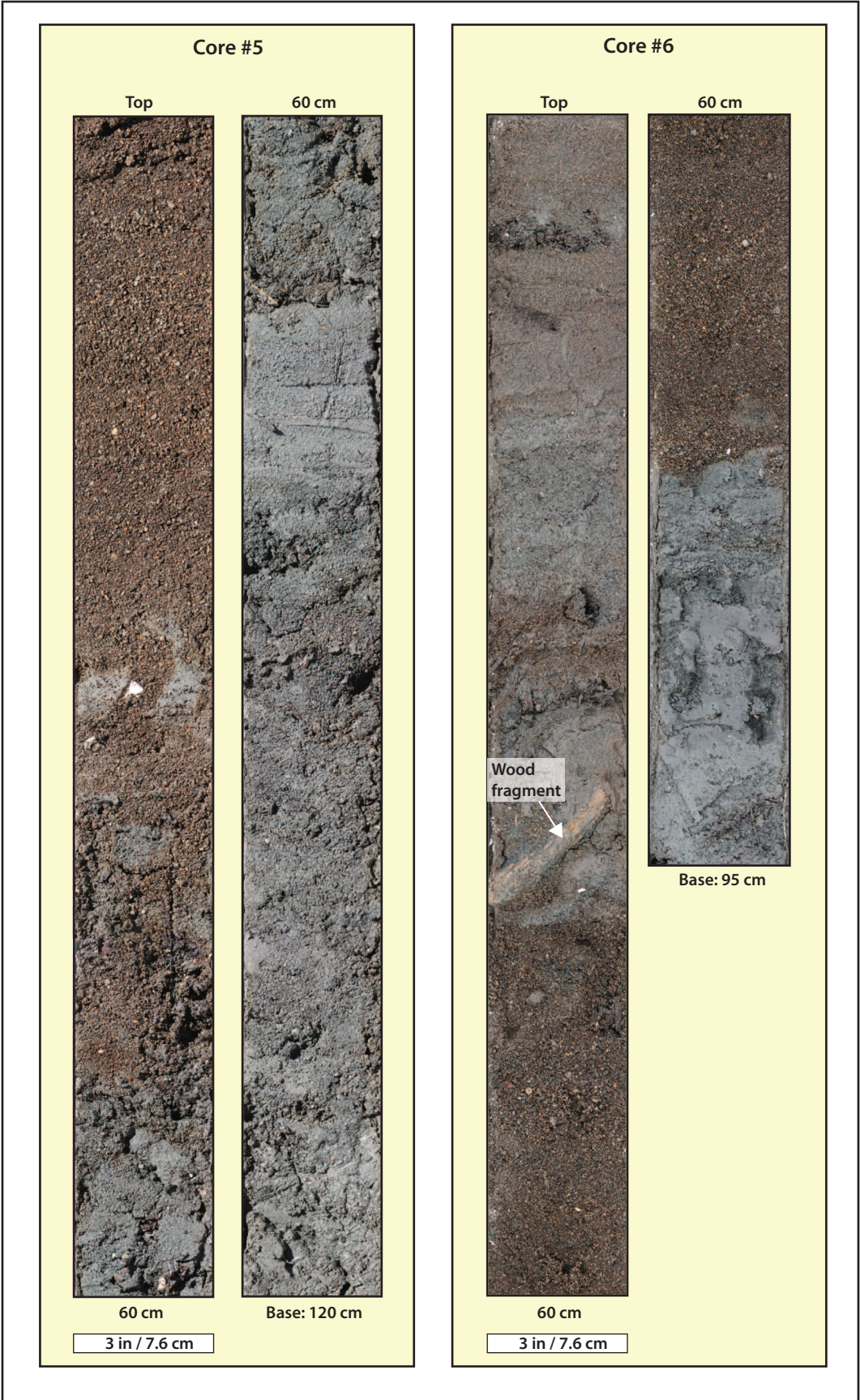


Figure 2-23. Sediment logs of vibracores retrieved from the free-meandering river point bars near Kilchis Point. Fining- and coarsening-upward layers can be observed, along with common to abundant wood fragments. Interbeds of mud and sand occur dominantly in the lower portions of cores #4 and #5, below a depth of 75 centimeters. Moderately well-sorted sediment is present in the cores, with occasional very coarse sand, gravel, and pebble layers. Aerial photograph courtesy of Don Best, Best Impressions Picture Co., used by permission.

Maximum Depth: 120 cm

Figure 2-24. Core examples from the inner estuary bayhead delta. Note the massive-appearing texture of the muddy sand, sand, and mud layers in cores #5 and #6. Wood fragments are common to abundant, as are granules. Medium sorted sediment is common in the sand intervals, with bioturbation structures largely absent.



Facies Association	Facies	Facies Contacts	Sedimentary Characteristics	Neoichnological Characteristics	Interpretation
<p>Bayhead Delta and Shore-Attached Tidal Flats Facies Association (FA2)</p>	<p>Facies 1 (Z2F1) Clay with interlaminated to interbedded sand</p>	<p>Facies 1, when present, is the lowermost facies observed in core, thus no lower contact is discernible. There is a relatively abrupt transition from Facies 1 into either Facies 2 or Facies 4 above.</p>	<p>Massive appearing, grey colored clay with interspersed muddy to clean coarse grained sand. No discernable sedimentary structures. If facies present, thickness ranges between 5 cm to 20 cm, with sand interlaminae or interbeds that are typically 0.5 cm to 2 cm thick.</p>	<p>Bioturbation is rare to absent. The only observable trace is a 1 cm diameter <i>Thalassinoides</i>-like burrow in clay that is infilled via coarse grained sand from an overlying interlamina.</p>	<p>Middle channel to channel edge mud</p>
	<p>Appendix B Core Figure Reference(s): B-3; B-4</p>	<p>Where Facies 2 is present, there is a sharp contact between Facies 2 and underlying Facies 1 or 4. There is also a sharp contact between Facies 2 and overlying Facies 3 or 4.</p>	<p>Predominantly massive, grey to brown colored, muddy very fine to very coarse grained sand with gradational intervals of silt 0.5 cm to 7 cm thick. Sedimentary structures are rare, but when observed consist of slightly inclined planar laminae with possible ripples. The low angle laminae are usually clay rich. Wood fragments are sparse to locally abundant. Sporadic granules and pebble sized grains are also present in this facies. This facies, when present, is usually between 40 cm to 55 cm thick.</p>	<p>Bioturbation is sparse to absent in Facies 2, with only observable trace as a possible <i>Thalassinoides</i>-like burrow in a transitional silt to muddy sand interval.</p>	<p>River mouth channel edge to channel-adjacent sand flats</p>
<p>Facies 2 (Z2F2) Massive to planar laminated muddy sand and silt</p>	<p>Appendix B Core Figure Reference(s): B-3; B-4</p>	<p>Table 2-2: Summary of Facies Characteristics for Bayhead Delta and Shore-Attached Tidal Flats (Zone 2)</p>			

Facies Association	Facies	Facies Contacts	Sedimentary Characteristics	Neochronological Characteristics	Interpretation
<p>Bayhead Delta and Shore-Attached Tidal Flats Facies Association (FA2)</p>	<p>Facies 3 (Z2F3) Low angle planar laminated and rippled sand</p>	<p>Facies 3 is overlain and underlain by Facies 4 with the contact between facies as being gradational to abrupt.</p>	<p>Dominantly brown colored, fine to medium grained fairly clean sand. Contains abundant sedimentary structures, such as inclined planar bedding and ripples. Usually only up to 5 cm thick.</p>	<p>Bioturbation absent.</p>	<p>Channel-adjacent sand tidal flats</p>
	<p>Appendix B Core Figure Reference(s): B-4</p>	<p>Facies 4 is prevalent through all cores sampled in Zone 2. Facies 4 can overlay and/or underlay any of the previous 3 facies mentioned for Zone 2.</p>	<p>Dominantly massive, brown colored, fine to very coarse grained, fairly clean sand. Accessory granule to pebble sized grains, wood clasts, and shell fragments present. These accessories are common as lags within Facies 4. A 2 cm – 3 cm thick clay horizon bisected by a slightly inclined, sand-infilled area, is observed that may be a mud rip-up clast or bioturbation associated structure. Most prevalent facies of the Bayhead Delta and Shore-Attached Tidal Flats (Zone 2). As little as 5 cm thick to over 110 cm thick.</p>	<p>Bioturbation is likely absent, however there is evidence for a possible bioturbation structure in the single muddy interval encountered within this facies.</p>	<p>Free-meandering channel: channel base to channel edge</p>
<p>Appendix B Core Figure Reference(s): B-2; B-3; B-4; B-5</p>	<p>Facies 4 (Z2F4) Massive fine to coarse sand</p>	<p>Facies 4 is prevalent through all cores sampled in Zone 2. Facies 4 can overlay and/or underlay any of the previous 3 facies mentioned for Zone 2.</p>	<p>Dominantly massive, brown colored, fine to very coarse grained, fairly clean sand. Accessory granule to pebble sized grains, wood clasts, and shell fragments present. These accessories are common as lags within Facies 4. A 2 cm – 3 cm thick clay horizon bisected by a slightly inclined, sand-infilled area, is observed that may be a mud rip-up clast or bioturbation associated structure. Most prevalent facies of the Bayhead Delta and Shore-Attached Tidal Flats (Zone 2). As little as 5 cm thick to over 110 cm thick.</p>	<p>Bioturbation is likely absent, however there is evidence for a possible bioturbation structure in the single muddy interval encountered within this facies.</p>	<p>Free-meandering channel: channel base to channel edge</p>

Table 2-2 (continued): Summary of Facies Characteristics for Bayhead Delta and Shore-Attached Tidal Flats (Zone 2)

Zone 2 Facies 2 (Z2F2) –Massive to planar laminated muddy sand and silt

Facies 2, like Facies 1, is also observed in free-meandering point bar and cut-bank locales, but is situated above Facies 1 either directly or indirectly (Fig. 2-23; Fig 2-24; Table 2-2). When present, this facies is usually between 40 cm to 55 cm thick. In one core it appears to fine upwards while in another core it appears to coarsen upwards. Facies 2 is predominantly massive, grey to brown colored, muddy very fine to very coarse grained sand with gradational intervals of silt 0.5 cm to 7 cm thick. Sedimentary structures are rare, but when observed consist of slightly inclined planar laminae with possible ripples. The low angle laminae are usually clay rich. Wood fragments are sparse to locally abundant. Sporadic granules and pebble sized grains are also present in this facies. Bioturbation is sparse to absent in Facies 2, with the only trace observed being a possible *Thalassinoides*-like burrow in a transitional silt to muddy sand interval. When present, there is a sharp contact between Facies 2 and underlying Facies 1 or 4. There is also a sharp contact between Facies 2 and overlying Facies 3 or 4.

Zone 2 Facies 3 (Z2F3) –Low angle planar laminated and rippled sand

Facies 3 is only observed in vibrocore from a free-meandering point bar locale. When observed, Facies 3 is usually only up to 5 cm thick. Facies 3 is dominantly composed of brown colored, fine to medium grained fairly clean sand. This facies also contains abundant sedimentary structures, such as inclined planar bedding and ripples. Bioturbation is absent from this facies. Facies 3 is overlain and underlain by Facies 4 with the contact between facies as being gradational to abrupt.

Zone 2 Facies 4 (Z2F4) –Massive fine to coarse sand

Facies 4 is the most prevalent facies of the Bayhead Delta and Shore-Attached Tidal Flats (Zone 2) occurring along cutbanks and aggrading point

bars of free-meandering river channels, as well as along areas dominated by tidal flats. Facies 4 can be as little as 5 cm thick to over 110 cm thick. Dominantly massive, brown colored, fine to very coarse grained, fairly clean sand characterizes Facies 4. Occasional granule to pebble sized grains and wood clasts are observed as sedimentary accessories. These granule to pebble sized grains and wood clasts typically occur in greatest abundance as lags at or near the base of the facies interval where they are common to abundant. There are also sparse occurrences of shell fragments. Facies 4 observed along a cored cutbank interval contained a 2 cm – 3 cm thick clay horizon that was bisected by a slightly inclined structure infilled by the surrounding sand. This structure may be the only evidence of bioturbation or may be a potential mud rip-up clast, otherwise bioturbation is absent from this facies. Facies 4 is occasionally the only facies recovered in select cores retrieved from Zone 2, especially if associated with tidal flats, but can occur in conjunction with other facies as well. Facies 4 can overlay and/or underlay any of the previous 3 facies mentioned for Zone 2.

Zone 2: Bayhead Delta and Shore-Attached Tidal Flats Interpretations

The four facies described for the Bayhead Delta and Shore-Attached Tidal Flats (Zone 2) are interpreted as: Facies 1 (Z2F1: Middle channel to channel edge mud); Facies 2 (Z2F2: River mouth channel edge to channel-adjacent sand flats); Facies 3 (Z2F3: Channel-adjacent sand tidal flats); and Facies 4 (Z2F4: Free-meandering channel: channel base to channel edge). These interpreted facies comprise the Bayhead Delta and Shore-Attached Tidal Flats Facies Association (FA2) (Table 2-2). An interpreted idealized vertical succession from the Bayhead Delta and Shore-Attached Tidal Flats Zone would ideally consist of a full sequence from Facies 2 (Z2F2) to Facies 4 (Z2F4) through to Facies 1 (Z2F1) and finally up to Facies 3 (Z2F3) (Fig. 2-25).

Numerous fining- and coarsening-upward successions are observed and interpreted to likely represent the rapidly migrating nature of fluvial-tidal and tidal channels. In the salt-marsh adjacent part of the bayhead delta, channel margin deposits, as well as gravel flats and mud flats, occur in areas that are laterally-restricted by vegetated salt marshes. Downstream of the river mouths, bayhead delta channels, sand flats and sand bars migrate laterally. Highly varying energy levels and sedimentation rates in the bayhead delta region, combined with no lateral migration restrictions (such as vegetated salt marshes), result in a complex vertical succession of fining-upward and coarsening-upward channel, sand flat and sand bar deposits.

Salt marsh-adjacent bayhead delta flats

Deposits of the bayhead delta contain a number of facies that transition laterally from one to another over relatively short distances. The range in facies, from mud-dominated through to muddy sand-dominated, and finally to coarse sand- and gravel-dominated, represents the large variation in current energies and suspended sediment concentrations input into this region of the estuary, as shown in the interpreted vertical succession (Fig. 2-25). The presence of salt marsh deposits acting as boundaries to the lateral extent of facies, in addition to their effect on baffling currents and providing an environment for sediment to settle out of suspension, has a major effect on the location and lateral variability of sediment.

The mud-dominated, sheltered salt marsh area, likely experiences low-current energies that allow the deposition of fine particles (clay and/or silt) to settle from suspension. Concomitantly, the presence of salt marsh deposits provides a source of organic nutrients and shelter from hydraulic energy, both parameters related to the colonization of organisms in an area. The intertidal nature of deposits in this sub-environment also means that the sediments are periodically sub-aerially exposed twice daily. Stabilization of this area by grass

species allows for lateral migration and formation of new salt marsh deposits in the downstream (bayward) direction.

One hundred meters downstream from the mud-dominated sheltered area, along the channel edge, the sediment is coarser, with a significant amount of pebble and gravel content, along with lower bioturbation intensity. This is likely due to strong fluvial current – during freshets – exposure along the bank causing erosion. As the fast-flowing, straight-oriented currents come in contact with the river cut-bank, their energy is dissipated along the cut-bank curvature. This can be enough to erode away most clay or silt material already deposited on its surface, along with finer-grained sand that can be easily re-suspended. Therefore, the sediment left behind is dominantly coarse grained (with medium to high gravel content). The inclination of the beds of gravel perpendicular to the river flow is a direct effect of the steepness of the cut-bank and channel edge due to the action of erosion. With an already inclined surface present, the coarse grained sand is deposited in inclined layers dipping shallowly from near the salt marsh, towards the channel edge, and in more steeply inclined layers at the most proximal channel edge and along the cut-bank.

The lack of sedimentary structures observed along the extensive gravel tidal flats of the bay-head delta region, other than the higher relief gravel ridges present near the channel edge, indicate that higher than normal current energies are likely involved in the sediment deposition process.

High energy river currents in this area can explain the apparent lack of clay and silt content. If the current energies are strong enough to transport and deposit flat-lying, planar-bedded gravel-sized sediment, finer grained portions are not deposited. Therefore, clay and silt, along with finer sand portions, continue to be suspended in the water column and continue downstream, where they enter the bay proper and are deposited in various zones of the estuary (Allen, 1982; Chaumillon et al., 2013). If any finer grained materials are deposited in this sub-environment they are likely short lived and eroded swiftly

by the strong currents; potentially causing the “deflation lag” texture of the tidal flat, with only the coarser fraction left behind after erosion (Allen, 1982).

The presence, locally, of gravel ridge structures on the channel edge, are likely a result of a high rate of deposition of gravel, in conjunction with high current energies. As observed, the gravel ridges slope gently away from the channel onto the gravel tidal flat and more steeply towards the channel side.

The area of extensive rippled medium- and coarse-grained sand, compared to the coarse or mud-dominated areas observed upstream, may be due to the fact that currents, having passed through the highly meandering, high current energy zone, are now approaching a wider, less confined zone, where energies are dissipated over a larger surface area. Due to this, finer sand portions are also able to settle on the tidal flats adjacent to the channels. Adding to this are fluvial currents, and strong ebb-tidal currents acting on the sediment in the same direction, thus resulting in the asymmetrical, ebb-oriented combined-flow ripples observed.

The exfiltration of water from the tidal flat, during the lowering ebb tide, results in the crests of ripples being the first to lose their sediment water saturation and become drier. Due to continuing wind and/or sun exposure, the ripple crest sediment continues to dry. During the drying process, the lack of (or small amounts of) surrounding water film between sand grains, and therefore the lack of capillary pressure holding grains together, enhances saltation of sand grains by the wind. The wind-blown, saltating sand grains accumulate in ripple troughs, where wind eddies and turbulence is reduced to a threshold where grains are allowed to settle out. The continued accumulation of wind-blown sediment in ripple troughs can eventually fill those troughs whereby small wind ripples form on the surface. This may be one mechanism where sand sheet formation is initiated. Occasionally, stronger wind gusts, or sustained wind velocities, potentially result in longer range transport of wind-blown sand grains down-wind from their point of origin.

The lack of bioturbation in this area may be explained by the high wind energies and constantly-shifting sediment, which may cover burrow openings and restrict access to the sediment water-interface for filter-feeders, in addition to high levels of desiccation stress.

There is a substantial reduction in the amount of mud within the confines of tidal and drainage creeks within this sub-environment, where the sediment deposited is dominantly medium- to coarse-grained sand forming downstream-oriented asymmetrical current ripples. Common to abundant plant material is found within the small fluvial creek, and bioturbation is lacking. All of the aforementioned combined factors indicate a high energy environment within the boundary of the creek facies, and a correspondingly high erosion rate that prevents mud deposition. The formation of ripples and sediment accumulation around tree branches is indicative of high sedimentation rates. Supporting this interpretation is the absence of bioturbation within the creek boundary. Also, the occurrence of abundant, open-to-surface burrows found directly adjacent to the creek edge in the muddy sand, demonstrate that lower current energies and lower sedimentation rates occur on the tidal flat of this area. The burrows occur in very high numbers over a small surface area, indicating an abundance of nutrient availability that can sustain a large concentration of organisms.

Bayhead delta free-meandering channel point bars and adjacent sand flats

The shore-attached tidal flats of Zone 2 are observed to contain various sedimentary structures, indicative of a range of current energies. Sedimentation rates, though not directly observed, may sometimes be inferred through observations of sedimentary structures present, along with the degree of bioturbation. Sedimentation rate can have an important effect on the distribution of incipient trace assemblages, with other major factors being aerial exposure and sediment grain size (Dashtgard, 2011). Near river mouths,

high fluvial discharges may also have an increased effect on the distribution of traces by introducing salinity and turbidity stresses (Dashtgard, 2011).

Areas adjacent to Kilchis Point experience very rapid changes in sedimentary environments and therefore structures observed, due to the highly-varying current energies and sediment grain sizes delivered to the bay via the Kilchis River mouth. Due to higher sedimentation rates, bioturbation intensity is also relatively low to moderate in this area, and any traces present are usually created by the burrowing activity of the sand shrimp *Neotrypaea californiensis*.

A change in current energy is outlined very well by the presence of primary lineation features. Parting lineation, or primary current lineation structures (Stokes, 1947) are “parallel ridges and hollows of low relief developed in flat-bedded sandstones on the upper surfaces of the component laminae” (Allen, 1963). They consist mainly of stream-lined sand grains oriented parallel with the current direction (Stokes, 1947). Ridges and hollows are offset and pass from one form into the other along their length (Allen, 1963). It is inferred that primary current lineation forms under upper flow regime conditions, either in the case of swash and back-swash currents on beaches, or unidirectional currents in river or tidal channels (Allen, 1963). Given the proximity of observed parting lineation to the free-meandering channel, it is likely that supercritical flow resulted in their creation.

One possible explanation for the abrupt transition of parting lineations into low-relief sand dunes, as observed at Tillamook Bay, is the origin or initiation (e.g. large wood fragments trapping sediment) of the dune formation on the tidal flat. However, the resulting decrease in current flow energy, when coming in contact with the stoss side of dunes, may cause the hydrodynamic regime to drop below supercritical, thus resulting in the formation of linguoidal to longitudinal ripples observed on the stoss side of dunes.

Marginal sand and muddy sand flats

In areas where the currents are strong, or where there is ample space for sediment to be distributed, sediment remains in suspension and continues to be distributed until the total energy of the system drops enough to allow for mud deposition. However, suspended mud particles transported towards the edge of the bay, between Goose Point and Kilchis Point, settle out of suspension due to lower current energy. As fine sediment also contains higher concentrations of organic matter, the available food resources for burrowing organisms are also higher. This is reflected in the higher bioturbation intensities observed in these areas. Similarly, the gradual reduction in grain size, from very coarse grained sand to medium grained sand is reflected by a slight increase in bioturbation and more complex sedimentary structures.

Areas located closer to the Bay City Channel, are more exposed to tidal currents, and also less restricted to the fluvial currents at the mouth of the Kilchis River. A gradual grain size decrease, from very coarse to medium grained sand to medium and fine grained sand is observed. The range of sedimentary structures observed is distinctly different from that of the previously mentioned quiescent area of this sub-environment. This can be attributed to the action of tidal and wave currents, and to a lesser extent, fluvial currents. The presence of low-relief dunes, as well as the variety of ripple structures, ranging from transverse to linguoidal, indicates that wave energies are much more significant than in the more sheltered areas of this sub-environment. Bioturbation intensity increases towards the shoreline (and away from the tidal channel), where clay content also increases. These factors, combined with an increase in eelgrass concentration, points to the more sheltered nature of the tidal flat, where organics are trapped more effectively, thus providing an important food source for burrowing organisms. It appears that bioturbation intensity and distribution, as well as the various sedimentary structures observed, are directly linked to total current energies in the system.

Zone 3: Isolated Tidal Sand Bar Descriptions and Results

Sedimentological and Neoichnological Features of Zone Sub-environments

Zone 3, part of the inner estuary, covers an area that includes one of the largest isolated tidal sand bars within Tillamook Bay. The sand bar is elongate and oriented along the ebb-flood tidal current directions, or in a north-south general orientation. The highest relief is observed in the center of the sand bar, furthest away from the two tidal channels towards which the bar surface dips at a shallow angle. Horizontal heterolithic stratification and inclined heterolithic stratification are observed in vibracores and trenches from the middle part of the sand bar, as well as at the inclined bar edge. Zone 3 is separated into three sub-environments (Fig. 2-26), with their boundaries arbitrarily assigned where significant changes in depositional environments are observed. Grain size varies from muddy very fine- to fine-grained sand, to medium-grained sand, along with total organic carbon values between 1.41% and 2.23% (Fig. 2-27). Given the location of the sand bar, changes in current energies are not as abrupt as near the river mouths, resulting in a more even distribution of sedimentary and biogenic characteristics over the area of the Zone 3 sand bar.

Channel-flanked, transverse-rippled deposits

Sedimentology-

The most proximal area of this sub-environment is dominated by relatively clean, well sorted, transverse rippled sand deposits (Fig. 2-28 A,B; Fig. 2-29 A,B). The ripples are slightly asymmetrical, and have low amplitudes of approximately 8-10 millimeters on average. Fecal pellets commonly accumulate in the ripple troughs (Fig. 2-29 B,C). Tidal creek facies are observed to incise into the bar surface. Algae mud mounds occur in these facies and are

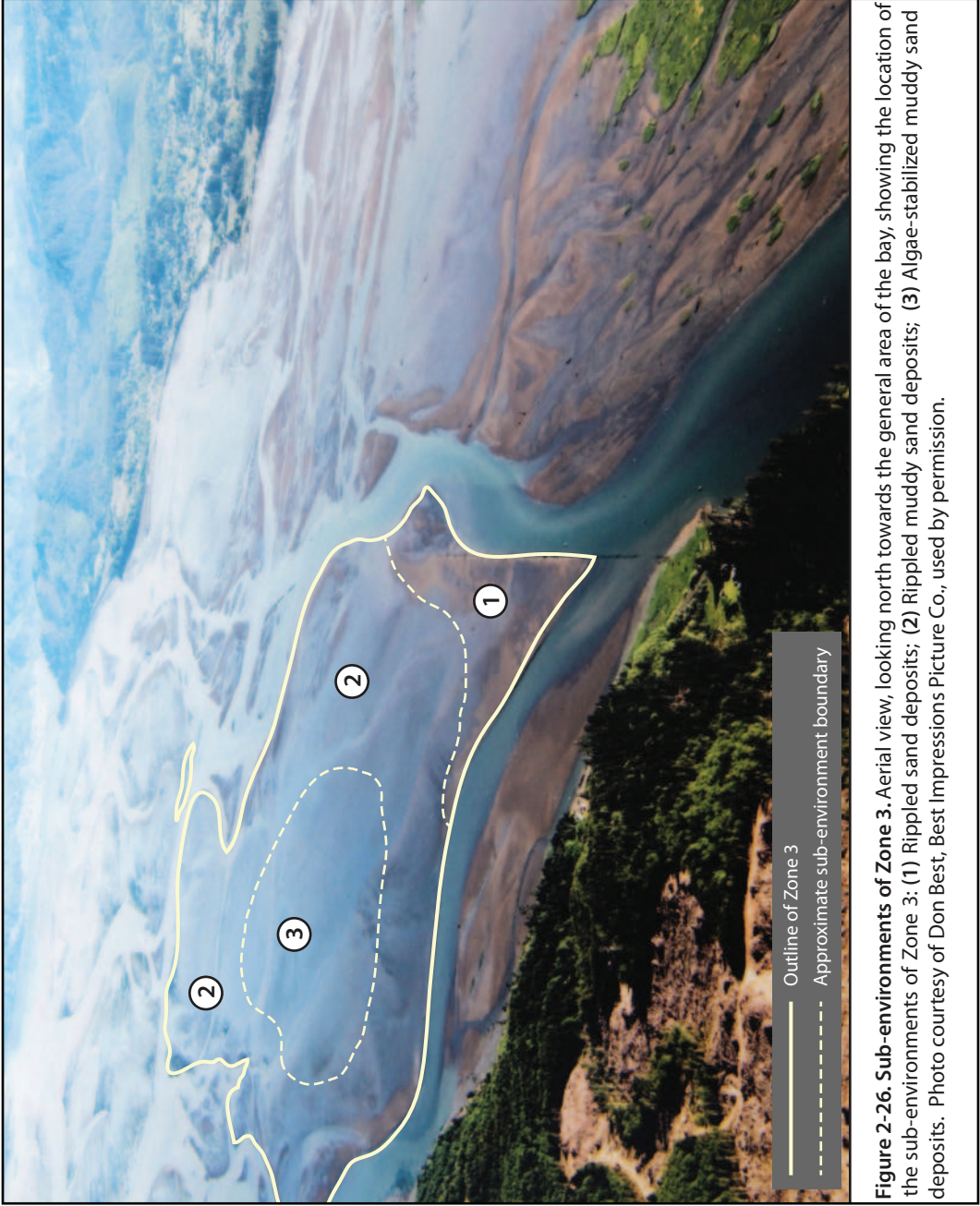
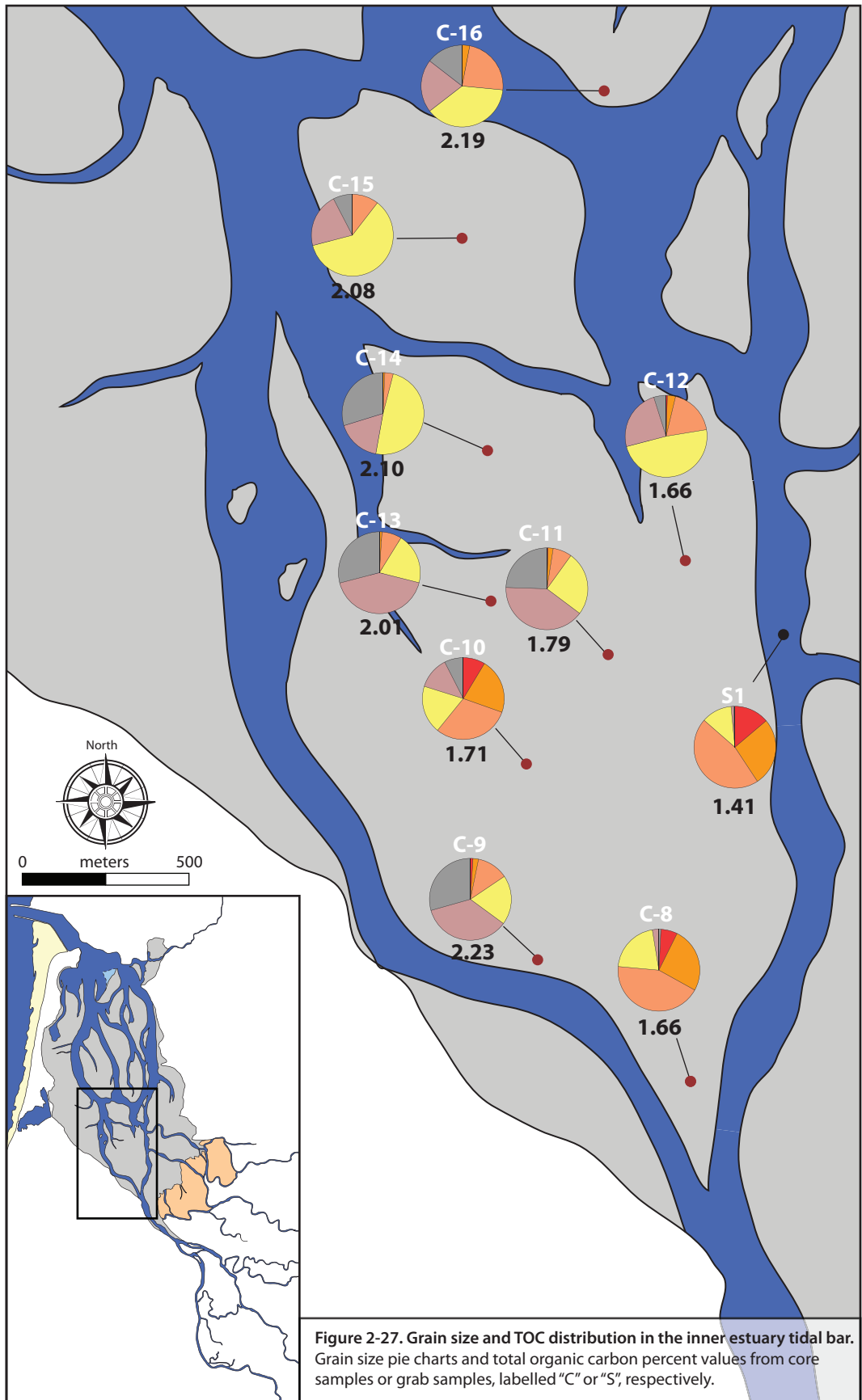


Figure 2-26. Sub-environments of Zone 3. Aerial view, looking north towards the general area of the bay, showing the location of the sub-environments of Zone 3: (1) Rippled sand deposits; (2) Rippled muddy sand deposits; (3) Algae-stabilized muddy sand deposits. Photo courtesy of Don Best, Best Impressions Picture Co., used by permission.





A



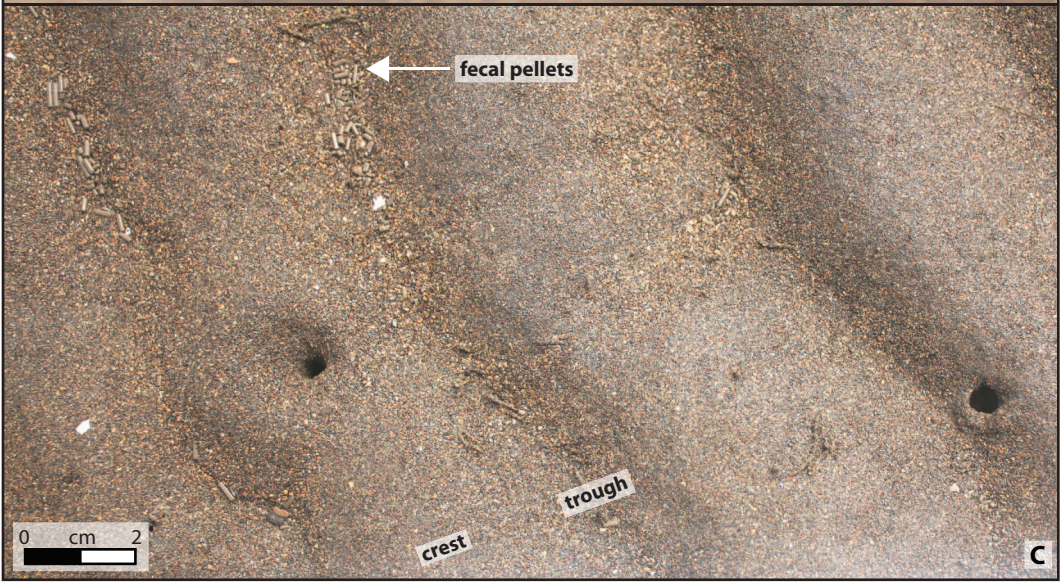
B

0 cm 2

C

Figure 2-28. Sedimentary features and traces of the channel-flanked, transverse-rippled deposits sub-environment, Zone 3. (A) Overview of tidal flat surface displaying dominantly straight to sinuous crested wave-formed ripples. (B) Alternate view of dominantly wave generated ripples where the straight to sinuous crested nature is more readily observed. (C) Unlined to slightly mucous lined *Arenicolites*-like burrow observed in the sub-surface.

Figure 2-29. Fecal pellets and incipient biogenic flasers of the channel-flanked, transverse-rippled deposits sub-environment, Zone 3. (A) View of the rippled surface at the southern tip of the tidal bar of Zone 3. **(B)** Cross-sectional to oblique view of nearly symmetrical ripples, showing the accumulation of fecal pellets in the ripple troughs. Ruler top scale is in centimeters. **(C)** Top view of the ripples and burrows, with sediment and fecal pellets expelled by the burrowing invertebrates, surrounding the burrow openings. Note the accumulation of fecal pellets in the troughs of ripples. The accumulation of fecal pellets, and their subsequent burial and compression, may lead to the formation of biogenic flasers.



sporadically distributed along the length of tidal creeks. They are oriented in a downstream direction, parallel to the drainage direction of the tidal creeks, towards the main tidal channel. Boxcores taken in creek sediments reveal a layered muddy sand and sand texture, with abundant plant fragments and organics.

At the sand bar edge, alternating sand and mud layers are observed in a 50 cm deep trench dug perpendicular to the bar edge. The layers range in thickness from 1-5 cm, have relatively sharp, flat contacts, and dip towards the channel at an angle of approximately 11° (Fig. 2-30 A,B,C).

Neoichnology-

Bioturbation is sparse to common, and occurs in the form of vertical, sub-vertical, and U-shaped burrows, all with small burrow diameters of 3-6 mm on average. Traces observed include *Arenicolites*-like burrows of *Nereis* sp. worms (Fig. 2-28 C), and *Siphonichnus*- and *Skolithos*-like burrows made by the soft-shell clam *Mya arenaria*. In a small number of thin, <5 mm burrows, iron staining is observed. Mud lining is observed on many burrow walls of *Arenicolites*-like burrows, and more rarely on the walls of *Skolithos*-like burrows. A smaller number of *Thalassinoides*-like burrows of the sand shrimp *Neotrypaea californiensis* are also observed, often cross-cutting vertical and sub-vertical burrows. Sediment appearing to have massive texture, and no discernable traces, is also observed, possibly due to the effect of cryptic bioturbation.

A higher concentration of *Nereis* sp. worm burrows occurs in the muddy tidal creek facies. Burrows commonly observed in the tidal creek environment, include U-shaped, *Arenicolites*-like burrows, and *Skolithos*-like burrows. Locally, *Thalassinoides*- and possibly *Palaeophycus*-like burrows are also observed. The rippled sand bar surface, dominated by cleaner sediment, contains traces similar to those observed in the tidal creek facies (Fig. 2-31 A,A',B). In front of the sand bar edge, however, the burrow morphologies, as well as the sediments they are found within, contrast with the ripple bar surface. These

Figure 2-30. Inclined heterolithic stratification, sand bar edge, channel-flanked, transverse-rippled deposits sub-environment, Zone 3. (A) Trench showing inclined sand and muddy sand interbeds at the edge of the sand bar of Zone 3. Note inclination of the beds towards the tidal channel seen nearby. (B) Close up view of the trench sidewall, showing more distinctly the sand and muddy sand (white arrows) interbeds. (C) Along-strike view of the a sidewall from the same trench, this time showing apparently flat-lying interbeds of sand and muddy sand.



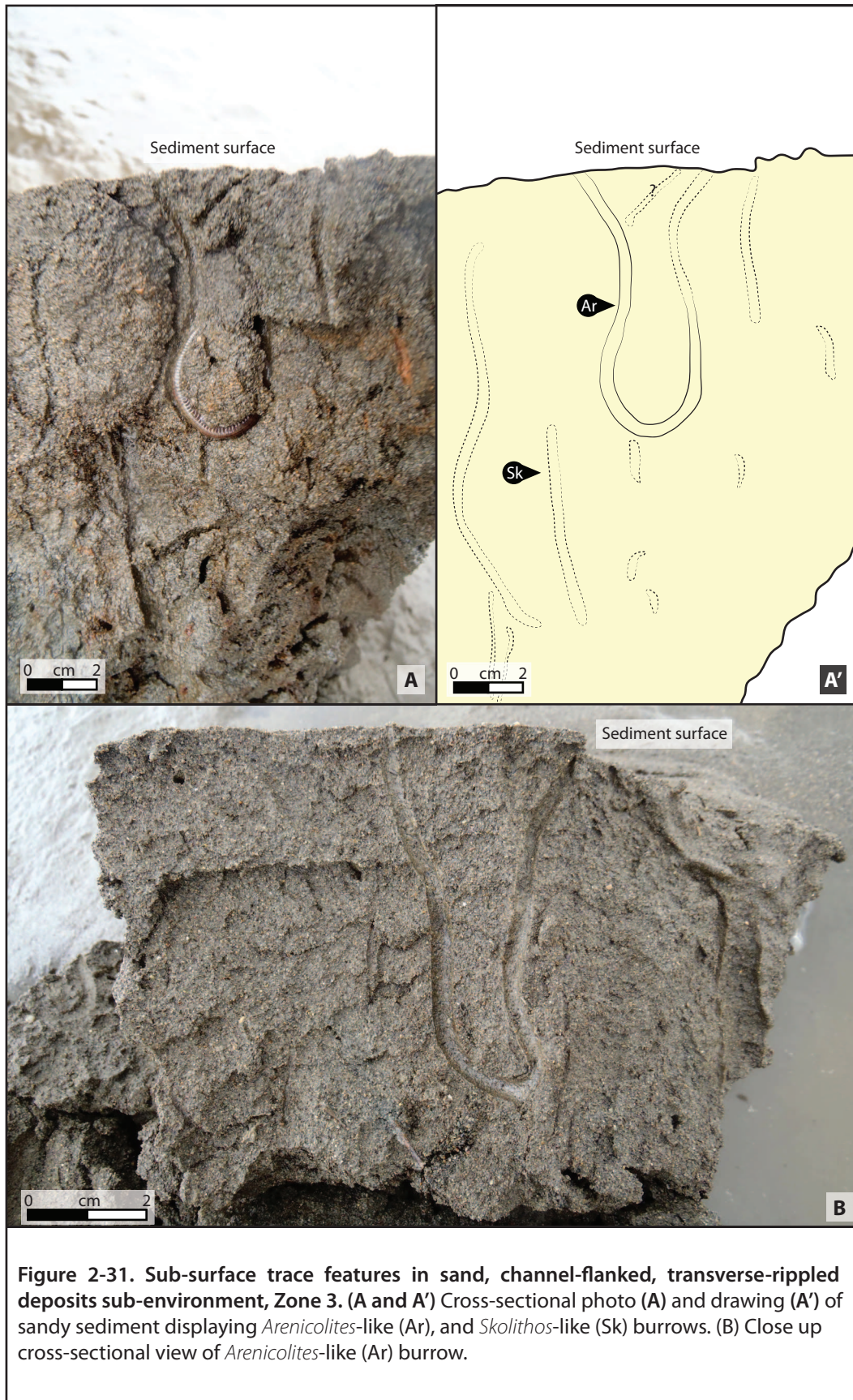


Figure 2-31. Sub-surface trace features in sand, channel-flanked, transverse-rippled deposits sub-environment, Zone 3. (A and A') Cross-sectional photo (A) and drawing (A') of sandy sediment displaying *Arenicolites*-like (Ar), and *Skolithos*-like (Sk) burrows. (B) Close up cross-sectional view of *Arenicolites*-like (Ar) burrow.

areally-restricted, burrowed, mud-dominated areas (Fig. 2-32 A) contain small, <5 mm, vertical, open-to-surface burrows (Fig. 2-32 B).

On the inclined portion of the bar, in heterolithic clean sand and muddy sand layers, vertical and sub-vertical traces are present when viewed in trenches oriented parallel to the bar edge (Fig. 2-33). At approximately 17 centimetres below the surface, U-shaped, vertical, and sub-vertical burrows occur in both layer types. The burrows, on occasion, extend into underlying layers of contrasting sediment character (Fig. 2-33 B,B'), have diameters of <5 mm, and vary in length from four to seven centimeters (Fig. 2-33 A,B,C; Fig. 2-34 A,A').

Rippled muddy sand deposits

Sedimentology-

This sub-environment flanks the algae-stabilized muddy sand deposits sub-environment and is bound by the channel-flanked, transverse-rippled deposits sub-environment on the most proximal tidal bar portion. Wood clasts and organic, carbonaceous debris are common to abundant. Highly organic or anoxic, dark layers, are common at about 3-4 centimeters below the sediment surface, and are commonly observed to have an irregular distribution and orientation, both vertically and horizontally. As with the previous sub-environment, tidal creeks commonly incise into the bar surface, and generally flow in a south, southeasterly orientation, towards the most proximal sub-environment of Zone 3 (Fig. 2-26) and the Bay City Channel. This sub-environment also has a high variety of ripple structures. Low-relief, elongate, muddy combined-flow ripples are common, as are "rolling" ripples, with an irregular pattern of equally-sized mound-like structures. Algae mounds are locally common and quite large, having diameters of approximately 1 metre. At the distal end of the tidal bar, the sediments dip at a very shallow angle and gradually transition into coarser-grained sediments of the tidal channel. This

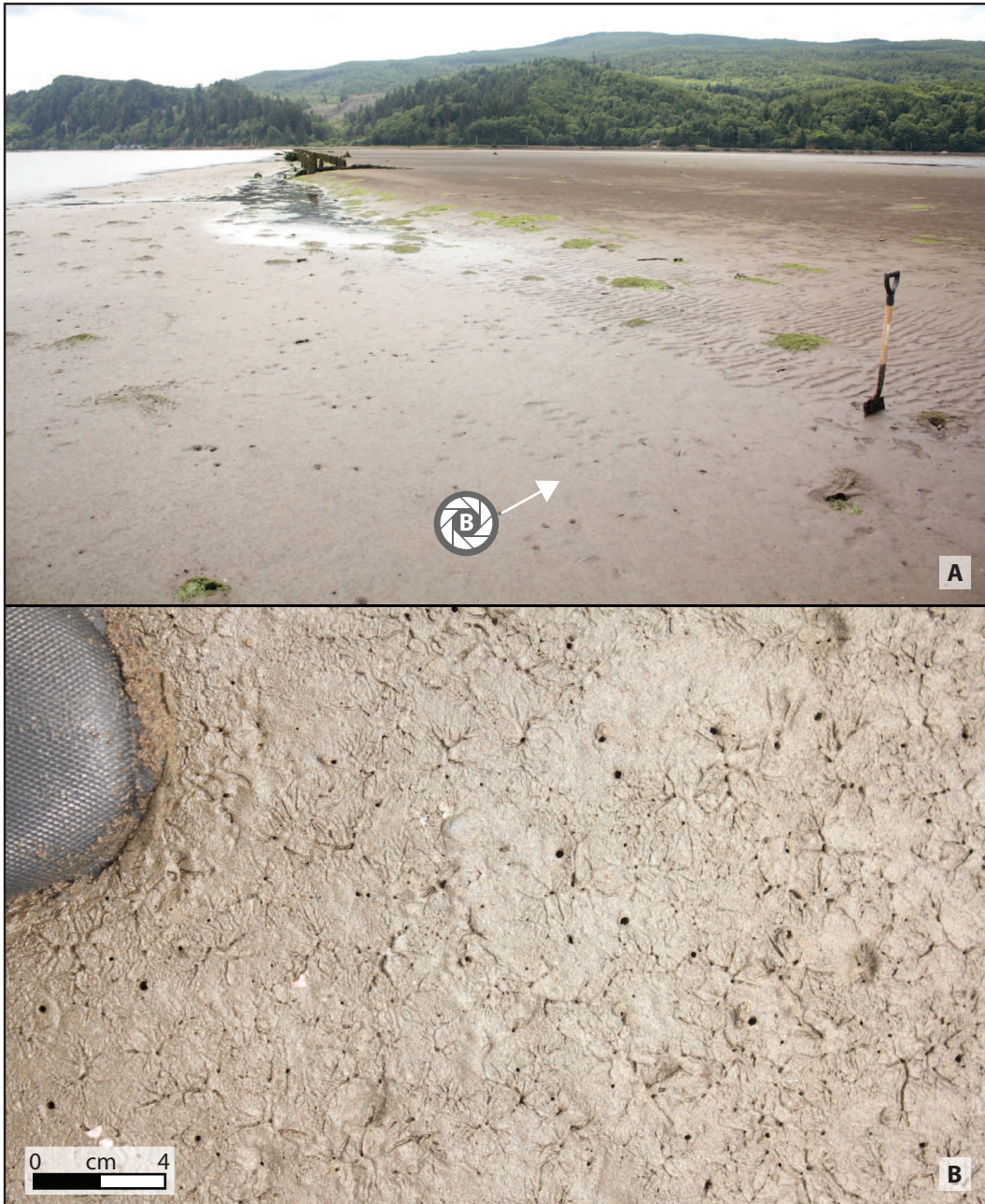
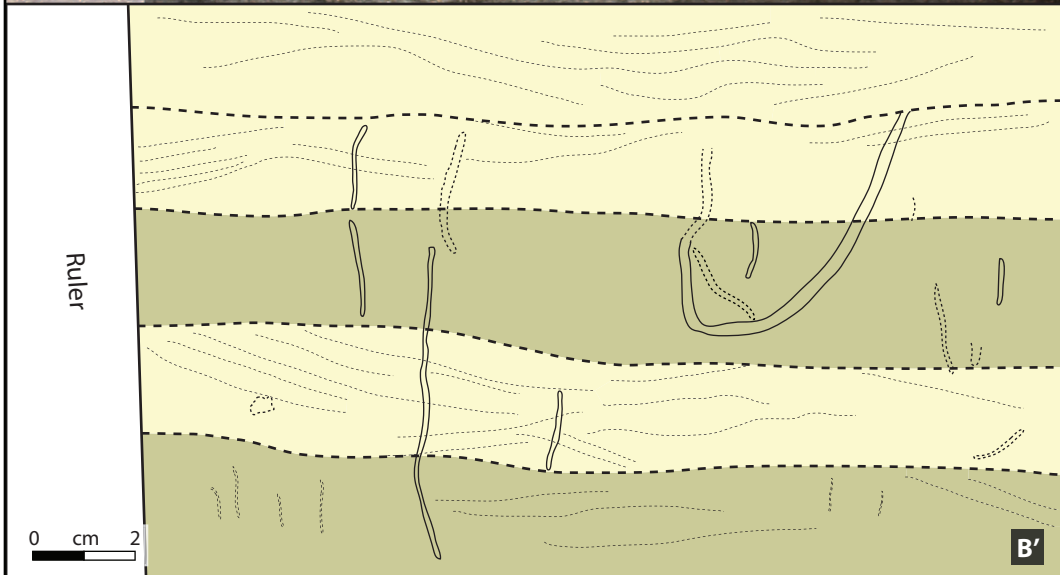
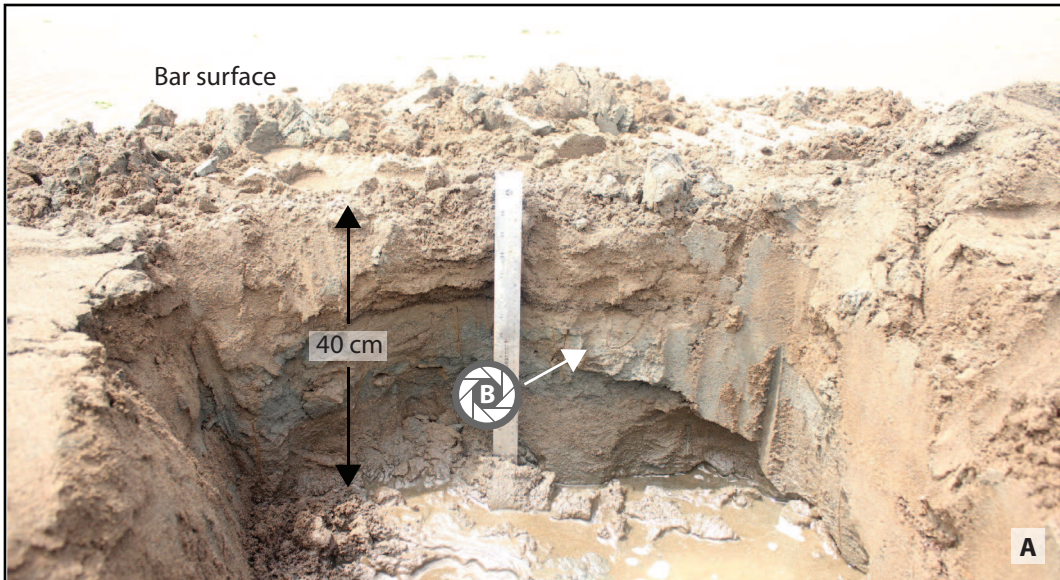


Figure 2-32. Burrowed, muddy sediment at the sand bar edge, channel-flanked, transverse-rippled deposits sub-environment, Zone 3. (A) View to the south, parallel to the sand bar edge, showing the sharp transition (see location of shovel) between the rippled, inclined sand bar edge and the relatively flat-lined mud-dominated sediment at the base of the inclined edge. (B) Close-up top view of the burrowed muddy sediment, with small, <0.5 centimeter burrow openings, and small mud cracks.

Figure 2-33. Burrowed layers of the inclined heterolithic stratification, sand bar edge, channel-flanked, transverse-rippled deposits sub-environment, Zone 3. (A) General view of the location of burrows observed in a trench near the sand bar edge. (B and C) Close-up photograph and drawing of the vertical *Skolithos*-like burrows and U-shaped, *Arenicolites*-like burrow. Note the trace of current and possible wave ripples structures observed within the sand layers.



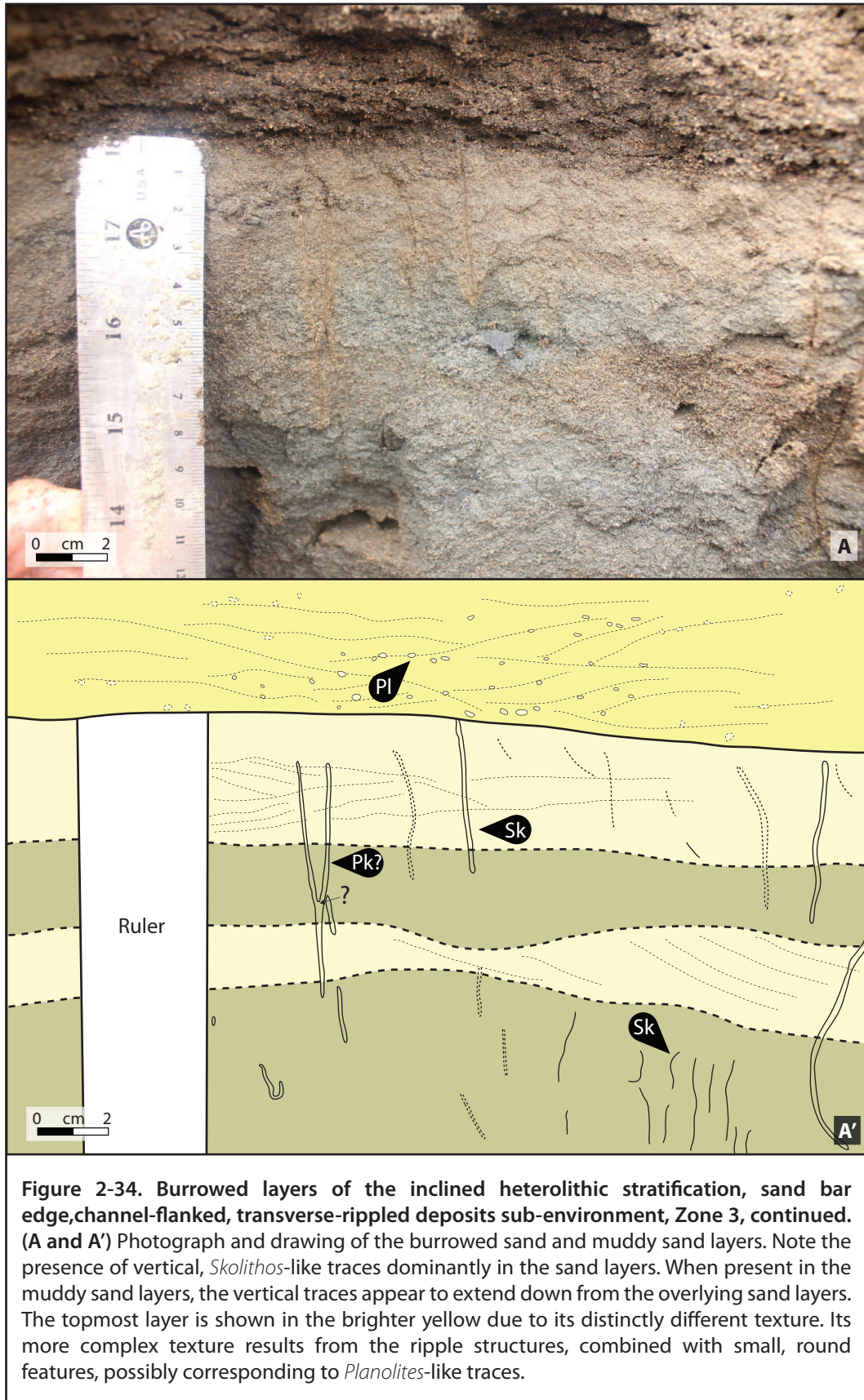


Figure 2-34. Burrowed layers of the inclined heterolithic stratification, sand bar edge, channel-flanked, transverse-rippled deposits sub-environment, Zone 3, continued. (A and A') Photograph and drawing of the burrowed sand and muddy sand layers. Note the presence of vertical, *Skolithos*-like traces dominantly in the sand layers. When present in the muddy sand layers, the vertical traces appear to extend down from the overlying sand layers. The topmost layer is shown in the brighter yellow due to its distinctly different texture. Its more complex texture results from the ripple structures, combined with small, round features, possibly corresponding to *Planolites*-like traces.

area is also the first to become submerged during flood tides, and experiences rapid water migration over the sediment surface due to the shallow slope.

Neoichnology-

The muddy deposits of this particular sub-environment show higher bioturbation intensity compared to the previously mentioned sub-environment. However, the neoichnological assemblage is similar, consisting of vertical and sub-vertical *Skolithos*-like burrows; thin, 5-10 mm *Siphonichnus*-like burrows; *Arenicolites*-like burrows; *Planolites*-like burrows; and *Palaeophycus*-like burrows. Algae roots are observed to penetrate into the top 10 cm of sediment. Burrows occur in both muddy sand layers, and layers with lower mud content, and have dominantly mud-lined burrows walls. Tracemakers include *Mya arenaria*, *Macoma balthica*, *Nereis* sp. worms, and the purple varnish clam *Nuttallia obscurata*. Although the most common burrow morphologies are vertical, sub-vertical, U-shaped, and occasional horizontal to vertical burrows also occur. They are likely *Skolithos*- and *Thalassinoides*-like burrows of the mud shrimp *Upogebia pugettensis* (Fig. 2-35 A,A',B,B'). Sand-infilled burrows are observed to be interconnected, forming a network of coarser-grained sand where the burrow boundaries are indistinct (Fig. 2-36 A,A'). Highly-bioturbated areas, with abundant *Thalassinoides*- and *Skolithos*-like burrows are commonly observed (Fig. 2-37 A,A',B,B'). Burrow walls are often oxidized and thus have an orange coloration. Mud lining is observed in many of the vertical and sub-vertical burrows, with the exception of *Siphonichnus*-like burrows. *Piscichnus*-like traces of possibly feeding fish, as well as *Nereis* sp. worm burrows are commonly observed along areas adjacent to the main channel.

Figure 2-35. Sub-surface sedimentary features and traces, rippled muddy sand deposits sub-environment, Zone 3. (A and A') Cross-sectional photo (A) and drawing (A') of sand (lighter beige colored layer in A') and organic rich muddy sand (grey colored layer in A') displaying unlined to slightly lined *Skolithos*-like (Sk), *Siphonichnus*-like (Si), *Planolites*-like (Pl) and *Thalassinoides*-like (Th) burrows. Note *in situ* bivalve associated with the *Siphonichnus*-like trace and multiple tiny wood clasts (wd) associated with the lower sandy layer. **(B and B')** Cross-sectional photo (B) and drawing (B') of sand (lighter beige colored layer in B'), organic rich muddy sand (grey colored layer in B'), and muddy sand (darker beige-green colored layers in B') displaying unlined to slightly lined *Skolithos*-like (Sk) traces with possible *Siphonichnus*-like (Si), and *Thalassinoides*-like (Th) burrows. Note *in situ* deceased bivalve associated tiny wood clasts (wd).

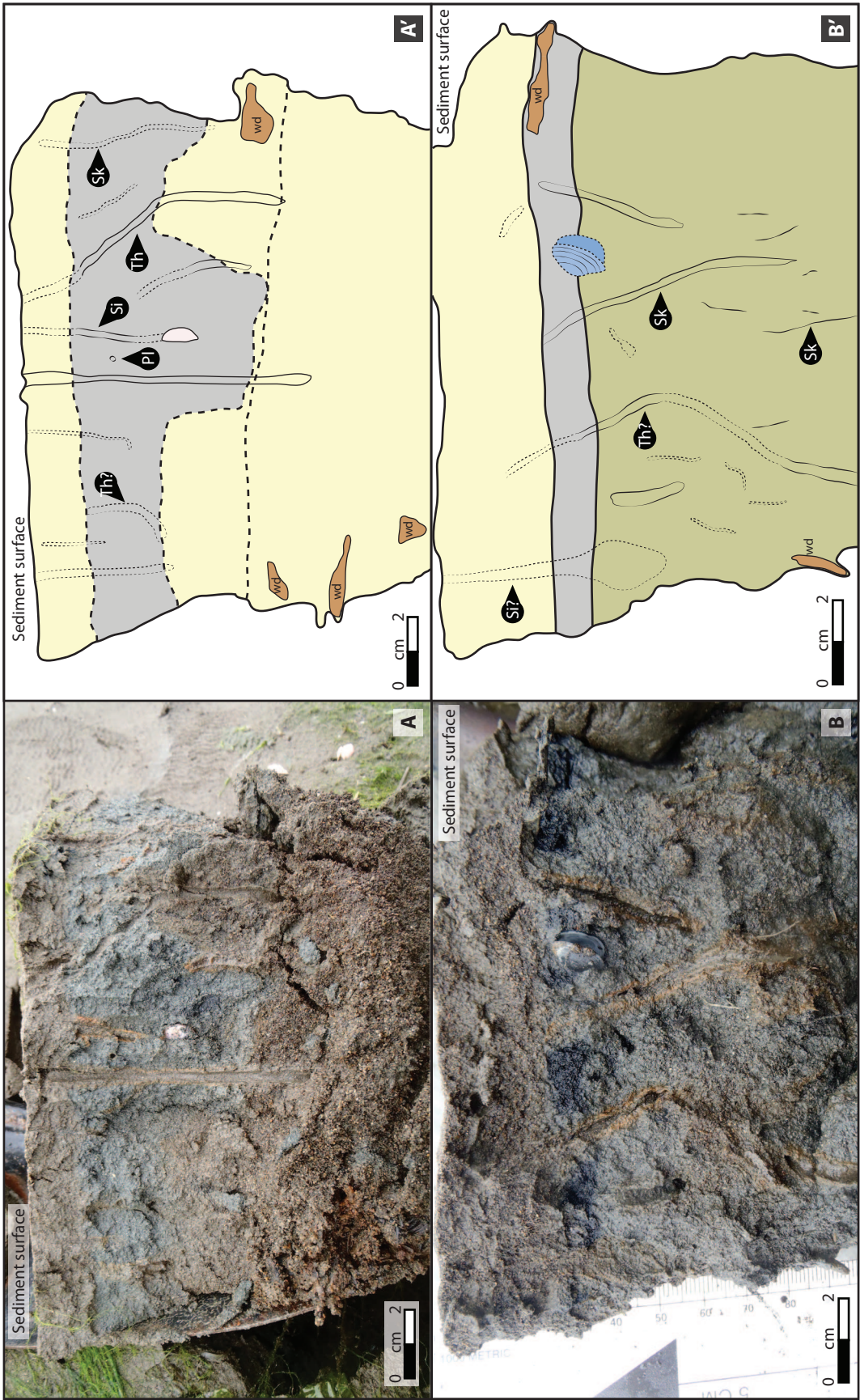


Figure 2-36. Sub-surface sedimentary features and traces as observed in a boxcore from the rippled muddy sand deposits sub-environment, Zone 3. (A) Photo of boxcored dominantly muddy sand to sandy sediment displaying faint laminae and beds as well as multiple infilled, but relatively indistinct, burrows. Note that the burrows are infilled with slightly coarser sediment than that which comprises the majority of laminae or beds. (A') Interpreted drawing of sediment in A that portrays a slightly clearer distinction of laminae and burrow morphology.

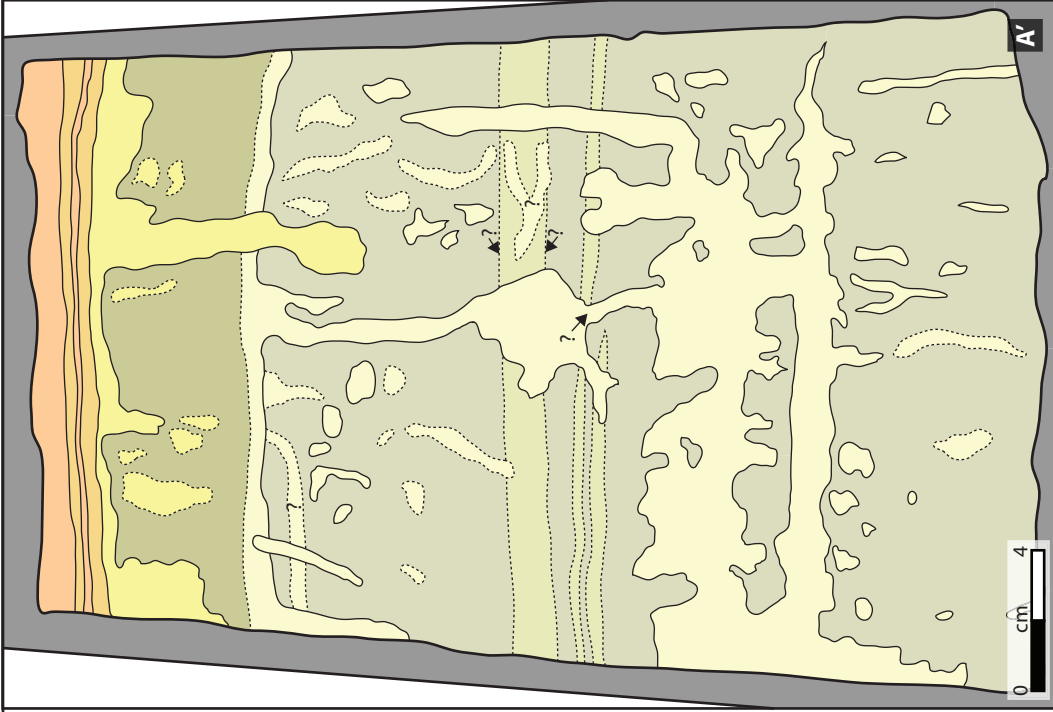
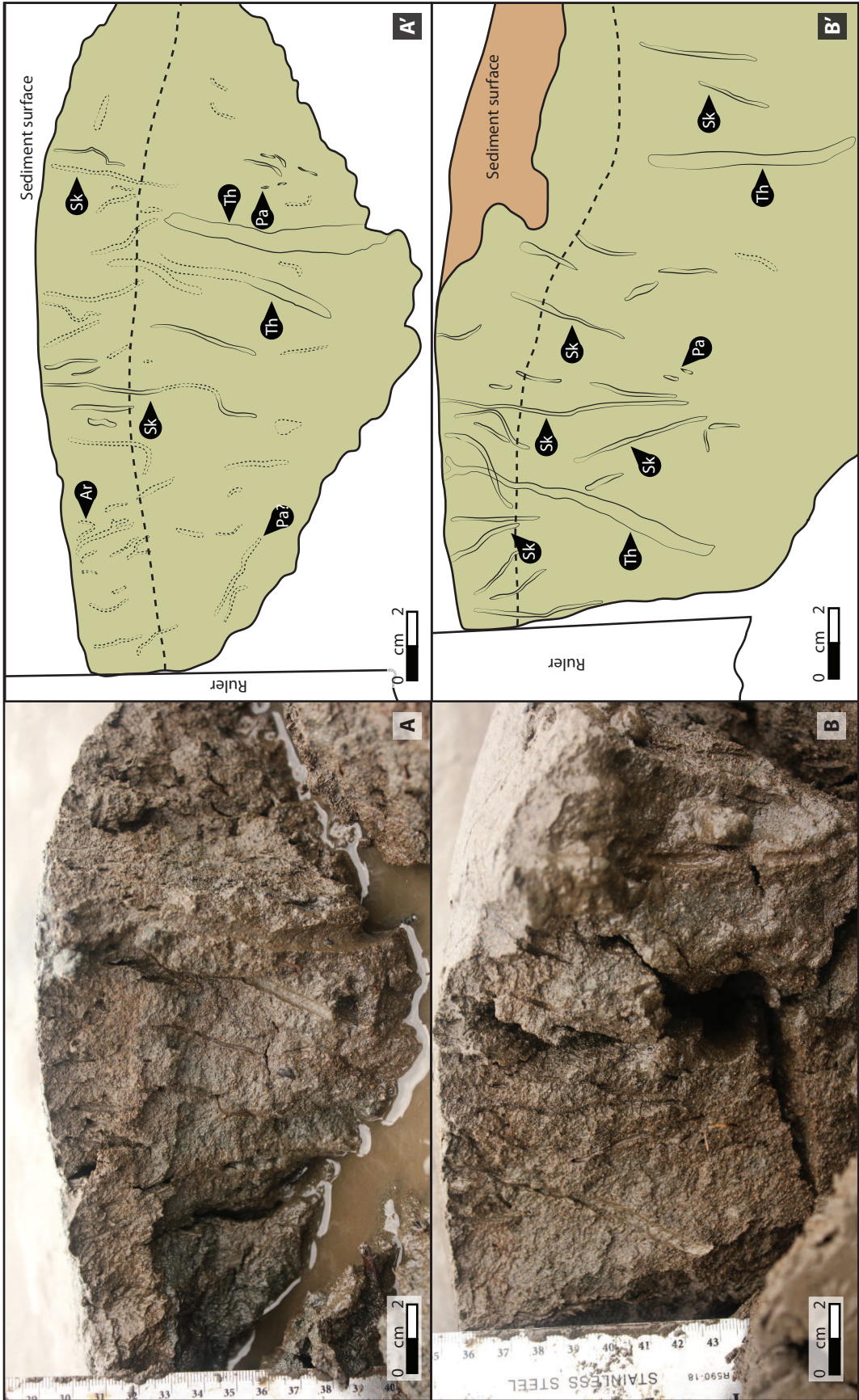


Figure-specific legend:

- Fine/medium sand
- Medium/coarse sand
- Mixed muddy/clean sand
- Oxidized(?) medium sand
- Clean, fine-grained sand
- Medium-grained sand
- Muddy, fine-grained sand

Figure 2-37. Sub-surface sedimentary features and traces, rippled muddy sand deposits sub-environment, Zone 3, continued. (A) Photo showing cross-sectional view of tidal flat sediment where muddy sand dominates. The upper 2 cm appears slightly more red-brown in color. Burrows are common and are highlighted in **A'** for clarity. **(A')** Drawing of **A** distinguishes *Skolithos*-like (Sk), *Arenicolites*-like (Ar), *Palaeophycus*-like (Pa) and *Thalassinoides*-like (Th) burrows. **(B)** Photo also displaying cross-sectional view of tidal flat sediment dominated by muddy sand where the upper 2 cm appears slightly more red-brown in color compared to sediment below. Burrows are common and are highlighted in **B'** for clarity. **(B')** Drawing of **B** distinguishes *Skolithos*-like (Sk), *Palaeophycus*-like (Pa) and *Thalassinoides*-like (Th) burrows.



Algae-stabilized muddy sand deposits

Sedimentology-

Abundant algae in this sub-environment are distributed evenly on the bar surface, drastically influencing the sedimentation trend and the character of the sedimentary structures. At the sub-environment edge, sinuous to linguoidal combined-flow ripples are common (Fig. 2-38 A,B,C); eelgrass and algae occur in small concentrations, often being trapped on large wood fragments and tree branches (Fig. 2-38 C). Towards the central portions, an increase in eelgrass and mud concentration is observed. Large, hummocky mud mounds occur extensively throughout the area. In the central part of this sub-environment, algae cover up to approximately 60-70% of the bar surface, and possibly more locally (Fig. 2-39 A,B,C).

Neoichnology-

Thalassinoides-like burrows of the mud shrimp *Upogebia pugettensis* are common to abundant (Fig. 2-40 A,A') in the central part of the sub-environment, with the sand shrimp *Neotrypaea californiensis* dominating the area marked by the transition into the rippled muddy sand bar surface (Fig. 2-39 D). *Macoma balthica* and *Mya arenaria* form *Siphonichnus*-like and *Skolithos*-like burrows. *Nereis* sp. worms are abundant and form *Skolithos*-like and *Arenicolites*-like U-shaped burrows (Fig. 2-40 A,A'). Small, one to four centimeter long, and <5 mm in diameter, S-shaped burrows are common to abundant. Most appear to be oblique sectional views of much longer burrows. Small, *Planolites*-like burrows occur in smaller concentrations. In areas of lower algal concentration, *Siphonichnus*-like traces of the purple varnish clam *Nuttallia obscurata* are present. Numerous small burrows occur on the surface of muddy sediments, which are often devoid of well-developed ripple structures (Fig. 2-39 B).

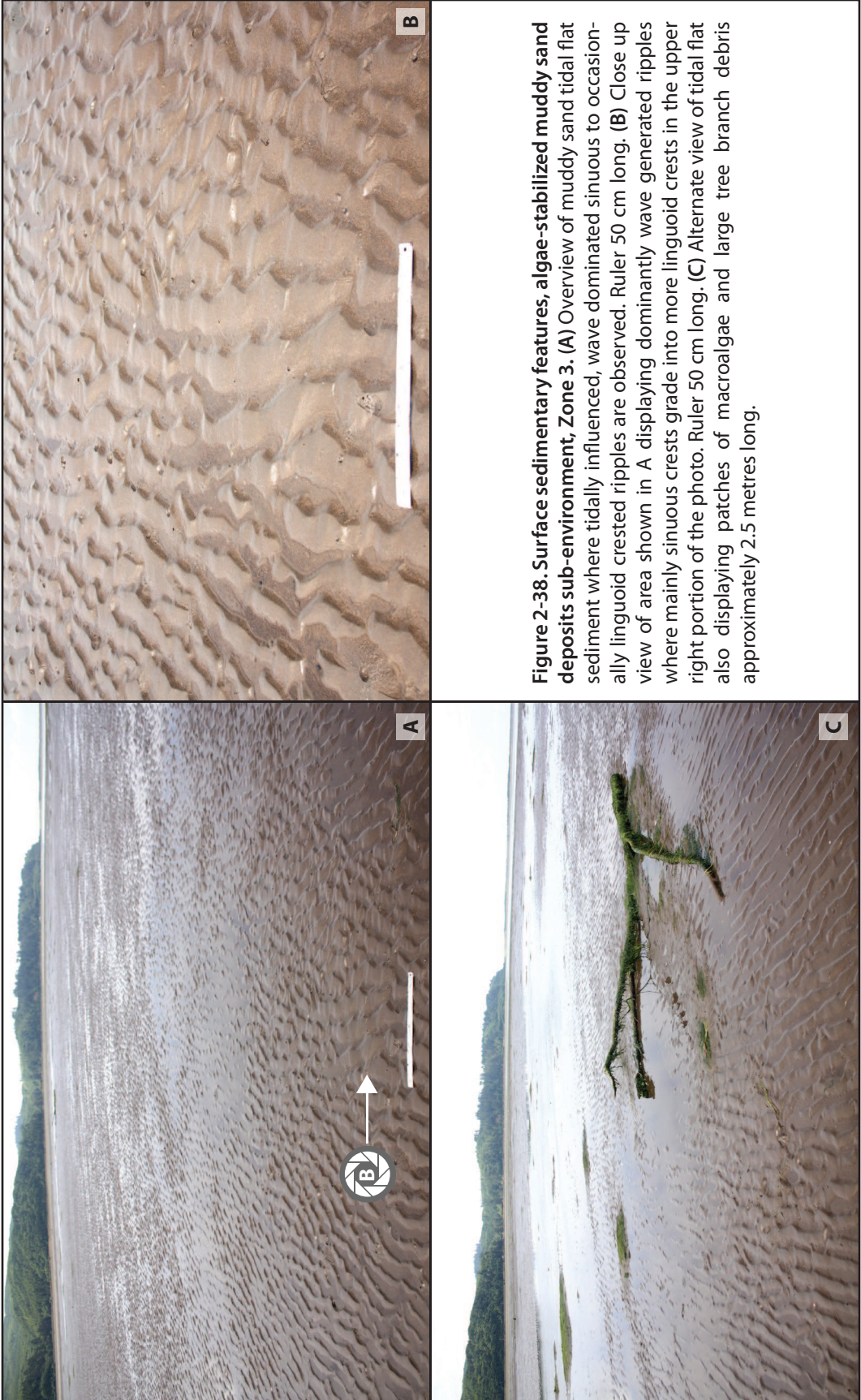


Figure 2-38. Surface sedimentary features, algae-stabilized muddy sand deposits sub-environment, Zone 3. (A) Overview of muddy sand tidal flat sediment where tidally influenced, wave dominated sinuous to occasionally linguoid crested ripples are observed. Ruler 50 cm long. **(B)** Close up view of area shown in A displaying dominantly wave generated ripples where mainly sinuous crests grade into more linguoid crests in the upper right portion of the photo. Ruler 50 cm long. **(C)** Alternate view of tidal flat also displaying patches of macroalgae and large tree branch debris approximately 2.5 metres long.

Figure 2-39. Surface sedimentary features and traces, algae-stabilized muddy sand deposits sub-environment, Zone 3. (A) Overview of tidal flat displaying expanses of eelgrass and sporadic macroalgae with burrow mounds obvious especially in patches without eelgrass. Shovel for scale is ~1 m. **(B)** Alternative view of tidal flat with virtually no eelgrass present but with multiple burrow mounds still obvious. Shovel for scale is ~1 m. **(C)** View of a small, macroalgal stabilized mound with multiple large burrow openings. Shovel for scale is ~1 m. **(D)** Side view of probable *Neotrypaea californiensis* burrow mound.



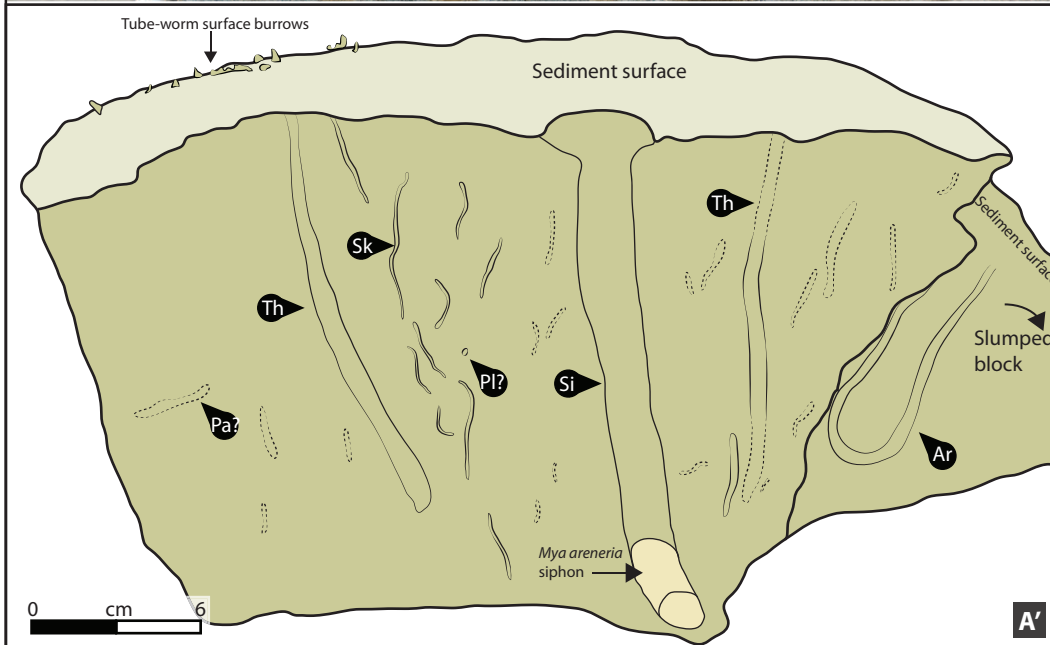


Figure 2-40. Sub-surface trace features in muddy sand, algae-stabilized muddy sand deposits sub-environment, Zone 3. (A and A') Cross-sectional photo (A) and drawing (A') of muddy sand displaying *Arenicolites*-like (Ar), *Skolithos*-like (Sk), *Siphonichnus*-like (Si), and *Thalassinoides*-like (Th) burrows with possible *Planolites*-like (Pl) and *Palaeophycus*-like (Pa) burrows. Note *Nereis* sp. worm in *Arenicolites*-like burrow of slumped block and partially exposed *Mya arenaria* siphon in the partially exposed *Siphonichnus*-like trace. Also note surficial expression of tube worm burrows on the sediment surface.

Zone 3 Isolated Tidal Sand Bar Vibracore Facies Descriptions

Vibracores of the Isolated Tidal Sand Bar Zone 3 show the highest variation in mud and sand layer thicknesses. Heterolithic stratification (HS) and inclined heterolithic stratification (IHS) is commonly observed, in the form of sand and mud interbeds and interlaminae (Fig. 2-41 Part I A,B,C,D,E,F; Fig. 2-41 Part II A,B,C,D,E,F; Fig. 2-42 Part I; Fig. 2-42 Part II; Fig. 2-42 Part III), both at the edge of the isolated sand bar, as well as in the center, furthest away from tidal channels. Dominantly muddy, as well as sandy HS and IHS are observed. Muddy HS and IHS are mainly observed in thick mud units, with thinner sand layers occurring within these thicker units (e.g. cores 11 and 14, Figs B-9 and B-12, respectively). Sandy IHS, as observed in core 12 (Fig. B-10) and 13 (Fig. B-11), contains thin mud layers, with respect to the overall sand layers they are found in. Fine- to medium-grained sand dominates the sediment observed in cores of Zone 3, with grain size variations common in all cores observed. Shell fragments are rare to common, unlike the abundant wood fragments that commonly occur as wood lags at the bottom of sand layers. Organic laminae are sporadically to commonly observed within sand layers. Bioturbation, where observed, is difficult to interpret due to poorly preserved burrow structures. Sedimentary structures, on the other hand, are more easily distinguishable in both visual analysis of the cores and x-rays of the cores; the most common sedimentary structures are current ripples, as well as fine laminae. Low-angle, as well as wavy bedding is also observed, though to a lesser extent. A total of nine cores ranging from 130 cm to 240 cm long were recovered from Zone 3. Four facies are identified from the Isolated Tidal Sand Bar (Zone 3) according to distinct sedimentary and neoichnological characteristics. These facies are summarized in Table 2-3, with supplementary references to vibracore logs located in Appendix B.

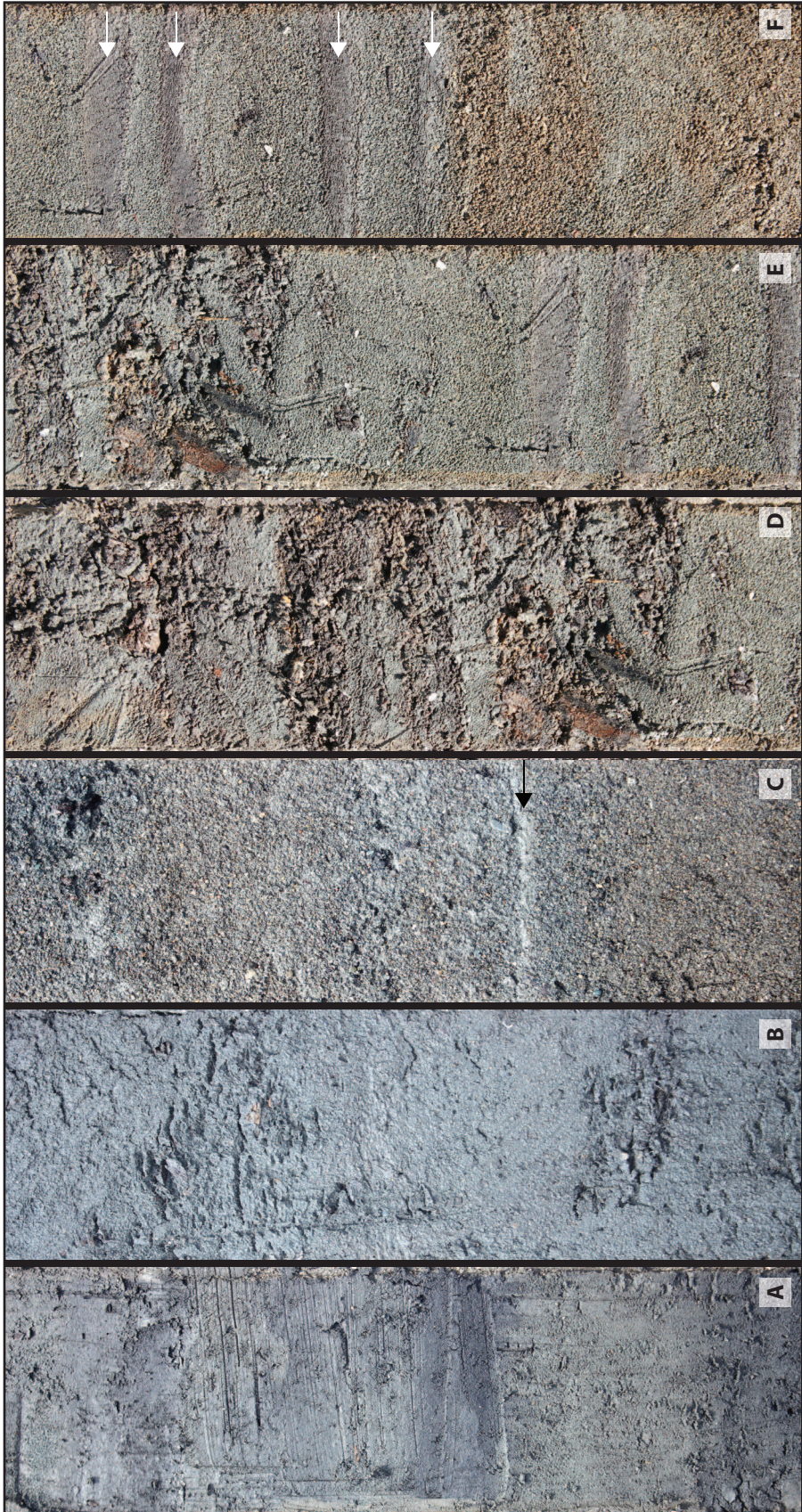


Figure 2-41. Part 1. Vibracore examples from the inner estuary tidal bar, Zone 3. Examples of the typical sedimentary features observed in the mixed sand and mud inclined heterolithic stratification of the inner estuary. (A) Mixed mud (dark bluish-grey) and muddy sand (light grey) interbeds. (B) Dominantly muddy sand, with a distinct, thin mud lamina observed (black arrow). (D, E, and F) Photo series of a continuous core, showing interlaminated to interbedded muddy sand and organic-rich mud layers (D), and interlaminated to interbedded sand and mud (white arrows) layers (E and F). Note the relatively uneven thickness of mud layers.

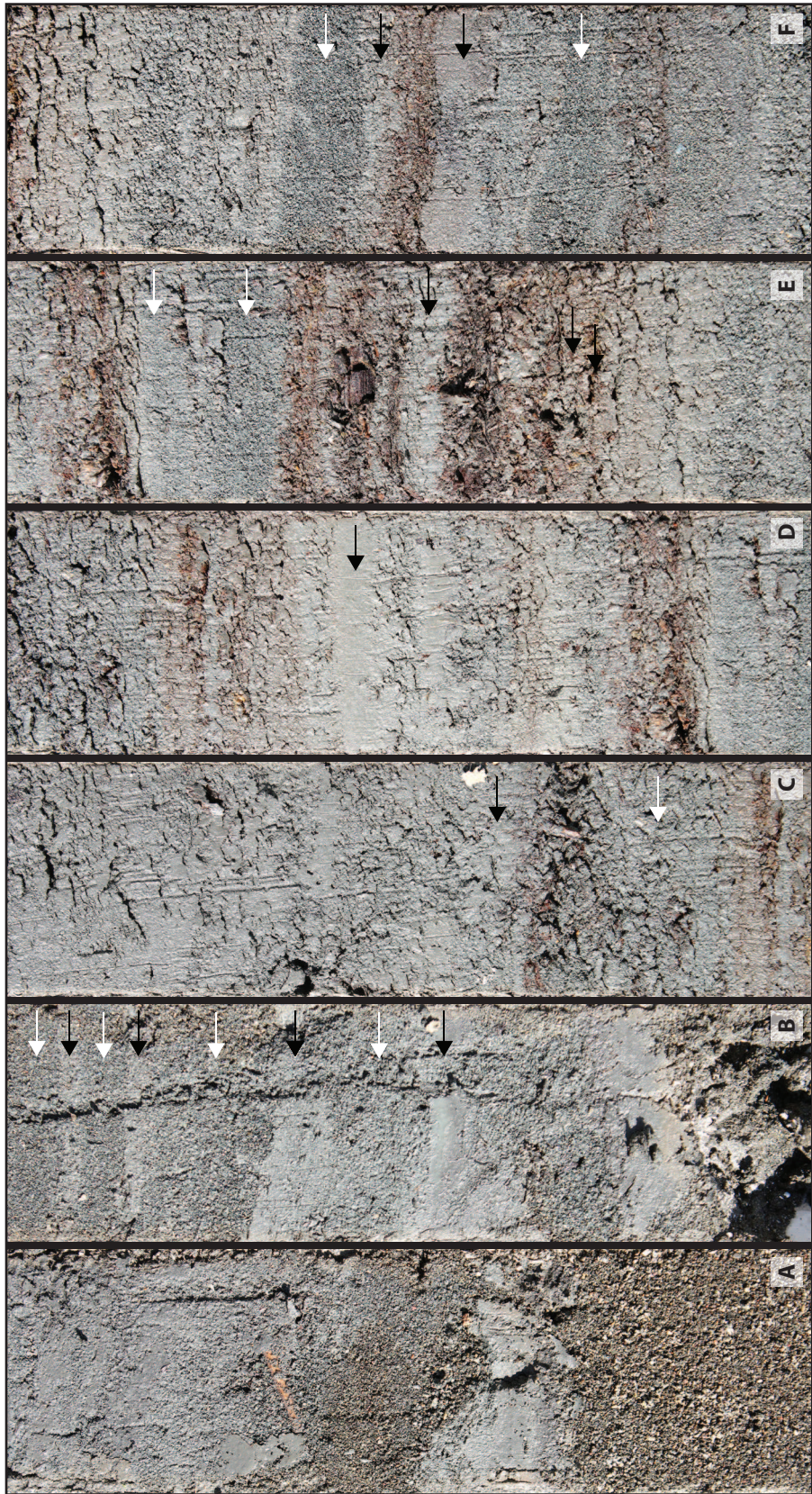


Figure 2-41. Part II. Vibracore examples from the inner estuary tidal bar, Zone 3. Examples of the typical sedimentary features observed in the mixed sand and mud inclined heterolithic stratification of the inner estuary. (A) Medium-grained sand layer, containing a mud bed, overlain by a thicker mixed mud and muddy sand layer. (B) Mixed muddy sand (white arrows) and mud (black arrows) layers. (C, D, E, and F) Photo series of a continuous core, showing interlaminated to interbedded, muddy sand (white arrows) and mud (black arrows) layers. Organic and wood fragment rich muddy layers, are common and seen in the photos as brown colored.

Figure 2-42, Parts I, II, and III (next three pages). Sediment logs of the inner estuary sand bar, Zone 3. Sediment logs for vibracores #8 to #16. Cores #10 and #14 appear as duplicates in part I and II, and part I and III, respectively. This is to allow the reader to visualize the connection between each part, and observe trends between cores oriented lengthwise along the sand bar, as well as widthwise along the bar. Note the variation in grain size of the coarse members. Heterolithic stratification, in the form of coarse (i.e. sand) and fine (i.e. clay and silt) members is abundant. Common sedimentary structures, though difficult to observe in cores or x-radiographs, are current ripples. Bioturbation was very seldomly observed; wood fragments, as well as occasional shell fragments, are common. Aerial photo, appearing in each part, courtesy of Don Best, Best Impressions Picture Co., used by permission.

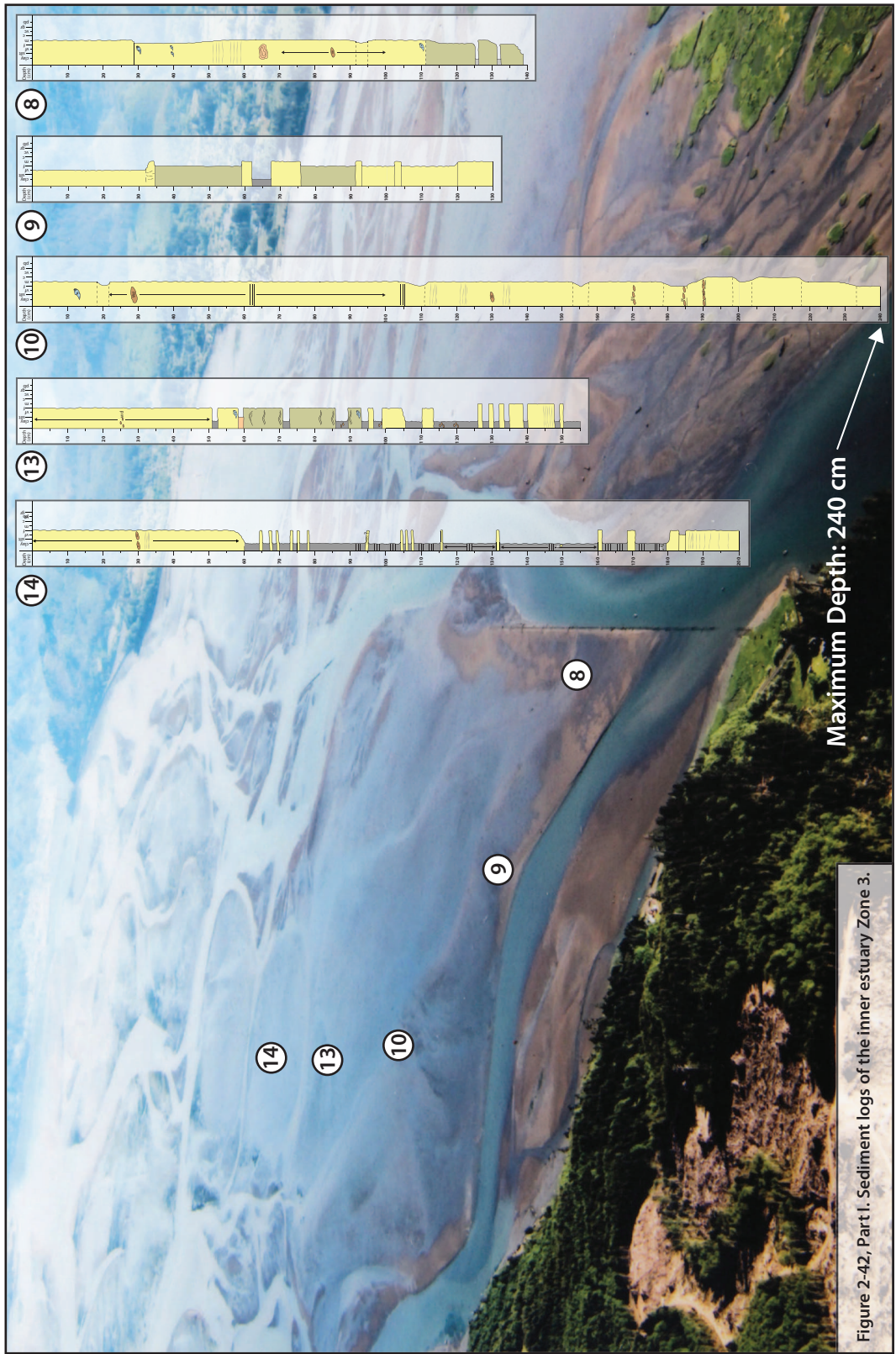
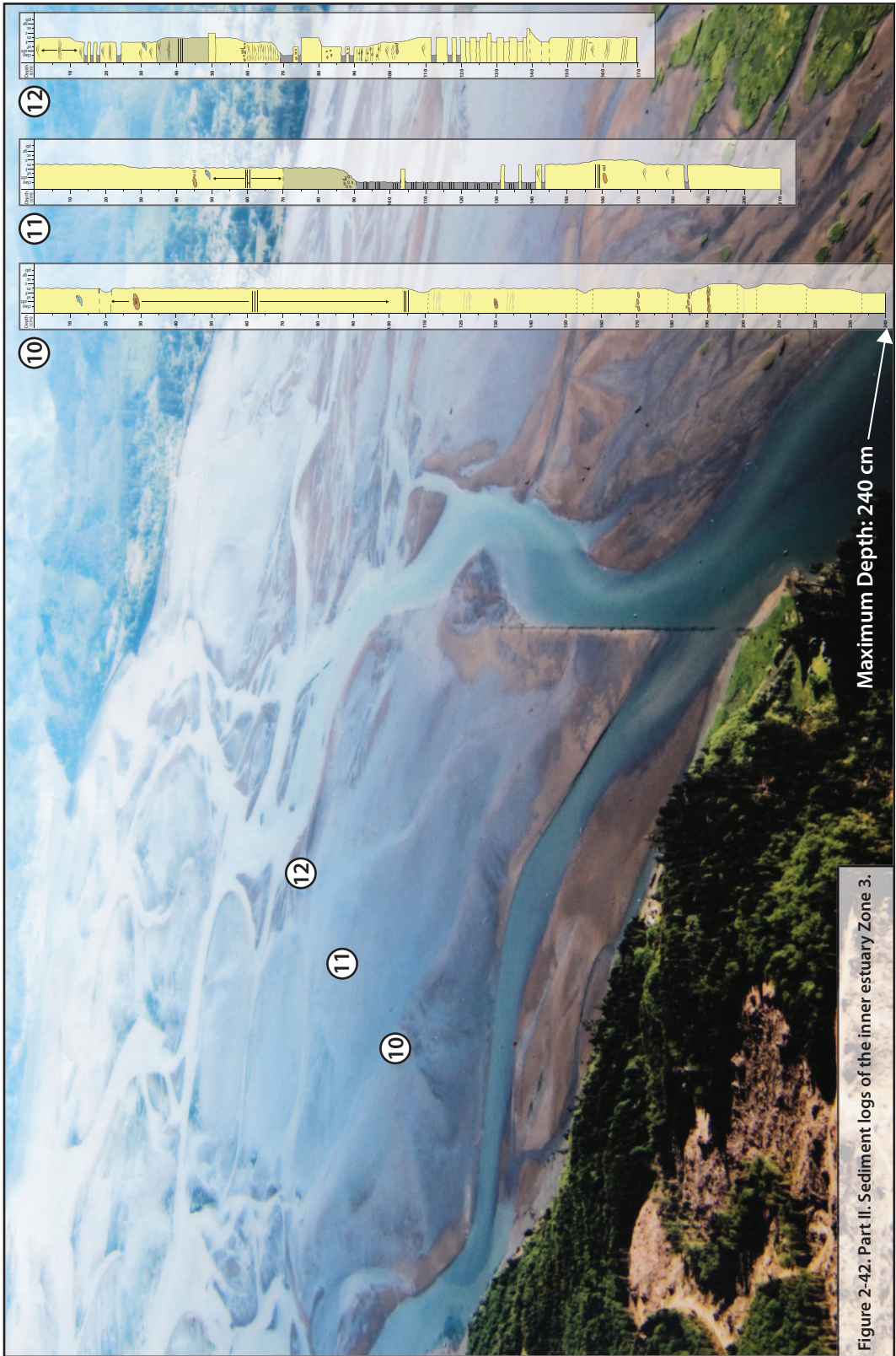
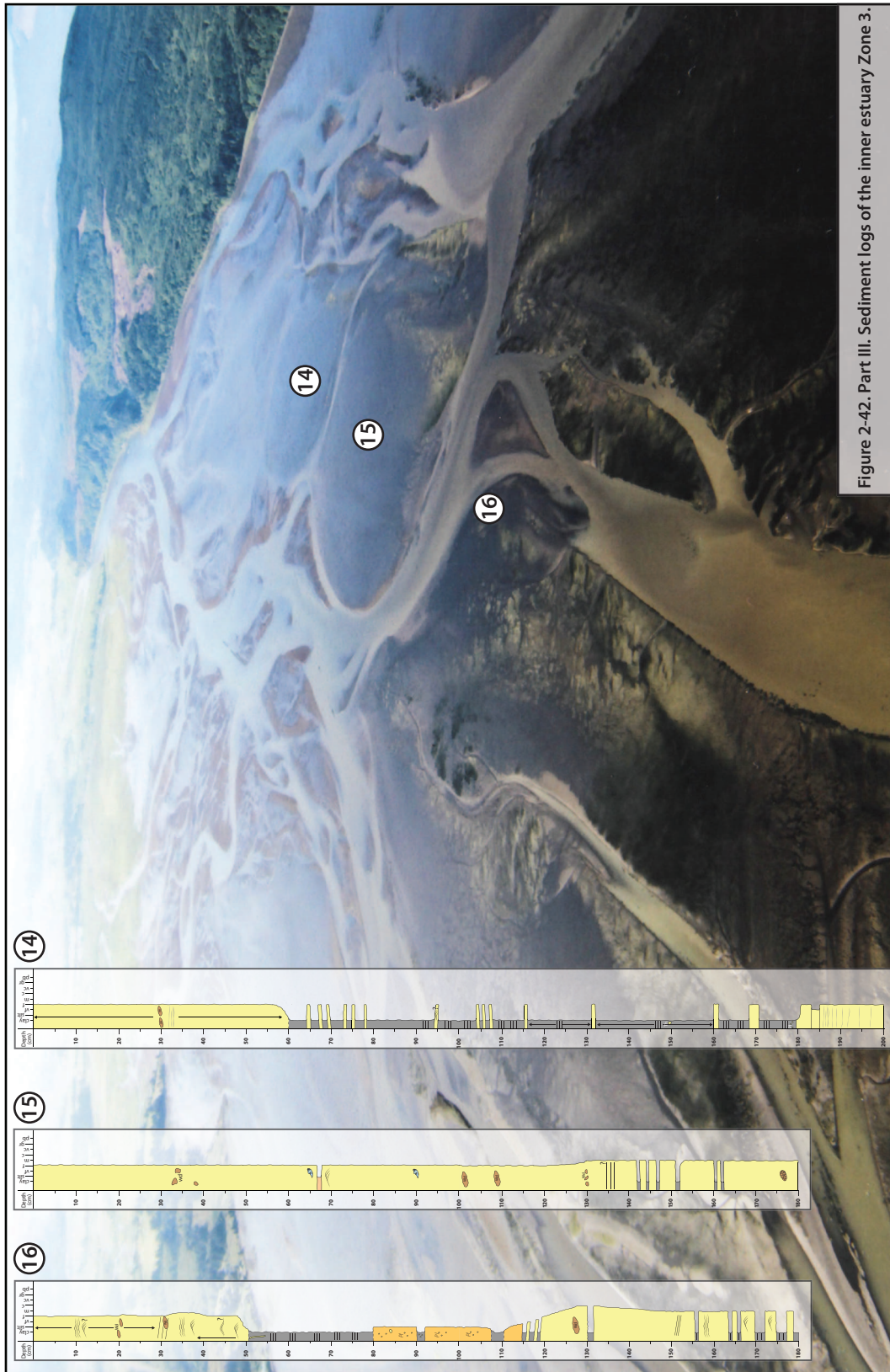


Figure 2-42, Part I. Sediment logs of the inner estuary Zone 3.





Facies Association	Facies	Facies Contacts	Sedimentary Characteristics	Neoichnological Characteristics	Interpretation
<p style="text-align: center;">Isolated Tidal Sand Bar Facies Association (FA3)</p>	<p>Facies 1 (Z3F1) Massive to planar laminated clay and silt</p>	<p>Underlying Facies 3 gradually transitions into this facies, while there is an abrupt but indistinct change from Facies 1 into overlying Facies 7 above.</p>	<p>The clay portion, however, is the most dominant grain size within Facies 1 and consists of a continuous 30 cm thick sequence of planar laminated clay. The silt interval is reworked by bioturbation, with sporadic occurrences of bioturbation in clay interbedded with silt as well. Thickness of Facies 1 is 65 cm with the silt portion typically 5 cm to 15 cm thick and the clay portion between silt 2.5 cm to 5 cm thick.</p>	<p>Bioturbation is absent to locally abundant. <i>Planolites</i>-like traces dominate these bioturbated silt intervals. Another possible vertical burrow, 1 cm in diameter and 5-6 cm long, appears in the planar laminated clay and is infilled by sand from overlying Facies 7.</p>	<p>Tidal creek to mud-dominated bar surface</p>
	<p>Appendix B Core Figure Reference(s): B-14</p>	<p>When present, and where contacts are discernable, Facies 7 can underlay Facies 2 abruptly, but indistinctly. Facies 7 and 4 can overlay Facies 2 abruptly, but indistinctly to gradationally.</p>	<p>This facies ranges in thickness from 50 cm to 120 cm. Massive to planar laminated clay dominates the sequence and can be up to 20 cm thick without interruption from sand laminae or beds. Clean, fine to dominantly medium grained sand commonly occurs as laminae within the clay, but can be up to 10 cm thick, especially in basal parts of the facies. The sand present is usually massive in appearance, possibly due to biogenic reworking, or can be occasionally planar laminated to rippled, especially in the finer grained portions. Wood fragments are common in the clay portion (up to 40-60%).</p>	<p>Bioturbation is absent to sparse. <i>Planolites</i>-like burrows are evident at some locales in basal portions of this facies occurrence. A possible sand-infilled, 1 cm in diameter <i>Thalassinoides</i>-like burrow is evident at one locale in a portion of planar laminated clay.</p>	<p>Central muddy tidal bar to tidal bar margin</p>

Table 2-3: Summary of Facies Characteristics for Isolated Tidal Sand Bar (Zone 3)

Facies Association	Facies	Facies Contacts	Sedimentary Characteristics	Neochronological Characteristics	Interpretation
<p>Isolated Tidal Sand Bar Facies Association (FA3)</p>	<p>Facies 3 (Z3F3) Sand-dominated HS and/or IHS</p>	<p>When observed, in proximal settings this facies is gradationally overlain and underlain by Facies 4, Facies 5, Facies 6 and/or Facies 7; while in distal settings this facies is gradationally overlain by either Facies 6 or Facies 7</p>	<p>Clean, moderately to well sorted, fine to dominantly medium grained sand with interbedded to interlaminated clay, typically 0.5 cm – 2.5 cm thick. Sharp, undulatory contacts present between laminae or beds. Lesser amounts of v.f. grained sand, organic fragments, and wood fragments can be common. Sed. structures include horizontal planar, low angle parallel, wavy to rippled laminae. Sand layers dip at ~2-3° at two locales. The typical thickness of Facies 3 is 25 cm – 65 cm, however it can be as low as 10 cm to 15 cm.</p>	<p>Bioturbation appears absent.</p>	<p>Central sandy tidal bar to tidal bar margin</p>
	<p>Appendix B Core Figure Reference(s): B-7; B-10; B-13; B-14</p>	<p>Depending on sub-environment Facies 4 is: gradationally to abruptly overlain or underlain by Facies 6 or Facies 3; abruptly overlain by Facies 7 and abruptly underlain by Facies 6; and finally gradationally overlain by either Facies 6 or 7, and gradationally underlain by Facies 2</p>	<p>The muddy sand dominantly appears massive to biogenically reworked, but can also display planar, to inclined planar, to wavy and rippled laminae. Rare shell fragments and locally abundant wood fragments can be found. Sporadic lenses of clay may also be observed. The facies is 15 cm to 40 cm in thickness and dominated by muddy fine to medium grained sand.</p>	<p>Bioturbation is usually absent but can be locally abundant, although traces are indiscernible.</p>	<p>Central muddy tidal bar</p>
<p>Table 2-3 (continued): Summary of Facies Characteristics for Isolated Tidal Sand Bar (Zone 3)</p>					

Facies Association	Facies	Facies Contacts	Sedimentary Characteristics	Neochronological Characteristics	Interpretation
Isolated Tidal Sand Bar Facies Association (FA3)	Facies 5 (Z3F5) Laminated organic rich sand Appendix B Core Figure Reference(s): B-10	Facies 5 is gradational with Facies 3.	Typically only 5 cm to 20 cm thick and is dominated by planar to rippled, organic rich laminae in dominantly fine sand. Abundant wood fragments can also be present.	Bioturbation absent.	Tidal creek to central muddy tidal bar
	Facies 6 (Z3F6) Massive sand Appendix B Core Figure Reference(s): B-6; B-7; B-8; B-9; B-11; B-13	Complex facies relations with other facies. Facies 6 is observed to be gradational to abrupt with underlying Facies 3, 4, or 7 and overall abrupt with overlying Facies 2, 4 and 7.	Clean, well sorted, fine to medium grained massive sand dominates. Wood clasts are rare to common. Shell fragments sporadic. Wood and shells may form a lag. Very rare thin clay or silt laminae associated with potential faint ripples. The thickness of Facies 6 observed in vibracores ranges greatly but is typically between 20 cm to 50 cm thick, however intervals up to 100 cm – 140 cm are not uncommon.	Bioturbation is common, but generally indiscernible as to classifying specific traces.	Burrowed central tidal bar to bar margin
	Facies 7 (Z3F7) Planar to rippled sand Appendix B Core Figure Reference(s): B-6; B-8; B-9; B-10; B-12; B-14	Complex facies relations with other facies. Facies 7 is underlain by any of the previous six facies of Zone 3, while it is overlain by Facies 3 through 6, with all contacts being mainly gradational	Planar, low angle to wavy and rippled laminae in clean, fine to medium grained sand characterizes Facies 7. Clay laminae, wood fragments and shell fragments are sporadically encountered. A slightly mottled texture observed locally. Facies 7 is typically 10 cm to 20 cm thick in core but is occasionally witnessed to be up to 60 cm, and even as high as 120 cm thick.	A mottled texture may be apparent in some intervals and may indicate sporadic bioturbation, otherwise bioturbation is largely, if not wholly, absent from Facies 7.	Tidal bar margin

Table 2-3 (continued 2): Summary of Facies Characteristics for Isolated Tidal Sand Bar (Zone 3)

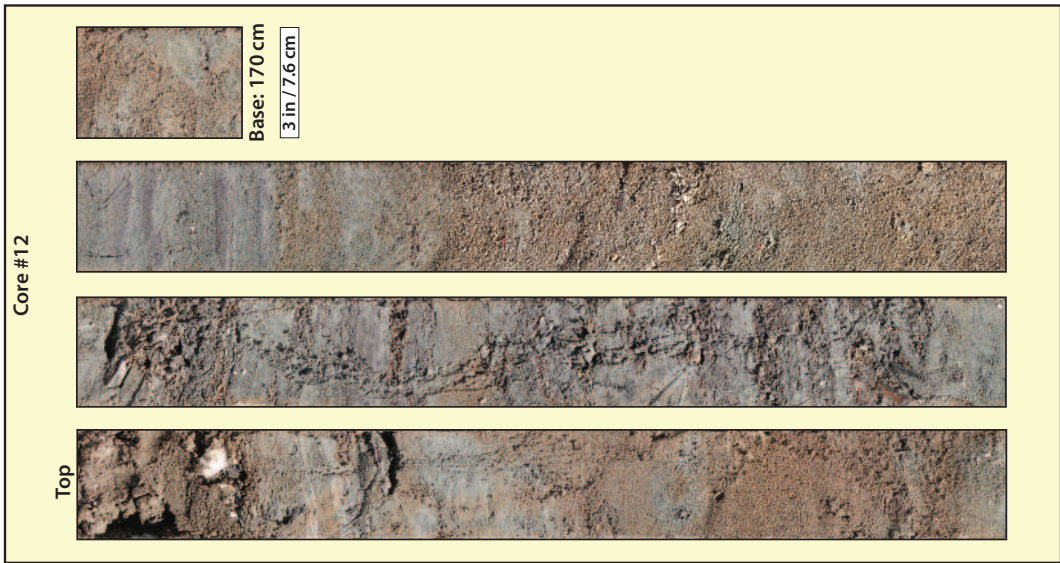
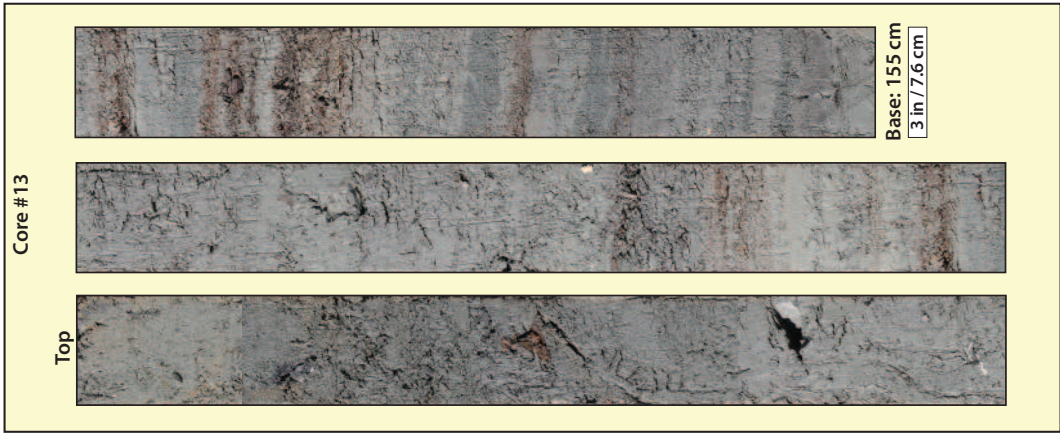
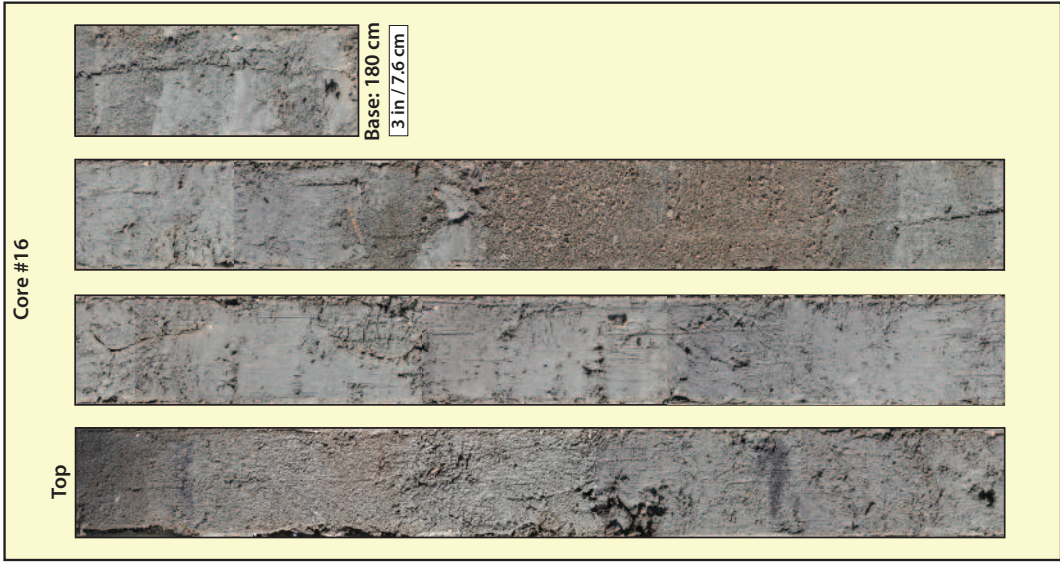
Zone 3 Facies 1 (Z3F1) – Massive to planar laminated clay and silt

Facies 1 is only observed in the most (seaward) vibracore from Zone 3 (Fig. 2-42 Part I; Fig 2-42 Part II; Fig. 2-42 Part III; Figure 2-43; Table 2-3). Thickness of Facies 1 is 65 cm with the silt portion typically 5 cm to 15 cm thick and the clay portion between silt 2.5 cm to 5 cm thick. The clay portion, however, is the most dominant grain size within Facies 1 and consists of a continuous 30 cm thick sequence of planar laminated clay. The silt interval is reworked by bioturbation, with sporadic occurrences of bioturbation in clay interbedded with silt as well. Bioturbation is absent to locally abundant. *Planolites*-like traces dominate these bioturbated silt intervals. Another possible vertical burrow, 1 cm in diameter and 5-6 cm long, appears in the planar laminated clay and is infilled by sand from overlying Facies 7. Underlying Facies 3 gradually transitions into this facies, while there is an abrupt but indistinct change from Facies 1 into overlying Facies 7 above.

Zone 3 Facies 2 (Z3F2) – Mud-dominated HS and/or IHS

Facies 2 is found in vibracores from the algae-stabilized muddy sand deposits sub-environment to the distal reaches of the rippled muddy sand deposits sub-environment (Fig. 2-42 Part I; Fig 2-42 Part II; Fig. 2-42 Part III; Figure 2-43; Table 2-3). This facies ranges in thickness from 50 cm to 120 cm. Massive to planar laminated clay dominates the sequence and can be up to 20 cm thick without interruption from sand laminae or beds. Clean, fine to dominantly medium grained sand commonly occurs as laminae within the clay, but can be up to 10 cm thick, especially in basal parts of the facies. The sand present is usually massive in appearance, possibly due to biogenic reworking, or can be occasionally planar laminated to rippled, especially in the finer grained portions. Wood fragments are common in the clay portion, with up to 40-60% of the portion being composed of wood fragments. Bioturbation is absent to sparse. *Planolites*-like burrows are evident at some locales in basal portions of this facies occurrence. A possible sand-infilled, 1 cm in diameter

Figure 2-43. Core examples from the inner estuary Zone 3. A large variation of sedimentary bedding styles and sediment character is observed in sediments of the isolated tidal sand bar, or Zone 3. Core 12: heterolithic stratification, in the form of sand, muddy sand, and mud interbeds is observed in the lower half of the core. A relatively high percentage of sand is observed, as compared to core 13. High organic and wood content is observed in thin lenses and layers. Core 13: note the interbedded sand and mud layers, with high to very high wood fragment content, as well as the massive-appearing muddy sand and sand layer in the top half of the core. Core 16: heterolithic stratification is observed, though not as well developed as that observed in cores 12 and 13. Sand layers and mud and silt layers have a massive appearance, with occasional faintly-observable laminae present. Small, 0.5 cm wide sand-filled burrows are observed in the mud and silt layers.



Thalassinoides-like burrow is evident at one locale in a portion of planar laminated clay. Where Facies 2 is observed, it is sometimes the lowermost facies observed in core and therefore no discernable contact is determined below. However, if present, Facies 7 sometimes underlay Facies 2 where there is a relatively abrupt, but indistinct, contact between the two. Facies 7 can also be found to overlay Facies 2 where the contact between them is still relatively abrupt, but indistinct. Facies 4 can also be seen to overlay Facies 2 at some locales with the contact appearing gradational.

Zone 3 Facies 3 (Z3F3) – Sand-dominated HS and/or IHS

Facies 3 is observed from vibracores obtained proximal to tidal channels in the rippled muddy sand deposits sub-environment (Fig. 2-42 Part I; Fig 2-42 Part II; Fig. 2-42 Part III; Figure 2-43; Table 2-3). The typical thickness of Facies 3 is 25 cm – 65 cm, however it can be as low as 10 cm to 15 cm. Clean, fine to dominantly medium grained sand and interbedded to interlaminated clay, typically 0.5 cm – 2.5 cm thick (up to 7 cm thick), characterizes the facies. The sand is moderately to well sorted. Sharp, undulatory contacts are usually present between laminae or beds within this facies. There are subordinate fractions of very fine grained sand where organic and wood fragments (up to 20% in abundance) become common. Sand dominated IHS may have horizontal planar, low angle parallel, wavy to rippled laminae in the fine sand portions or appear massive. Sand layers were observed dipping at approximately 2-3° at two locales. Bioturbation appears absent. When observed in proximal settings this facies is gradationally overlain and underlain by Facies 4, Facies 5, Facies 6 and/or Facies 7. When observed in more distal settings this facies is gradationally overlain by either Facies 6 or Facies 7, but is usually the lowermost facies observed in vibracore so a lower contact cannot be established.

Zone 3 Facies 4 (Z3F4) – Muddy sand

Facies 4 is observed in vibracores that cross the whole range of sub-environments witnessed in Zone 3 (Fig. 2-42 Part I; Fig 2-42 Part II; Fig. 2-42 Part III; Figure 2-43; Table 2-3). The facies is 15 cm to 40 cm in thickness and dominated by muddy fine to medium grained sand. The muddy sand dominantly appears massive to biogenically reworked, but can also display planar, to inclined planar, to wavy and rippled laminae. Rare shell fragments and locally abundant wood fragments can be found. Sporadic lenses of clay may also be observed. Bioturbation is usually absent but can be locally abundant, although traces are indiscernible. In the channel-flanked, transverse-rippled deposits sub-environment Facies 4 is gradationally to abruptly overlain or underlain by Facies 6 or Facies 3. Facies 4 is the lowermost core at one locale within the aforementioned sub-environment and therefore no discernable contacts are seen. In the rippled muddy sand deposits sub-environment Facies 4 is abruptly overlain by Facies 7 and abruptly underlain by Facies 6. In the algae-stabilized muddy sand deposits sub-environment Facies 4 is gradually overlain by either Facies 6 or 7, and gradually underlain by Facies 2.

Zone 3 Facies 5 (Z3F5) – Laminated organic rich sand

Facies 5 is observed to occur solely in channel adjacent core 12 from the rippled muddy sand deposits sub-environment of Zone 3 (Fig. 2-42 Part I; Fig 2-42 Part II; Fig. 2-42 Part III; Figure 2-43; Table 2-3). It is typically only 5 cm to 20 cm thick and is dominated by planar to rippled, organic rich laminae in dominantly fine sand. Abundant wood fragments can also be present. Bioturbation is absent. Facies 5 is gradational with Facies 3.

Zone 3 Facies 6 (Z3F6) – Massive sand

Facies 6 is observed in vibracores that cross the whole range of sub-environments witnessed in Zone 3 (Fig. 2-42 Part I; Fig 2-42 Part II; Fig. 2-42 Part

III; Figure 2-43; Table 2-3). The thickness of Facies 6 observed in vibracores ranges greatly but is typically between 20 cm to 50 cm thick, however intervals up to 100 cm – 140 cm are not uncommon. Clean, well sorted, fine to medium grained massive sand characterizes this facies. Wood clasts are rare to common and sporadic shell fragments are also observed. Very rare thin clay laminae or possible ripples associated with silty lenses may have been observed in a couple 2 cm to 4 cm thick intervals. Wood clasts and shell fragments may form lags in generally medium grained sand associated with potential silty, or finer grained, laminae directly above. Bioturbation is common, but generally indiscernible as to classifying specific traces. The relationship of Facies 6 with other facies of Zone 3 is complex since it is so prevalent. Facies 6 is occasionally witnessed as the uppermost or lowermost facies in core and thus no observation of upper or lower contacts can be made. However, Facies 6 is observed to be gradational to abrupt with underlying Facies 3, 4, or 7 and overall abrupt with overlying Facies 2, 4 and 7.

Zone 3 Facies 7 (Z3F7) – Planar to rippled sand

Facies 7 is observed in vibracores that cross the whole range of sub-environments witnessed in Zone 3 (Fig. 2-42 Part I; Fig 2-42 Part II; Fig. 2-42 Part III; Figure 2-43; Table 2-3). Facies 7 is typically 10 cm to 20 cm thick in core but is occasionally witnessed to be up to 60 cm, and even as high as 120 cm thick. Planar, low angle to wavy and rippled laminae in clean, fine to medium grained sand characterizes Facies 7. Clay laminae, wood fragments and shell fragments are sporadically encountered. A mottled texture may be apparent in some intervals and may indicate sporadic bioturbation, otherwise bioturbation is largely, if not wholly, absent from Facies 7. Like Facies 6, Facies 7 is ubiquitous throughout Zone 3 and thus its relationship with other facies of this zone is complex. Facies 7 is usually gradational with other facies. In some distal portions Facies 7 appears at the top of the cored intervals and therefore no

upper contact is observed. Facies 7 is underlain by any of the previous six facies of Zone 3, while it is overlain by Facies 3 through 6.

Zone 3: Isolated Tidal Sand Bar Interpretations

The seven facies described for the Isolated Sand Bar (Zone 3) are interpreted as: Facies 1 (Z3F1: Tidal creek to mud-dominated bar surface); Facies 2 (Z3F2: Central muddy tidal bar to tidal bar margin); Facies 3 (Z3F3: Central sandy tidal bar to tidal bar margin); Facies 4 (Z3F4: Central muddy tidal bar); Facies 5 (Z3F5: Tidal creek to central muddy tidal bar); Facies 6 (Z3F6: Burrowed central tidal bar to bar margin); and Facies 7 (Z3F7: Tidal bar margin). These interpreted facies comprise the Isolated Sand Bar Facies Association (FA3) (Table 2-3). There is a complex interrelationship between facies. A gradual transition exists from tidal channel flanked sediment (i.e. bar margin) to central bar sediment. This gradual transition is dependent on local current energies, sedimentation rates, and sediment input. Ideally, channel sands would be found at the base of an interpreted idealized vertical succession from the Isolated Sand Bar Zone 3 sequence, progressing up into facies that are interpreted as bar margin sediment up to facies that are interpreted to represent central bar sediment (Figure 2-44, Parts I,II,III). Thus, with respect to the interpreted facies for Zone 3, Facies 2; Facies 3; and Facies 4 are interpreted as being associated with bar margin sediment, occurring right above idealized channel sediment (Figure 2-44, Parts I,II,III). These interpreted facies are gradational up into Facies 6, and finally up into Facies 7, associated with the central bar environment (Figure 2-44, Parts I,II,III). Facies 1 and Facies 5 can occur along any point in the interpreted succession (Figure 2-44, Parts I,II,III).

Sediments of the isolated tidal sand bar vary over a much larger area than those observed in other regions of the inner estuary. The dominant sand component, combined with lower concentrations of mud, facilitates the formation of inclined heterolithic stratification and horizontal heterolithic

Figure 2-44, Part 1. Schematic vertical succession from the proximal end of an inner estuary tidal sand bar. Vertical profile of deposits found in the proximal end of an isolated tidal sand bar, as interpreted from core and surface observations from Tillamook Bay. A fining-upward succession is observed, starting with coarse sand in the channel base, and transitioning into interbedded sand and mud inclined heterolithic stratification in the tidal bar margin. The succession is capped by bioturbated sand and muddy sand deposits on the bar surface, away from the tidal channels that flank the tidal sand bar.

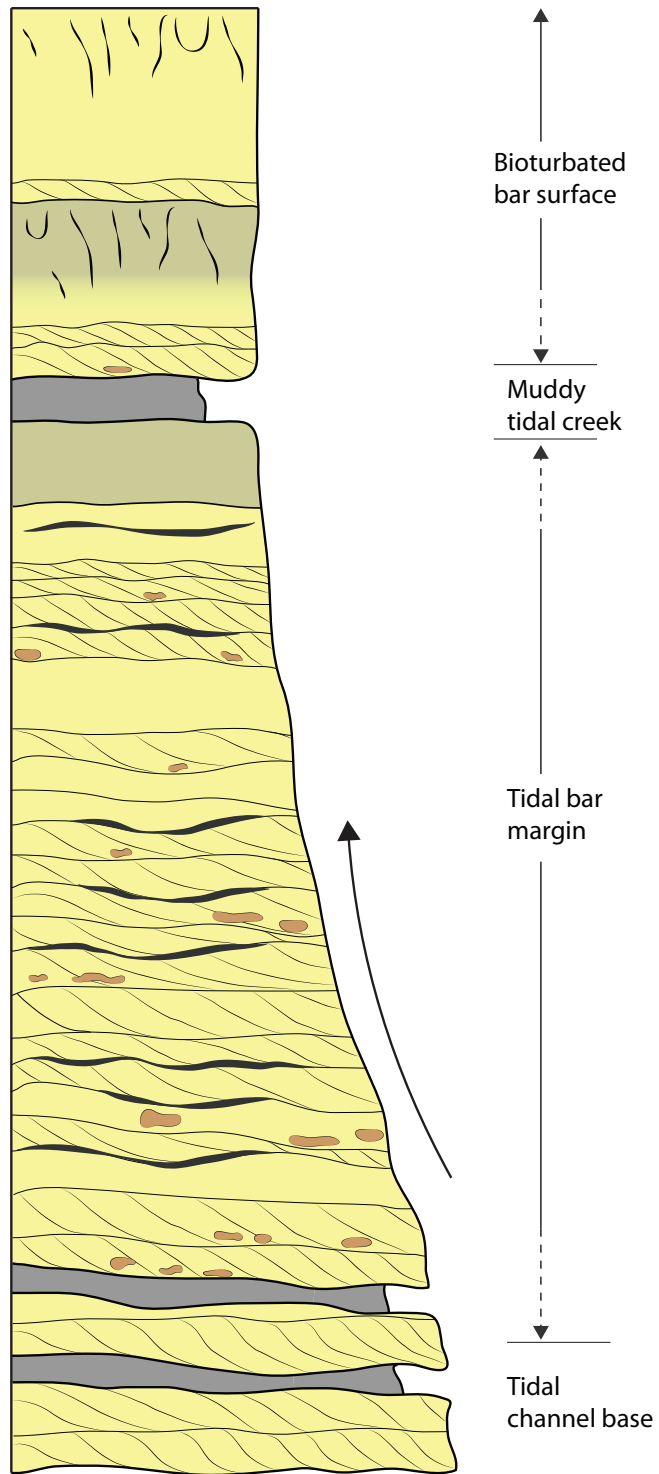


Figure 2-44, Part 2. Schematic vertical succession from the central part of an inner estuary tidal sand bar. Vertical profile of deposits found within the central, muddy region of an isolated tidal sand bar, as interpreted from core and surface observations from Tillamook Bay. Well-developed sand and mud inclined heterolithic stratification (IHS) is observed in interpreted channel-flanked bar margin deposits. Fining- and coarsening-upward successions are observed in the bar margin IHS, and are possibly indicative of laterally migrating tidal channels, and consequently, migrating tidal bar edge. In the central part of the sand bar, an increase in organic and clay content occurs. Bioturbation intensity is also higher in these deposits, as is generally observed in bar surface deposits located away from the tidal channels and bar margins.

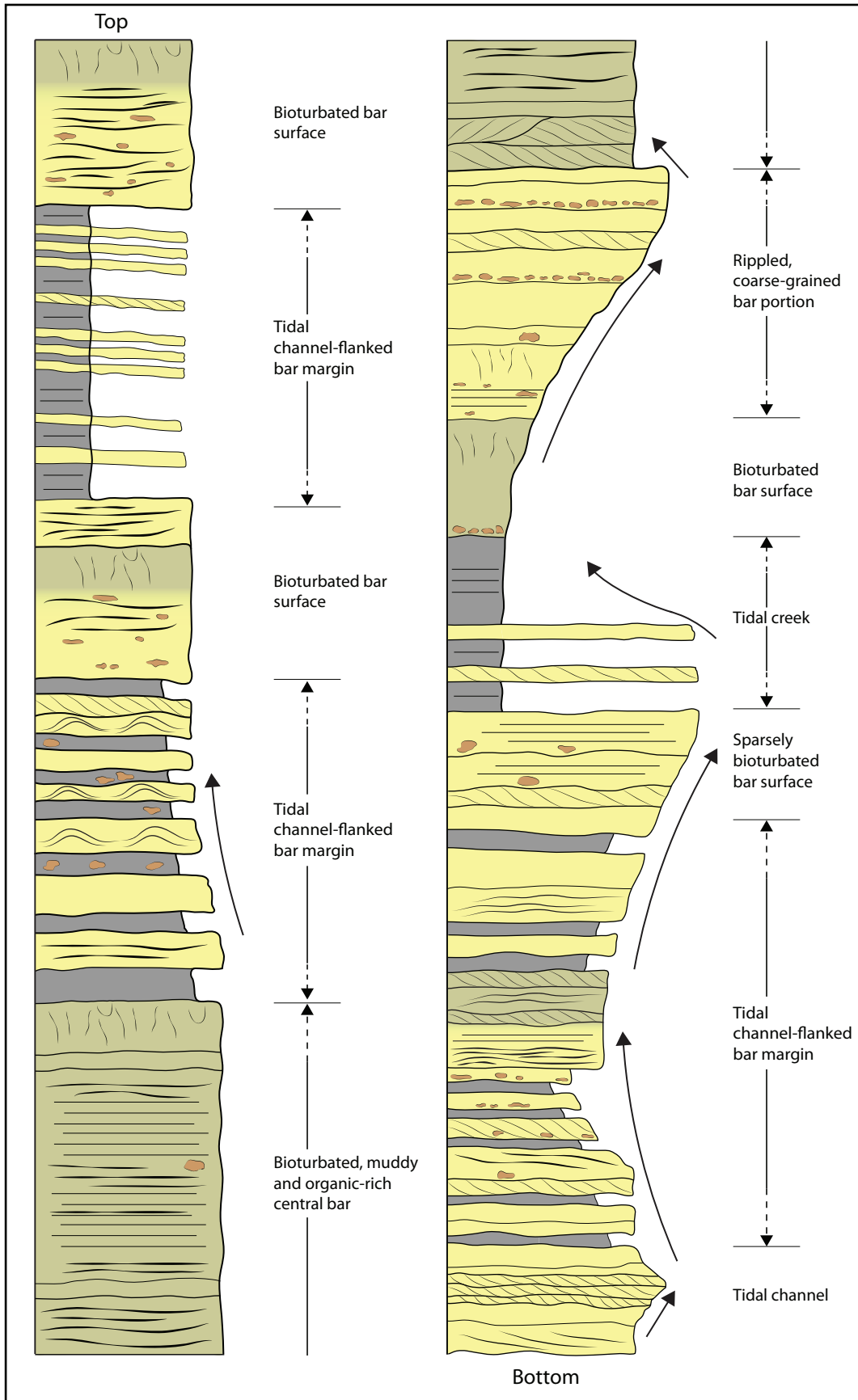
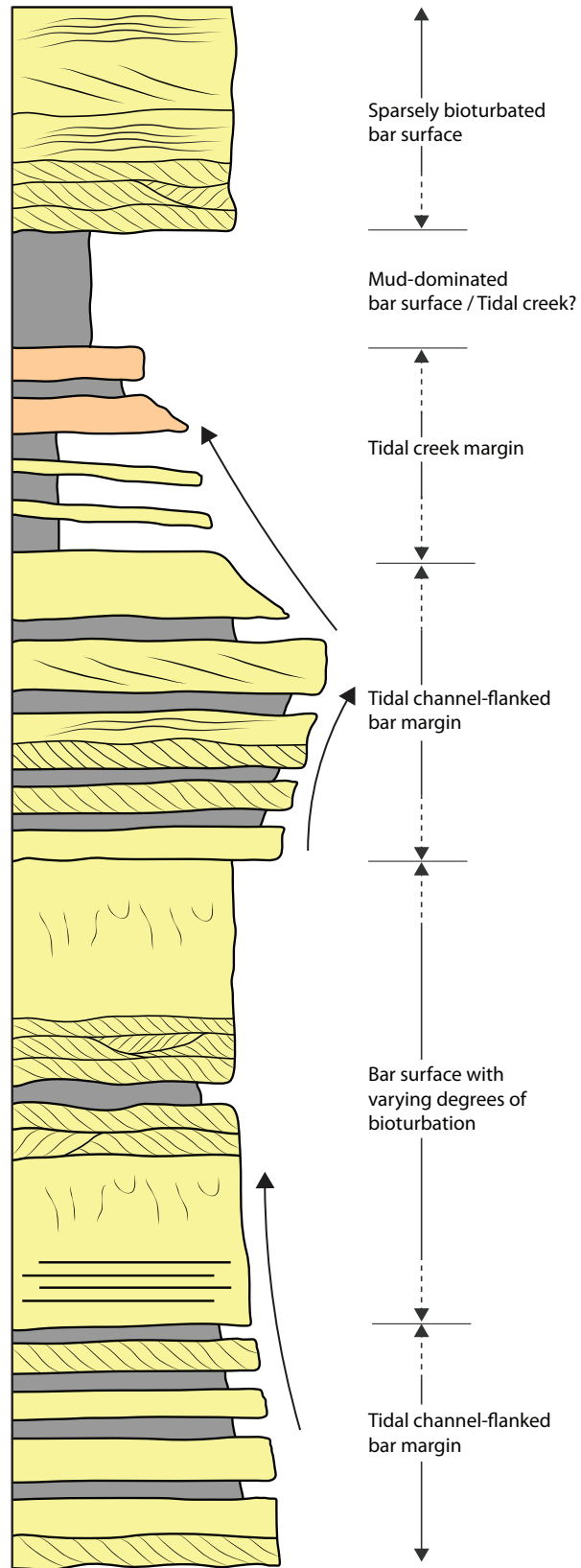


Figure 2-44, Part 3. Schematic vertical succession from the distal end of an inner estuary tidal sand bar. Vertical profile of deposits found in the distal end of an isolated tidal sand bar, as interpreted from core and surface observations from Tillamook Bay. An overall fining-upward succession is observed, with smaller-scale coarsening upward successions present within. Well-developed sand and mud inclined heterolithic stratification is observed in interpreted bar margin deposits, and to a lesser extent in tidal creek margins deposits. Sparsely bioturbated to highly bioturbated sand-dominated bar surfaces overlie bar margin and tidal creek margin inclined heterolithic stratification.



stratification (Figure 2-44; Parts 1 to 3). Muddy facies are common to abundant along various sub-environments of the sand bar. Bioturbation is most abundant in the muddy facies of the central part of the bar. The higher elevation, reduced current energy, muddier content of the sediment, and increased eelgrass abundance of the elevated central bar area likely results in the increased bioturbation witnessed.

The presence of thin mud layers in the deposits of the sand bar result from large storm events in the mountains east of the bay. A high rate of rainfall, erosion, and fluvial sediment load can result in sporadic fluxes of fine-grained material being delivered to the bay during the wet season. The thicker mud layers are likely deposited in a similar fashion. Their thick, massive character, suggests that they are likely the result of rapid depositional events due to sudden increases in fluvial runoff into the bay.

The high rate of fluvial discharge during the winter months can be expected to cause the freshwater to flow over the denser sea water. This factor is complicated by the fact that channels in the inner estuary zone, especially those flowing around the sand bar analyzed, are quite shallow, ranging from 0.5 metres to approximately 2.0 metres in depth, locally, at low tide. As a result, no discernible salinity stratification should be observed in the channels during low tide. However, salinity stratification has been shown to occur in Tillamook Bay, as well as in other bays and estuaries along the Oregon coast (Burt and McAlister, 1958).

The mixing of freshwater and seawater, which results in flocculation of river-derived clay (Middleton, 1980; Chaumillon et al., 2013), creates a salinity node in an estuary. Suspended sediment has a tendency to settle from fresh water into the denser inflowing seawater, producing a turbidity maximum (Amos and Lang, 1980), which does not necessarily coincide with the location of the salinity node at all times through the various seasons.

Though tidal currents are strongest in the main tidal channels, it is obvious from the ebb-oriented current ripples found extensively over the

surface of the sand bar, that tidal currents influence the formation of sedimentary structures. This is not unexpected, as the influence of tidal currents occurs over a continuum, as opposed to areas strictly defined to subtidal hydrographic zones, where currents definitely influence the formation of sedimentary structures. Intertidal sand bars are a continuation of similar forms that occur in subtidal zones (McCann, 1980).

Channel-flanked, transverse-rippled sand

It is highly probable that the presence of a long jetty, constructed in the earlier part of the 20th century, has had an influence on the sedimentation and bioturbation pattern of this sub-environment. The jetty, which runs parallel to, and outlines the eastern edge of the sub-environment as it comes in contact with the Bay City channel, likely promotes the formation of a boundary between the tidal flat and channel edge, which has changed minimally over a period of decades. The high current energies present in the Bay City channel, when coming in contact with the southern edge of the tidal sand bar, are minimally able to erode the banks as they are protected by the jetty pillars. These pillars keep the sediment relatively stable, and reduce the current energies and erosion rates of the bar. Lateral deposition of sediment on the angled bar edge is limited by high current velocities and concomitant sediment removal in the main river channel. As a result, this particular sub-environment is sand-dominated and well-sorted, with negligible mud content. It consists dominantly of fine- to medium-grained, rippled sand. Bioturbation (mostly *Skolithos*- and *Arenicolites*-like burrow), is sparse to common, depending on relative current energy and amount of shifting substrate.

Muddy, tidal creeks that incise into the sand-dominated deposits of this sub-environment form due to the overall flow of tidal creek water into the main river channel during the ebb tide. The muddy character is possibly due to the more quiescent periods experienced during high tide, allowing deposition of

fine sediment portions. Abundant fecal pellets found on the tidal bar can be transported by currents and deposited in the lower-energy tidal creek, to be later redistributed along its length and to increase the overall mud content.

Rippled muddy sand

These deposits occur in an open part of the bay, unobstructed by any artificial barriers. Muddy sand deposits are observed throughout the area, and are dominated by flat-lying, smooth to irregular tidal flat surfaces, with massive texture, as well as high bioturbation intensity and trace diversity. Bioturbation increases away from the tidal channels, in areas where common to abundant algae allow settling of fines and organics, and thus also provide abundant food resources to be exploited by organisms.

Areas of negligible eelgrass amounts are possibly due to stronger currents, particularly along the tapered northern end of the sub-environment, pointing in the ebb-tidal current direction, and terminating in a tidal channel at its northern edge. As a result, during the flood-tidal periods, this area is the first to experience the effect of strong tidal and wave currents flowing through the tidal channel and over the bar surface. Currents reaching the middle of the sand bar are therefore attenuated by the time they reach the respective area, likely allowing for the growth of algae and drastically different sedimentary environments.

Algae-stabilized muddy sand

This sub-environment contains extensive, dense eelgrass coverage over its surface, and, concomitantly, a much higher mud concentration. The effect of the eelgrass in baffling current energies is significant, forming abundant hummocky muddy sand mounds. Sedimentary structures in the form of ripples are, locally, non-existent, due to the effect of muddy mound formation and their lateral migration. Deposition of mud to the inner estuary likely occurs

during the rainy winter months, when total discharge is highest. Freshwater (and suspended fines) transported into the estuary interacts with seawater brought into the estuary by strong flood tidal currents, thus promoting flocculation and deposition. The high concentration of eelgrass on the highest-relief portions of the sand bar are likely due to more quiescent water conditions and even sediment distribution across the surface, where rapid changes in current energies do not occur (Middleton, 1980).

Closer to the sub-environment edge, sinuous to linguoidal combined-flow ripples occur, commonly with abundant fecal pellets accumulated in the ripple troughs. Such accumulations of fecal pellets, when later buried and compacted, may form biogenically-mediated flaser bedding. In the rock record, such biogenic flaser bedding may be impossible to distinguish from “regular” flaser bedding; the flattening and compression of modern fecal pellets results in the “deposition” of mud in the troughs, and destruction of the original pellet morphology. The hydrodynamic significance of flaser beds of this type is high but has not yet been investigated in detail.

Zone 4: Mud and Muddy Sand Flats Descriptions and Results

Sedimentological and Neoichnological Features

This zone is a small area where vibracores are collected from. It is not studied in detail (i.e. descriptions and observations of sedimentary and biogenic structures); therefore it is only briefly mentioned here. The zone consists of mud-dominated tidal flats, extending to the southern, forested shoreline of the bay. From aerial views, a complex network of tidal creeks can be observed on its surface, draining the area to the South Channel (Fig. 2-45 A,B,C). Near the very edge of the tidal flats, along the shoreline, the sediment layers appear to have the highest mud content. Relative sand concentration increases away from the shoreline towards the South Channel. In vibracores

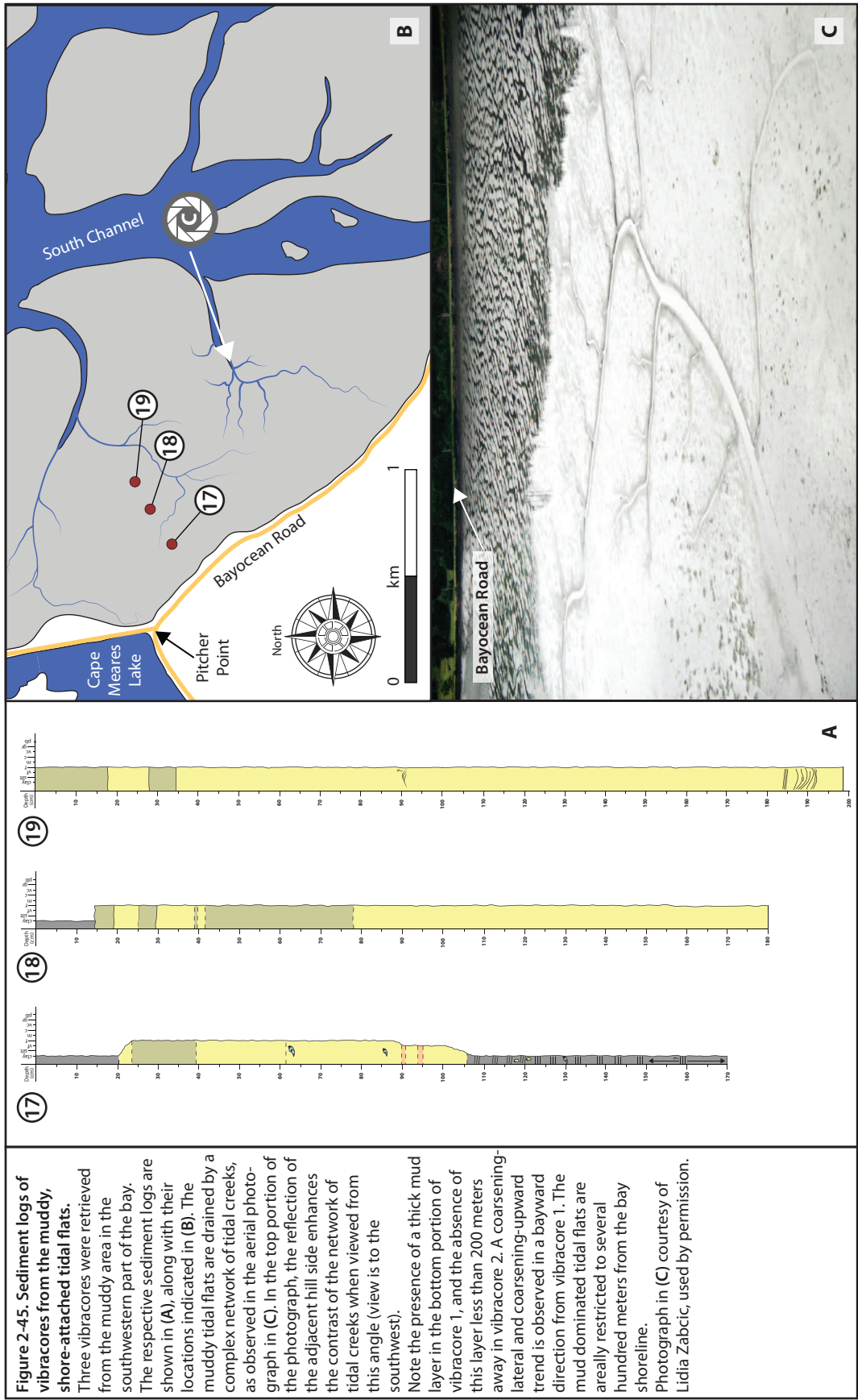


(Fig. 2-45 A,B,C; Fig. 2-46 A,B,C,D,E), it can be observed that the thickest mud layers are observed near the shoreline. Muddy sand layers occur in a bayward direction.

Zone 4: Mud and Muddy Sand Flats Vibracore Facies Descriptions

A total of three cores were recovered from Zone 1, with each recovered core ranging from 170 cm – 198 cm in length. Four facies are identified from the Mud and Muddy Sand Flats (Zone 4) according to distinct sedimentary and neoichnological characteristics. These facies are summarized in Table 2-4, with supplementary references to vibracore logs located in Appendix B.

Zone 4 Facies 1 (Z4F1) – Massive to planar-and/or low-angle-laminated mud

Facies 1 occurs in most vibracore from Zone 4, but is not found in the outermost, distal core (Fig. 2-45; Fig. 2-46; Fig. 2-47; Table 2-4). The thickness of Facies 1 decreases bayward towards these more distal areas. In proximal areas Facies 1 is 20 cm to 65 cm thick, decreasing to about 15 cm thick in the uppermost reaches of more distal core, before becoming absent in the most distal core. Facies 1 is defined by massive to planar- and/or low-angle-laminated grey mud. Massive clay usually occurs in the uppermost portions of retrieved vibracore with faint to distinct planar to low angle laminae observable in Facies 1 from deeper cored intervals. Shell fragments are sporadic and although bioturbation is largely absent, there is a rare occurrence of possible sand-filled burrows, 1 cm in diameter. In proximal core Facies 1 defined the upper- and lower-most facies and therefore does not have an upper or lower contact associated with those areas, respectively. However, Facies 1 appears to quickly, but indistinctly transition into Facies 3 located in the middle of the proximal core observed. Progressing to more distal core Facies 1 only occurs in the uppermost vibracored interval and thus has no

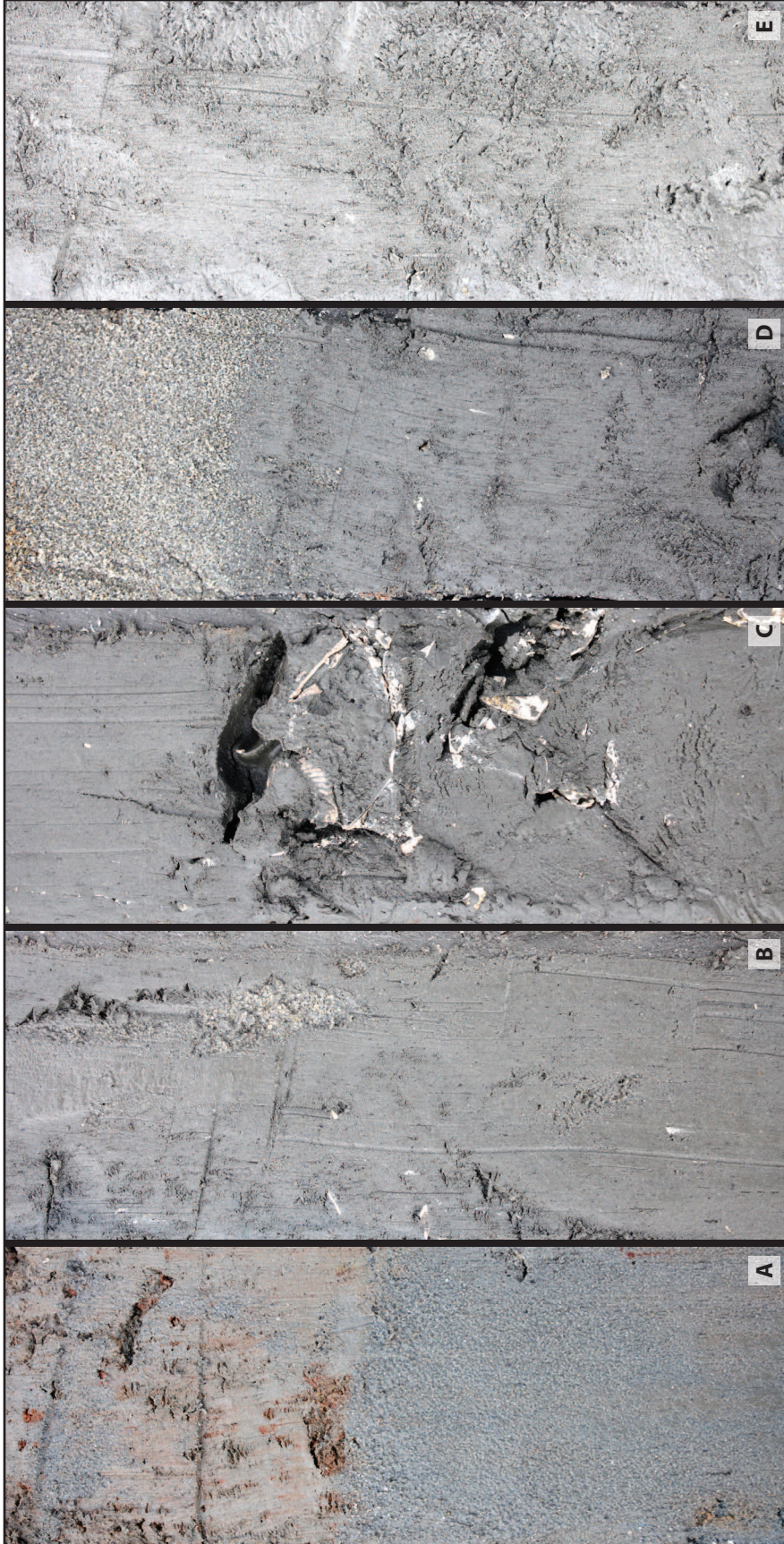
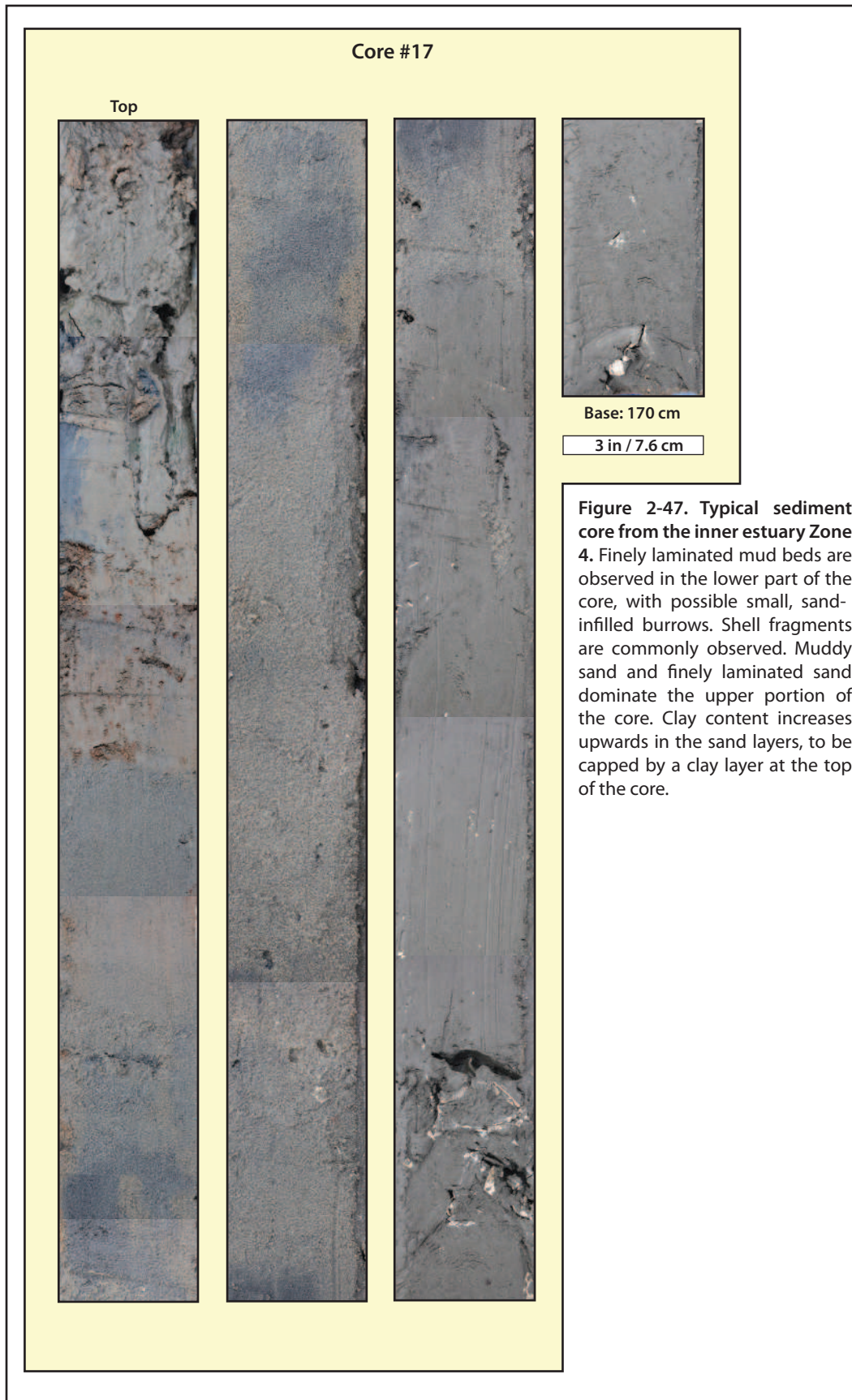


Figure 2-46. Vibracore examples from Zone 4. Examples of the typical sedimentary features observed in vibracores from Zone 4. From left to right, the first three photos from core 17 show muddy sand (A and B) and mud-dominated (C) beds. Note the brown-colored layer, rich in organics, that overlies the muddy sand layer in A, as well as a possible sand-filled burrow in B. Cross-sectionally split cockle clam shell fragments can be seen within the mud layer in C. Clean, well-sorted sand from core 20 is seen in photo D, where it overlies a silty sand to silt-dominated layer. The silt-dominated layer can be seen lower in core 20, as shown in photo E. Long grooves seen in some photos are the result of strings of aluminum that formed during the cutting and splitting of the core, and that could not be removed after smoothing of the core surface.



Facies Association	Facies	Facies Contacts	Sedimentary Characteristics	Neochronological Characteristics	Interpretation
<p>Mud and Muddy Sand Flats Facies Association (FA4)</p>	<p>Facies 1 (Z4F1) Massive to planar-and/or low-angle-laminated mud</p> <p>Appendix B Core Figure Reference(s): B-15; B-16</p>	<p>If observable, Facies 1 appears to quickly, but indistinctly transition into Facies 3. In distal cores Facies 1 only occurs in the uppermost vibracored interval and thus has no discernable upper contacts, and is usually sharply bound by underlying Facies 2.</p>	<p>Facies 1 is defined by massive to planar-and/or low-angle-laminated grey mud. Massive clay usually occurs in the uppermost portions of retrieved vibracore with faint to distinct planar to low angle laminae observable in Facies 1 observed deeper in cored intervals. Shell fragments are sporadic. The thickness of Facies 1 decreases bayward towards these more distal areas. In proximal areas Facies 1 is 20 cm to 65 cm thick, decreasing to about 15 cm thick in only upper reaches of more proximal core, before becoming absent in the most proximal core.</p>	<p>Bioturbation is rare to absent. There is a rare occurrence of possible sand-filled burrows, 1 cm in diameter.</p>	<p>Tidal creek to mud-dominated tidal flat</p>
	<p>Facies 2 (Z4F2) Muddy sand</p> <p>Appendix B Core Figure Reference(s): B-15; B-16; B-17</p>	<p>Facies 2 forms a gradational to sharp contact with Facies 3, but sometimes Facies 2 occurs as the uppermost facies observed in core, in distal areas, and therefore no upper contact is discerned. Occasionally, bound by a sharp upper boundary with Facies 1.</p>	<p>Facies 2 is characterized by distinct muddy fine sand. Distinct sedimentary structures are absent. It is typically 5 cm to 35 cm thick.</p>	<p>Bioturbation is absent.</p>	<p>Tidal creek to muddy tidal flat</p>

Table 2-4: Summary of Facies Characteristics for Mud and Muddy Sand Flats (Zone 4)

Facies Association	Facies	Facies Contacts	Sedimentary Characteristics	Neoichnological Characteristics	Interpretation
<p>Mud and Muddy Sand Flats Facies Association (FA4)</p>	<p>Facies 3 (Z4F3) Massive Sand</p>	<p>Facies 3 has no observable contact in distal cores, and is sharply overlain by either Facies 1 of 2. In muddier proximal cores Facies 3 is bound above and below by a transitional, but rapid contact into Facies 1.</p>	<p>Facies 3 is defined by the presence of massive, clean, fine grained sand. There are no discernable sedimentary features associated with this facies, but rare shell fragments can appear interspersed within it. Intervals of Facies 3 can be as little as 10 cm thick but generally it occurs in much thicker packages and can be up to 140 m thick.</p>	<p>Bioturbation appears absent.</p>	<p>Possibly bioturbated sand flat to tidal channel-adjacent sediments</p>
	<p>Facies 4 (Z4F4) Laminated Sand</p>	<p>Occasionally there is no lower contact for Facies 4, as it is the most basal unit observed at one locale, but otherwise Facies 4 is bound by Facies 3 and is transitional with this facies.</p>	<p>When present, Facies 4 is up to 10 cm thick and appears gradually continuous with the clean, fine grained sand of Facies 3. Slightly inclined planar laminae characterize Facies 4. Weakly laminated areas are also present. Possible soft sediment deformation and rare potential ripples are also observed.</p>	<p>Bioturbation is absent.</p>	<p>Sand flat to tidal channel-adjacent sediments</p>
<p>Appendix B Core Figure Reference(s): B-15; B-16; B-17</p>					
<p>Appendix B Core Figure Reference(s): B-15; B-17</p>					

Table 2-4 (continued): Summary of Facies Characteristics for Mud and Muddy Sand Flats (Zone 4)

discernable upper contacts, and is usually sharply bound by underlying Facies 2.

Zone 4 Facies 2 (Z4F2) – Muddy sand

Small intervals of Facies 2 is evident in all vibracore observed from Zone 4 (Fig. 2-45; Fig. 2-46; Fig. 2-47; Table 2-4). It is typically 5 cm to 35 cm thick. Facies 2 is characterized by distinct muddy fine sand. Distinct sedimentary and bioturbation structures are absent. Facies 2 typically forms a gradational to sharp contact with Facies 3, but sometimes Facies 2 occurs as the uppermost facies observed in core, in distal areas, and therefore no upper contact is discerned. Occasionally, it is bound by a sharp upper boundary with Facies 1.

Zone 4 Facies 3 (Z4F3) – Massive Sand

Facies 3 is the most prevalent facies of Zone 4 and occurs in all vibracore, becoming increasingly common bayward (to more distal areas) (Fig. 2-45; Fig. 2-46; Fig. 2-47; Table 2-4). Intervals of Facies 3 can be as little as 10 cm thick but generally it occurs in much thicker packages and can be up to 140 m thick. Facies 3 is defined by the presence of massive, clean, fine grained sand. There are no discernable sedimentary features associated with this facies, but rare shell fragments can appear interspersed within it. Bioturbation appears absent. In more distal locations Facies 3 does not have a lower contact as it is the lowermost facies observed in vibracore; however it is usually sharply overlain by either Facies 2 or Facies 1. In proximal locations, where muddier sediment is more prevalent, Facies 3 is bound on the top and bottom by a transitional, but rapid, contact into Facies 1.

Zone 4 Facies 4 (Z4F4) – Laminated Sand

Facies 4 is a thin, but distinct facies, within otherwise massive sand and can be found sporadically throughout distal to proximal core of Zone 4 (Fig. 2-45; Fig. 2-46; Fig. 2-47; Table 2-4). When present, Facies 4 is up to 10 cm thick and

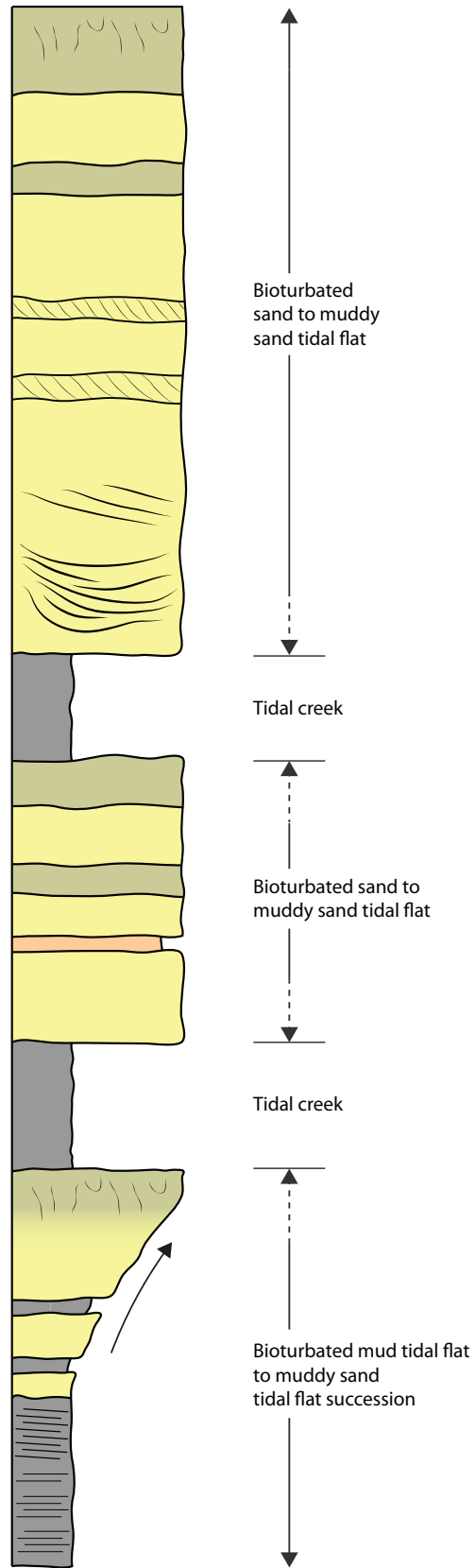
appears gradually continuous with the clean, fine grained sand of Facies 3. Slightly inclined planar laminae characterize Facies 4. Weakly laminated areas are also present. Possible soft sediment deformation and rare potential ripples are also observed. Bioturbation is absent. Occasionally there is no lower contact for Facies 4, as it is the most basal unit observed at one locale, but otherwise Facies 4 is bound by Facies 3 and is transitional with this facies.

Zone 4: Mud and Muddy Sand Flats Interpretations

The four facies described for the Mud and Muddy Sand Flats (Zone 4) are interpreted as: Facies 1 (Z4F1: Tidal creek to mud-dominated tidal flat); Facies 2 (Z4F2: Tidal creek to muddy tidal flat); Facies 3 (Z4F3: Possibly bioturbated sand flat to tidal channel-adjacent sediments); and Facies 4 (Z4F4: Sand flat to tidal channel-adjacent sediments). These interpreted facies comprise the Mud and Muddy Sand Flats Facies Association (FA4) (Table 2-4). The interpreted idealized vertical succession from the Mud and Muddy Sand Flats (Zone 4) ideally consists of a full sequence displaying a gradational change from proximal-to-shore mud (Facies 1 and Facies 2) up to sandier facies, near tidal channel sediments (Facies 3 and Facies 4) (Fig. 2-48).

As has been observed from other shore-attached tidal flats in Tillamook Bay (e.g. sheltered, quiescent area between Goose Point and Kilchis Point), silt and clay tends to be trapped and deposited where tidal and wave currents are slowed down by the shoreline. The location of this zone, at the southwesterly part of the bay, though not necessarily protected by strong currents, does indicate – as interpreted in Figure 2-48 - a change in bay shoreline orientation, starting at Pitcher Point (Fig. 1-2; Part II). As wave and tidal currents are dominantly oriented towards the south during flood tide, these currents are expected to be slowed down, and possibly even refracted to the southwest. This zone contains a high percentage of mud, likely due to the slowing down of currents transporting suspended sediment in the water column. Due to the

Figure 2-48. Schematic vertical succession from a muddy tidal flat succession. Vertical profile of muddy tidal flat deposits, as interpreted from core and surface observations from Tillamook Bay. Sand and muddy sand tidal flat successions are observed within the vertical profile, constructed from three vibracores. Sedimentary structures are generally sparse, and are a possible indication of high bioturbation intensity resulting in their obliteration, as well as the mixing of the sand and mud layers into more homogeneous layers. Numerous tidal creeks incise the tidal flat deposits of Zone 4, where the current succession is interpreted from. High mud accumulations observed in tidal creeks lead to the interpretation of thick mud layers as being of probable tidal creek origin. Extensive mud deposits, likely distributed over the area of the tidal flat by tidal current, can, however, also be observed in the region, and are another possible interpretation.



proximity of the zone to the Bayocean Peninsula storm breach of 1952, it is probable that some of the sand is beach-derived as a result of the breach. However, a distinct surface (i.e. an erosional surface or abrupt change in sediment character) was not noted.

Middle Estuary Characteristics

Zone 5: Marginal Tidal Flats Descriptions and Results

Sedimentological and Neoichnological Features of Zone Sub-environments

The Middle Estuary Zone 5 examined in this study is located along the western margin of Tillamook Bay, directly adjacent to Bayocean Peninsula (Fig. 2-49). It is bound to the east by the South Channel, and to the west by the consolidated dunes of the peninsula. At its southern and northern ends, it gradually transitions into muddier sediments of the inner estuary and sandy sediments of the outer estuary, respectively. The dune deposits on Bayocean Peninsula are well-stabilized and vegetated, and occur in terraces above estuary intertidal sandy deposits. The anthropogenically-altered terraces, are flanked by large boulders used to stabilize them and prevent erosion. Large drift logs, likely sourced from the peninsula, lay oriented parallel to the tidal flat edge and terraces. Grassy areas cover part of the intertidal flat, and often occur adjacent to the forested area that protrudes eastward into the flats.

Tidal sand flat

Sedimentology-

Although facies do vary in this zone, overall, the sandy, bay-margin intertidal flats examined here show high consistency in terms of grain size and total organic carbon (TOC) distribution, with the main grain size observed

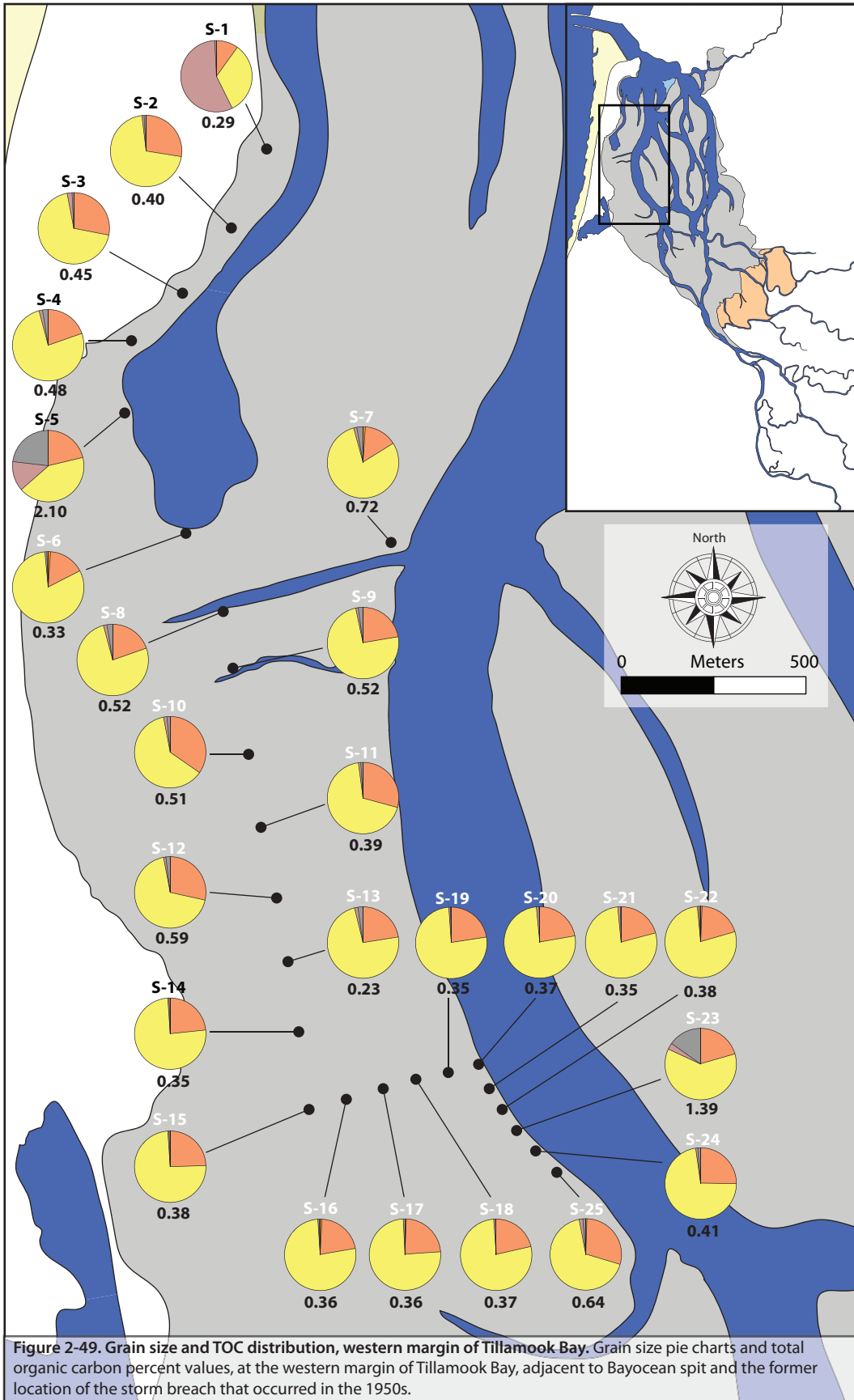


Figure 2-49. Grain size and TOC distribution, western margin of Tillamook Bay. Grain size pie charts and total organic carbon percent values, at the western margin of Tillamook Bay, adjacent to Bayocean spit and the former location of the storm breach that occurred in the 1950s.

being fine sand, and average TOC value being 0.53% (Fig. 2-49). Higher relief portions of the tidal flat, aided by the presence of common grassy areas, exhibit sinuous, nearly symmetrical combined-flow ripples (Fig. 2-50 A,B,C).

High-wavelength, relatively low-relief dunes are observed to form throughout this area. The dunes are oriented in two directions: northwest to southeast, and southwest to northeast, relative to the north-south oriented western margin of the bay (Fig. 2-51 A). They are similar in morphology to ridge and furrow structures, but because of their dual orientation, the term "dune" is preferred here. Wavelengths of the dunes range between approximately 10-15 meters.

Some areas observed have more symmetrical, transverse ripples that are often oriented parallel to sub-parallel to the bay margin (Fig. 2-51 B), and subsequently have an oblique orientation relative to the orientation of the dunes. Stabilized, organic-rich areas (possible algae), give the sediment a muddy appearance, and overlay and destroy ripple structures, forming mounds of sediment higher in organics and troughs. Red algae, although sparse, are observed to give the sediment a brown red coloration.

Neoichnology-

Bioturbation is sparse on the higher relief portions of the tidal flat, but is a common occurrence in the sinuous, nearly symmetrical, low relief rippled sandy tidal flats of Zone 5 (Fig. 2-50 A,B,C,D). These low relief rippled sandy tidal flats contain common to abundant bioturbation, with a large majority of burrows made by the soft-shell clam *Mya arenaria* and the sand shrimp *Neotrypaea californiensis* (Fig. 2-51 C). The level of bioturbation in some areas is high enough to rework the surface ripples, giving the sediment a bumpy texture, especially in the case of mud surface burrows (i.e. shrimp sand volcanoes).

The stabilized, organic-rich areas show abundant bioturbation, though the tracemaker was not observed. A very sharp transition in bioturbation

Figure 2-50. Sedimentary features of the shore-attached tidal flats, western margin, Zone 5. (A) View to the east, showing the burrowed and rippled tidal flat. Note the presence of high-wavelength dunes (outlined by water pooled in the dune troughs), oriented obliquely to the shoreline (present behind the photographer). **(B)** Close-up view of the complex, low-amplitude ripples, with numerous burrow openings observed on the surface. **(C)** View to the north, largely parallel to the shoreline, showing the high-density *Neotrypaea californiensis* surface burrows and associated sand volcanoes. **(D)** Slightly oblique view of the sediment surface, showing the early stages of formation of a bacterial mat; a thin microfilm covers the sediment surface, resulting in the “oily” lustre observed. Note the presence of burrow openings, as well as trackways (tracemaker unknown) or possible water rill marks on the sediment surface.

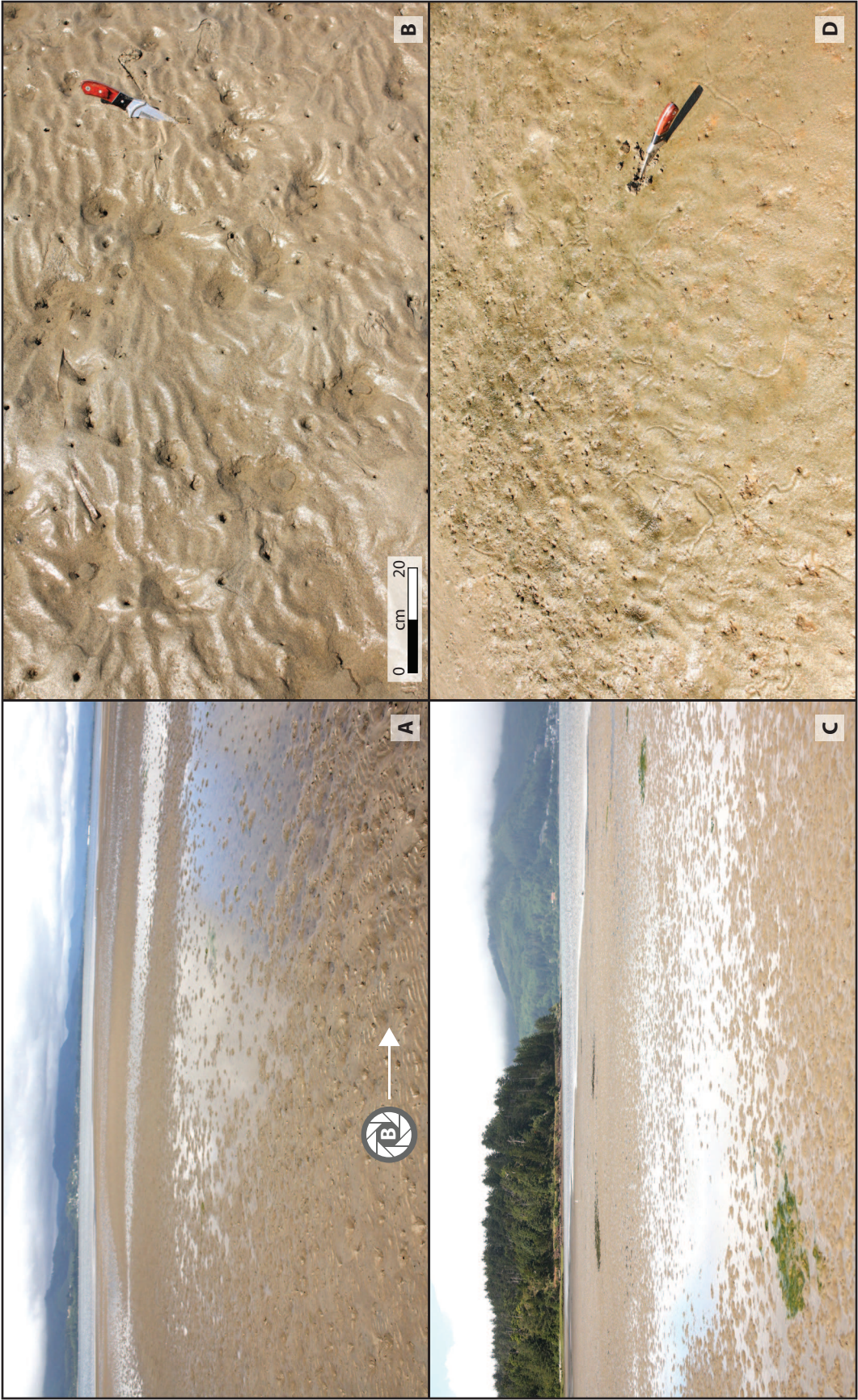
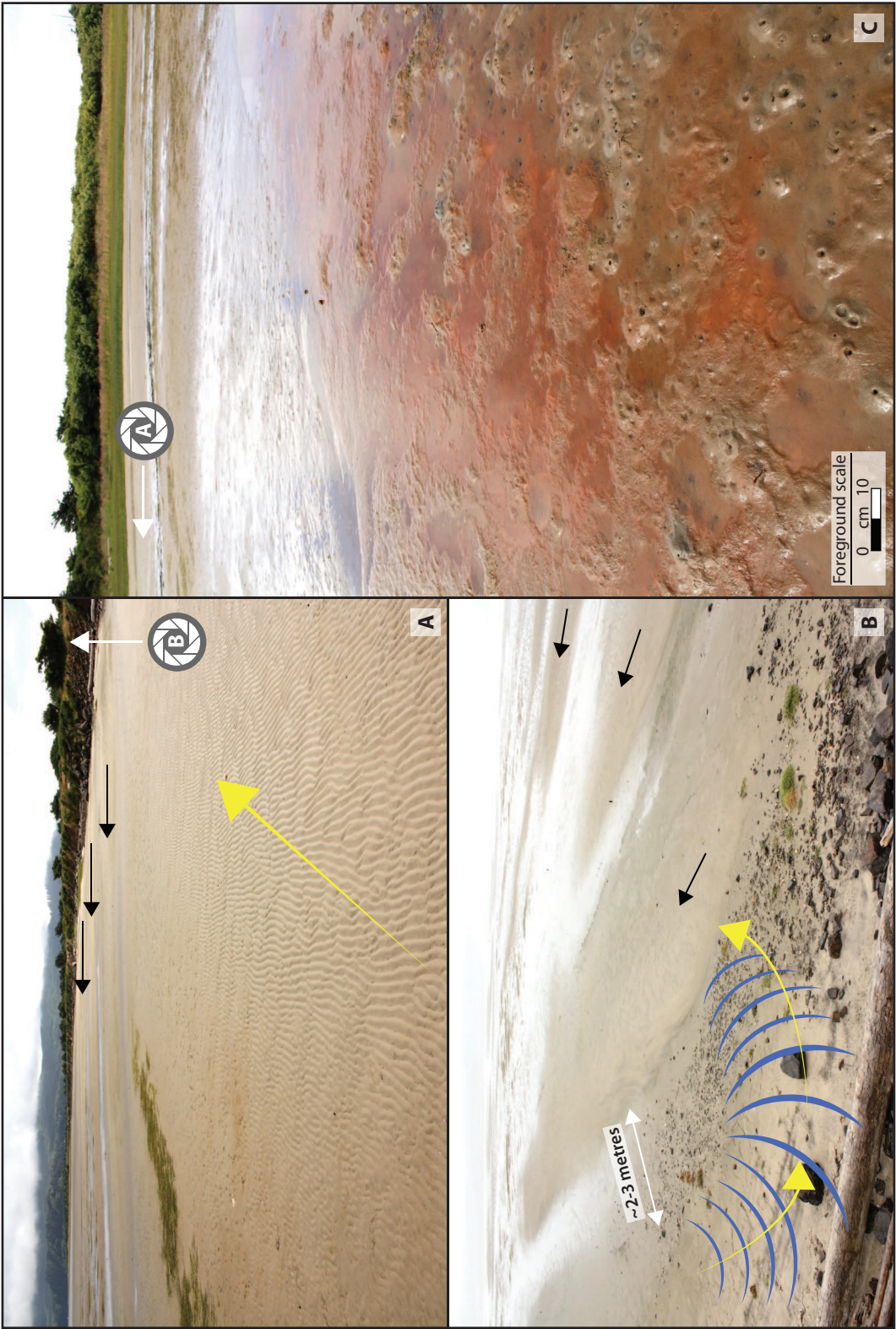


Figure 2-51. Wave refraction and formation of high-wavelength dunes, Zone 5. (A) View to the south, parallel to the shoreline and adjacent Bayocean Spit, observed near the top of the photograph. The yellow arrow indicates the general direction of wave current propagation towards the shoreline; the black arrows indicate the presence of dunes, also observed in (B). Note also the transverse ripples of mixed wave-current origin, and possibly also eolian origin during periods of low tide. (B) View from a higher-relief point on Bayocean Spit, looking east. The bay shoreline edge is present at the bottom of the photograph, near the large log, which is also seen in photo (A). Note the oblique orientation of dunes (black arrows), which are observed from the level of the tidal flat in (A); their orientation is interpreted to result from wave refraction (shown by the blue curved lines) of the wave current propagation (yellow arrow). (C) Burrowed tidal flat between troughs of dunes; note red-colored sediment, likely due to bacterial activity.



intensity occurs from the un-reworked, un-stabilized sediment, to the highly organic, stabilized sediment. Locally, gastropod surface tracks are also observed, commonly in areas of the low-relief, sinuous, asymmetrical ripples, and close to the algae-stabilized sediment (Fig. 2-50 D).

Areally-restricted firmground

Though not initially part of this study, this part of the middle estuary was inspected out of interest where an areally-restricted *Glossifungites* surface is observed. As such, it is passively noted here. Due to a camera malfunction and time constraints, no photos are taken of the *Glossifungites* surface itself. However, a representative sample was collected, as shown in photos from Figure 2-52 (A,A',B,C). The surface observed at this location has a very limited areal extent of approximately 50 m², and the layer is composed of sandy mud and possible peaty material at an average thickness of 4 centimeters.

Burrows are common to abundant, vertical through sub-vertical, through to horizontal, and range from small, millimeter-scale burrows, to larger, centimeter-scale burrows. No burrowing organisms are observed, except for small bivalves emplaced in the firm layer that produce *Gastrochaenolites*-like traces. Other types of burrows observed include *Psilonichnus*-like traces of the hairy shore crab *Hemigrapsus oregonensis* (commonly seen in the area), *Thalassinoides*-like traces produced by the sand shrimp *Neotrypaea californiensis* (common to abundant in the area), and possible sub-vertical *Skolithos*-like traces of spionid worms (Fig. 2-52 A,A',B,C).

Zone 5: Marginal Tidal Flats Vibracore Facies Descriptions

A total of two cores were recovered from Zone 5, with each recovered core ranging from 175 cm – 200 cm in length. Two facies are identified from the Marginal Tidal Flats (Zone 5) according to distinct sedimentary and

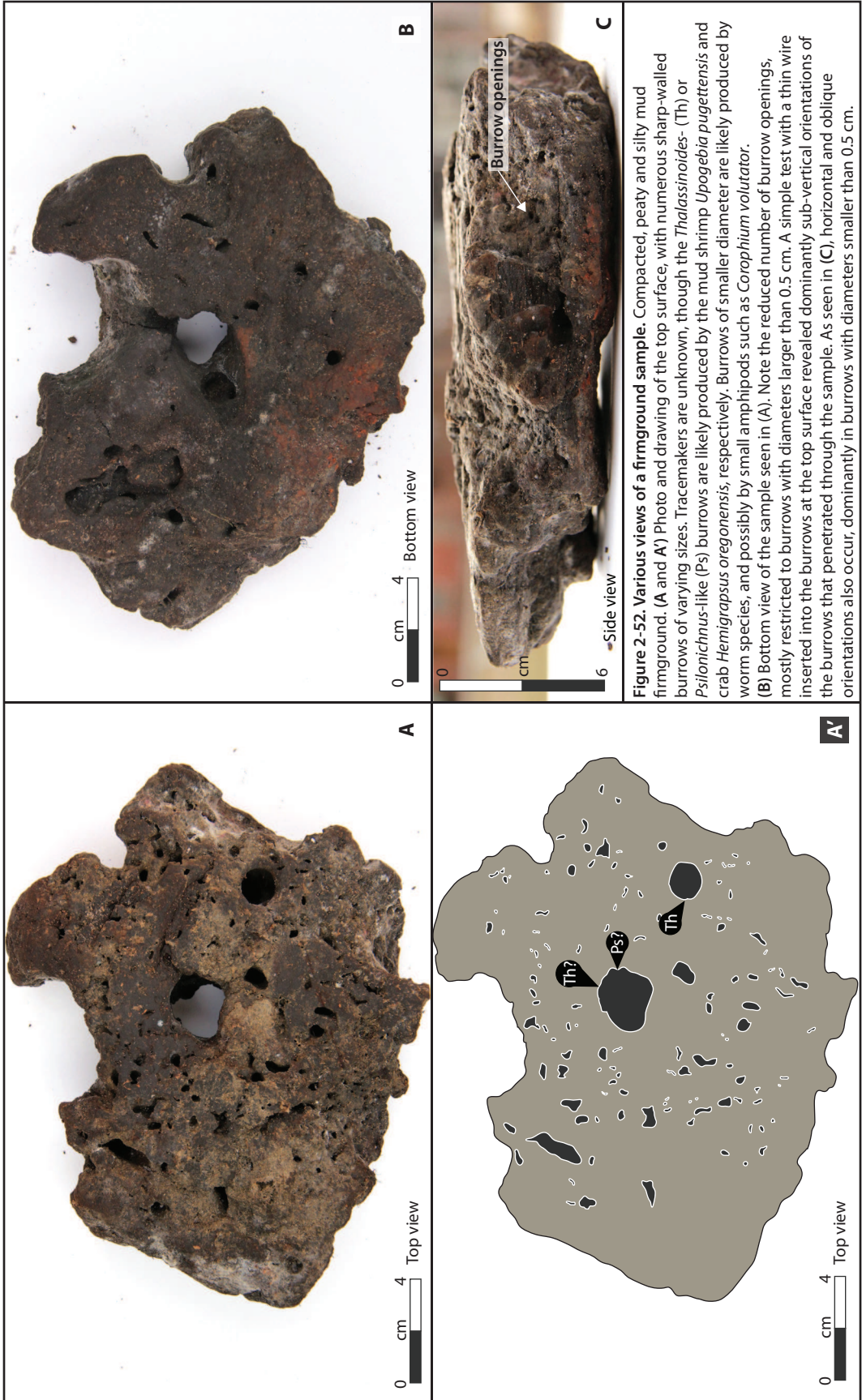


Figure 2-52. Various views of a firmground sample. Compacted, peaty and silty mud firmground. (A and A') Photo and drawing of the top surface, with numerous sharp-walled burrows of varying sizes. Tracemakers are unknown, though the *Thalassinoides*- (Th) or *Psilonichnus*-like (Ps) burrows are likely produced by the mud shrimp *Upogebia pugetensis* and crab *Hemigrapsus oregonensis*, respectively. Burrows of smaller diameter are likely produced by worm species, and possibly by small amphipods such as *Corophium volutator*. (B) Bottom view of the sample seen in (A). Note the reduced number of burrow openings, mostly restricted to burrows with diameters larger than 0.5 cm. A simple test with a thin wire inserted into the burrows at the top surface revealed dominantly sub-vertical orientations of the burrows that penetrated through the sample. As seen in (C), horizontal and oblique orientations also occur, dominantly in burrows with diameters smaller than 0.5 cm.

neiochnological characteristics. These facies are summarized in Table 2-5, with supplementary references to vibracore logs located in Appendix B.

Zone 5 Facies 1 (Z5F1) –Massive to rippled silt

Facies 1 is only observed in basal sections of the most proximal (most landward) vibracore of Zone 5 (Fig. 2-53 A,B,C; Table 2-5). Where observed, Facies 1 is 55 cm thick. It is characterized by dominantly massive appearing silt, with up to 10-15% fine sand. Ripples are apparent in an interval 15 cm thick, otherwise the facies appears massive throughout. Bioturbation is absent. There is no basal contact observed for Facies 1, but a sharp contact between overlying Facies 2 is observed.

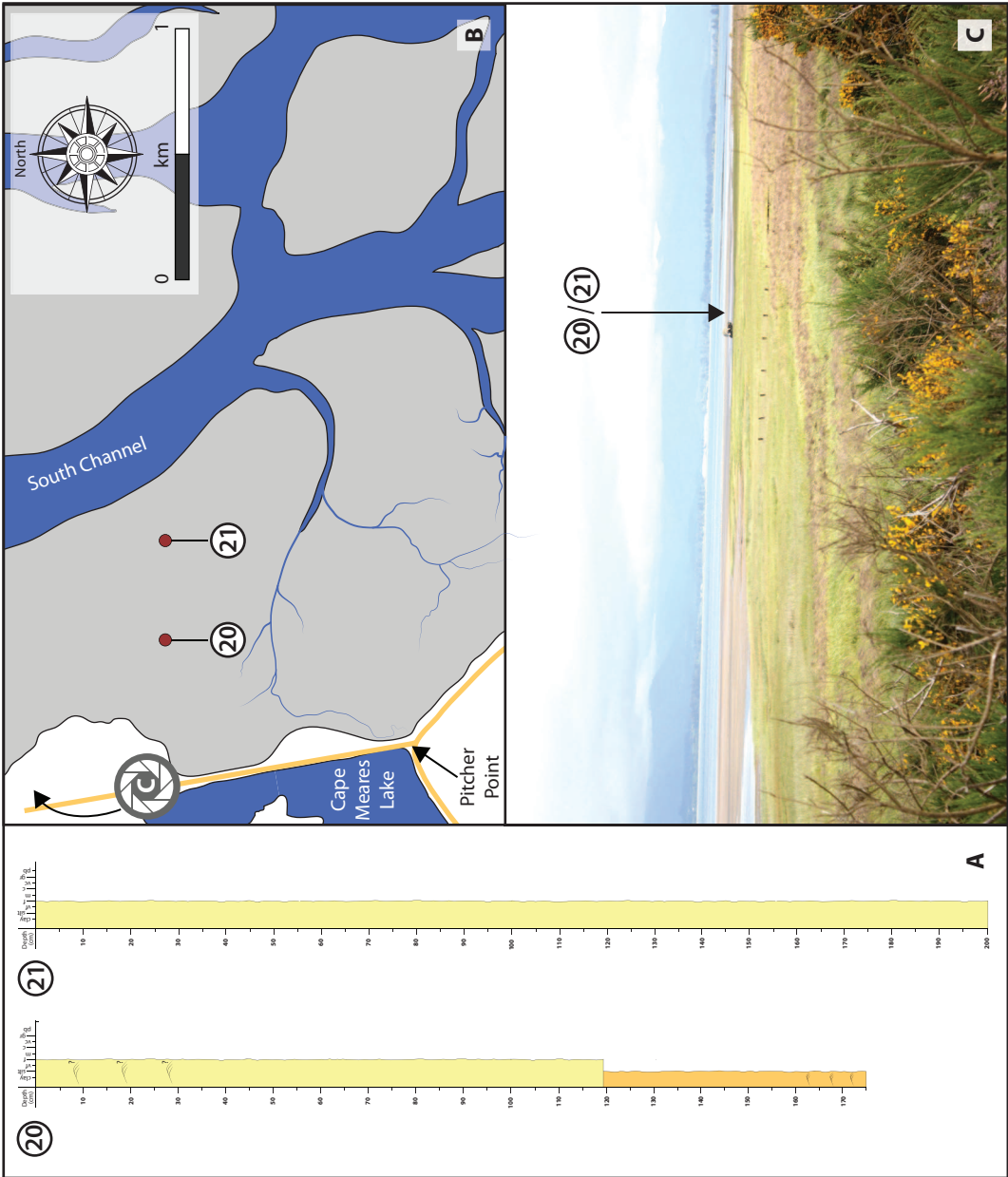
Zone 5 Facies 2 (Z5F2) –Massive sand

Facies 2 is the most prevalent facies observed in Zone 5 (Fig. 2-53 A,B,C; Fig. 2-54; Table 2-5). This facies is characterized by clean, very well sorted, massive appearing, fine, quartz-rich sand. Due to the very good sorting of the sediment, layer boundaries, as well as any surfaces, are very difficult to observe (Fig. 2-53 A,B,C). This is reflected in core 21, where no discernable boundaries could be observed, as well as no discernable grain size variation. Vaguely-observable current ripples may be present in core 20. Both cores from this zone are located in the path of the sediment deposited into the bay after the storm breach of 1952. Bioturbation is absent. The only observable contact is a sharp contact between underlying Facies 1 in the most landward (proximal core), otherwise Facies 2 is the only facies observed in Zone 5.

Zone 5: Marginal Tidal Flats Interpretations

The two facies described for the Marginal Tidal Flats (Zone 5) are interpreted as: Facies 1 (Z5F1: Bay margin silty tidal flat); and Facies 2 (Z5F2: Bay margin well-sorted tidal flat). These interpreted facies comprise the Marginal

Figure 2-53. Sediment logs from the sand-dominated, western part of Tillamook Bay. As can be seen from the sediment logs of cores 20 and 21 (A), thick layers of well-sorted, dominantly fine sand, with possible current ripples are observed. A thick silt-dominated layer can also be observed in the bottom portion of core 20. (B) Map indicating location of the two cores, as well as the location of the photo taken from Bayocean Peninsula and looking east-southeast. (C) Overview of the vegetated environment on Bayocean Peninsula, showing the approximate location of where cores 20 and 21 were retrieved from on the tidal flats.





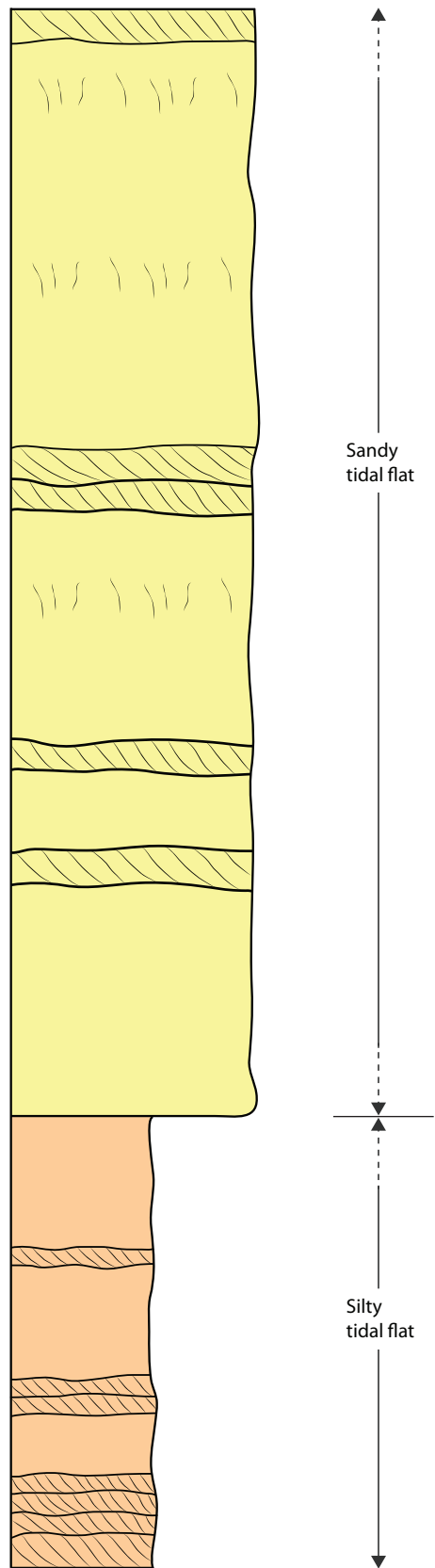
Facies Association	Facies	Facies Contacts	Sedimentary Characteristics	Neochronological Characteristics	Interpretation
<p align="center">Marginal Tidal Flats Facies Association (FA5)</p>	<p>Facies 1 (Z5F1) Massive to rippled silt</p>	<p>There is no basal contact observed for Facies 1, but a sharp contact between overlying Facies 2 is observed.</p>	<p>It is characterized by dominantly massive appearing silt, with up to 10-15% fine sand. Ripples are apparent in an interval 15 cm thick, otherwise the facies appears massive throughout. Where observed, Facies 1 is 55 cm thick.</p>	<p>Bioturbation is absent.</p>	<p align="center">Bay margin silty tidal flat</p>
	<p>Appendix B Core Figure Reference(s): B-18</p>	<p>The only observable contact is a sharp contact between underlying Facies 1 in the most landward (proximal core), otherwise Facies 2 is the only facies observed in Zone 5.</p>	<p>This facies is characterized by clean, very well sorted, massive appearing, fine, quartz-rich sand. Due to the very good sorting of the sediment, layer boundaries, as well as any surfaces, are very difficult to observe (Fig. 2-53 A,B,C). This is reflected in core 21, where no discernable boundaries could be observed, as well as no discernable grain size variation. Vaguely-observable current ripples may be present in core 20. Both cores from this zone are located in the path of the sediment deposited into the bay after the storm breach of 1952.</p>	<p>Bioturbation is absent.</p>	<p align="center">Bay margin well-sorted sand tidal flat</p>
<p>Appendix B Core Figure Reference(s): B-18; B-19</p>	<p>Facies 2 (Z5F2) Massive sand</p>				

Table 2-5: Summary of Facies Characteristics for Marginal Tidal Flats (Zone 5)

Tidal Flats Facies Association (FA5) (Table 2-5). The interpreted idealized vertical succession from the Marginal Tidal Flats (Zone 5) ideally consists of a full sequence from silt flats (Facies 1) up to sandy bay margin tidal flats (Facies 2) (Fig. 2-55).

The transition between the inner estuary and middle estuary, as observed on the western shore of Tillamook Bay, occurs gradually between mud-dominated and muddy-sand tidal flats, to well-sorted, clean sand-dominated tidal flats (Fig. 2-55). The extensive tidal flats adjacent to Bayocean Peninsula, and extending to the South Channel running in a north-south orientation, are dominated by the relatively clean, fine-grained sands of largely quartz mineralogy. The sands are similar in texture to those observed on the Pacific Ocean shoreline along the Bayocean Peninsula. Given the presence of high-wavelength, relatively low-relief dunes on the tidal flats of Zone 5, it is interpreted that deposition and distribution of these features is largely controlled by the combined action of tidal and wave currents. The sediment in this part of the estuary, as observed by Komar et al. (2004) is delivered to the bay from the Pacific Ocean, via the bay mouth. The transport of sediment likely follows the tidal and wave currents through the South Channel as soon as they enter the bay area. Due to the bay morphology in the area of Zone 5 (i.e. the curvature of the shoreline outlined by the peninsula), the currents are forced to follow a similar orientation, flowing in a south, southwesterly direction. The consolidated sediments found in the terraces of the peninsula act to refract currents, and possibly create or amplify more wave currents in the process. Refraction of currents is a dominant control on the orientation of high-wavelength dunes (Allen, 1982); this can be observed in the dune orientations, which are largely oblique to the western shoreline of the bay, and are oriented in southwest to northeast and northwest to southeast orientations. One set of dunes are clearly created by primary currents flowing in a general southeasterly direction; the other set are created by secondary currents,

Figure 2-55. Schematic vertical succession from a sandy tidal flat succession. Vertical profile of sandy tidal flat deposits, as interpreted from core and surface observations from Tillamook Bay. Tidal and wave currents entering the estuary transport marine-sourced sand into the outer part of Tillamook Bay, as well as the western margin, where the current vertical succession is interpreted from. The well-sorted nature of the sand, combined with moderate to high bioturbation (interpreted from surface observations), is interpreted to lead to the obliteration of sedimentary structures. Very few ripple structures were observed in sediment cores, and this is likely due to the lack of contrasting sediment types in this region, and the unconsolidated nature of the sediment.



generated by current refraction that changes current flow to a southeasterly direction.

The presence of very well-sorted, fine-grained sand, combined with the presence of well-developed, high-wavelength dunes indicates that Zone 5 experiences higher total energies than the adjacent, muddy inner estuary. Zone 5 is unique in the sense that it displays sedimentary features consistent with both the inner estuary and outer estuary observations. For example, extensive burrowing by *Neotrypaea californiensis* observed in the middle estuary Zone 5, is also observed abundantly on the sand bar of inner estuary Zone 3 as well as in the bayhead delta region of Zone 2. In a similar way to the outer estuary Zone 6, very-well sorted, fine-grained sands, with well-developed dunes are observed in Zone 5. The term “middle estuary” is subjective, and is used loosely to define Zone 5 and emphasize the transition from inner estuary towards the more middle part of the estuary. The true “middle estuary”, though not studied, is observed passively to consist of eelgrass-stabilized tidal bars. Based on observations of the inner estuary, such an environment is expected to contain high concentrations of fine sediment (i.e. clay), as well as high bioturbation intensities. Heterolithic stratification and inclined heterolithic stratification may also be present in the true “middle estuary”, but they are certainly not observed in Zone 5, on the western bay margin.

The areally-restricted compact sandy mud / peaty surface observed midway along the western margin of Tillamook Bay is of high importance in interpreting the history of possible Pleistocene terraces at Tillamook Bay. A similar, peaty-clay firmground surface was observed in Netarts Bay, located approximately 15 kilometres south of Tillamook Bay (Hodgson, 2013). This exhumed, compacted, peaty-clay firmground is potentially of Pleistocene age and is sporadically exposed along the eastern margin of Netarts Bay, where coastal terrace deposits, of Late Pleistocene age, have been reported (Peterson et al., 1988; Hodgson, 2013). Sporadically located Pleistocene terraces are found along the extent of the Oregon-Washington coastline, with one of the

most laterally-continuous terraces, the Whiskey Run terrace, being approximately 83,000 years in age (West and McCrumb, 1988). The peaty-clay firmground present at Netarts Bay displays a stepwise topography where the lower bayward down-step portions are covered by a surficial veneer of sediment (Hodgson, 2013). This stepwise phenomenon observed in exhumed, compacted, bay margin, clay-dominated substrates, was also observed in Willapa Bay, Washington (Gingras et al., 2001). The limited areal extent of the sandy-mud / peaty surface observed at Tillamook Bay may also exhibit a stepwise topography and be largely covered by a layer of surficial sediment of varying depths, but further observation and analysis are needed in order to validate this hypothesis.

The traces observed in the peaty-clay firmground at Netarts Bay can be ascribed to the *Glossifungites* Ichnofacies assemblage (Hodgson, 2013). They include larger diameter *Thalassinoides*-, *Psilonichnus*-, and *Gastrochaenolites*-like traces; and smaller diameter *Skolithos*-, *Arenicolites*-, *Diplocraterion*-, *Rhizocorallium*-, and *Polykladichnus*-like traces (Hodgson, 2013). The *Gastrochaenolites*-like burrows are exclusively found within the peaty-clay firmground layer (Hodgson, 2013). The larger diameter *Thalassinoides*-, *Psilonichnus*-, and *Gastrochaenolites*-like traces are constructed by *Upogebia pugettensis*, *Hemigrapsus* spp., and *Zirfaea pilsbryi*, respectively (Hodgson, 2013). *Polydora* spp. creates the smaller diameter *Skolithos*-, *Arenicolites*-, *Diplocraterion*-, and *Rhizocorallium* - like traces, while nereid polychaetes construct the *Polykladichnus*-like traces (Hodgson, 2013). These observations, though inclusive of a more diverse ichnofossil assemblage, are consistent with those found in Tillamook Bay during this study and also lend further assistance to the interpretation of potential tracemakers that are not observed.

The *Glossifungites* Ichnofacies demarcates discontinuities that may have sequence-stratigraphic importance, or which can be autogenically derived (MacEachern et al., 2010). Given that the firmground surface observed at Tillamook Bay is areally-restricted to the west by the consolidated dunes of

Bayocean Spit, it is possible that intertidal sandy mud flat deposits are periodically aerially exposed and dewatered; or buried, compacted and dewatered during the Holocene, and exhumed at a later time. This Holocene age, however, is speculative, and has to be scrutinized using radiocarbon-dating techniques. Another possible Holocene-age scenario is that of the formation of firm sandy mud deposits due to their dewatering on a tidal channel cut-bank. The firmground surface is currently situated close to the relatively steep banks of the tidal channel that runs sub-parallel western bay margin. Given the relatively stable nature of intertidal features, such as tidal bars, observed at Tillamook Bay, it is possible that the existence of this tidal channel at this location over a long period of time may enhance dewatering and increase the firmness of the mud deposits. This can be compared to observations of enhanced drainage occurring on cutbanks of intertidal creek deposits at Willapa Bay, adjacent to a dewatered substrate (of limited areal extent) which contains *Psilonichnus*-like burrows (Gingras et al., 2000). A Pleistocene-age interpretation, though possible, requires sandy mud flat deposits to be buried, compacted, and later exhumed. However, the drowned-valley nature of Tillamook Bay estuary clearly indicates that, starting with the rise in sea level at the end of the last glaciation, rivers deposited sediment on top of Pleistocene deposits (Glenn, 1978). In a sediment core, located approximately 200 metres south-east of to the firmground surface observed the thickness of the Holocene fill is reported to be more than 32 metres, resting on Pleistocene bedrock (Glenn, 1978). It is therefore possible that the firmground surface observed is of Pleistocene age, and possibly may have been exposed as a terrace.

Outer Estuary Characteristics

Zone 6: Isolated Tidal Sand Bar Descriptions and Results

Sedimentological and Neoichnological Features of Zone Sub-environments

Zone 6 of the outer estuary is in contrast with zones of the inner estuary, and to a lesser extent with Zone 5 of the middle estuary. It is dominated by large, ebb-oriented dunes that cover the majority of the tidal bar surface (Fig. 2-56). The dunes are mainly located in the northern portion of Zone 6, and are intertidal to subtidal in nature, forming on a shallowly dipping, bay mouth-oriented sand bar surface. Sediments of this zone are well sorted and dominated by fine grained sand. Total organic carbon percentage is relatively low and consistent in all samples analyzed. Bioturbation is very low to moderate. Zone 6 is divided into three sub-environments for clarity.

The hydrodynamic energy of this region, on first observation, appears much higher than in the inner estuary region. Outgoing and incoming tidal currents are observed to have higher energies, especially in the deep channels in this part of the estuary. On occasion, strong wind currents are observed to create short wavelength (~3-6 meters), medium to large amplitude (1.0-1.5 meter estimated amplitude) waves, much larger than the waves observed in the inner estuary.

Rippled sand deposits

Sedimentology-

The southern tip of Zone 6 contains very low-relief dunes (Fig. 2-57 A,B,C), as compared to the northern tip, which contains higher-relief dunes (described in the following sub-environment section). The most common sedimentary structures observed are linguoidal combined-flow ripples, located

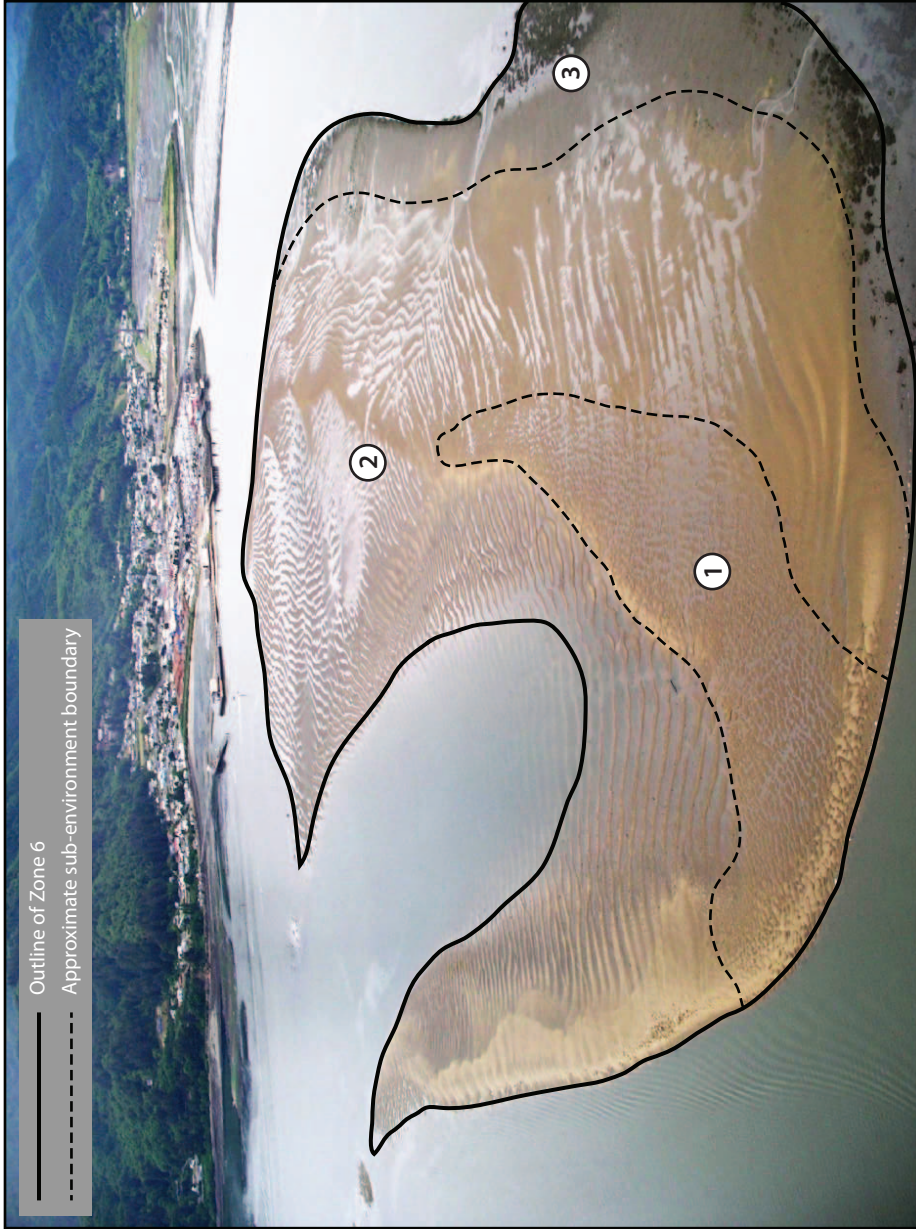
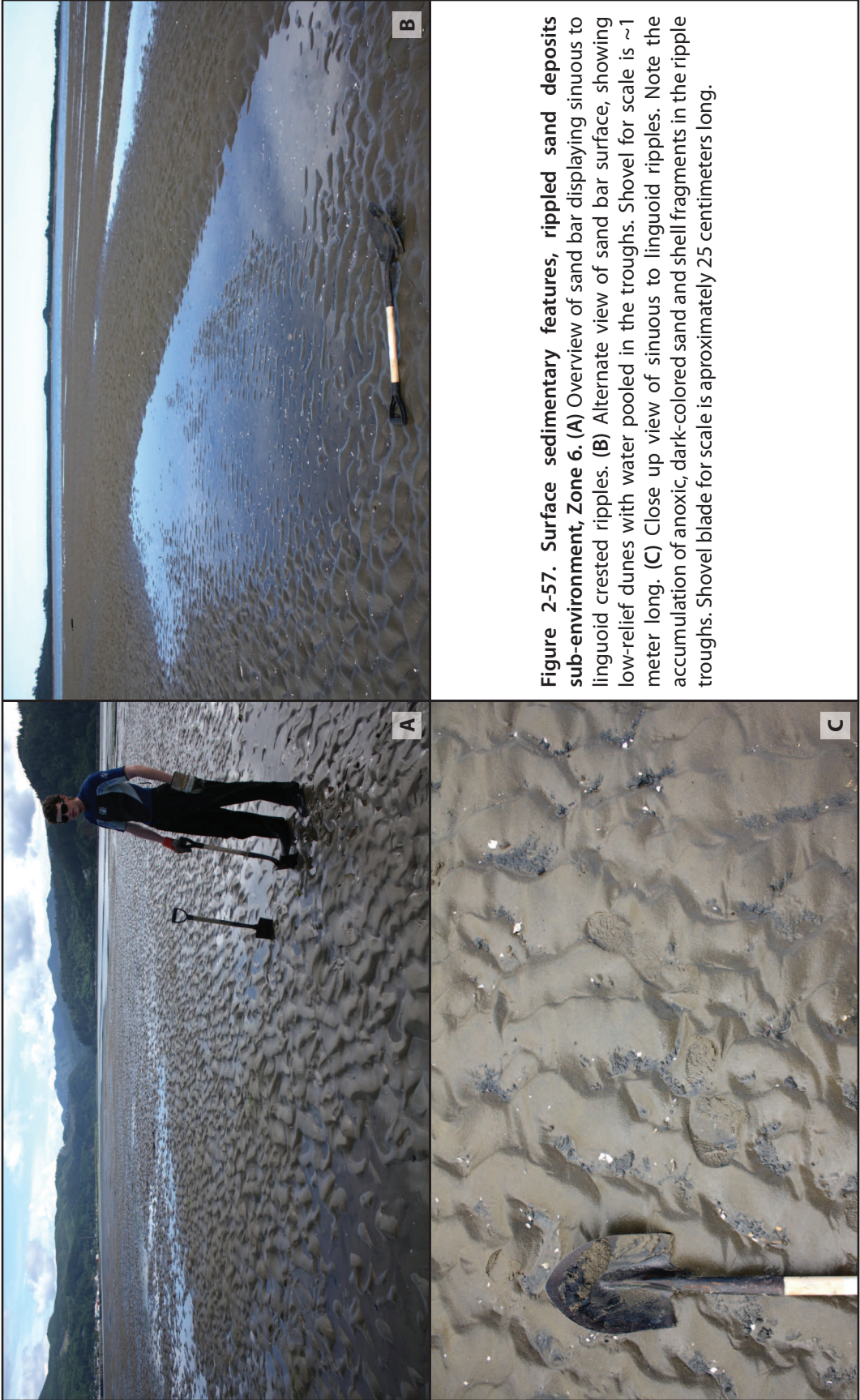


Figure 2-56. Sub-environments of Zone 6. Aerial view, looking north towards Zone 6 and its sub-environments: (1) rippled sand deposits and low-relief dunes; (2) medium-relief dunes; (3) algae-covered muddy sand deposits. The City of Garibaldi and the Garibaldi marina can be seen in the background. Photo courtesy of Lidia Zabcic, used by permission.



both on the dune crests and troughs. The majority of dune troughs have water pooled over the surface during low tide. These troughs are observed to have a high concentration of shell fragments, as well as a high number of accumulations of dark, anoxic sand. The dunes troughs and crests are irregular to straight-oriented. In the majority of dunes observed, no clear lee or stoss side is observed; dunes dip at similar angles in every direction towards the troughs.

The north-western edge of this area contains slightly higher-relief dunes, with more distinct lee and stoss sides, and a straight-crested morphology. Abundant shell fragments are not only observed in the troughs, but also in accumulations on the lee side of dunes. Being able to more clearly observe the lee side, it is also observed that the dunes in this area are oriented in a flood orientation, as opposed to the more dominant ebb orientation observed at the northern tip of the sand bar.

Neoichnology-

Traces observed in this sub-environment are made by the following burrowing organisms: *Clinocardium nuttallii* and *Tresus capax*, both forming *Skolithos*- and *Siphonichnus*-like burrows; and *Notomastus* threadworms, forming thin *Skolithos*-like burrows; the beach hopper *Traskorchestia traskiana*, is also observed, but no discernible traces of this organism are seen. Accumulations of dark, anoxic sand are often observed occurring near burrow openings. However, the tracemaker is not observed, as all attempts digging into the water-saturated sediment are unsuccessful due to caving in of sediment and inflow of water.

Medium-relief dunes

Sedimentology-

The southern half of this sub-environment, located between sub-environment 1 and 2 (Fig. 2-56), consists of rippled sand flats and better defined, ebb-oriented, low-to-medium-relief dunes (Fig. 2-58 A,B,C). The ebb-oriented dunes occur from the eastern to western part of this sub-environment. The dunes are sinuously- to straight-crested, with varying angles of repose on the lee sides, ranging from approximately 10°-30°. Pooled water is observed in the troughs, and the pools are either connected in an elongate trough, or stand on their own. Linguoidal combined-flow ripples are superimposed on the dune surfaces, forming right up to the downstream end of the dune crest, at the upper reach of the lee side. Interconnected dune troughs contain sediment flows in the form of microscale delta lobes (~ 1-2 metres length, decimeter-scale width at the lobe front), as shown in Figure 2-59 (A,B). A suboxic, grey layer is observed at approximately 9-10 centimeters depth. Grey sand mounds, distinctly formed on the sediment surface and associated with burrow openings, have the exact same color as the underlying, suboxic sand layer, and are common in the area.

At the western edge of this area, the sand flat surface is observed to dip into a lower-elevation part of the sand flat. This sand flat contains straighter-crested combined-flow ripples, and common to abundant algae covering the surface. This surface dips at a shallow to moderate angle towards the deeper channel waters westward, and towards the algae-covered muddy sand deposits, sub-environment 3 (Fig. 2-56).

The northern half of this sub-environment has a surface fully covered by medium-relief dunes, from the eastern margin, where it is bound by the tidal channel to the western margin, and where the dunes continue on a shallow angle into a subtidal portion of the bar. As is characteristic of the area, well sorted, fine sand dominate. Linguoidal ripples are superimposed on the stoss

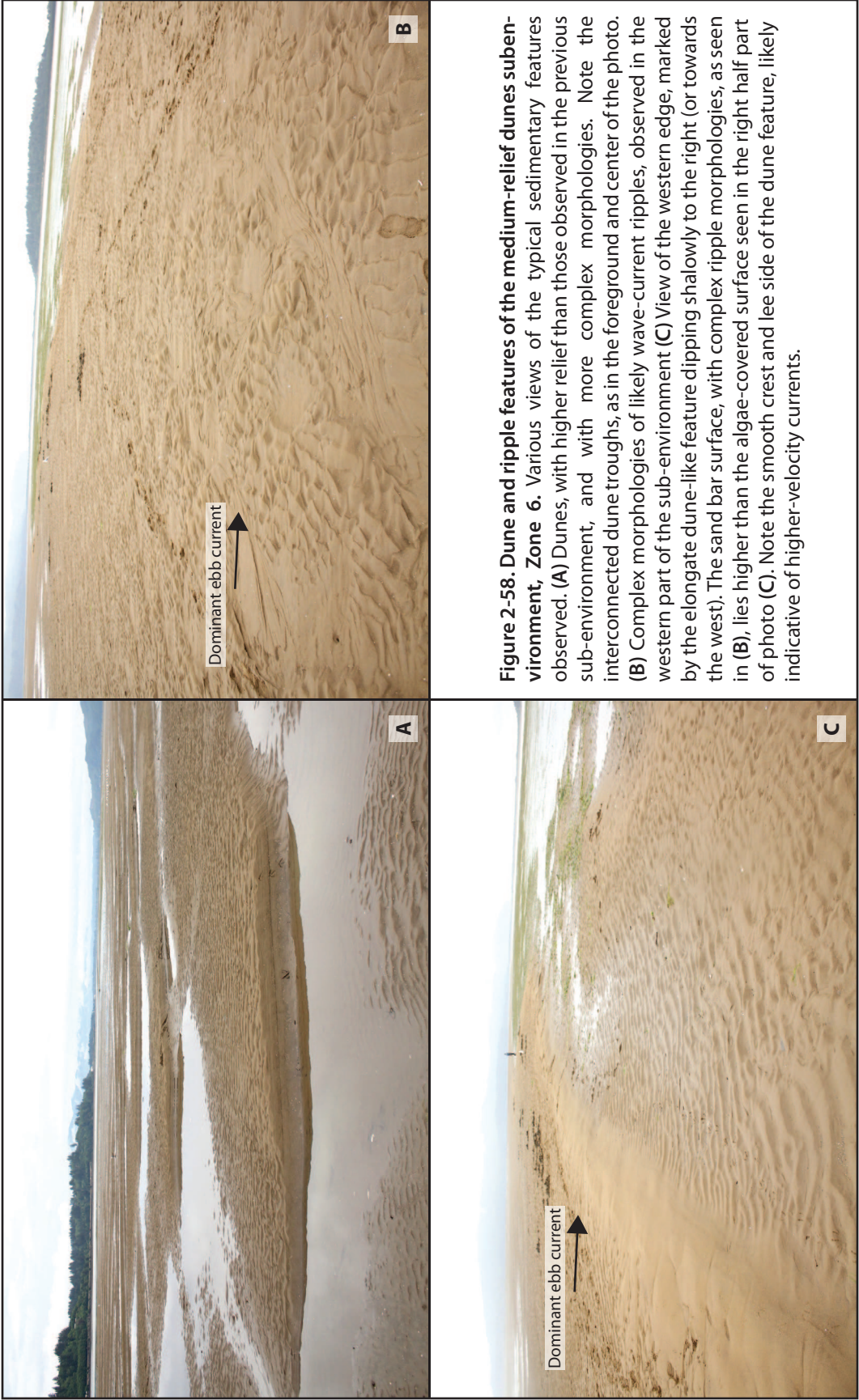


Figure 2-58. Dune and ripple features of the medium-relief dunes sub-environment, Zone 6. Various views of the typical sedimentary features observed. (A) Dunes, with higher relief than those observed in the previous sub-environment, and with more complex morphologies. Note the interconnected dune troughs, as in the foreground and center of the photo. (B) Complex morphologies of likely wave-current ripples, observed in the western part of the sub-environment (C) View of the western edge, marked by the elongate dune-like feature dipping shallowly to the right (or towards the west). The sand bar surface, with complex ripple morphologies, as seen in (B), lies higher than the algae-covered surface seen in the right half part of photo (C). Note the smooth crest and lee side of the dune feature, likely indicative of higher-velocity currents.



Figure 2-59. Complex dune morphologies, medium-relief dunes sub-environment, Zone 6. (A) View of a micro-delta and its lobes, formed due to sediment being transported from one dune trough (seen towards the center of the photo) to another (largely outside of the field of view, its edge seen in the foreground). The delta lobe is approximately 45 centimeters across at its widest part. Note the complex dune morphologies, and sinuous to linguoid ripples superimposed on the dune crests and stoss sides. (B) View of a typical dune trough morphology, with complex linguoid ripples observed on the dune stoss sides.

side of dunes. The dunes are relatively large features, having lengths of tens of metres. Dune amplitudes range from 30 centimeters to 80 centimeters, and wavelengths range on average from 3 to 5 meters (Fig. 2-60 A,B,C; Fig. 2-61 A,B,C). The crests are dominantly straight to occasionally sinuous. Troughs are most often separated from each other, but locally they connect and appear to cut across and interrupt a continuous dune crest. They also occur as isolated "lenses", several meters in length, and 1-2 meters in width. The linguoidal ripples superimposed on the dune stoss sides are usually observed to range from the troughs to just near the dune crest (Fig. 2-62 A,B,C). They are rarely present at the dune crest, usually forming on the lower-relief range of dunes. Ripples are also present at the base of the lee slope of dunes. These ripples have a straight to curved morphology, and are most commonly oriented at an oblique to right angle in relation to the lee slope of the dune, only to grade smoothly into linguoidal ripples in the troughs (Fig. 2-61 A,B,C). As shown in Figure 2-61 (A,B,C) the current ripples are oriented at an oblique angle when not in direct contact with the lee slope, and curve when located closer to the slope; in that case, they form a straight angle. Shell fragments are common in the troughs, and are often concentrated at the base of the lee slopes.

A black colored layer of anoxic sand is found under the dune crests at approximately 30 centimeters depth. The location of the anoxic layer in the troughs could not be accurately determined, due to the water-saturation and caving in of sediment. X-radiographs are able to discern shell fragment accumulations that aid in outlining cross-bed surfaces (Fig. 2-63 A,A').

The lower-intertidal portion of the tidal sand bar contains dunes that are a continuation of the aforementioned medium-relief dunes, and at the time and tidal range of initial observation, are located underwater, with features only briefly observed in the shallower areas, under about 10-30 centimeters of water. Past this point, the ebb-oriented character of those dunes can be inferred by walking in a direction parallel to their migration direction, and

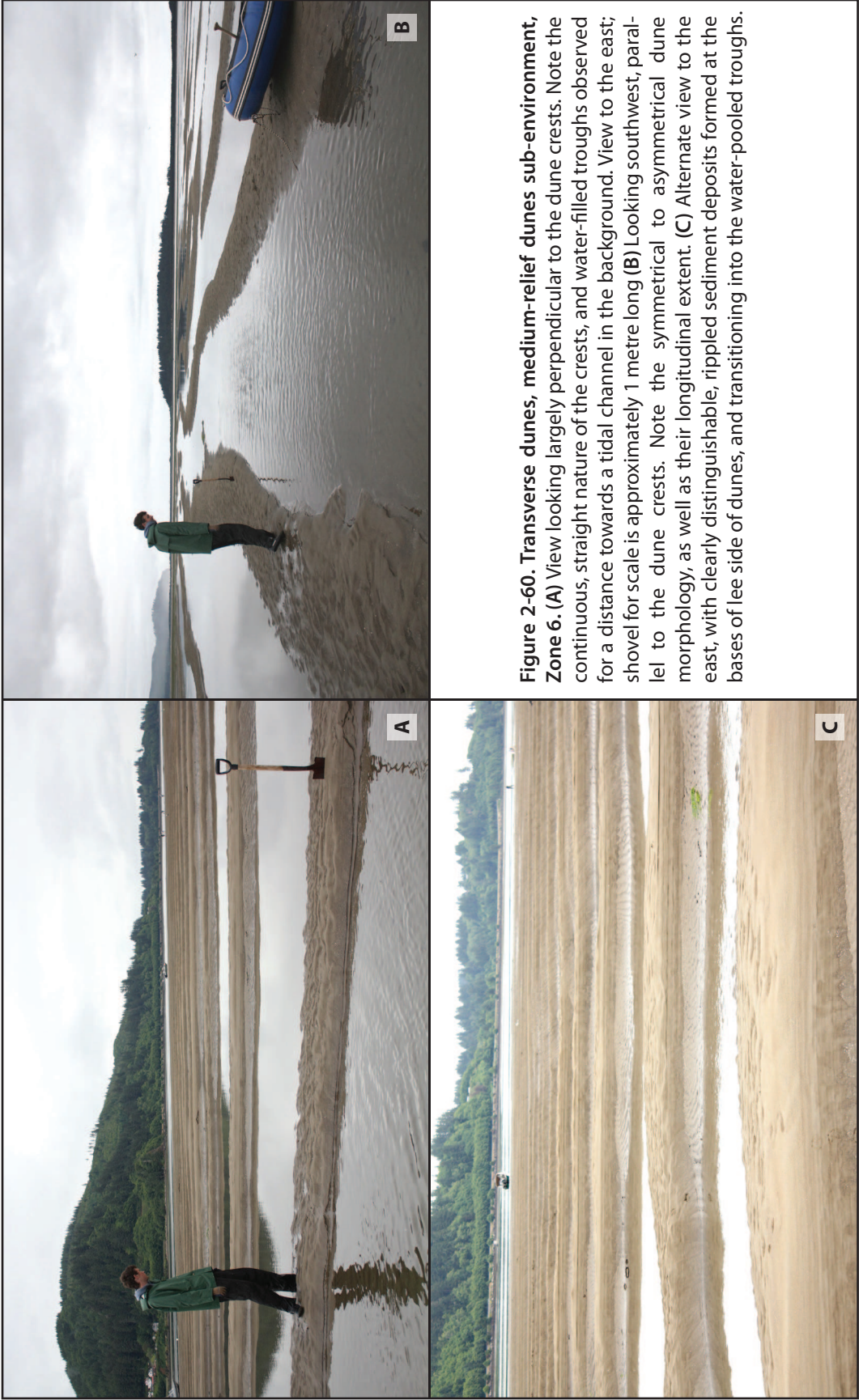
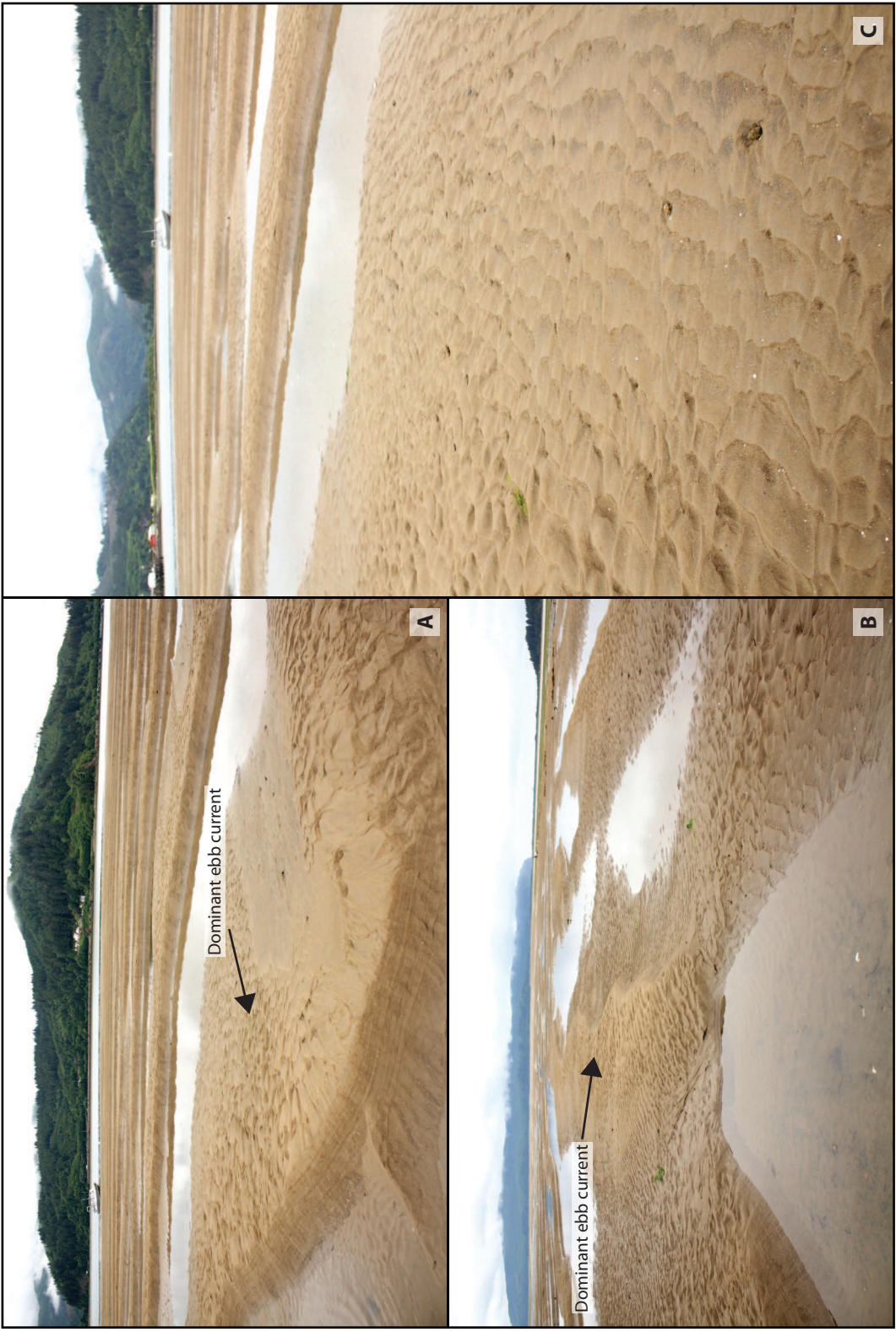


Figure 2-60. Transverse dunes, medium-relief dunes sub-environment, Zone 6. (A) View looking largely perpendicular to the dune crests. Note the continuous, straight nature of the crests, and water-filled troughs observed for a distance towards a tidal channel in the background. View to the east; shovel for scale is approximately 1 metre long **(B)** Looking southwest, parallel to the dune crests. Note the symmetrical to asymmetrical dune morphology, as well as their longitudinal extent. **(C)** Alternate view to the east, with clearly distinguishable, rippled sediment deposits formed at the bases of lee side of dunes, and transitioning into the water-pooled troughs.

Figure 2-61. Rippled sediment deposits at the base of dune fronts. (A) Rippled sediment, deposited in front of transverse dunes. As indicated on the features in the foreground, the mentioned rippled sediment contains ripples oriented obliquely to the dune strike orientation. They are likely the result of subordinate ebb currents flowing through the dune troughs. The dominant ebb current is therefore oriented largely perpendicular to the dune strike orientation. (B) Top view of a dune crest, lee side, and the ripple sediment at the base of the dune. Note the curvature of the ripple crests in front of the dune, likely due to increased friction along the dune lee surface. Also note the relatively high concentration of shell fragments at the contact between the lee surface and rippled sediment. Shovel for scale is approximately 1 metre long, and points in the ebb current direction. (C) View parallel to the inferred sub-ordinate current direction. The thickness of the rippled sediment deposits appears to vary, and locally, it approaches the level of the dune crest, as observed near the central and center-right part of the photo.



Figure 2-62. Complex dune morphologies, medium-relief dunes sub-environment, Zone 6. (A) View to the northeast, showing the more complex - when compared to the transverse dunes also observed -, sinuous dune forms. Note the linguoid ripples superimposed on the dune stoss side in the foreground, as well as the water line marks on the dune lee side. **(B)** View to the south, parallel to the overall, strike orientation of the dunes. The sinuous crests and complex troughs are more clearly observed when viewed from this angle. **(C)** Closer view of the transverse to linguoid ripples superimposed on dunes stoss sides.



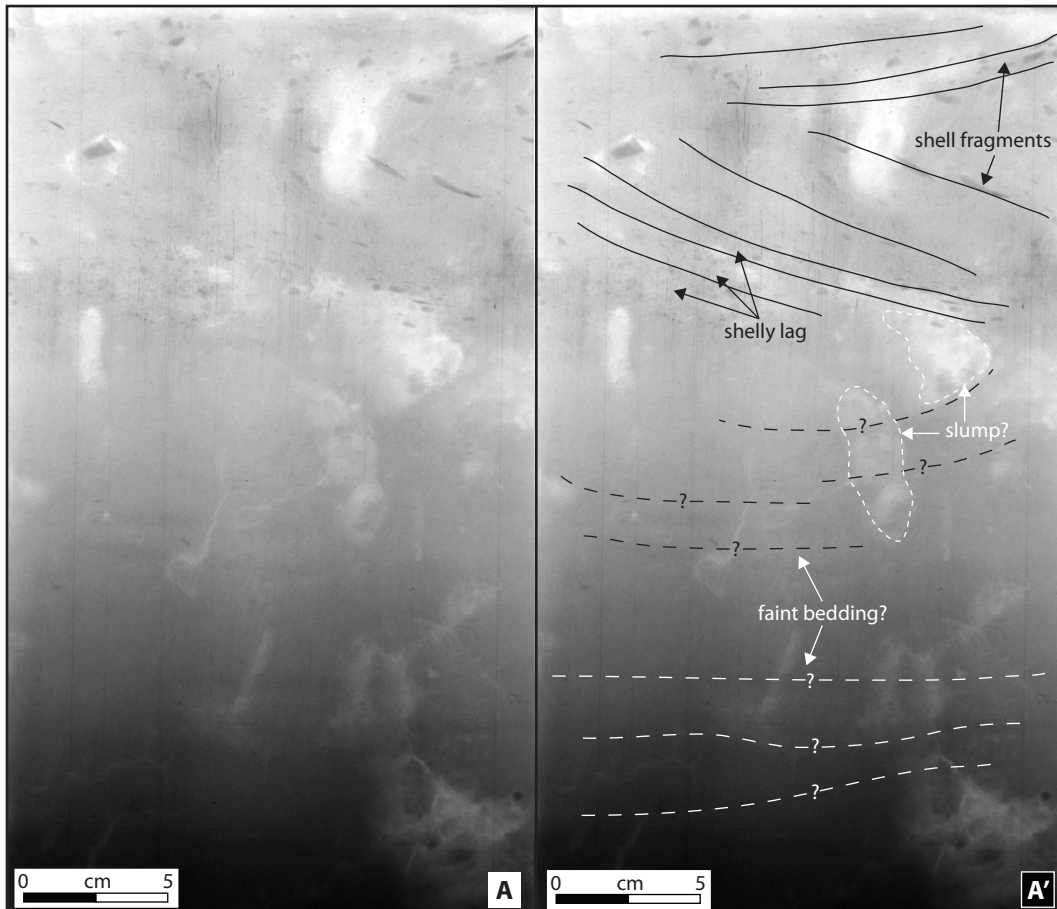


Figure 2-63. X-radiograph of cross-bedded dune sediments, Zone 6. (A) Raw x-radiograph (x-ray) of cross-bedded sand, sampled from a dune crest using a boxcore. **(A')** Annotated x-ray, shows shell fragment accumulations along interpreted cross-bed surfaces. Faintly-observable bedding is likely also observed. Due to the well-sorting nature of sediment, mineralogical and/or sedimentological contrast is lacking, and therefore layers of sediment tend to 'blend in" together.

observing the variation in slope between the stoss sides and lee sides. Thus, the lower reaches of this area can fall in the lower intertidal to high subtidal realm.

Neoichnology-

The tracemaker associated with the grey sand mounds is unknown, but other burrowing organisms are observed such as *Notomastus* sp. threadworms, *Tresus capax*, *Macoma secta*, small individuals of *Nereis* sp. and *Nephtys* sp. worms, and rarely, the ribbon worm *Paranemertes peregrina*. These organisms are rarely observed together, except in the case of *Notomastus* sp. worms and small clam siphons of an unknown tracemaker. *Tresus capax* clams burrow deeply into the sediment, and are found at a depth of approximately 50 cm.

Overall, bioturbation is generally low to medium on the medium-relief dune areas (Fig. 2-64 A,B,C,D; Fig. 2-65 A,B,C), consisting of the following traces: *Skolithos*- and *Siphonichnus*-like traces made by the bivalves *Clinocardium nuttallii* and *Macoma secta*; *Skolithos*- and *Planolites*-like burrows made by *Nephtys* sp. worms; *Thalassinoides*-like burrows made by *Neotrypaea californiensis*; and surface tracks made by *Pagurus hirsutiisculus* and seagulls. Rare ribbon worms (*Paranemertes peregrine*) are also observed, but their incipient trace(s) cannot be determined.

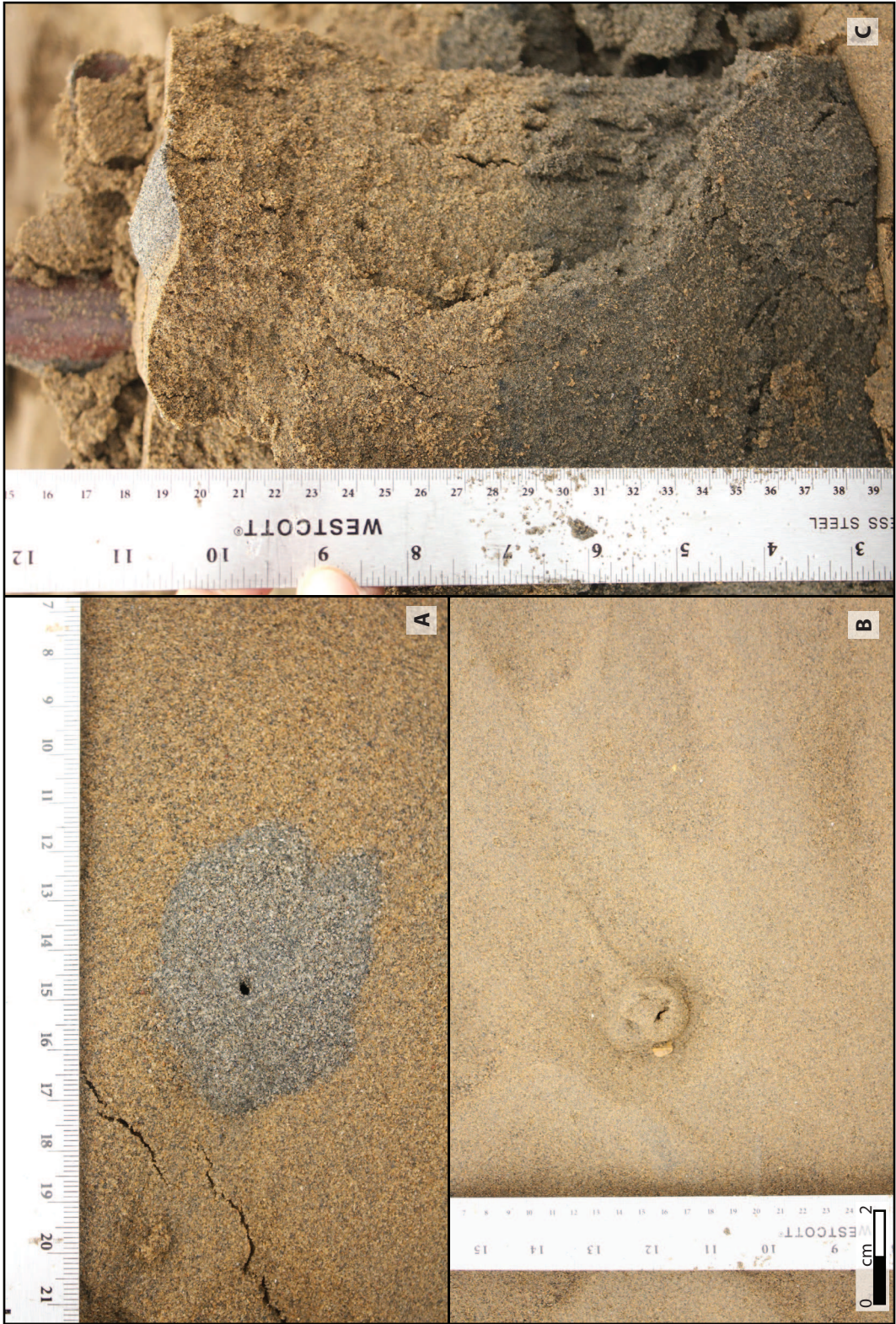
Algae-covered muddy sand deposits

Sedimentology-

This sub-environment, observed on the eastern part of the previously-described isolated sand bar, as well as part of a sand bar adjacent to the one previously described, is briefly examined and is mentioned here for a short comparison. Algae cover almost the entire area of this sub-environment, to approximately 60-70% coverage. This does not, however, apply to the full surface of the sand bar, which at its southern portion, does not appear to be covered in algae. Together with the algae-stabilized zone, the sediment has a



Figure 2-65. Trace features of medium-relief dunes sub-environment, Zone 6, continued. (A) Close up view of burrow with mound of excavated sand formed around burrow opening. (B) Small column of sand around, and partially enclosing, a burrow opening. (C) Cross-sectional view of grey sands below and beige sands above with burrow seen in A on top. Note that the excavated sands around the burrow opening originated from the grey layer below.



significant concentration of mud, estimated at 30-40%. Sedimentary structures in the form of ripples are not observed. In turn, however, hummocky mud mounds are common to abundant and varied in diameter from centimeter scale to decimeter scale. These hummocks are similar in nature to the ones previously observed in the central portion Zone 3 of the inner estuary.

Where eelgrass is abundant (generally the central and east-central part of the sub-environment) the maximum reach (depth-wise) of roots could not be determined. The abundant rootlets made it difficult to dig trenches deeper than 20-30 centimeters. From what could be observed in the top 30 centimetres, no direct distinction between oxic, suboxic, and anoxic layers is evident. Muddy sand of varying shades of grey color is observed, but the highly reworked sediment destroyed the boundary between the aforementioned layers.

Neoichnology-

Bioturbation is common to abundant, consisting of both small, less than five centimeter burrows, as well as large, 1-2 centimeter burrows. The bar surface has an irregular surface, with numerous (tens of burrows openings per square meter) surface burrows, and visible highly-reworked sediment. Common traces observed are vertical *Thalassinoides*-like burrows, thin, *Skolithos*-like burrows, and *Planolites*-like burrows of *Nereis* sp. worms. Tracemakers are rarely observed, and they consist of dominantly small (~10 cm long, 0.3-0.5 centimeters wide) *Nereis* sp. worms. One large Nereid specimen is observed; its dimensions are approximately 40-50 centimeters long, 1.0-1.5 centimeters wide. The bivalve *Clinocardium nuttallii* is observed in small numbers, and shell fragments are present locally in quiescent, water pooled areas between hummocky mud mounds, where eelgrass is not as abundant. Given the obvious high sediment reworking, it is possible that the actual organism diversity (and associated incipient traces) may be higher. This is addressed in more detail in the interpretation section.

Zone 6: Isolated Tidal Sand Bar Vibracore Facies Descriptions

Vibracores of zone 6 (Fig. 2-66 Part 1 A,B,C,D,E,F; Fig. 2-66 Part II A,B,C,D,E,F; Fig. 2-67 Part I; Fig. 2-67 Part II) show the highest grain size consistency compared to the previous zones studied. Though very short, and providing limited data to base interpretations on, cores 22 through 32 show varying sedimentary structures, many associated with migrating dunes formed on the sand bar surface. The boundaries between three different layers are sometimes flat lined and easy to trace laterally, though they are often sporadically distributed and irregular in nature (Fig. 2-66 Part 1 A,B,C,D,E,F; Fig. 2-66 Part II A,B,C,D,E,F). Due to very good sorting of the sediment, layer boundaries, as well as sedimentary structures, are difficult to observe. In some cases, high-angle bedding is observed, aided by the fact that shell fragments are concentrated in lags, which are noted to be deposited on dipping surfaces. Shell fragments are commonly observed through most cores, while sparse wood fragments are present only in core 32. High-angle bedding, as well as low-angle bedding is observed in vibracores retrieved from areas dominated by well-developed, medium-relief dunes. A total of eleven cores were recovered from Zone 6, with each recovered core ranging from 65 cm – 130 cm in length. Six facies are identified from the Isolated Tidal Sand Bar (Zone 6) according to distinct sedimentary and neoichnological characteristics. These facies are summarized in Table 2-6, with supplementary references to vibracore logs located in Appendix B.

Zone 6 Facies 1 (Z6F1) –Burrowed massive sand

Facies 1 is found from one vibracore taken from the Algae-covered muddy sand deposits sub-environment (Fig. 2-66 Part 1 A,B,C,D,E,F; Fig. 2-66 Part II A,B,C,D,E,F; Fig. 2-67 Part I; Fig. 2-67 Part II; Table 2-6). This facies is defined by burrowed, massive, fine-grained sand. The burrows occur sparsely and are sand-filled, having diameters of 2 mm to 4 mm. Facies 1 is 50 cm thick.

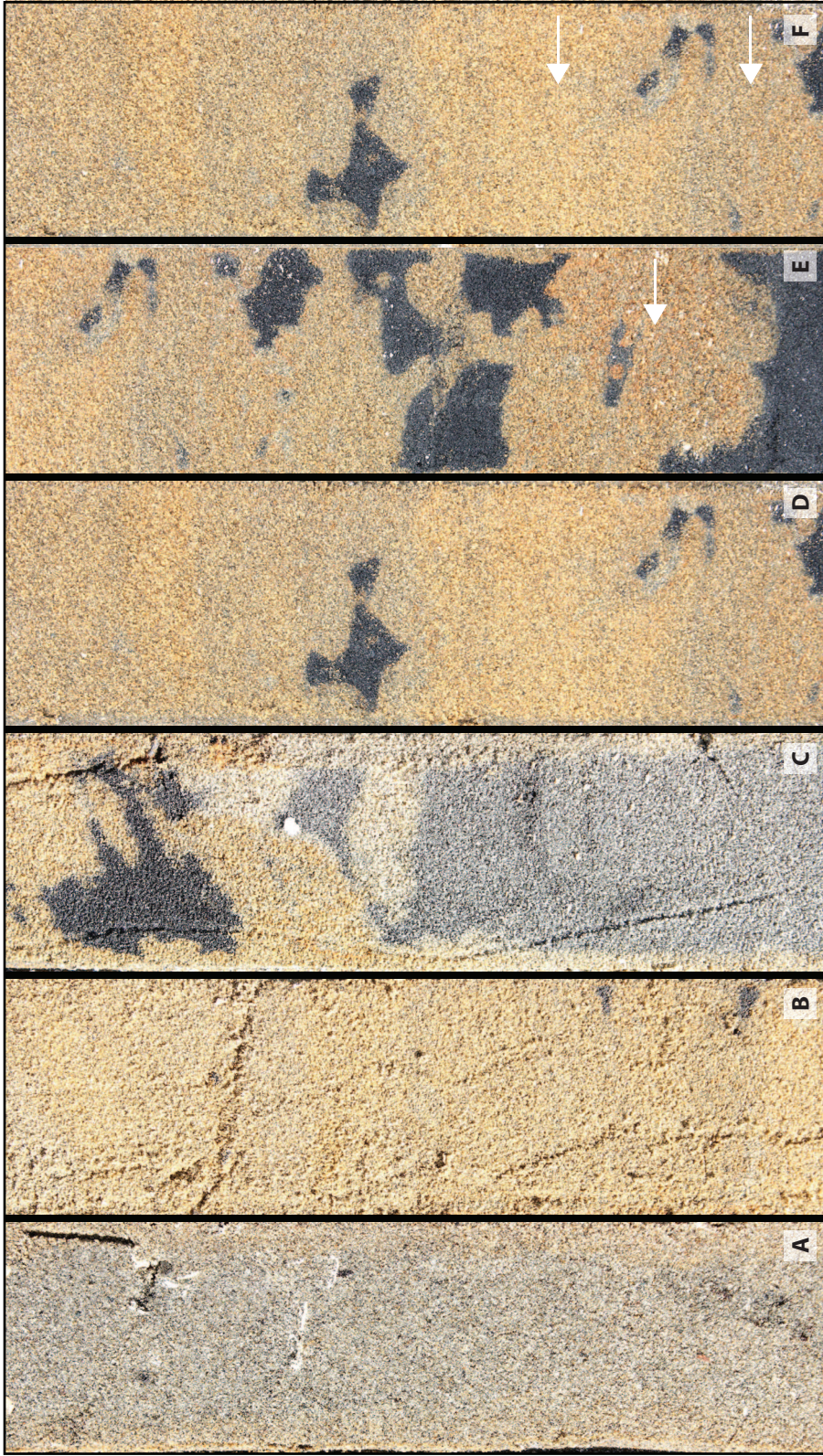


Figure 2-66, Part I. Vibracore examples from Zone 6. Examples of the typical sedimentary features observed in vibracores from the outer estuary tidal bar of Zone 6. Clean, fine-grained sands are present throughout core shown in A-F, with small, sporadic shell fragments in portions of the sampled core observed as white streak or small clumps. Variable zones of anoxic (beige sand), suboxic (light grey sand) and anoxic sand (dark grey to black sand) are also evident throughout A-F. Weakly developed foresets can be observed in E and F (white arrows).

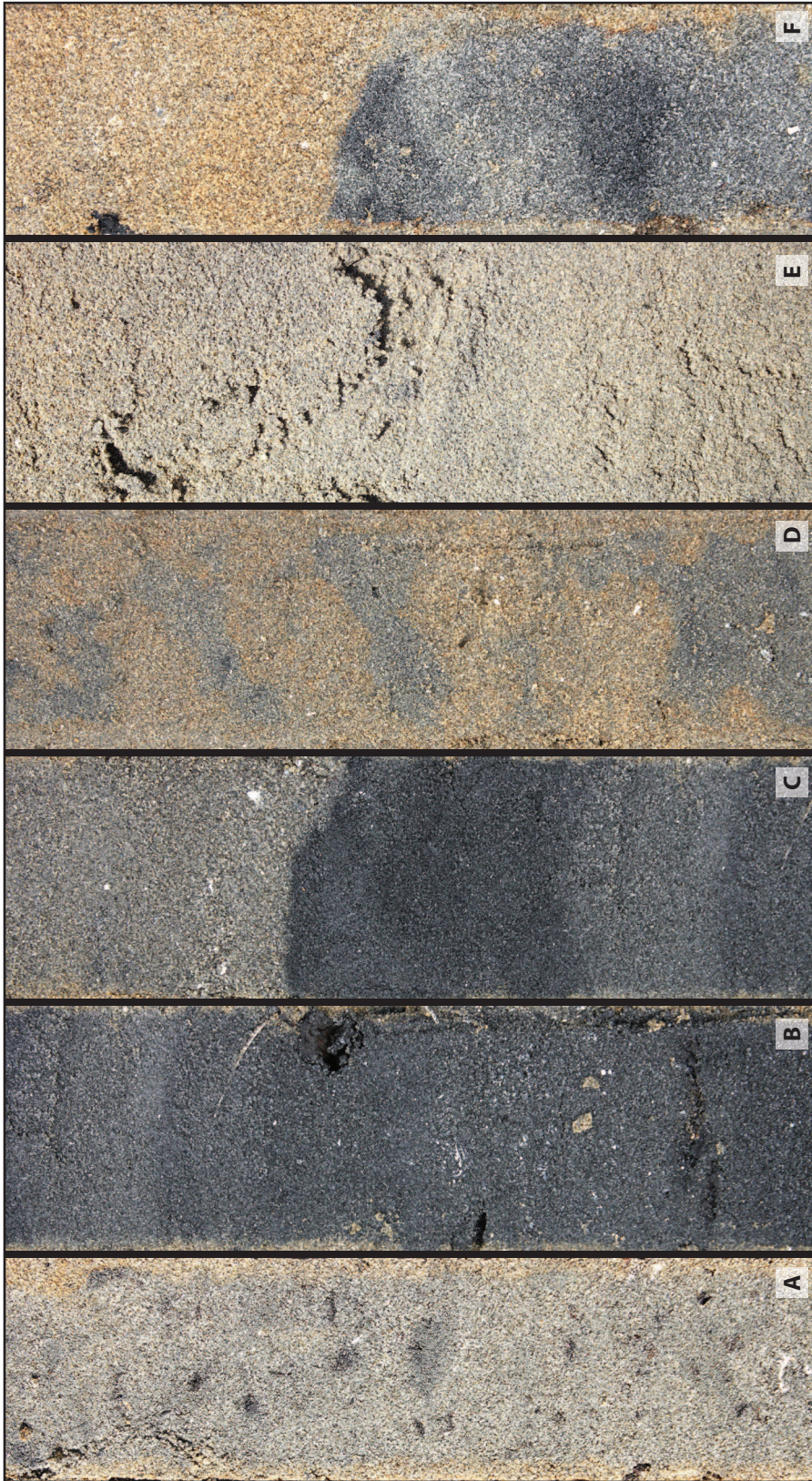
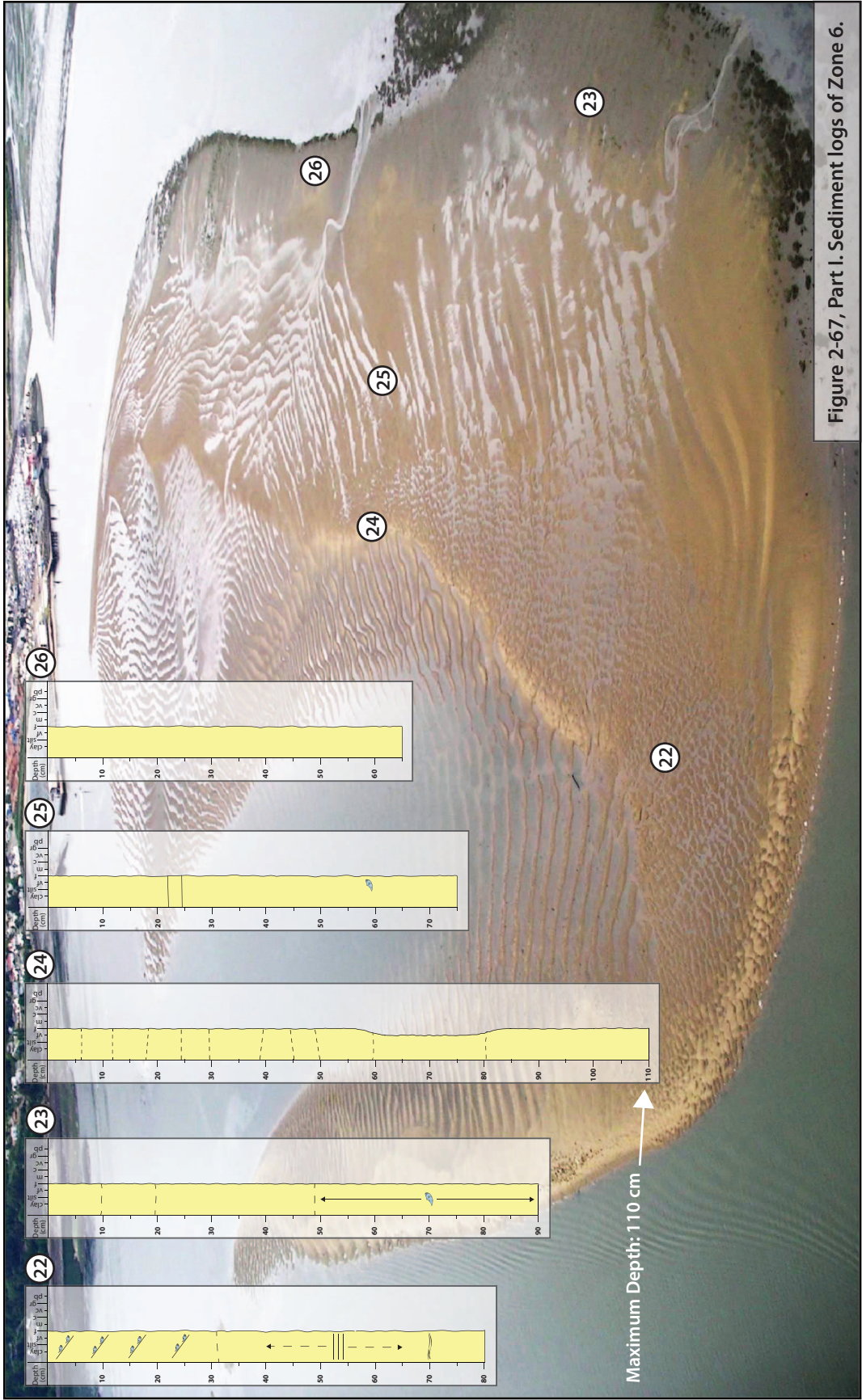


Figure 2-66, Part II. Vibracore examples from Zone 6. Examples of the typical sedimentary features observed in vibracores from the outer estuary tidal bar of Zone 6. Note possible small, <1 cm burrows (black arrows) in photo A. Small shell fragments, often deposited on faintly-observable foresets, can be seen in the rest of the photos, but especially in B and C, where the suboxic to anoxic, light to dark grey sand, are observed. Faint burrows observed in D with sporadic shell fragments. Note also the presence of faintly-observable foresets in D, E, and F.

Figure 2-67. Parts I and II (next two pages). Sediment logs of the outer estuary, Zone 6. Sediment logs for vibracores #22 to #32. As observed, the sediments of the outer estuary sand bar are well-sorted, with little grain size variation. Bedding contacts are faintly observable and difficult to distinguish at times. Cross-bedding is observed locally in some cores, and shell fragments are common to abundant in most cores. Aerial photos courtesy of Lidia Zabcic, used by permission.



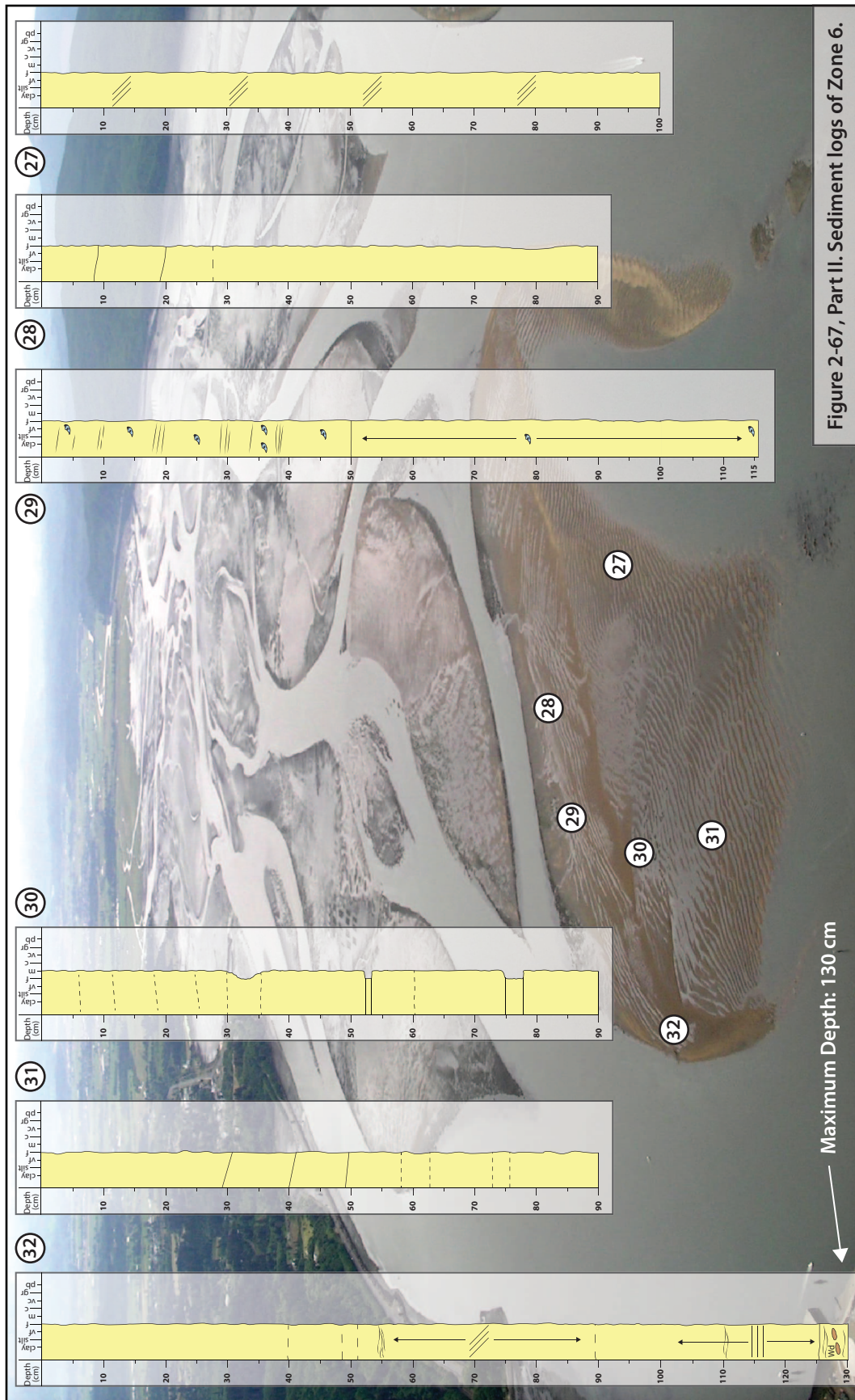


Figure 2-67, Part II. Sediment logs of Zone 6.

Maximum Depth: 130 cm

Facies 1 has no overlying facies and thus no overlying contact. There is a gradational contact with Facies 2 below.

Zone 6 Facies 2 (Z6F2) –Massive sand

Facies 2 is the most ubiquitous facies found throughout Zone 6 (Fig. 2-66 Part 1 A,B,C,D,E,F; Fig. 2-66 Part II A,B,C,D,E,F; Fig. 2-67 Part I; Fig. 2-67 Part II; Fig. 2-68; Table 2-6). It is commonly 20 cm to 60 cm thick. Facies 2 is characterized by massive, clean, well-sorted fine to medium grained sand. Small shell fragments are sporadically observed. Bioturbation appears largely absent, but possible sparse, 2-4 mm diameter, sand-filled burrows are observed. Facies 2 is gradational with Facies 1, 4, 5, and 6.

Zone 6 Facies 3 (Z6F3) –Laminated sand

Facies 3 is only observable in one vibracore obtained from the medium relief dune sub-environment (Fig. 2-66 Part 1 A,B,C,D,E,F; Fig. 2-66 Part II A,B,C,D,E,F; Fig. 2-67 Part I; Fig. 2-67 Part II; Table 2-6). The facies may be up to 50 cm thick; however it is only discernable as a 25 cm thick facies unit. Facies 3 is characterized by light brown coloured, clean, fine-grained sand with observable planar to inclined laminae. Bioturbation is absent. Facies 3 is gradational with Facies 4 and is underlain and overlain by this facies.

Zone 6 Facies 4 (Z6F4) –Planar-bedded sand

Facies 4 can be found throughout Zone 6 (Fig. 2-66 Part 1 A,B,C,D,E,F; Fig. 2-66 Part II A,B,C,D,E,F; Fig. 2-67 Part I; Fig. 2-67 Part II; Fig. 2-68; Table 2-6). It is commonly 10 cm to 30 cm thick. Facies 4 is characterized by planar-bedded, clean, well-sorted fine to medium grained sand. Fine grained sand dominates over the medium grained sand fraction. A lens of organic material is observed occurring with some planar beds. Small shell fragments are observed, commonly concentrated along bedding planes. Bioturbation is absent. Facies 4 is gradational with Facies 2, 3, 5, and 6.

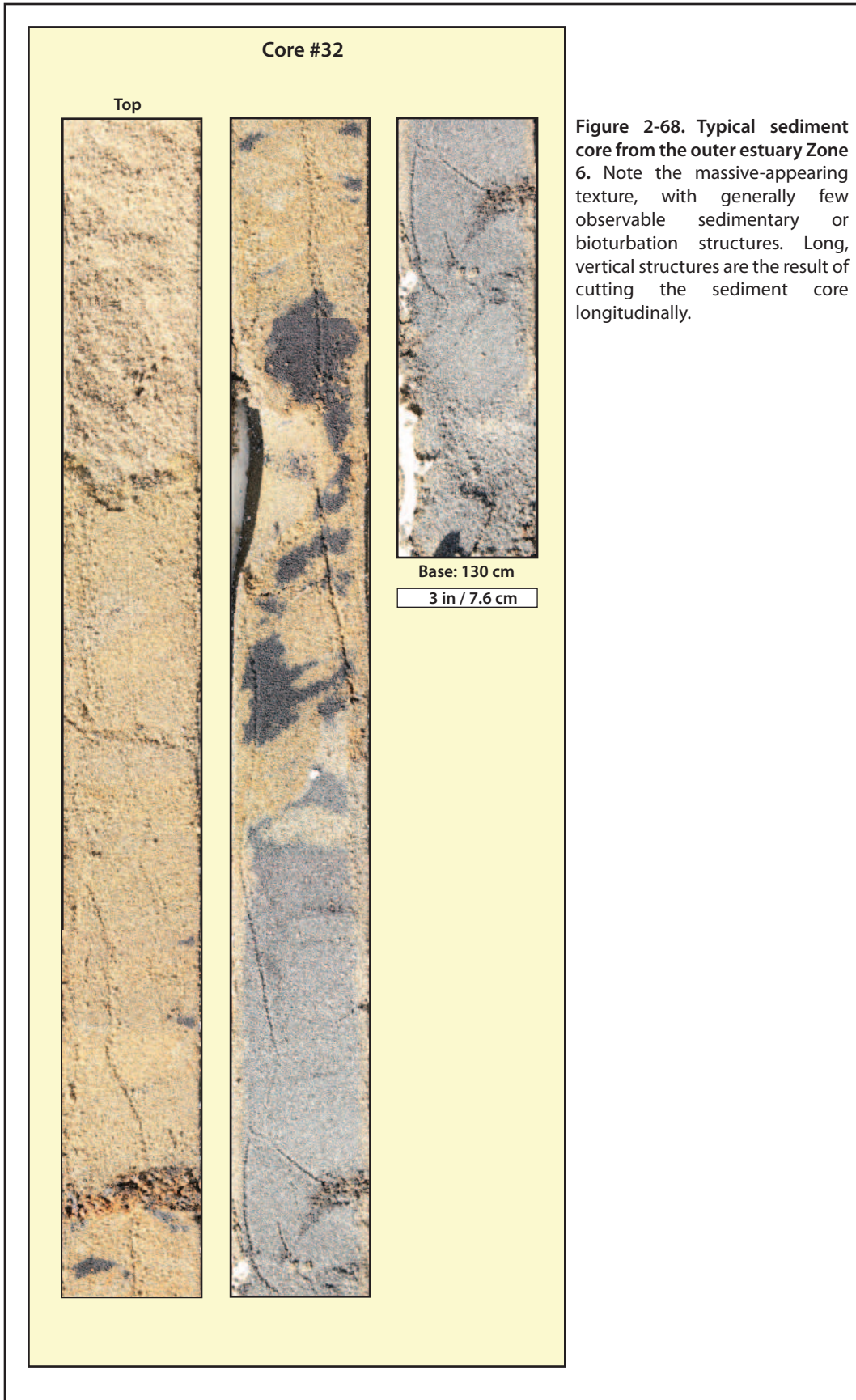


Figure 2-68. Typical sediment core from the outer estuary Zone 6. Note the massive-appearing texture, with generally few observable sedimentary or bioturbation structures. Long, vertical structures are the result of cutting the sediment core longitudinally.

Facies Association	Facies	Facies Contacts	Sedimentary Characteristics	Neoichnological Characteristics	Interpretation
<p style="text-align: center;">Isolated Tidal Sand Bar Facies Association (FA6)</p>	<p style="text-align: center;">Facies 1 (Z6F1) Burrowed massive sand</p>	<p>Facies 1 has no overlying facies and thus no overlying contact. There is a gradational contact with Facies 2 below</p>	<p>This facies is defined by burrowed, massive, fine-grained sand. Facies 1 is 50 cm thick.</p>	<p>The burrows occur sparsely and are sand-filled, having diameters of 2 mm to 4 mm.</p>	<p style="text-align: center;">Bioturbated, rippled tidal bar surface to low relief dune-covered tidal sand bar surface</p>
	<p style="text-align: center;">Facies 2 (Z6F2) Massive sand</p>	<p>Facies 2 is gradational with Facies 1, 4, 5, and 6.</p>	<p>Facies 2 is the most ubiquitous facies found throughout Zone 6. It is commonly 20 cm to 60 cm thick. Facies 2 is characterized by massive, clean, well-sorted fine to medium grained sand. Small shell fragments are sporadically observed.</p>	<p>Bioturbation appears largely absent, but possible sparse, 2-4 mm diameter, sand-filled burrows are observed.</p>	<p style="text-align: center;">Rippled tidal bar surface to low relief dune-covered tidal sand bar surface</p>

Table 2-6: Summary of Facies Characteristics for Isolated Tidal Sand Bar (Zone 6)

Facies Association	Facies	Facies Contacts	Sedimentary Characteristics	Neochronological Characteristics	Interpretation
Isolated Tidal Sand Bar Facies Association (FA6)	Facies 3 (Z6F3) Laminated sand	Facies 3 is gradational with Facies 4 and is underlain and overlain by this facies.	The facies may be up to 50 cm thick; however it is only discernable as a 25 cm thick facies unit. Facies 3 is characterized by light brown coloured, clean, fine-grained sand with observable planar to inclined laminae.	Bioturbation is absent.	Dune-associated, flat-lying tidal sand bar surface
	Appendix B Core Figure Reference(s): B-25	Facies 4 is gradational with Facies 2, 3, 5, and 6.	Characterized by planar-bedded, clean, well-sorted fine to medium grained sand. Fine grained sand dominates over the medium grained sand fraction. A lens of organic material is observed occurring with some planar beds. Small shell fragments are observed, commonly concentrated along bedding planes. It is commonly 10 cm to 30 cm thick.	Bioturbation is absent.	Low relief dune- to medium relief dune-covered tidal sand bar surface
	Facies 4 (Z6F4) Planar-bedded sand	Appendix B Core Figure Reference(s): B-20; B-21; B-25; B-26			

Table 2-6 (continued): Summary of Facies Characteristics for Isolated Tidal Sand Bar (Zone 6)

Facies Association	Facies	Facies Contacts	Sedimentary Characteristics	Neochronological Characteristics	Interpretation
<p style="text-align: center;">Isolated Tidal Sand Bar Facies Association (FA6)</p>	<p style="text-align: center;">Facies 5 (Z6F5) Low-angle bedded sand</p>	<p style="text-align: center;">Facies 5 is commonly observed to be gradational with Facies 2 and occasionally with Facies 4.</p>	<p>Commonly 15 cm to 25 cm thick, but can be up to 50 cm – 60 cm thick. Faint bedding, slightly inclined at an angle up to 5 degrees; in clean, well-sorted, fine to medium grained sand characterizes Facies 5. Small shell fragments (0.1 to 0.2 cm in diameter) are sporadically observed. Beds of fine and medium grained sand alternate and, in addition to small shell fragments, help in observation of the low-angle bedding.</p>	<p>Bioturbation is absent.</p>	<p style="text-align: center;">Low relief to medium relief dune-covered tidal sand bar surface</p>
	<p style="text-align: center;">Appendix B Core Figure Reference(s): B-21; B-23; B-24; B-25</p>	<p style="text-align: center;">Contacts with Facies 6 are gradational when present. Facies 4 is found to either overlay or underlay Facies 6, while Facies 2 is also observed to underlay Facies 6.</p>	<p>The facies was typically 30 cm thick, but was found to comprise the entirety of Core 27 at a thickness of 100 cm. Facies 6 is characterized by clean, well-sorted, fine-grained sand. Small shell fragments are observed concentrated along the high angled foresets. Typically, the cross beds are faintly observable.</p>	<p>Bioturbation is generally lacking but there is an occurrence of possible small, round, sand-filled burrows.</p>	<p style="text-align: center;">Medium relief dune-covered tidal sand bar surface</p>
<p>Table 2-6 (continued 2): Summary of Facies Characteristics for Isolated Tidal Sand Bar (Zone 6)</p>					

Zone 6 Facies 5 (Z6F5) –Low-angle bedded sand

Facies 5 can be found throughout Zone 6 (Fig. 2-66 Part 1 A,B,C,D,E,F; Fig. 2-66 Part II A,B,C,D,E,F; Fig. 2-67 Part I; Fig. 2-67 Part II; Table 2-6). It is commonly 15 cm to 25 cm thick, but can be up to 50 cm – 60 cm thick. Faint bedding, slightly inclined at an angle up to 5 degrees, in clean, well-sorted, fine to medium grained sand characterizes Facies 5. Small shell fragments (1 to 2 mm in diameter) are sporadically observed. Beds of fine and medium grained sand alternate and, in addition to small shell fragments, help in observation of the low-angle bedding. Bioturbation is absent. Facies 5 is commonly observed to be gradational with Facies 2 and occasionally with Facies 4.

Zone 6 Facies 6 (Z6F6) –High-angle x-bedded sand

Facies 6 is observed in vibracores from the rippled sand deposits and medium relief dunes sub-environments (Fig. 2-66 Part 1 A,B,C,D,E,F; Fig. 2-66 Part II A,B,C,D,E,F; Fig. 2-67 Part I; Fig. 2-67 Part II; Fig. 2-68; Table 2-6). The facies was typically 30 cm thick, but was found to comprise the entirety of Core 27 at a thickness of 100 cm. Facies 6 is characterized by clean, well-sorted, fine-grained sand. Small shell fragments are observed concentrated along the high angled foresets. Typically, the cross beds are faintly observable. Bioturbation is generally lacking but there is an occurrence of possible small, round, sand-filled burrows. Contacts with Facies 6 are gradational when present. Facies 4 is found to either overlay or underlay Facies 6, while Facies 2 is also observed to underlay Facies 6.

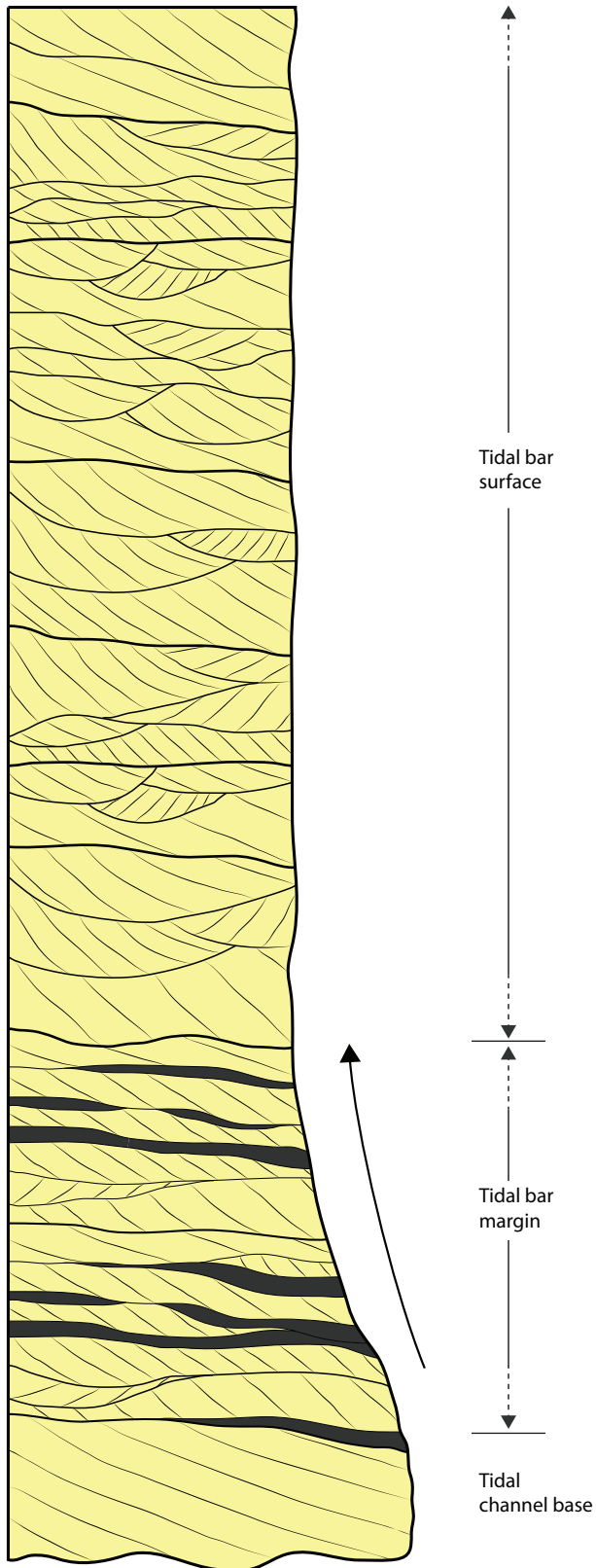
Zone 6: Isolated Tidal Sand Bar Interpretations

The six facies described for the Isolated Tidal Sand Bar (Zone 6) are interpreted as: Facies 1 (Z6F1: Bioturbated, rippled tidal bar surface to low relief

dune-covered tidal sand bar surface); Facies 2 (Z6F2: Rippled tidal bar surface to low relief dune-covered tidal sand bar surface); Facies 3 (Z6F3: Dune-associated, flat-lying tidal sand bar surface); Facies 4 (Z6F4: Low relief dune- to medium relief dune-covered tidal bar sand surface); Facies 5 (Z6F5: Low relief to medium relief dune-covered tidal sand bar surface); and Facies 6 (Z6F6: Medium relief dune-covered tidal sand bar surface). These interpreted facies comprise the Isolated Tidal Sand Bar Facies Association (FA6) (Table 2-6). Ideally, though not observed in vibracores, a succession may consist of channel coarse sand through to muddy sand and/or mud on the bar edge, followed by a complex interrelationship between all 6 facies interpreted from vibracores of Zone 6 (Fig. 2-69). There is no distinct sequence observed between interpreted facies of Zone 6, rather they are all related and form a complex outer bar facies association (Fig. 2-69).

The outer estuary tidal sand bar studied, due to its relatively small area and inter-relatedness of facies, will be interpreted here in one section (Fig. 2-69), comprising all sub-environments. The clean, well sorted sands of Zone 6, are clearly reworked both by tidal and wave currents, making this portion of the estuary the most mixed, in terms of current energy types. Deep tidal channels, between 2.5 - 6 metres deep, surround the tidal bars of the outer estuary. Zone 6 experiences strong tidal currents, due to its location relative to the tidal prism. Dune migration orientations, mostly parallel to the ebb tide currents, indicate a strong tidal influence on the sediments of the tidal bar (Allen, 1982). Well-developed troughs, as well as trough cross-bedding observed in cores and boxcores, indicates the effect of wave currents. This is to be expected, given the location of Zone 6 near the bay mouth and the direct connection to the Pacific Ocean. Trough cross-beds of the outer estuary indicate the combined influence of tidal and wave generated currents (Dashtgard, 2011). Large ocean swells or storm waves frequently affect the waters at the bay mouth, sending strong currents inward and forming waves inside the bay. During the summer season, when fieldwork was conducted,

Figure 2-69. Schematic vertical succession from an outer estuary tidal sand bar. Vertical profile of an isolated sand tidal bar, as interpreted from core and surface observations from Tillamook Bay. On the laterally-aggrading side of the bar, mud deposits are interbedded with complex rippled sand and low-relief dunes. In the central region of the bar, low-relief to medium-relief dunes, with complex ripples superimposed on their surface, are widely observed. High angle bedding and trough cross-bedding, interpreted largely from surface observations, are widely distributed. High wave influence affects the sorting of sediment and the formation of sedimentary structures. Due to the well-sorted nature of the marine-sourced sediment, sedimentary structures, as well as bioturbation structures, are difficult to observe in sediment cores. They are, however, better observed in surface sediments. Bioturbation structures, where present on the bar surface, are absent to moderate in concentration, but most are poorly preserved. Dune structures, along with their interpreted high-angle bedding and trough-cross bedding, are largely oriented in the ebb-tidal current direction.



strong, wind-induced waves were observed. The lack of significant amounts of silt and clay, especially the main tidal bar studied, can be explained by the hydraulic energies affecting this area. Large tides, creating strong tidal currents, prevent the deposition and/or preservation of mud in areas other than those close to shorelines or in deep water (Middleton, 1980). Although tides at Tillamook Bay fall in the mesotidal range, a medium sized tidal prism, combined with wave action, may be able to create currents in the outer estuary strong enough to prevent any significant mud deposition and erode any previously deposited mud layers. The dunes described in this zone may fall into the category of “megaripples” (Dalrymple et al., 1978).

The dunes of the outer estuary, although resembling ridge and runnel topography (King and Williams, 1949), are different from the latter, which form due to wave and storm erosion on tidal beach deposits, and have a beach-parallel morphology, cut by drainage channels oriented perpendicular to the beach (Masselink et al 2006). Intertidal bars of low-amplitude ridges (i.e. ridge and runnel topography) rarely exceed 1 metre amplitude, and are generally widely spaced apart, at approximately 100 metres (Masselink et al 2006). Though the “low-amplitude ridges” and dunes of the outer estuary of Tillamook Bay are similar the dune wavelength (i.e. spacing) is much smaller, on the order of several meters. The combined tidal and wave influence, along with a different depositional setting and different energy system, indicates the reason behind the morphological contrast between ridge and runnel topography and outer estuary dunes.

Given the relatively low total organic carbon (TOC) values present in the sediment of the outer estuary bar, it is likely that lower concentrations of deposited food and nutrients are available in this zone. This may explain the comparatively low bioturbation intensity and reduced organism diversity, relative to the muddier, higher TOC zone of the inner estuary, where bioturbation is more intense and deposited food is abundant. A possible source of nutrients, however, is the transport of plankton during flood tides, as

noted by Ricketts et al. (1985). It is important to note that, although bioturbation structures were not observed in high concentrations, this does not necessarily imply low bioturbation intensity. Given the well-sorted character of sediments in the outer estuary, and the fact that a lack of contrasting sediment character is observed, both sedimentary and biogenic structures may be obliterated due to cryptic bioturbation and the high reworking of sediment.

DISCUSSION

Sedimentological Facies Model and Controls on Sedimentation

Tidal bars, being dominant geomorphologic features in Tillamook Bay, occur in various areal extents throughout the estuary, ranging from the largest bars in the inner estuary, and gradually decreasing in size to the smallest bars in the outer estuary. As shown in Figure 2-70, much of the sediment in the inner estuary is river-derived, and ranges widely from very coarse sand in the bayhead delta, to fine-grained sand and muddy sand at the ebb-oriented end of the tidal bar of Zone 3. Tidal bars are tidally generated sand bodies with their long axes oriented largely parallel to the dominant currents (Olariu et al., 2012). Tidal bars, described in estuaries, deltas, and open shelf settings, have a strong component of lateral migration, and often migrate when adjacent to migrating channels (Olariu et al., 2012). Tidal bars formed in marginal marine setting, such as estuaries, have a fining upward succession, whereas those formed in shelf settings, where tidal channels do not exist, exhibit a coarsening upward profile (Olariu et al., 2012).

The location of the turbidity maximum in meso- and macro-tidal estuaries is directed dominantly by the gravitational circulation mechanism (Hughes et al., 1998). The mechanism relies on the interplay between low-density, seaward-directed surface flows of freshwater carrying suspended

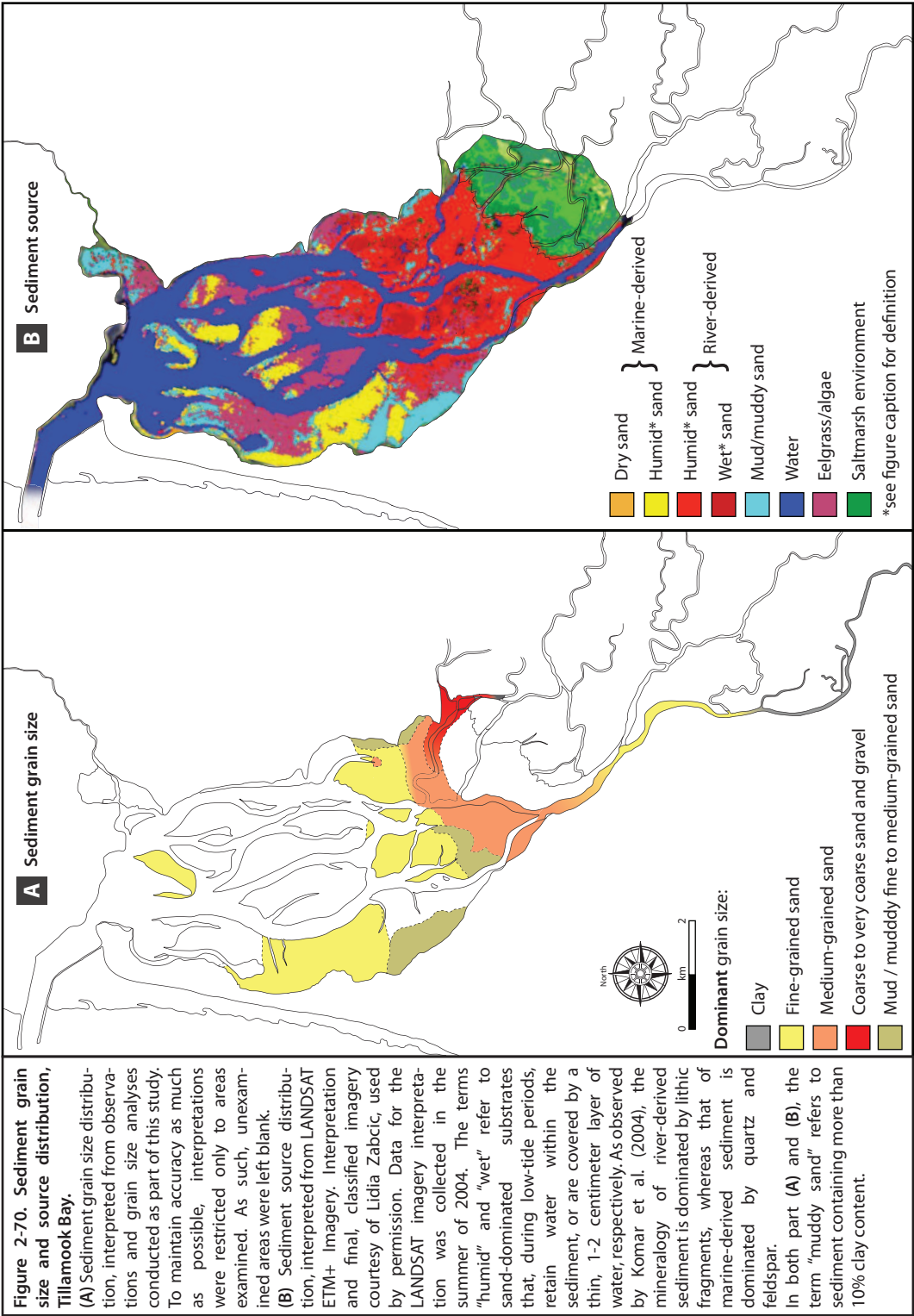


Figure 2-70. Sediment grain size and source distribution, Tillamook Bay. (A) Sediment grain size distributions, interpreted from observations and grain size analyses conducted as part of this study. To maintain accuracy as much as possible, interpretations were restricted only to areas examined. As such, unexamined areas were left blank. (B) Sediment source distribution, interpreted from LANDSAT ETM+ Imagery. Interpretation and final, classified imagery courtesy of Lidia Zabcic, used by permission. Data for the LANDSAT imagery interpretation was collected in the summer of 2004. The terms "humid" and "wet" refer to sand-dominated substrates that, during low-tide periods, retain water within the sediment, or are covered by a thin, 1-2 centimeter layer of water, respectively. As observed by Komar et al. (2004), the mineralogy of river-derived sediment is dominated by lithic fragments, whereas that of marine-derived sediment is dominated by quartz and feldspar. In both part (A) and (B), the term "muddy sand" refers to sediment containing more than 10% clay content.

sediment, and the higher-density, landward-directed bottom-flow of saline water. At the point of mixing between saline and fresh water, the change in water salinity induces the clumping together of fine particulate matter, which then settles (flocculates) out of suspension (Dyer, 1986; Hughes et al., 1998). Highly-concentrated clay suspensions may result in the formation of fluid muds (Einstein and Krone, 1962; Hughes et al., 1998).

Salinity stratification (Fig. 2-71; Fig. 2-72) in Tillamook Bay occurs dominantly during the wet, rainy season, when fluvial, freshwater discharge is highest and able to advance farther downstream during both the low and high tides. River-derived, suspended sediment also increases in concentration during the wet season. During the dry season, flood tides overpower the fluvial currents, causing the mixing zone to migrate upstream into the fluvial-tidal transition (Fig. 2-71). The migration of the freshwater front (and the turbidity maximum, as shown in Figure 2-73) has an effect on the location where flocculation can take place, as it can advance quite far into the estuary (Fig. 2-72). As a result, mud deposition, controlled by the mixing of freshwater versus marine water and thus by flocculation, takes place in inner estuary fluvial-tidal transition areas during the dry season (Fig. 2-71), and in the inner estuary sand bars and tidal flats during the wet season (Fig. 2-72).

It is possible that many of the mud beds observed in the intertidal flats of Tillamook Bay are fluid mud deposits. Fluid mud has concentrations higher than 10 g/L, and commonly occurs at the area of turbidity maximum in tidally-influenced estuaries (Ichaso and Dalrymple, 2009). Fluid mud consists of dense accumulations of clay and silt-sized sediment, and can move in response to gravity, as gravity flows, or in response to shear stresses induced by flows in the tidal and fluvial water mixing zone (Ichaso and Dalrymple, 2009). The minimum thickness of homogeneous mud layers, interpreted to be deposited as fluid mud, is higher than approximately one centimeter in modern settings (Dalrymple et al., 2003). In the Tilje Formation in Norway, thick mud beds were

Figure 2-71. Salinity stratification during the dry season. Cross-sectional schematic view of salinity measurements, recorded during the low tide and high tide periods on July 23, 1958. Figure compiled using data from Burt and McAlister (1958).

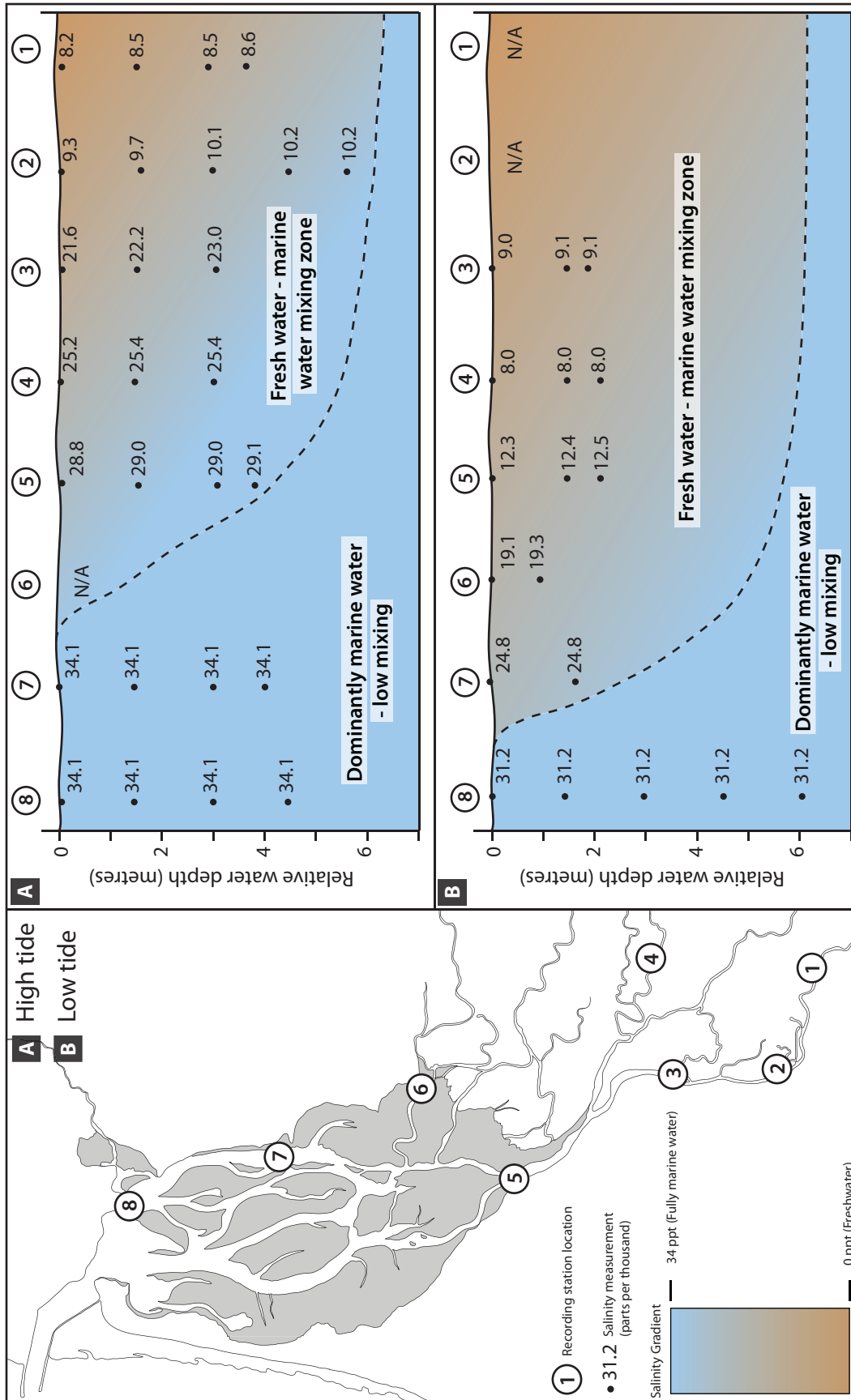
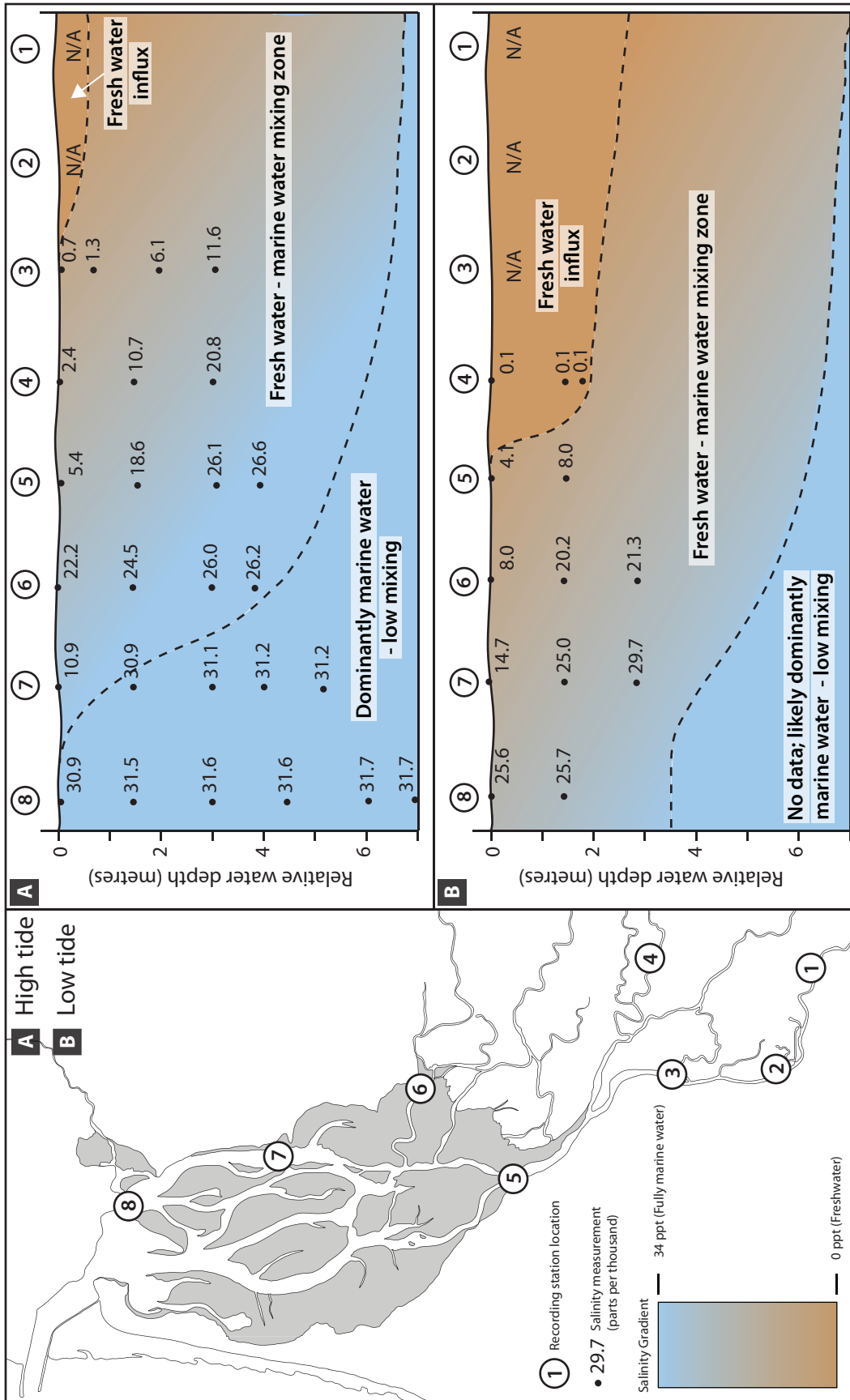


Figure 2-72. Salinity stratification during the wet season. Cross-sectional schematic view of salinity measurements, recorded during the low tide and high tide periods on January 4, 1958. Figure compiled using data from Burt and McAlister (1958).



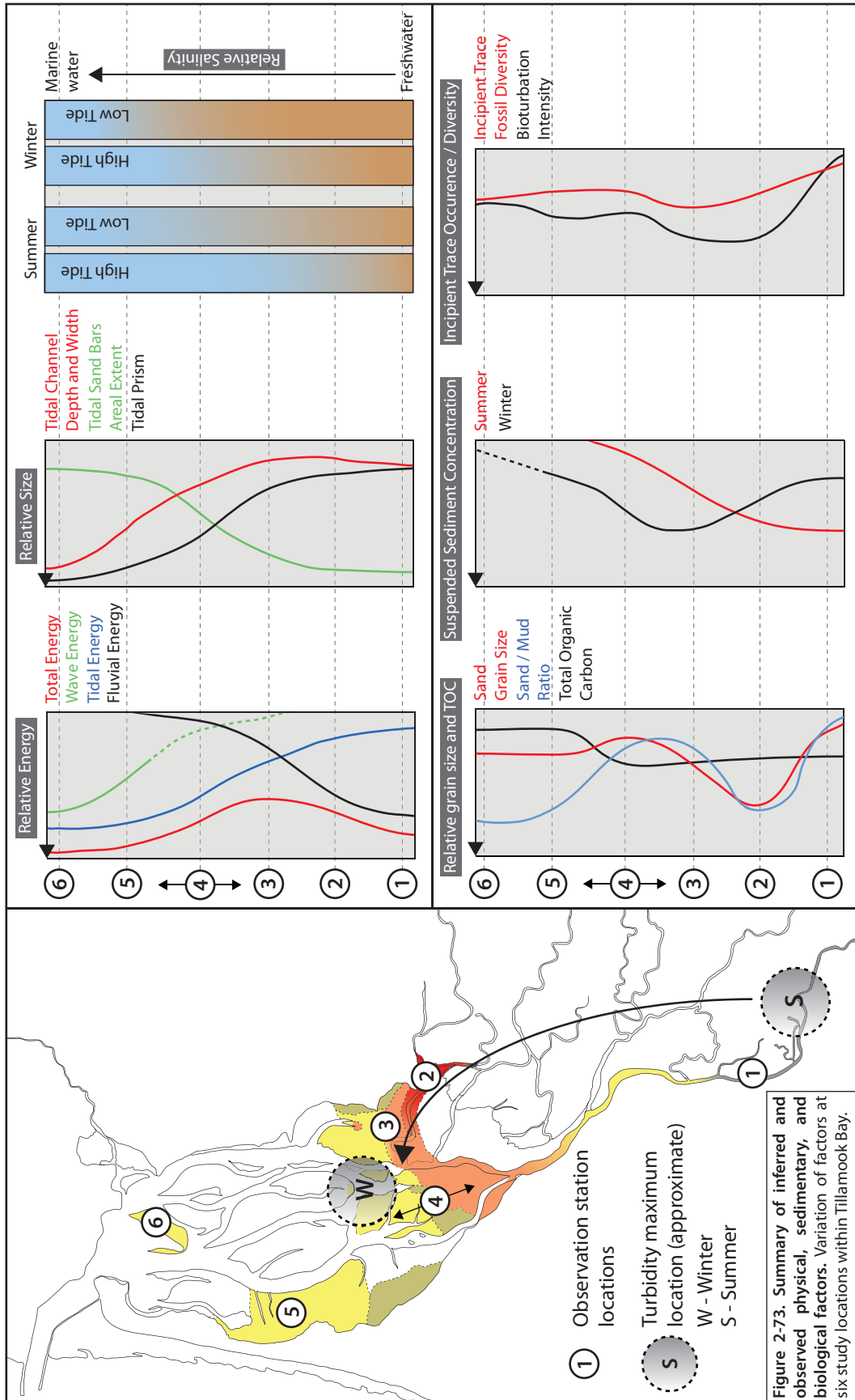


Figure 2-73. Summary of inferred and observed physical, sedimentary, and biological factors. Variation of factors at six study locations within Tillamook Bay.

observed at the bottom of tidal-fluvial channel deposits, interpreted to have formed as channel-bottom fluid mud (Ichaso and Dalrymple, 2009).

Given the wave-influenced geomorphology of the Tillamook Bay estuary, and the largely constant bay width between the baymouth and bayhead regions, tidal range is unlikely to be increased due to a gradually-restricted morphology, as is the case with idealized funnel-shaped, tide-dominated estuaries. Moreover, the relatively shallow channels of the inner estuary reduce the surface area that otherwise increases frictional forces acting on tidal currents. As such, the tidal asymmetry mechanism of forming a turbidity maximum (Dyer, 1986; Hughes, 1998), if occurring in Tillamook Bay, likely has a subordinate importance and impact.

Tidal bars studied at Tillamook Bay indicate a fining of sediment in a lateral direction, away from tidal channels and towards the central portions of the bars. As seen in Figure 2-74, Part I and II, tidal channels maintain relatively stable positions within the estuary over a time-span of several decades. Channel widths, on the other hand, vary more widely, as do corresponding bar migrations. Over a 34-year period, the most significant bar migrations occur in the middle and outer estuary, with smaller changes occurring in the inner estuary, except for the bay-head delta zone near the mouth of the Kilchis River. The bay-head delta region is expected to receive large amounts of sediment of varying grain sizes, and as such, it is not surprising that significant changes in sedimentation patterns and bar migrations occur here. The inner estuary tidal bar (Zone 3) examined in this study appears to migrate over relatively short distances in a time span of 34 years. The most significant changes occur at the ebb-oriented tip of the bar, with more minor changes at the flood-oriented tip. As it transitions into the middle estuary, the ebb-oriented tip may experience – as the rest of the middle and outer estuary – more significant wave influence. In an upstream direction, closer to the mouth of Tillamook River and other rivers entering the bay, the bar migration is reduced possibly due to reduced wave influence relative to the middle and outer estuary zones. In this scenario, tidal

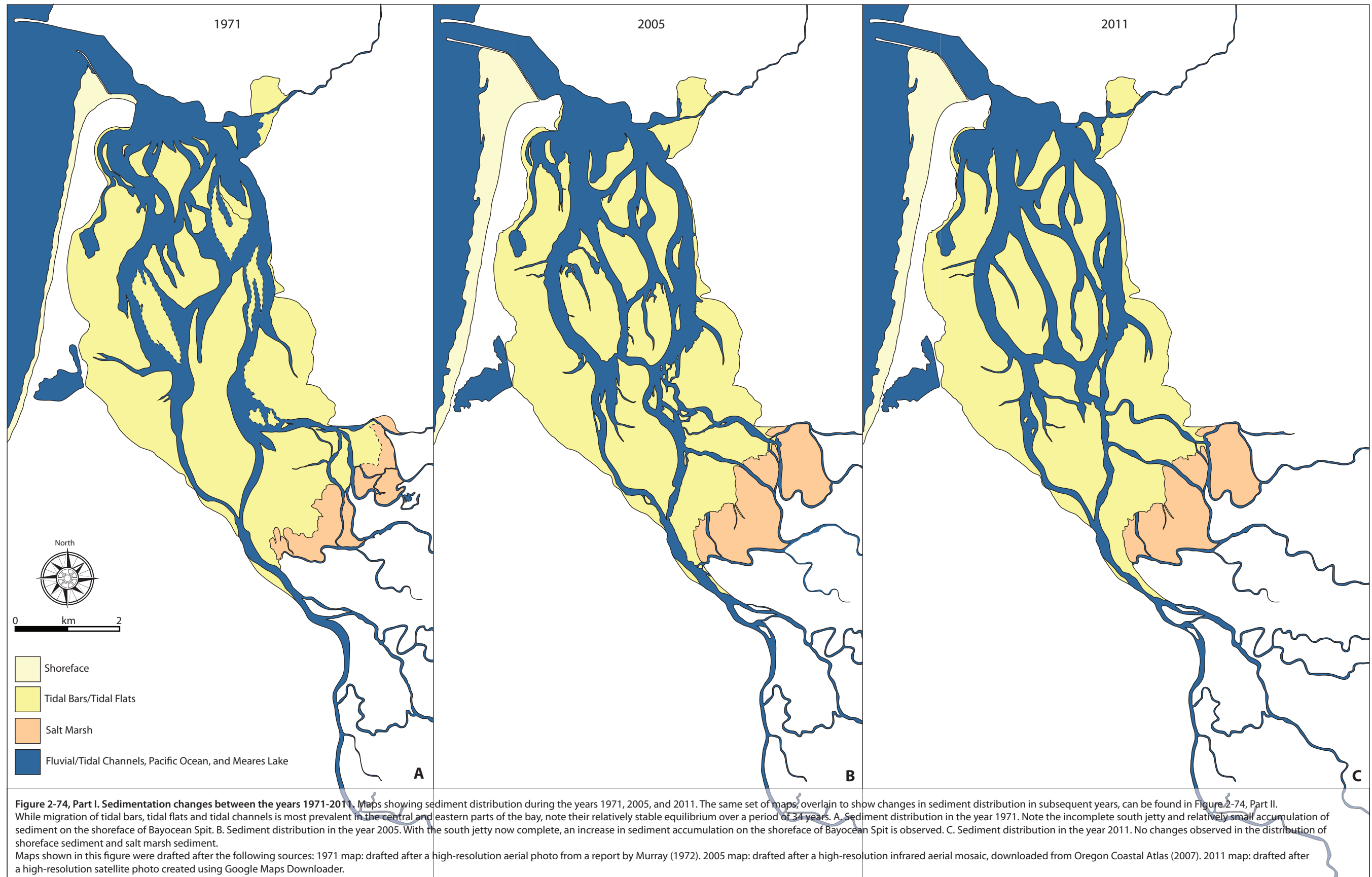


Figure 2-74, Part II. Sedimentation changes between the years 1971-2011.

Maps showing sediment distribution during the years 1971, 2005, and 2011. The maps are overlain and sediments shown in contrasting colors in order to show areas of no change and areas of significant change in subsequent years. It is important to note that the maps show distributions at the beginning and end of each time period, and not at any time in between. Therefore, the changes observed should be interpreted as a general, simplified view of sedimentation and migration patterns of geomorphological features such as tidal bars.

Individual maps (i.e. with no overlays) can be found in Figure 2-74, Part I.

(A) Sedimentation changes over a period of 34 years, between 1971 and 2005, of shoreface sediments, tidal bar and tidal flat sediments, and salt marsh sediments.

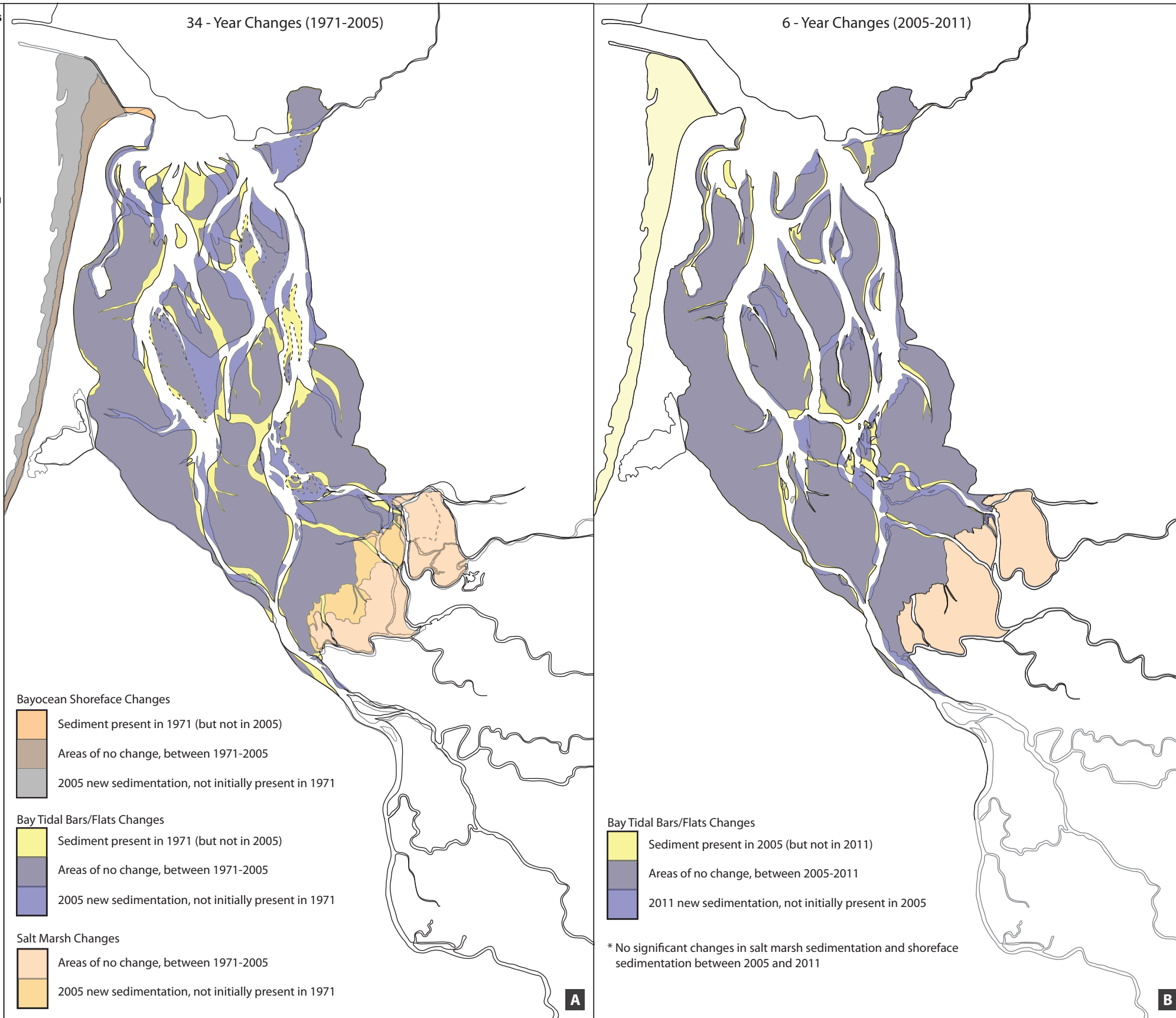
(B) Sedimentation changes over a period of 6 years, between 2005 and 2011, of tidal bar and tidal flat sediments. Note the relatively insignificant changes to shoreface and salt marsh sedimentation.

Maps shown in this figure were drafted after the sources described below.

1971 map: drafted after a high-resolution aerial photo from a report by Murray (1972)

2005 map: drafted after a high-resolution infrared aerial mosaic, downloaded from Oregon Coastal Atlas (2007).

2011 map: drafted after a high-resolution satellite photo created using Google Maps Downloader.



currents – of limited strength due to a smaller tidal prism in this region – partly act on sediment delivery and total energy in the tidal channels. On the edges of tidal bars, adjacent to tidal channels, trenches dug into the sloping bars reveal the presence of inclined heterolithic stratification, with burrows occurring in both finer and coarser members. Vibracores both at the edge of the tidal bar and within the center of the bars also reveal heterolithic stratification, with alternating mud and sand layers on both centimeter and decimeter scales. Because of limitations due to the diameter of the cores, the inclined nature of the layers could not be easily observed, though in some cases the beds are clearly inclined. Inclined heterolithic stratification was also observed within deposits of the free-meandering Kilchis River, at the site of the bayhead delta.

It is interpreted that deposition of sand and mud beds at Tillamook Bay is seasonally-controlled. Mixing of freshwater and marine water, during dry and wet seasons results in thorough mixing, or salinity stratification, respectively. The presence of salinity stratification promotes flocculation of suspended sediment, and with the seasonal migration of the turbidity maximum, mud deposition takes place either in the fluvial channels of the fluvial-tidal transition zone, or on tidal bars and tidal flats inside the bay. During periods of fluvial discharge, the turbidity maximum moves in a bayward direction, and suspended sediment is thus transported past the river mouths, into the bay, where it is reworked by tides, and settles in quiescent, intertidal areas. Similar processes have been observed on a tidal bar of the Fraser River, British Columbia (Sisulak and Dashtgard, 2012). Seasonal variations in fluvial discharge result in the rapid deposition of sand and mud beds during freshet conditions, and deposition of mud during base-flow conditions. The freshet-deposited sand and mud beds lack bioturbation, due to reduced salinity and increased sedimentation rate, whereas the mud deposited during base-flow, brackish-water conditions, contains *Arenicolites*-, *Skolithos*-, *Palaeophycus*-, and *Polykladichnus*-like traces (Sisulak and Dashtgard, 2012).

Three lithofacies models have been proposed for meandering river conditions, based on outcrop and modern settings (Smith, 1987). The three models that can occur within the same fluvial-estuarine system include: continuous sand, irregular sand, and rhythmic sand and mud facies, corresponding to increasingly higher tidal influence (Smith, 1987). The rhythmic sand and mud, observed within inner estuary and middle estuary zones, corresponds to the epsilon cross-stratification put forth by Allen (1963).

The terms *Inclined Heterolithic Stratification* (IHS) and *Inclined Stratification* (IS), have been widely used to describe dominantly lithologically heterogeneous sediments from siliciclastic sedimentary environments (Thomas et al., 1987). While useful as descriptive terms in many important studies (e.g. Pemberton et al., 1982), the term, as applied to modern intertidal sedimentary features, may not be fully descriptive of the specific environment of deposition (e.g. bayhead delta, channel margin, tidal channel, shore-attached tidal flats etc.) The classification put forth by Allen (1963), though highly complex, if used carefully and with the right amount of supporting data, can be more descriptive in assigning certain facies to depositional environments, as listed above. The high sedimentological contrast between bayhead-delta, inner-estuary tidal bars, and outer estuary tidal bars, for example, shows that the term *Inclined Heterolithic Stratification* (IHS) and *Inclined Stratification* (IS), applied to the first two, and latter environments, respectively, do not imply bedform stacking patterns and geometries. By observing the morphological characteristics (such as dip angles of channel margins) of sedimentary environments, the locations within the estuary depositional complex, the sediment caliber, and sedimentary structures present, it can be assessed that the overall nature of the stacking patterns in each environment can greatly differ. As a result, assigning the term IHS to heterolithic strata of the inner estuary, and IS to largely homogeneous strata of the outer estuary, may provide "lower-resolution" descriptions and interpretations, and tend to over-generalize the sedimentary units observed.

The deposition and redistribution of mud within the estuary, though largely controlled by the migration of the turbidity maximum between the wet and dry seasons, can also be controlled by the presence of areally-extensive eelgrass stabilized flats, as well as high concentrations of filter-feeding or deposit-feeding organisms. In the case of eelgrass, high concentrations on tidal flats and bars allow the baffling of currents, therefore causing suspended material to settle out of suspension (Boothroyd et al., 1985). This leads to higher-relief (compared to the surrounding area), dome-shaped mud accumulations around eelgrass concentrations.

Similarly, fecal pellets produced by suspension-feeding organisms, as well as benthic organisms such as polychaete worms, can accumulate in large quantities in estuarine environments. Some studies have shown that the amount of fecal pellets produced by estuarine organisms can be on the order of tens of metric tons (dry weight) over the course of even a month (Haven and Morales-Alamo, 1968). Large numbers of pellets, as high as 40,000 pellets/m³ (Haven and Morales-Alamo, 1968) can be found suspended in the water column; the increased weight of those compacted fine sediment particles can thereby accelerate the sedimentation of finer, uncompacted suspended sediment. Within subtidal zones of tidal creeks – which incise into tidal bars and flats at Tillamook Bay – high concentrations of fecal pellets are observed to be transported by water currents flowing during the outgoing tide. The high fecal pellet accumulations coincide with high accumulations of small plant fragments, both of which are observed to be freely moved by currents in a downstream direction, away from the higher-relief portions of the tidal bars and tidal flats. Observations of the cross-sectional sedimentary layers within tidal creeks reveal a high mud concentration, even in zones where the laterally-adjacent, non-tidal-creek sediments are sand-dominated. It is therefore possible that the reworking and re-suspension of fecal pellets by tide and wave currents during tidal cycles, may be a driving factor in the re-distribution of mud within the estuary, or within sub-environments within the estuary. As

such, large tidal creeks with high cross-sectional surface areas, capable of transporting high amounts of water and fecal pellets, may be able to provide high amounts of mud to their lower reaches. High accumulations of fecal pellets in sand-dominated areas, under the influence of tidal and wave currents, tend to be transported and deposited in ripple troughs. This may give rise to flaser and lenticular bedding (depending on relative mud and sand content), even in clean, sand-dominated settings, such as beaches (Frey and Pemberton, 1985). The formation of biogenic flasers – due to the excretion and preservation of fecal pellets in sedimentary environments – therefore falls under the category of biodeposition structures (Frey and Pemberton, 1985).

Dunes, observed in the mixed-energy outer estuary of Tillamook Bay, and visibly influenced by tides, are significantly smaller in scale than those mentioned by Olariu et al. (2012) as having “a strong component of forward migration”. However, similar conditions likely affect the deposition of those dunes, on a smaller scale. Likely due to mixed energy conditions and good sorting, dunes in Zone 6 are not observed to coarsen upward. The difference may be accounted for by the strong wave influence in the outer estuary, along with a large tidal prism, thus having the ability to erode and/or flush suspended sediment through the deep channels. These factors, causing the sediment to become very well sorted, also indirectly result in their homogenization. Therefore, the difference in current energies between dune troughs and crests – interpreted to cause the coarsening upward of tidal dunes (Olariu et al., 2012) – are not expected to result in a segregation of sediment particles of varying sizes. It should be noted, however, that shell lags are observed along the foresets and bottomsets of dunes in Zone 6. In cross-stratified siliciclastic sandstones of the Baronía Sandstone, dual-oriented foresets, along with absent to sparse bioturbation (BI 0 to 1) have been observed (Olariu et al., 2012). Such deposits have been interpreted to have formed under tens of meters of water, under the influence of bi-directional tidal currents in proximity to a marine strait or constriction of an embayment.

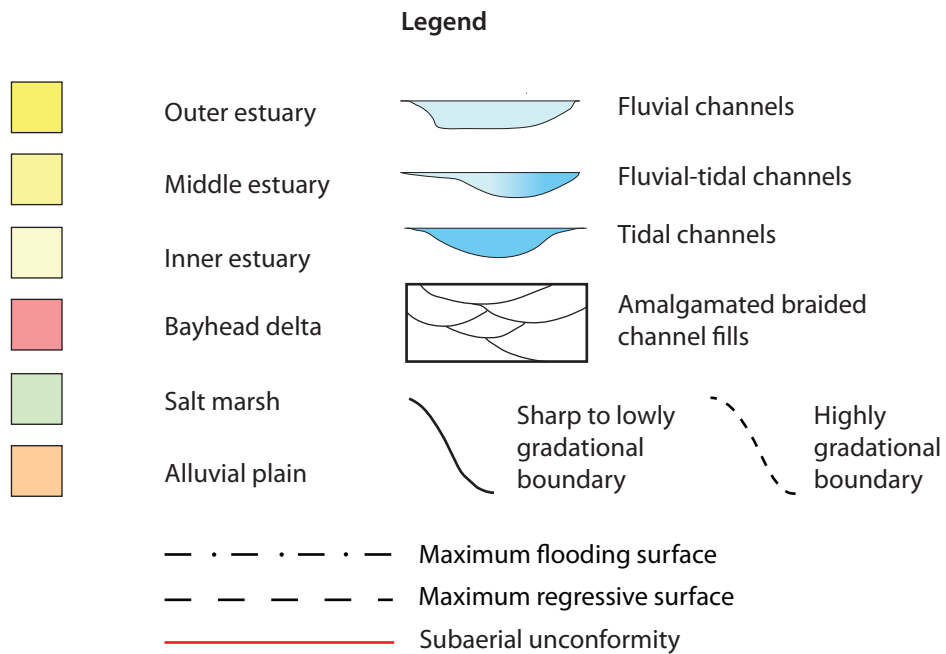
Although markedly different in many respects, the morphological difference between tidal bars and tidal dunes described by Olariu et al. (2012) likely applies to bars and dunes formed in shallow waters of Tillamook Bay. Tidal bars are oriented parallel to sub-parallel to the axis of dominant flood and ebb currents, and migrate laterally as channels migrate laterally (Chaumillon et al., 2013). Tidal dunes, on the other hand, migrate forward under the influence of strong ebb currents of the large tidal prism draining Tillamook Bay at every tidal cycle. The relief of a tidal bar and tidal dune varies in relation to water flow height, being more than 20%, and less than 20%, respectively, of the flow height (Dalrymple and Rhodes, 1995).

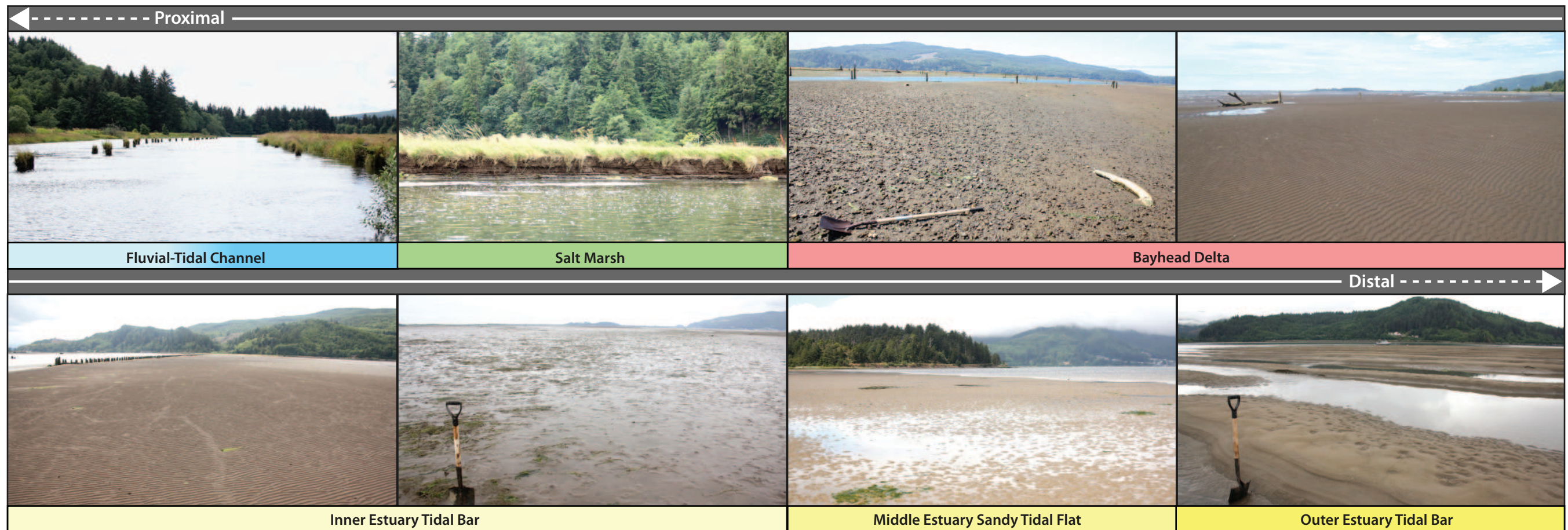
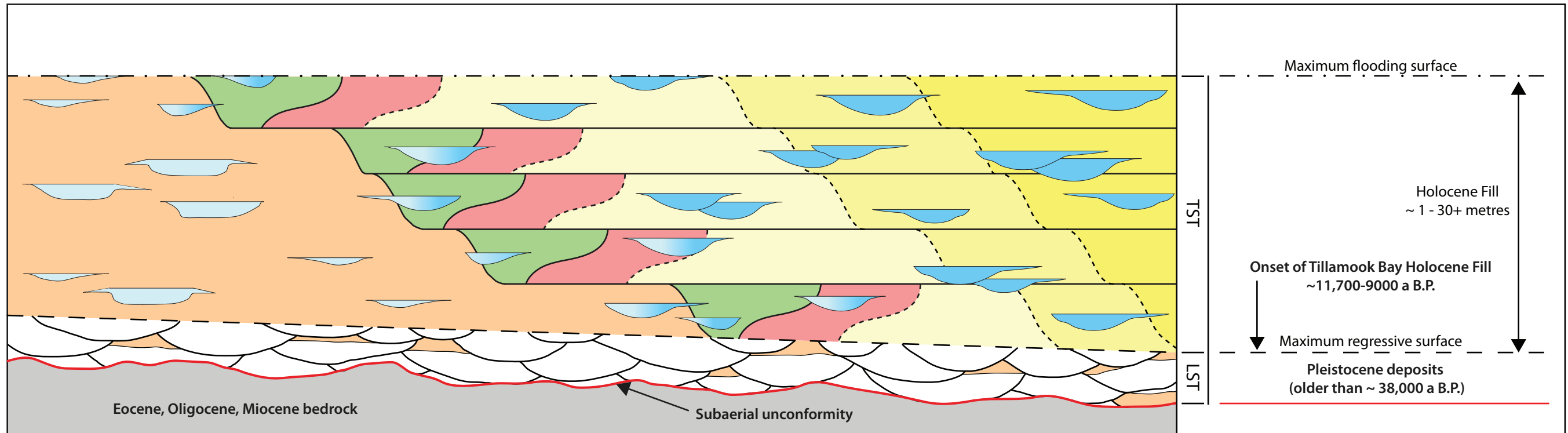
An overall schematic dip-oriented cross section of Tillamook Bay (Fig. 2-75) and a three-dimensional vertical succession facies model (Fig. 2-76) are constructed to show an idealized stratigraphic succession of the bay. Backstepping estuarine successions are interpreted in the schematic cross-section from fluvial-tidal channels through to outer estuary facies as occurring in the transgressive systems tract (TST). These TST deposits overlie lowstand systems tract (LST) deposits that are thought to correspond to the Pleistocene deposits observed by Glenn (1978). Additionally, the three-dimensional model shows schematic vertical successions of typical facies showing grain size trends in various estuarine settings from proximal to distal regions. A similar LST to TST to HST trend within the Gironde Estuary, France, has been described, as a result of Holocene drowning of an incised fluvial valley (Allen and Posamentier, 1993).

Neoichnological Facies Model

To aid in the understanding of biological, physical and sedimentological co-interactions within the bay an ichnological and sedimentological facies model of Tillamook Bay Estuary was generated (Fig. 2-77). An important contrast between energy fluctuations (caused by wave and/or tidal currents) in

Figure 2-75. Schematic dip-oriented cross-section of Tillamook Bay. Cross-sectional view shows the backstepping pattern of fluvial-tidal channels through outer estuary facies, as occurring in the transgressive systems tract (TST) and infill of the mixed-energy Tillamook Bay estuary. The TST deposits overlie the lowstand systems tract (LST), which are interpreted to correspond to the Pleistocene deposits observed by Glenn (1978). The thickness of the Holocene fill, along with the approximate dates shown in the figure, are also based on the observations and interpretations of Glenn (1978). Figure modified from Kerr et al. (1999) and Catuneanu (2006).





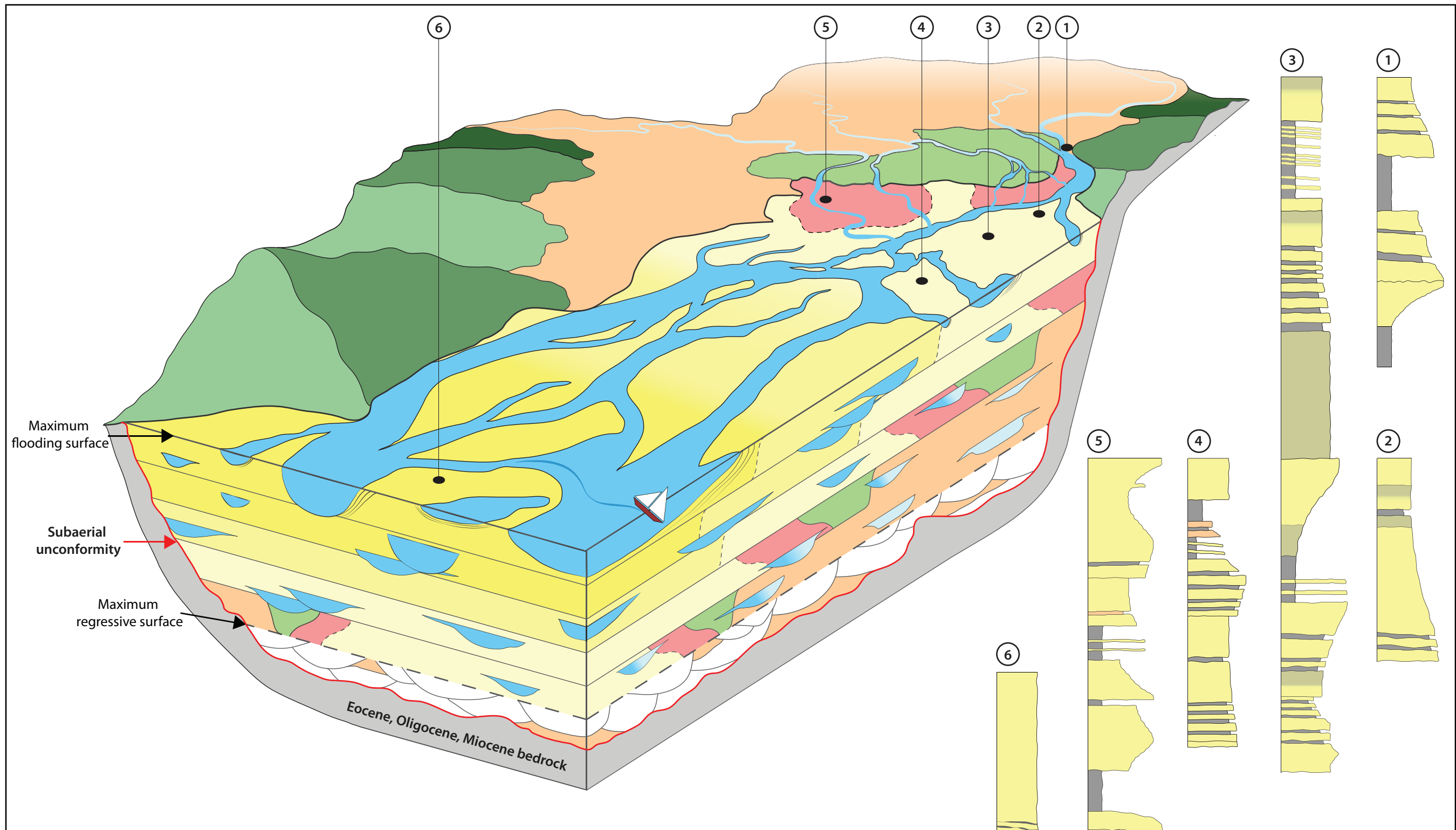
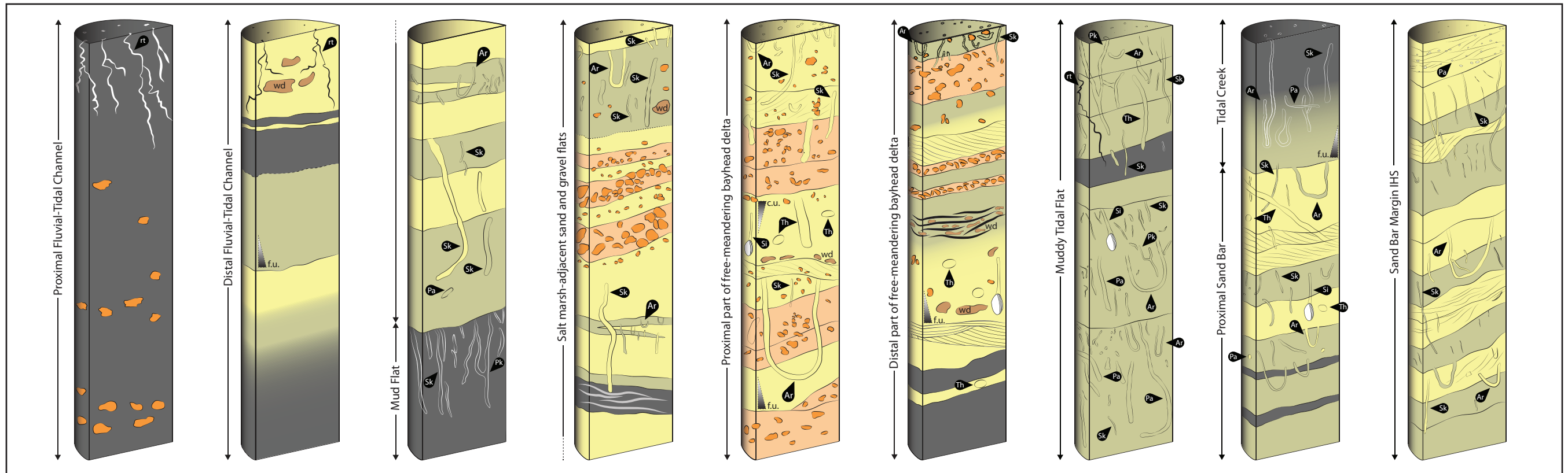


Figure 2-76. Schematic three-dimensional and vertical succession facies model. Representation of the three-dimensional (3D) nature of estuarine deposits at Tillamook Bay. The top surface of the 3D model shows the morphology of the intertidal features as of 2011. The backstepping nature of the channels and other estuarine features is based on the general rise in sea level; small-scale fluctuations in sea level are ignored. For a legend of the 3D model, see Figure 2-75. The schematic vertical successions show an indication of the typical facies and grain size trends observed in select estuarine settings from the proximal to distal regions. They do not represent a full vertical profile to the base of the estuarine fill. For a detailed view of each vertical succession, see the interpretation section of Zones 1, 2, 3, and 6. Vertical successions of Zone 4 and 5 fall in regions outside of the field of view of the 3D model, and are therefore not included.

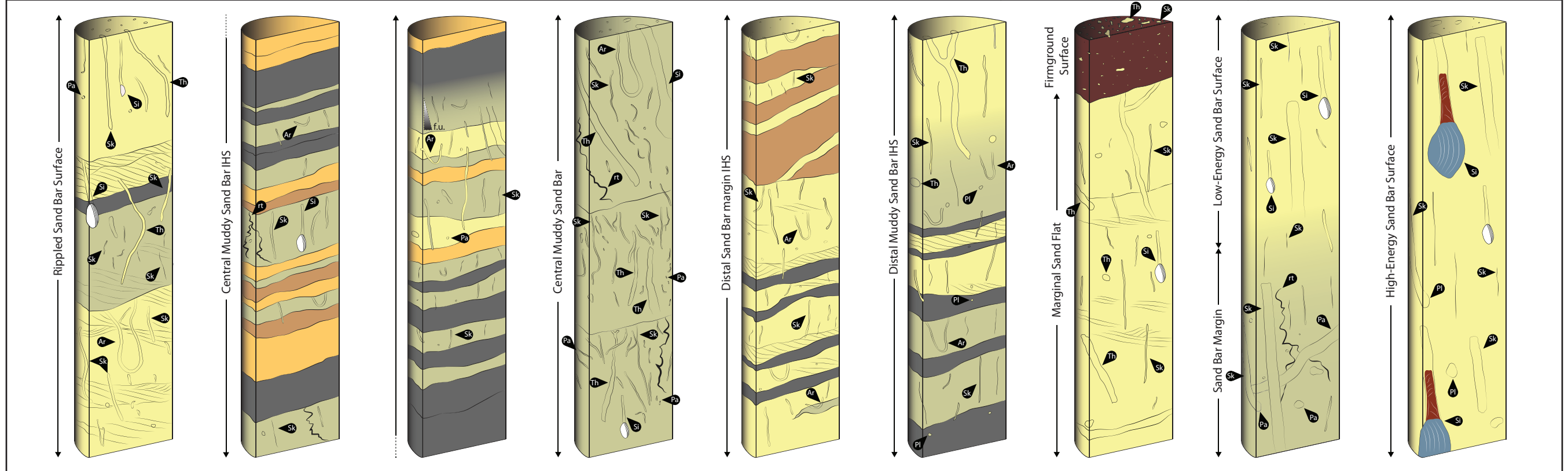
Figure 2-77. Ichnological and sedimentological facies model of Tillamook Bay Estuary. Facies model interpreted from a combination of core, surface, and x-ray observations. The model indicates the possible ichnological and sedimentological features that could be observed in sediment cores if most features were preserved. Drawings are based on the work of Dr. Kerrie L. Bann, as appearing in MacEachern et al. (2007).



Proximal Inner Estuary Fluvial-Tidal Channels

Inner Estuary Bayhead Delta

Inner Estuary Muddy Tidal Flat



Isolated Inner Estuary Tidal Sand Bar

Middle Estuary Marginal Sand Flat

Outer Estuary Isolated Tidal Sand Bar

Distal

various estuarine regions is due to the fact that different sediment calibers may be preferentially deposited. As an example, it has been observed that wave influence may inhibit mud deposition (as observed in bays), whereas tidal currents may mobilize and promote the sedimentation of fluid mud (Gingras and MacEachern, 2012). The important factors influencing bioturbation distribution in tidal settings are: sedimentation rate, tidal currents (observed to result in a landward increase in bioturbation, in the middle of estuaries), and the distribution of food resources (Gingras and MacEachern, 2012).

Characteristics of brackish-water trace-fossil suites are, among others, low trace fossil diversity, an impoverished marine assemblage, and morphologically-simple vertical and horizontal structures (Pemberton et al., 1982; Gingras et al., 2011). Common occurrences of *Gyrolithes*, *Palaeophycus*, *Cylindrichnus*, *Arenicolites*, *Skolithos*, and *Thalassinoides*, to name a few, indicates the trophic-generalist behaviour of the tracemakers, in an environment of widely-distributed, abundant food resources (Pemberton et al., 1982; Gingras et al., 2011).

Invertebrates are generally grouped into six main ethological classes (Frey and Pemberton, 1985); the two observed classes of traces at Tillamook Bay fall dominantly into the category of dwelling structures (*Domichnia*), as well as the category of feeding structures (*Fodinichnia*). Although dwelling traces are commonly mud-lined, some are likely not maintained permanently, as is the case with *Thalassinoides*-like burrows created in medium-to-coarse sand at the mouth of the Kilchis River. Although such burrows may collapse more easily due to high water saturation and poorer sediment sorting, they still record dwelling behaviour of the *N. californiensis* shrimp.

Tillamook Bay, being a mixed-energy estuary, with significant influences from both tide and wave currents, exhibits a correspondingly mixed distribution of sediment type, bar morphologies, and bioturbation intensities. In estuaries with large tidal prisms, salinity changes are more gradual, and animal distributions are more evenly distributed, differing little between distal

and proximal settings (Gingras et al., 2011). As a result, the dominant controls on biogenic structure distributions are related to sediment caliber, sedimentation rates, water turbidity, and hydraulic energies. In the case of Tillamook Bay, a “medium” sized tidal prism, combined with wave energies, results in less mixing of fluvial and tidal water, and correspondingly variable salinity fluctuations. As shown by Burt and McAlister (1958), salinity variations occur in Tillamook Bay during winter and summer months. These variations can be observed in a lateral, as well as vertical orientation (i.e. salinity stratification) during low and high tide periods. Salinity stratification is observed only during the wet, winter season; in the dry season, salinity stratification is insignificant and thorough mixing occurs.

In the case of settings with large tidal prisms, maximum bioturbation intensities occur in proximal parts, where burrow sizes are also smallest on a proximal to distal spectrum, and where mixed-feeding ethologies characterize the burrowing assemblages (Gingras et al., 2011).

Many of the burrows observed in the medium- to highly-burrowed, muddy central portion of the inner estuary tidal bar, show possible cross-cutting relationships, with morphologies that pass from one form into another (e.g. vertical to horizontal) and diameters that vary from 5-10 millimeters, to less than five millimetres. Such combination of burrows, known as compound traces, or composite biogenic structures have been observed in the form of *Heteromastus* sp. burrows and *Nereis* sp. burrows connected to *Psilonichnus*-like burrows of crabs, among others such as *Mya arenaria* burrows sharing the same siphon passage (Gingras et al., 2002a). Behaviours likely indicate beneficial effects of organisms taking advantage of larger, existing burrow structures, with benefits that include: presence of an oxygenation zone deeper below the surface (and further away from predators), ‘pooling’ of water in larger burrows during periods of low tide, and presence of organic-rich detritus and fecal pellets accumulated in large burrows by incoming and outgoing tide currents (Gingras et al., 2002a, 2012a).

The presence of a brackish-water suite of trace fossils in facies of an ancient reservoir may not necessarily indicate tidal influence, given that such suites have been observed in wave-dominated bays and estuaries (Gingras and MacEachern, 2012). Characteristic sedimentary structures, often interpreted in a tidal context, include herringbone cross-stratification, and flaser, wavy, and lenticular bedding. With the exception of the rare presence of rhythmic stratification in burrow infills, and variations of bioturbation intensities in different beds, biogenic structures do not show direct evidence for tidal influence (Gingras and MacEachern, 2012).

Regular heterogeneity of trace fossils, common in inclined heterolithic stratification, is characterized by the regular repetition of similarly burrowed layers, separated by unburrowed layers (Gingras and MacEachern, 2012). This is observed at the tidal bar margin in the inner estuary of Tillamook Bay, but on a scale that may be deemed insufficient to conclusively demonstrate the influence of tidal action and regular heterogeneity of traces in this part of the estuary. However, the burrowed tidal flats and tidal bars of the inner estuary zones show sub-environments with regular, heterogeneous lateral distributions of burrows near the surface. On a larger scale, encompassing multiple sub-environments, a more irregular, heterogeneous distribution of burrows is observed. This, however, is expected, given the proximity of certain sub-environments to the river mouths, and, indirectly, to varying current energies and sedimentation rates. Given that seasonal episodes of erosion and/or sedimentation occur in Tillamook Bay, it is not surprising that overall, regular heterogeneity of bioturbation is observed in the inner-estuary zones. Bioturbation within IHS deposits has been interpreted to respond to seasonal river discharge fluctuations, with highly burrowed layers deposited during periods of low sedimentation and low fluvial discharge of summer months, and layers with low to absent bioturbation deposited during high sedimentation episodes associated with high-fluvial discharge during winter months (Lettley

et al, 2007; Gingras and MacEachern, 2012; Gingras et al., 2002b; Pearson and Gingras, 2006).

The delivery of marine plankton to bays and estuaries, due to tidal currents, provides an important and abundant resource to burrowing infauna (Newell, 1979). Combined with this, the growth of algae on tidal flats and bars promotes the baffling of sediment and concentration of organics. Organic matter, found in fine grained siliciclastic sediments, can, based on its chemical make-up, be an energy sources for organisms (Risk and Yeo, 1980). The two types of organic matter are:

1. Organic matter derived from marine phytoplankton (such as remains of unicellular algae), known as Type II kerogen. This type of organic matter is widely decomposed in oxygenated environments by aerobic organisms, but also by anaerobic ones. When present in sufficiently large quantities in buried siliciclastic environments, Type II kerogen may generate oil (Gautier et al. 1985).
2. River transported organic matter, largely derived from terrestrial plants, and is known as Type III kerogen. Being depleted of hydrogen (when compared to Type II kerogen), this type of organic matter is not decomposed as much by aerobic and anaerobic organisms. When present in sediment of the rock record, it may generate mostly thermal gas (Gautier et al. 1985).

High tidal prisms that allow circulation of estuarine waters, as well as processes that allow settling and trapping of organics at the sediment-water interface, are important in optimizing food resources (Gingras et al., 2011). Exploitation of food resources is often observed in the inferred feeding behaviours of brackish-water trace-fossil suites (Gingras et al., 2011). The trapping of organics on tidal flats during slack water periods, combined with low sedimentation rates, can result in completely bioturbated sediments due to high population densities of organisms (Gingras et al., 2011). Given that organics are not easily trapped in subtidal, higher energy settings, where

sedimentation rates are also high, it is observed that a vertical and lateral increase in bioturbation takes place between sparsely bioturbated, subtidal settings, to highly bioturbated, intertidal flat settings (Gingras et al., 2011).

In the muddy sand bar deposits (Zone 3) of Tillamook Bay, vertical trace morphologies, though possibly produced by siphons of filter-feeding bivalves, are often observed in bioturbated sediments where *Nereis* sp. worms are common to abundant. As such, the exploitation of highly-organic deposits may result in burrow morphologies that are difficult to differentiate between those of filter-feeding organisms or deposit-feeding organisms. There is, however, a potential value in recognizing structures that may be related to interface-deposit feeding behaviours, as opposed to the normal associations with filter-feeding behaviours (Gingras et al., 1999; 2001). Found in muddy tidal flats, molluscs are subjected to variations in salinity, as well as the presence of mud. Although mud increases the turbidity of the water, it also contains more organic matter. Molluscs, such as *Mya arenaria* and *Macoma balthica* use their siphonal tubes to filter fine particulate matter, or to reach out in the surrounding sediment and pick up food items via deposit feeding (Rasmussen, 1973; McLusky and Elliott, 1981). The organic-rich content of mud in estuaries provides a valuable food source for *Nereis* sp. worms, whose distribution is governed by strategies for physiological and ecological adaptation (Mettam, 1981).

Modern Estuary Comparison

Before assigning the neoichnological observations from this study to a specific ichnofacies, a comparison to a similar estuarine setting is addressed. In this section, the morphology of tidal bars in Tillamook Bay estuary is compared to the morphology of tidal bars in the Bombetoka Bay Estuary (also referred to as the Betsiboka Estuary), in northwestern Madagascar (Fig. 2-78). This estuary was chosen because of several similarities to Tillamook Bay: (1) sediment is

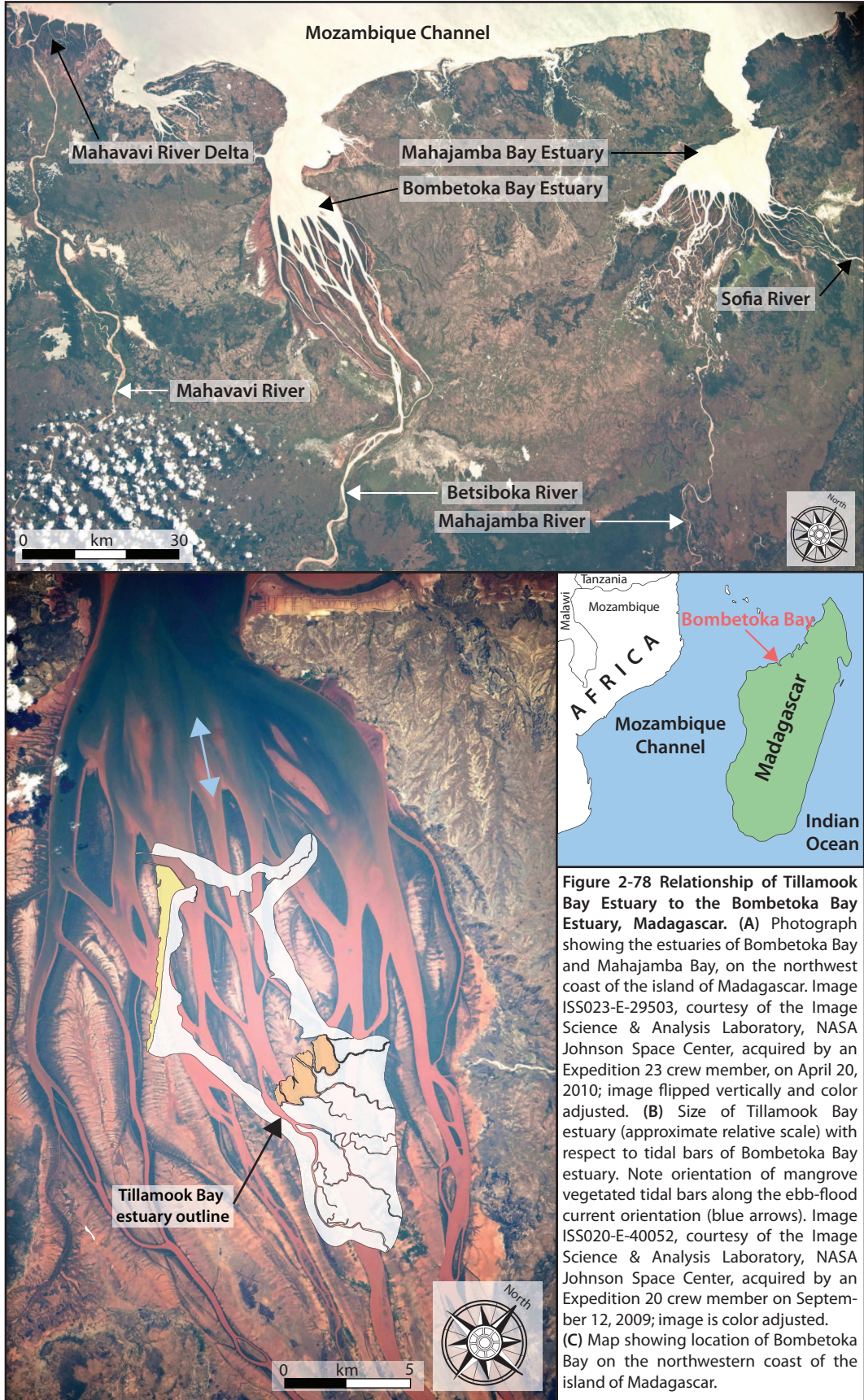


Figure 2-78 Relationship of Tillamook Bay Estuary to the Bombetoka Bay Estuary, Madagascar. (A) Photograph showing the estuaries of Bombetoka Bay and Mahajamba Bay, on the northwest coast of the island of Madagascar. Image ISS023-E-29503, courtesy of the Image Science & Analysis Laboratory, NASA Johnson Space Center, acquired by an Expedition 23 crew member, on April 20, 2010; image flipped vertically and color adjusted. (B) Size of Tillamook Bay estuary (approximate relative scale) with respect to tidal bars of Bombetoka Bay estuary. Note orientation of mangrove vegetated tidal bars along the ebb-flood current orientation (blue arrows). Image ISS020-E-40052, courtesy of the Image Science & Analysis Laboratory, NASA Johnson Space Center, acquired by an Expedition 20 crew member on September 12, 2009; image is color adjusted. (C) Map showing location of Bombetoka Bay on the northwestern coast of the island of Madagascar.

deposited within Bombetoka Bay, which is partially enclosed, with an opening to a fully marine setting; (2) strong tidal currents shape the elongate tidal bars; and (3) the estuary receives high fluvial discharge and sediment load during the wet, rainy season, and deposition of mud takes place largely during those time periods.

Betsiboka River in Madagascar, at 600 km long, transports lateritic soils and sediments, eroded by heavy tropical rainstorm in the highlands of Central Madagascar (Raharimahefa and Kusky, 2010). The river discharges into Bombetoka Bay, forming what is referred to as Bombetoka Bay Estuary. A bayhead delta is also present at the upstream, eastern end of the estuary. The tropical climate of Madagascar, combined with high deforestation rates and exploitation of natural resources in recent decades, has resulted in high sedimentation rates within the estuary (Raharimahefa and Kusky, 2010). The intertidal bars, and tidal flats, observed in images from the International Space Station (Fig. 2-78), have grown rapidly in the last three decades. The shallow area defined by these features has increased by as much as 800% between the years 1973 and 2000 (Raharimahefa and Kusky, 2010). Muddy sedimentation is interpreted to occur dominantly during rainy seasons and periods of high fluvial discharge, due to high concentrations of suspended material and high flocculation rates. High suspended sediment concentrations, combined with strong tidal currents, have also resulted in sedimentation occurring “offshore” into the Mozambique Channel, in the form of an ebb delta. Compared to the approximate relative size of Tillamook Bay (Fig. 2-78), the tidal bars and flats of Bombetoka Bay Estuary are much larger. This is to be expected if the basin area to be filled is larger, and other factors such as sedimentation and tidal prism also act on a much larger scale.

After comparing the intertidal bars of Tillamook Bay Estuary to those of Bombetoka Bay Estuary (both estuaries that have experienced high sedimentation rates and shallowing in recent decades), it can be observed that the relative areal extent of bars in the outer estuary is smaller than the areal

extent of bars and tidal flats of the inner estuary. This, again, is expected due to higher tidal prisms and deeper channels located in the outer estuary compared to the inner estuary. A major distinction between the tidal bars of Bombetoka Bay Estuary and those of Tillamook Bay Estuary is the relative influence of wave versus tidal currents. Observing the morphology of bars in Tillamook Bay, it can be interpreted with a high degree of certainty that the mixed-energy setting, with significant wave influence, results in the reworking of sediment, and the morphology of the bars observed in aerial photography is dominantly oriented parallel to the ebb and flood tidal current directions, with a smaller lateral component perpendicular to those current directions. However, tidal bars of Bombetoka Bay Estuary have much more elongate morphologies, and those are most likely due to a larger influence of tidal currents. While wave currents may still be present, their influence on sedimentation and bar morphology is likely negligible or overshadowed by the much stronger tidal currents.

With the above points in mind, it becomes clear by examining a simple comparison between a mixed-energy estuary (Tillamook Bay) and a tidally-influenced estuary (Bombetoka Bay Estuary) that the term "brackish-water ichnofacies" may not be correctly assigned, or too broad of a term to be applied in every brackish-water setting. It is true that some characteristics of brackish-water settings recur in many modern environments, as well as ancient examples. Dominant energy is just one of the many factors that can control both sedimentation patterns and bioturbation intensity distribution throughout an estuary. It then becomes more necessary for a refined model of the "brackish-water ichnofacies" to be put forth, and described from the standpoint of several possible scenarios of brackish-water settings. Certainly, the use of more ichnofacies can become problematic and may create more confusion among workers in academia and the hydrocarbon exploration industry. While existing ichnofacies models have been used successfully in interpreting many ancient outcrops and/or subsurface reservoirs, there still

exists the need for improved models, especially for environments interpreted to have formed in brackish-water settings.

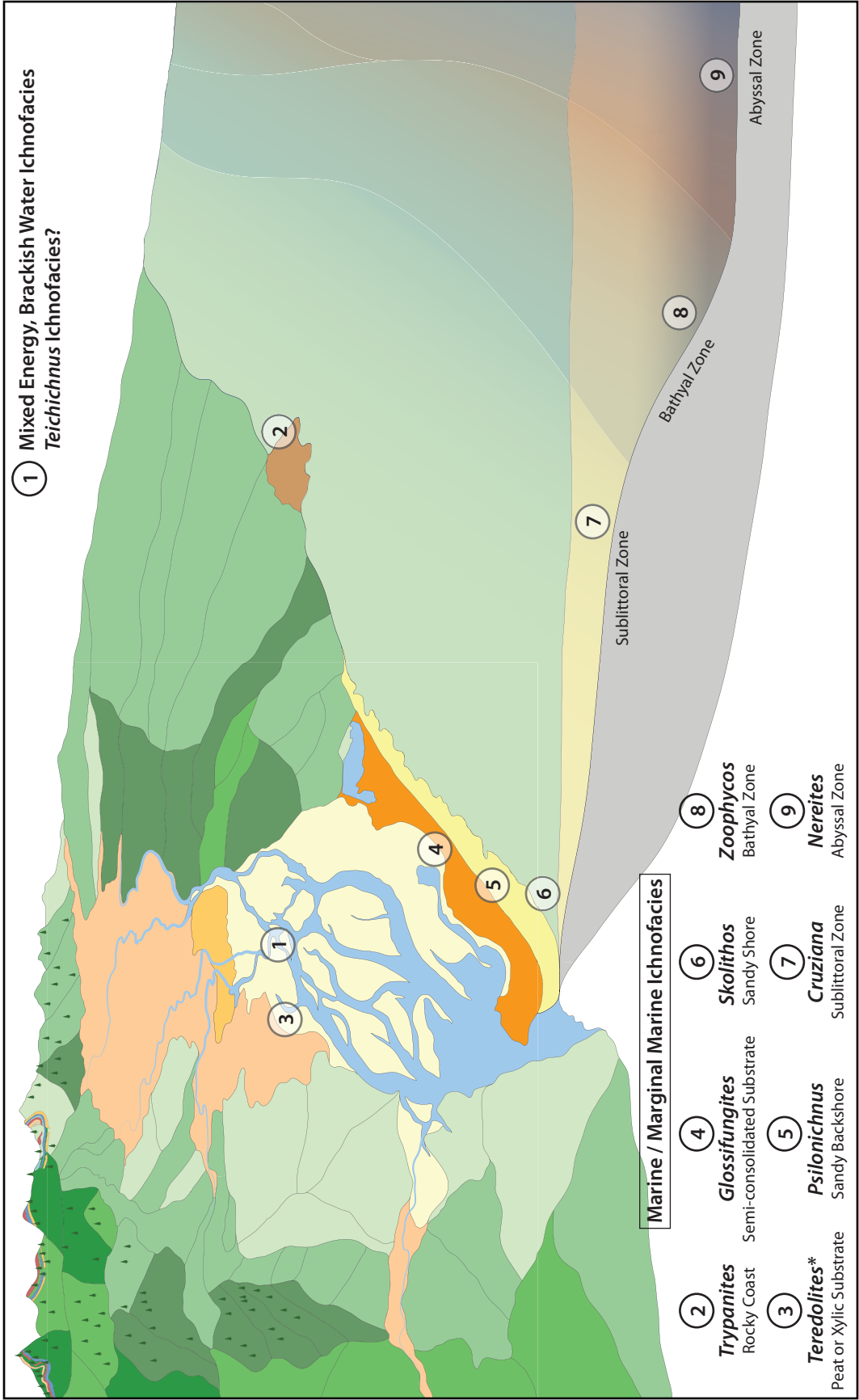
One such ichnofacies, assigned to brackish-water settings, has been proposed (Pemberton et al., 2009; 2010). A difficulty exists in recognizing trace fossil assemblages in salinity-stressed settings. The behaviours of organisms in such settings reflect their need to construct semi-permanent dwellings for feeding purposes, as well as protection purposes (from outside climatic elements, from predation, and from salinity changes). The biogenic structures created therefore are morphologically-simple, smaller in size than their marine counterparts, and correspond to a relatively low number of suites (Pemberton et al., 2009; 2010). Based on the major characteristics mentioned above, the *Teichichnus* Ichnofacies has been proposed (Pemberton et al., 2009; 2010).

This proposal was much needed in both academia and the hydrocarbon industry, where traditionally, trace fossil suites in interpreted brackish-water settings have been assigned to expressions of two fully marine ichnofacies, namely the *Skolithos* and/or *Cruziana* Ichnofacies, or the incorrectly applied (within an estuarine context) “mixed *Cruziana-Skolithos* Ichnofacies” (Gingras et al., 2012a; Gingras et al., 2012b). Although the relatively newly-proposed *Teichichnus* Ichnofacies appears to be a very good fit as an ichnological model of brackish-water settings, the term has yet to be formally described and presented in a peer-reviewed publication. Similarly, with the exception of a small number of authors (e.g. Phillips, 2011; Dicks, 2012), a review of recent literature reveals that the term has not been widely adopted by workers in this field. Of particular mention are peer-reviewed publications, none of which – in the accessible, searchable literature – make mention of the term “*Teichichnus* Ichnofacies”. This highlights the uncertainty and difficulty faced by many workers in interpreting brackish-water ichnology and neoichnology. The previously-used *Cruziana* and *Skolithos* Ichnofacies (as examples) have been widely used and have become the norm when discussing interpretations in the settings described above. As with any new terms, their ease of adaptability

rests on clear descriptions and definitions being made available, in order to restrict uncertainties in assigning interpretations to a particular ichnofacies. The *Teichichnus* Ichnofacies (Pemberton et al., 2009; 2010), has a high importance in more accurately delineating models for brackish-water ichnology. A formal, detailed description of the ichnofacies can be highly valuable, especially if it addresses the multitude of different brackish environments (e.g. restricted bay estuary settings versus open bay estuary settings, and tidally-dominated versus mixed-energy estuaries).

The dominant incipient traces observed at Tillamook Bay are in the form of *Skolithos*-, *Thalassinoides*-, *Siphonichnus*-, and *Palaeophycus*-like traces. No *Teichichnus*-like traces are definitively observed. However, their lack of presence may not necessarily reflect the complete absence of such traces. It is difficult to observe spreite in modern sediment, and this certainly is the case in sediments of tidal bars and flats of Tillamook Bay, where no discernable traces containing spreite are observed. However, if the modern sediments studied are to lithify, the compaction and sediment contrast are expected to most likely reveal not only traces containing spreite (such as possible *Teichichnus* and *Diplocraterion*), but other structures not easily recognized in modern settings. The neoichnological observations at Tillamook Bay certainly indicate that the suites are best assigned to an expression of the *Teichichnus* Ichnofacies. For this reason, the term “mixed-energy brackish-water” ichnofacies is used (Fig. 2-79), to emphasize the important factors (i.e. wave and tide currents) that control sedimentation, sediment reworking, to some extent sedimentation rates, and, indirectly, bioturbation concentrations throughout the estuary. Although the term “*Teichichnus* Ichnofacies” has not been formally described and defined in detail, the use of the term “mixed-energy brackish-water” ichnofacies, is not, by any means, necessarily correct. The term is used simply to indicate the need for mentioning an environment of deposition, and how ichnological or neoichnological features described within it, deviate from an archetypal

Figure 2-79. Marine to marginal marine ichnofacies. Schematic diagram showing the multitude of ichnofacies occurring in marine to marginal marine environments. The “mixed-energy, brackish water ichnofacies” observed at Tillamook Bay, and used here as an example, is most likely attributed to the *Teichichnus* Ichnofacies. Figure modified after Frey and Pemberton (1985). *The location of the *Teredolites* Ichnofacies is shown as an example of where such an ichnofacies is expected to be found; the *Teredolites* Ichnofacies is not observed at Tillamook Bay.



ichnofacies, in this case the *Teichichnus* Ichnofacies (Pemberton et al., 2009; 2010).

Reservoir Characterization Analogue

The study of modern sedimentary environments can greatly aid in producing reservoir analogues, to better delineate prospective reservoir sands in subsurface studies (Pemberton and Gingras, 2005). It is accepted that burrowing behaviour of organisms, and the presence of trace fossils in hydrocarbon reservoirs, may have a positive effect and improve the reservoir quality by enhancing permeability (Pemberton and Gingras, 2005; La Croix et al., 2013). Integrating neoichnological observations with observations about the sediment caliber, sediment sorting, sand/mud ratios, as well as thickness and volume of deposits at different locations within the estuary, a potential reservoir model can be created (Fig. 2-80).

As can be observed in Figure 2-80, sand bodies of the outer estuary have the highest reservoir potential, based on the seven criteria outlined. Differentiating between tidal dunes and tidal bars helps in identifying orientations of sedimentary bodies and orientations of accretion surfaces, from a petroleum exploration and reservoir characterization point of view (Fenies and Tastet, 1998; Olariu et al., 2012). Depending on the setting the dunes or bars form under (e.g. seaway versus open-coast), their orientation relative to paleo-shorelines can vary from perpendicular to parallel (Olariu et al., 2012). This has implications when trying to map ancient sand bodies in reservoirs with sparse subsurface data, as multiple depositional environments and therefore mapping styles may miss important hydrocarbon-bearing units.

In a study of the Gething Formation in northeastern British Columbia, it was concluded that potential reservoir sandstone bodies – within an interpreted paleobay – reside in the bayhead delta deposits, in the larger, medially-positioned tidal channel deposits of heterolithic to sand-rich

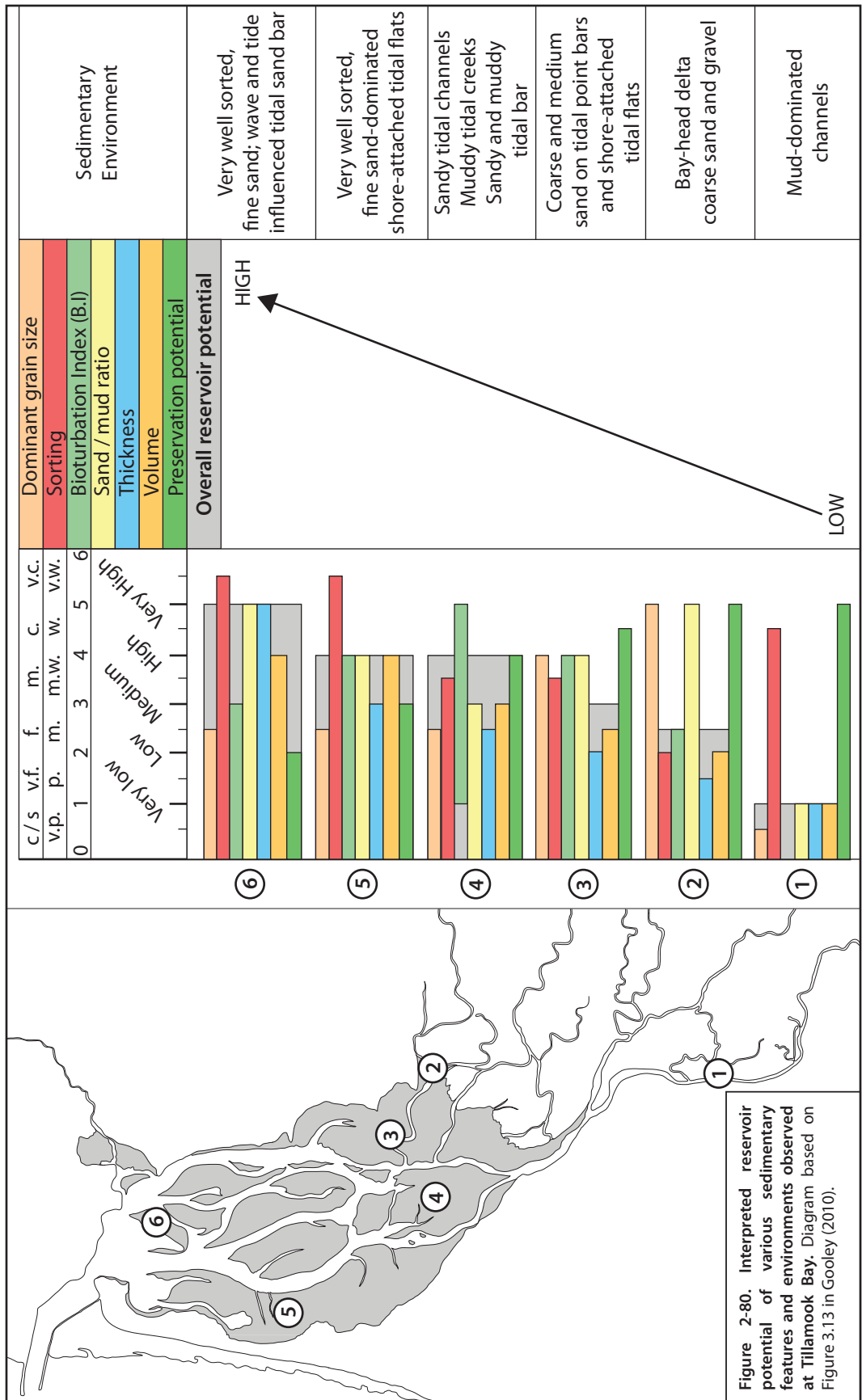


Figure 2-80. Interpreted reservoir potential of various sedimentary features and environments observed at Tillamook Bay. Diagram based on Figure 3.13 in Gooley (2010).

character, and in the even larger sand-rich bodies (e.g. flood-tidal delta, shoreface deposits) of the outer reaches of the bay (Gingras et al., 2010).

Understanding the lateral and vertical architecture of sedimentary facies within an interpreted sedimentary environment is important for the accurate mapping of reservoir facies. This has been shown, for example, in a study of internal stratigraphic architecture of an interpreted bayhead delta within a partially-closed, brackish inland seaway from the McMurray Formation (Caplan and Ranger, 2011).

Larger scale studies have also shown that in bioturbated media, burrow permeability can be substantially higher than the matrix permeability, allowing fluid flow to take place via preferential pathways of interconnected burrows (Polo Camacho, 2013). As such, it is important to consider the bioturbation intensity (indicated by the bioturbation index, or B.I., in Figure 2-80) of sedimentary facies within a sedimentary environment, as they may have a positive effect on reservoir quality.

The overall reservoir potential of sedimentary facies observed at Tillamook Bay is assessed through the seven criteria in Figure 2-80, which indicates an overall interpreted increase in reservoir potential from the proximal facies of the inner estuary, to the distal facies of the outer estuary. During a transgressive phase, tidal bars of the outer estuary are expected to be the first facies exposed to erosional forces, and therefore have the lowest interpreted preservation potential. However, given the increased thickness (and therefore volume) of the bars in this zone of the estuary, combined with good sorting, low mud content, and a bioturbation index ranging from 0 to 3, bars of the outer estuary are interpreted to have the highest reservoir potential. The innermost inner estuary, dominated by mud-dominated fluvial-tidal channels of low areal extent and low thickness, are most likely to be preserved; however, given the low score of most criteria, this area is interpreted to contain limited reservoir potential, most likely restricted to the sandier, distal parts of the fluvial-tidal channels.

BIBLIOGRAPHY

- Allen, J.R.L.** (1963) The classification of cross-stratified units, with notes on their origin. *Sedimentology*, v. 2, p. 93-114.
- Allen, J.R.L.** (1982) *Sedimentary structures. Their character and physical basis.* Elsevier, Amsterdam, 2 volumes, v. 1 p. 612, v. 2 p. 678.
- Allen, J.P.** and **Posamentier, H.W.** (1993) Sequence stratigraphy and facies model of an incised valley fill: the Gironde Estuary, France. *Journal of Sedimentary Petrology*, v. 63, p. 378-391.
- Amos, C.L.** and **Lang, B.F.N.** (1980) The sedimentary character of the Minas Basin, bay of Fundy, In **McCann, S.B.**, ed. *The Coastline of Canada: Geological Survey of Canada*, Paper 80-100, p. 123-152.
- Boothroyd, J.C., Friedrich, N.E.** and **McGinn, S.R.** (1985) Geology of microtidal coastal lagoons: Rhode Island. *Marine Geology*, v. 63, p. 35-76.
- Burt, W.V.** and **McAllister, B.** (1958) Hydrography of Oregon estuaries. Data Report No. 3, School of Science, Oregon State College, Corvallis, Oregon, p. 18.
- Caplan, M.** and **Ranger, M.** (2001) Description and interpretation of coarsening-upward cycles in the McMurray Formation, northeastern Alberta; preliminary results. In: CSPG Annual Convention, 2001, v. 2001, p. 010-1 – 010-9
- Catuneanu, O.** (2006) *Principles of Sequence Stratigraphy.* Elsevier, p. 375.
- Chaumillon, E., Fenies, H., Billy, J., Breilh, JF.** and **Richetti, H.** (2013) Tidal and fluvial controls on the internal architecture and sedimentary facies of a lobate estuarine tidal bar (The Plassac Tidal Bar in the Gironde Estuary, France). *Marine Geology*, v. 346, p. 58-72.
- Dalrymple, R.W.** and **Choi, K.** (2007) Morphologic and facies trends through the fluvial-marine transition in tide-dominated depositional systems: A schematic framework for environmental systems: A schematic framework for environmental and sequence-stratigraphic interpretation. *Earth Science Reviews*, v. 81, p. 135-174.
- Dalrymple, R.W.** and **Rhodes, R.N.** (1995) Estuarine dunes and bars. in **Perillo, G.M.E.**, ed., *Geomorphology and Sedimentology of Estuaries.* Developments in Sedimentology: Elsevier, Amsterdam, v. 53. P. 359-422.
- Dalrymple, R.W., Knight, J.R.** and **Lambiase, J.J.** (1978) Bedforms and their hydraulic stability relationships in a tidal environment, Bay of Fundy, Canada. *Nature* v. 275, p.100-104.
- Dalrymple, R.W., Baker, E.K., Harris, P.T.,** and **Hughes, M.** (2003) Sedimentology and stratigraphy of a tide-dominated, foreland-basin delta (Fly River, Papua New Guinea). In: **Sidi, F.H., Nummedal, D., Imbert, P., Darman, H., Posamentier, H.W.** Eds., *Tropical Deltas of Southeast Asia – Sedimentology, Stratigraphy, and Petroleum Geology:* SEPM Special Publication, v. 76, p. 147–173.

- Dashtgard, S.E.** (2011) Linking invertebrate burrow distributions (neoichnology) to physicochemical stresses on a sandy tidal flat: implications for the rock record. *Sedimentology*, v. 58, p. 1303-1325.
- Dicks, R.** (2012) Neoichnology and sedimentology of the fluvial-tidal transition zone of the Columbia River Delta, Northwest U.S.A. Master of Science Thesis, Department of Earth and Atmospheric Sciences, University of Alberta, Edmonton, Alberta, Canada. p. 152.
- Doxaran, D., Froidefond, J.-M., Castaing, P. and Babin, M.** (2009) Dynamics of the turbidity maximum zone in a macrotidal estuary (the Gironde, France): Observations from field and MODIS satellite data. *Estuarine Coastal Shelf Science*, v. 81, p. 321–332.
- Dyer, K.R.** (1986) *Coastal and estuarine Sediment Dynamics*. John Wiley and Sons, Chichester, p. 358.
- Einstein, A.J. and Krone, R.B.** (1962) Experiments to determine modes of cohesive sediment transport in saltwater. *Journal of Geophysical Research*, v. 64, p. 1451-1461.
- Fenies, H. and Tastet, JP.** (1998) Facies and architecture of an estuarine tidal bar (the Trompeloup bar, Gironde Estuary, SW France). *Marine Geology*, v. 150, p. 149-169.
- Frey, R.W. and Pemberton, S.G.** (1985) Biogenic Structures in Outcrops and Cores: I. Approaches to Ichnology. *Bulletin of Canadian Petroleum Geology*, v. 33, no. 1, p. 72-115.
- Gautier, D.L., Kharaka, Y.K. and Surdam, R.C.** (1985) Relationship of organic matter and mineral diagenesis. *Society of Economic Paleontologists and Mineralogists. Short course no. 17*, p. 279.
- Gingras, M.K., Pemberton, S.G., Saunders, T. and Clifton, H.E.** (1999) The ichnology of modern and Pleistocene brackish-water deposits at Willapa Bay, Washington; variability in estuarine settings. *Palaios*, v.14, p. 353-374.
- Gingras, M.K., Pemberton, S.G., and Saunders, T.** (2000) Firmness profiles associated with tidal-creek deposits: the temporal significance of *Glossifungites* assemblages. *Journal of Sedimentary Research*, v. 7, p. 1017-1025.
- Gingras, M.K., Pemberton, S.G., and Saunders, T.** (2001) Bathymetry, sediment texture, and substrate cohesiveness; their impact on modern *Glossifungites* trace assemblages at Willapa Bay, Washington. *Palaeogeography, Palaeoclimatology, Palaeoecology*, v. 169, p. 1-21.
- Gingras, M.K., Pickerill, R. and Pemberton, S.G.** (2002a) Resin cast of modern burrows provides analogs for composite trace fossils. *Palaios*, v. 17(2), p. 206-211.
- Gingras, M.K., Räsänen, M. and Ranzi A.** (2002b) The significance of bioturbated inclined heterolithic stratification in the southern part of the Miocene Solimoes Formation, Rio Acre, Amazonia Brazil. *Palaios*, v.17, p. 591-601.
- Gingras, M.K., Zonneveld, J-P. and Blakney, B.J.** (2010) Preliminary assessment of ichnofacies in the Gething Formation of NE British Columbia. *Bulletin of Canadian Petroleum Geology*, v. 58, no. 2, p. 159-172.
- Gingras, M.K., MacEachern, J.A., and Dashtgard, S.E..** (2011) Process ichnology and the elucidation of physico-chemical stress. *Sedimentary Geology*, v. 237, p.115-134.

- Gingras, M.K. and MacEachern, J.A.** (2012) Tidal ichnology of shallow-water clastic settings. In **Davis Jr., R.A. and Dalrymple, R.W., eds. *Principles of Tidal Sedimentology***. Springer, p. 57-77.
- Gingras, M.K., MacEachern, J.A. and Dashtgard, S.E.** (2012a) The potential of trace fossils as tidal indicators in bays and estuaries. *Sedimentary Geology*, v. 279, p.97-106.
- Gingras, M.K., MacEachern, J.A., Dashtgard, S.E., Zonneveld, J.-P., Schoengut, J., Ranger, M.J. and Pemberton, S.G.** (2012b) Chapter 16: Estuaries. In **Knaust, D. and Bromley, R.G., eds. *Trace Fossils as Indicators of Sedimentary Environments. Developments in Sedimentology***. Elsevier, v. 64, p. 463-505.
- Glenn, J.L.** (1978) Sediment sources and Holocene sedimentation history in Tillamook Bay, Oregon: Data and Preliminary Interpretations. Open-file report 78-680: United States Department of the Interior Geological Survey, Denver, Colorado.
- Gooley, J.T.** (2010) Alluvial Architecture and Predictive Modeling of the Late Cretaceous John Henry Member, Straight Cliffs Formation, Southern Utah. Master of Science Thesis, Department of Geology and Geophysics, University of Utah, p. 377.
- Haven, D.S. and Morales-Alamo, R.** (1968) Occurrence and transport of faecal pellets in suspension in a tidal estuary. *Sedimentary Geology*, v. 2, p. 141-151.
- Hodgson, C.A.** (2013) Sedimentology and Neoichnology of a Wave-Dominated, Tidally-Influenced, Fully Marine Bay, Oregon, USA. Unpublished Master of Science Thesis, Department of Earth and Atmospheric Sciences, University of Alberta, Edmonton, Alberta, Canada, p. 312.
- Hughes, M.G., Harris, P.T. and Hubble, T.C.T.** (1998) Dynamics of the turbidity maximum zone in a micro-tidal estuary: Hawkesbury River, Australia.
- Ichaso, A.A. and Dalrymple, R.W.** (2009) Tidal and wave-generated fluid-mud deposits in the Tilje Formation (Jurassic), offshore Norway. *Geology*, v. 37, p. 539-542.
- Image Science and Analysis Laboratory** (2009) Image ISS020-E-40052. National Aeronautics and Space Administration (NASA), Johnson Space Centre. Accessed September 23, 2013, <eol.jsc.nasa.gov>.
- Image Science and Analysis Laboratory** (2010) Image ISS023-E-29503. National Aeronautics and Space Administration (NASA), Johnson Space Centre. Accessed September 23, 2013, <eol.jsc.nasa.gov>.
- Jones, K.L., Keith, M.K., O'Connor, J.E., Mangano, J.F., and Wallick, J.R.** (2012) Preliminary assessment of channel stability and bed-material transport in the Tillamook Bay tributaries and Nehalem river basin, northwestern Oregon. U.S. Department of the Interior, U.S. Geological Survey, Open-File Report 2012-1187, p. 121.
- Kerr, D., Ye, L., Bahar, A., Kelkar, B.G. and Montgomery, S.** (1999) Glenn Pool field, Oklahoma: a case of improved prediction from a mature reservoir. *American Association of Petroleum Geologists Bulletin*, v. 83, no.1., p. 1-18.

- King, C.A.M. and Williams, W.W.** (1949) The formation and movement of sand bars by wave action. *Geographical Journal*, v. 113, p.70-85.
- Komar, P.D., McManus, J. and Styllas, M.** (2004) Sediment accumulation in Tillamook Bay, Oregon: natural processes versus human impacts. *The Journal of Geology*, v. 112, p. 455-469.
- LaCroix, A.D., Gingras, M.K., Pemberton, S.G., Mendoza, C.A., MacEachern, J.A. and Lemiski, R.T.** (2013) Biogenically enhanced reservoir properties in the Medicine Hat gas field, Alberta, Canada. *Marine and Petroleum Geology*, v. 43, p. 464-477.
- Lettley, C.D., Gingras, M.K., Pearson, N.J., and Pemberton, S.G.** (2007) Burrowed stiffgrounds on estuarine point bars: modern and ancient examples, and criteria for their discrimination from firmgrounds developed along omission surfaces. In: MacEachern, J.A., Bann, K.L., Gingras, M.K., Pemberton, S.G. *Eds, Applied Ichnology. Society of Economic Paleontologists and Mineralogists: Short Course Notes v. 52*, p. 317–325.
- MacEachern, J.A., Pemberton, S.G., Bann, K.L. and Gingras, M.K.** (2007) Departures from the archetypal ichnofacies: effective recognition of environmental stress in the rock record, in **MacEachern, J.A., Bann, K.L., Gingras, M.K., and Pemberton, S.G.**, eds., *Applied Ichnology, SEPM Short Course Notes 52*, p. 65-93.
- MacEachern, J.A., Pemberton, S.G., Gingras, M.K., and Bann, K.L.** (2010) Ichnology and Facies Models, in **James, N.P. and Dalrymple R.W.**, eds., *Facies Models 4: Geological Association of Canada*, p.19-58.
- Masselink, G., Kroon, A. and Davidson-Arnott, R.G.D.** (2006) Morphodynamics of intertidal bars in wave-dominated coastal settings – a review. *Geomorphology*, v. 73, p. 33-49.
- McCann, S.B.** (1980) Classification of tidal environments, in McCann, S.B., ed., *Sedimentary processes and animal-sediment relationships in tidal environments*. Geological Association of Canada Short Course Notes: Halifax, Nova Scotia, v. 1, p. 1-24.
- McLusky, D.S. and Elliott, M.** (1981) The feeding and survival strategies of estuarine molluscs. In **Jones, N.V. and Wolff, W.J.**, *Eds.*, *Feeding and Survival Strategies of Estuarine Organisms*. Plenum Press, New York, p. 109-121.
- Mettam, C.** (1981) Survival strategies in estuarine *Nereids*. In **Jones, N.V. and Wolff, W.J.** (Editors): *Feeding and Survival Strategies of Estuarine Organisms*. Plenum Press, New York, p. 65-77.
- Middleton, G.V.** (1980) Physical Processes, in **McCann, S.B.**, ed., *Sedimentary processes and animal-sediment relationships in tidal environments*. Geological Association of Canada Short Course Notes: Halifax, Nova Scotia, v. 1, p. 25-58.
- Murray, T.J. and Associates** (1972) Development Program for Tillamook Bay, Oregon. Portland, Oregon, p. 82.
- Musial, G., Reynaud, J.-Y., Gingras, M.K., Féliès, R.L. and Parize, O.** (2012) Subsurface and outcrop characterization of large tidally influenced point bars of the Cretaceous McMurray Formation (Alberta, Canada). *Sedimentary Geology*, v. 279, p. 156-172.

- Newell, R.C.** (1979) *Biology of Intertidal Animals*. Marine Ecological Surveys Ltd., Faversham, Kent, p. 781.
- Olariu, C., Steel, R.J., Dalrymple, R.W. and Gingras, M.K.** (2012) Tidal dunes versus tidal bars: The sedimentological and architectural characteristics of compound dunes in a tidal seaway, the lower Baronia Sandstone (Lower Eocene), Ager Basin, Spain. *Sedimentary Geology*, v. 279, p. 134-155.
- Oregon Coastal Atlas** (2007) Intertidal Color Infrared Aerial Mosaic of Tillamook Bay Estuary, 2005. Oregon Department of Land Conservation and Development (DLCD), U.S. Environmental Protection Agency (EPA), U.S. Department of Agriculture. Accessed March 2013 via <www.coastalatlantlas.net>
- Pearson, N.J. and Gingras, M.K.** (2006) An ichnological and sedimentological facies model for muddy point-bar deposits. *Journal of Sedimentary Research*, v.76, p. 771-782.
- Pemberton, S.G., Flach, P.D. and Mossop, G.D.** (1982) Trace fossils from the Athabasca Oil Sands, Alberta, Canada. *Science*, v. 217, no. 4562, p. 825-827.
- Pemberton, S.G. and Gingras, M.K.** (2005) Classification and characterizations of biogenically enhanced permeability. *American Association of Petroleum Geologists (AAPG) Bulletin*, v. 89, no. 11, p. 1493-1517.
- Pemberton, S.G., Gingras, M.K., Dashtgard, S.E., Bann, K.L. and MacEachern, J.A.** (2009) The *Teichichnus* Ichnofacies: a temporally and spatially recurring ethological grouping characteristic of brackish-water conditions. Conference abstract: American Association of Petroleum Geologists (AAPG) Annual Convention and Exhibition, Denver, Colorado, June 7-10. AAPG Search and Discovery Article #90090.
- Pemberton, S.G., Gingras, M.K., Dashtgard, S.E., Bann, K.L. and MacEachern, J.A.** (2010) From salinity-stressed suite to recurring ethological grouping: the rise of the *Teichichnus* Ichnofacies. Conference abstract: GeoCanada 2010-Working with the Earth, Calgary, Alberta, May 10-14.
- Peterson, C.D., Darienzo, M.E., and Parker, M.** (1988) Coastal neotectonic field trip guide for Netarts Bay, Oregon. *Oregon Geology*, v. 50, p. 99-106.
- Phillips, J.M.** (2011) Sedimentology, ichnology and development of a sub-regional depositional and stratigraphic framework for the McMurray-Wabiskaw succession in the Mackay River area, northeastern Alberta. Unpublished Master of Science Thesis, Department of Earth and Atmospheric Sciences, University of Alberta, Edmonton, Alberta, Canada, p. 323.
- Polo Camacho, C.A.** (2013) Bioturbation and Resource Quality: a Case Study from the Upper Cretaceous Lysing and Nise Formations, Ellida and Midnatsoll Fields, Norwegian Sea. Unpublished Master of Science Thesis, Department of Earth and Atmospheric Sciences, University of Alberta, Edmonton, Alberta, Canada, p. 169.
- Raharimahefa, T. and Kusky, T.M.** (2010) Environmental monitoring of Bombetoka Bay and the Betsiboka Estuary, Madagascar, using multi-temporal satellite data. *Journal of Earth Science*, V. 21, no. 2, p. 210-226.

- Rasmussen, E.** (1973) Systematics and ecology of the Isefjord marine fauna (Denmark), *Ophelia*, v.11,p. 1-507.
- Ricketts, E.F., Calvin, J., and Hedgpeth, J.W.** (1985) Bays and Estuaries: in *Between Pacific Tides*. Stanford University Press, Stanford, California. 5th ed., p. 652.
- Risk, M.J. and Yeo, R.K.** (1980) Animal-sediment relationships in Minas Basin, Bay of Fundy. In: S.B. McCann, (Ed.), *Coastline of Canada*, Geological Survey of Canada, Paper 80-10, p. 189–194.
- Sisulak, C.F. and Dashtgard, S.E.** (2012) Seasonal controls on the development and character of inclined heterolithic stratification in a tide-influenced, fluvially dominated channel: Fraser River, Canada. *Journal of Sedimentary Research*, v. 82, p. 244-257.
- Smith, D.G.** (1987) Meandering River Point Bar Lithofacies Models: Modern and Ancient Examples Compared. In **Ethridge, F.G., Flores, R.M. and Harvey, M.D.** Recent Developments in Fluvial Sedimentology. Society of Economic Paleontologists and Mineralogists, Special Publication 39, p. 83-91.
- Stokes, W.L.** (1947) Parting lineation in fluvial sandstones: a criterion of current direction. *The Journal of Geology*, v. 55, no.1, p. 52-54.
- Thomas, R.G., Smith, D.G., Wood, J.M., Visser, J., Calverley-Range, E.A. and Koster, E.H.** (1987) Inclined Heterolithic Stratification – Terminology, Description, Interpretation and Significance. *Sedimentary Geology*, v. 53, p. 123-179.
- Tillamook Coastal Watershed Resource Center** (2002) Tillamook Bay Bathymetry [map]. Bay City, Oregon.
- West, D.O. and McCrumb, D.R.** (1988) Coastline uplift in Oregon and Washington and the nature of Cascadia subduction-zone tectonics. *Geology*, v. 16, p. 169-172.

CHAPTER 3 – CONCLUSIONS

This study examines the sedimentology and neoichnology of intertidal features located within Tillamook Bay Estuary, Oregon. Data and observations were gathered in order to try and understand the parameters controlling sedimentation and the distribution of burrowing infauna. Stemming from this, the data and observations were then used in constructing a sedimentological and neoichnological model for three zones of Tillamook Bay: the inner estuary, middle estuary, and the outer estuary. In environmental and paleoenvironmental studies, the variation of estuarine characteristics between the inner, middle, and outer estuary (or proximal to distal zones) has been shown to be important both from an academic, and a hydrocarbon exploration, point of view. With the above in mind, the main focus, or topic of this thesis, has been **to understand and determine the dominant controls on sedimentation and animal-sediment interactions from the inner estuary to outer estuary depositional environments.**

To address the aforementioned thesis topic the main thesis chapter (Chapter 2) examines in detail, the sedimentological and neoichnological characteristics observed in, or near, fluvial and tidal channels, tidal flats and tidal bars of the inner, middle, and outer estuary. Additionally, a discussion of microbially-induced sedimentary structure examples, showing the relationship between cyanobacterial activity, burrowed microbial mats, algal mats, and wrinkle marks, as well as their application in interpretation of intertidal sediments, sedimentation rates and cycles of sedimentation, is included in Appendix C. Boundaries between the three estuarine zones studied are arbitrarily assigned for ease of data presentation, as well as relating observations and interpretations between different depositional environments.

The sediment character in different zones of the bay varies widely in the inner estuary, but is much more consistent in the middle and outer estuary (Fig.

Tillamook Bay Estuary Characteristics

1 Inner Estuary

- Dominantly fluvial
- Low to medium
- Straight to meandering, ~40-200 m wide; >2 m - <1 m deep
- Interplay of fluvial, tidal, and wave currents, dependent on location; low to medium total energy
- Fluvial-tidal channels; salt marshes; tidal channels and creeks; bayhead delta; high energy and quiescent tidal flats; tidal sand bars
- Mud-dominated channels; gravel flats, transverse, sinuous, and linguoid ripples; muddy and sandy tidal creeks; low-relief dunes; eel grass-stabilized mud mounds, parting lineations; heterolithic and inclined heterolithic stratification; massive-appearing sand and mud layers; microbial mats
- Absent to high, appearing dominantly in the form of vertical, straight to U-shaped, *Skolithos*-, *Thalassinoides*-, *Siphonichnus*- and *Arenicolites*-like burrows. Largely concentrated in lower-energy settings, away from fluvial-tidal and tidal channels.

2 Middle Estuary (central)*

- Fluvial and marine sediment, reworked and mixed by tidal and wave currents
- Medium to high
- Straight to sinuous, ~100-300 m wide; >2 m - <1 m deep
- Dominantly tidal and wave currents; medium to high total energy
- Tidal channels and creeks; tidal flats; tidal bars
- Muddy or mud-dominated, eel grass-covered tidal flats and tidal bars; heterolithic and inclined heterolithic stratification probable; massive-appearing mud layers probable
- Medium to high, possibly controlled by quiescent settings and sediment rich in organics and food resources, deposited as a result of current baffling by abundant algae and eel grass

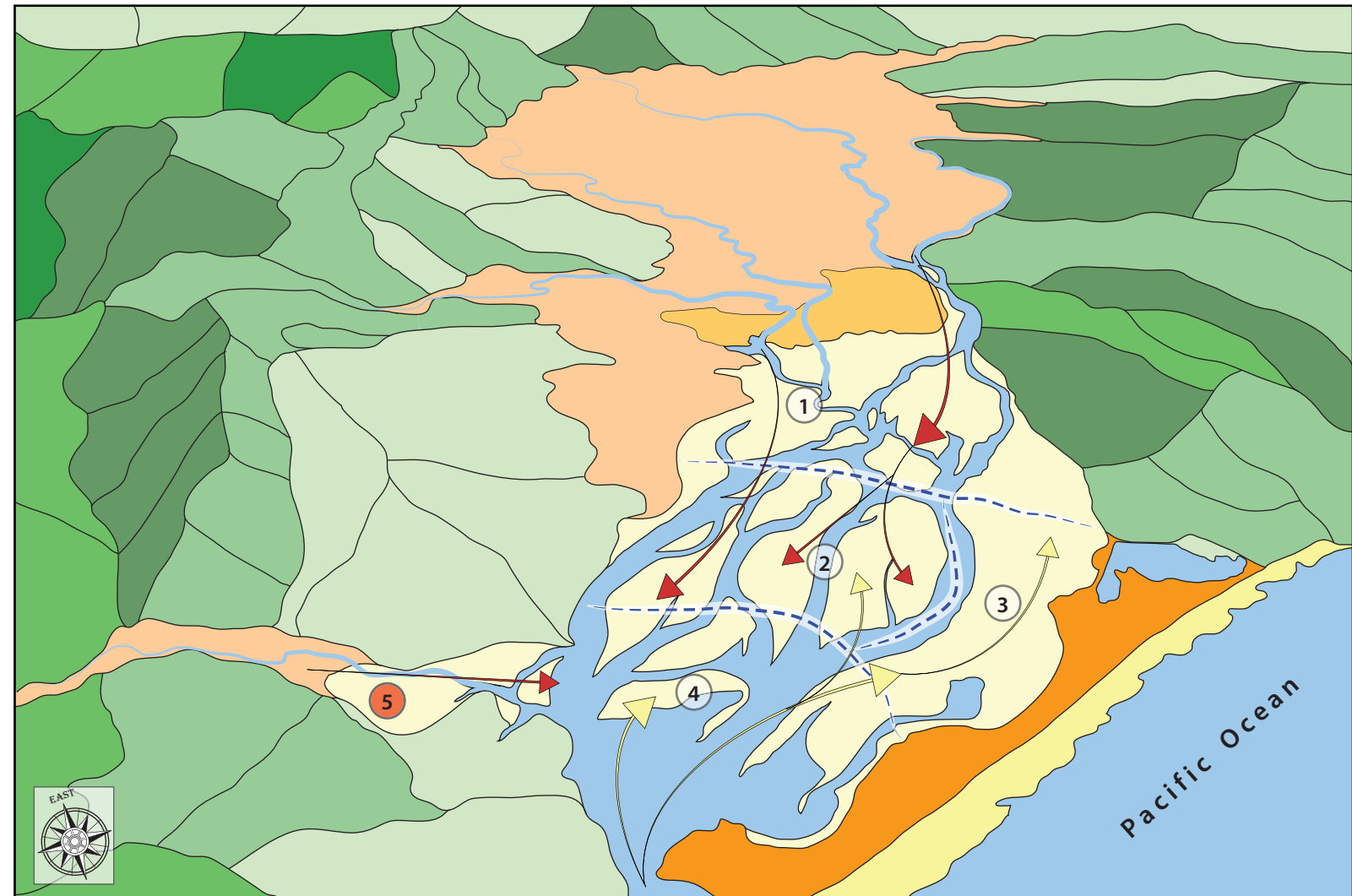
*The middle central estuary was not studied. It is included here for completeness, but the characteristics shown are hypothetical or interpreted from passive observations.

3 Middle Estuary (western margin)

- Dominantly marine
- Medium
- Straight to sinuous; ~250-300 m wide; >4 m - <1 m deep
- Tidal and wave currents; medium to high total energy
- Tidal sand flats, tidal channels and creeks
- Transverse and linguoid ripples; high-wavelength, low-relief dunes oriented obliquely to the bay shoreline; areally-restricted firmground surface; algal mats; wrinkle marks
- Low to moderate, dominantly in the form of vertical *Siphonichnus*- and *Thalassinoides*-like burrows. *Skolithos*- and *Psilonichnus*-like burrows, along with the former two, also observed in firmground surface

4 Outer Estuary

- Dominantly marine
- High
- Straight to sinuous; ~85-1000 m wide; >8 m - <1 m deep
- Tidal and wave currents; high total energy
- Tidal sand bars; tidal channels and creeks; tidal flats
- Transverse- to sinuous-crested, low- to medium-relief dunes; cross-stratified and trough cross-stratified sands; linguoid ripples
- Low to moderate, dominantly in the form of vertical *Siphonichnus*-, *Thalassinoides*-, and *Skolithos*-like burrows. *Planolites*-like burrows, and surface tracks also common.



Characteristics legend

- Sediment source
- Tidal prism
- Channel morphology
- Current type and energy
- Depositional environments
- Sedimentary features
- Bioturbation

Aerial view legend

- Fluvial channel / tidal channels / ocean water
- Alluvial plain sediments
- Salt marsh deposits
- Intertidal flats and sand bars
- Quaternary dune deposits
- Shoreface sands
- Hilly and mountainous terrain

- Marine-derived sediment
- Fluvially-derived sediment
- - - Inferred, arbitrary boundary between the inner, middle, and outer estuary

1

5

- Estuary zone mentioned and described in the characteristics
- Area not studied; see caption below

Figure 3-1. Tillamook Bay Estuary Characteristics. Aerial drawing showing the four main estuary parts. The boundary between each area is arbitrary, and used only as a general guideline to divide the observed estuary characteristics. The descriptions are based largely on observations and interpretations discussed in the thesis. Channel widths were approximated and measured digitally using Google Inc.'s Google Earth software. Channel depths were interpreted from field observations, as well as from a Tillamook Bay bathymetry map, published by the Tillamook Coastal Watershed Resource Center (2002).

Area 5, as labelled on the aerial drawing, was not studied. However, it is important to consider that the freshwater and sediment discharge of Miami River - the smallest of the five tributaries of Tillamook Bay - in this area, creates a "micro" estuary adjacent and connected to the larger Tillamook Bay Estuary. Though not directly observed, a rapid transition from an inner estuary to middle estuary to outer estuary likely occurs in this area.

3-1). Other variations in estuarine characteristics occur between the inner, middle, and outer estuary. Although the bulk of the middle estuary was not studied it is included in Figure 3-1 for completeness, to be able to relate the transition between proximal and distal features in the estuary.

The inner estuary, the largest in areal coverage, contains the highest variability in depositional environments, sediment character, sedimentary structures, and burrowing infauna distribution, diversity, and concentration. Beginning in the fluvial-tidal transition zone that extends at most ten kilometers upstream from the mouth of the Tillamook River, mud-dominated straight to meandering fluvial channels can be observed. With the exception of mud and occasional gravel, sediment of other grain sizes is transported bayward and deposited within the bay itself. Mud deposition in the fluvial-tidal channels is interpreted to occur during the dry season, when fluvial freshwater discharge is at its lowest. Due to low discharge, mixing of marine water and freshwater occurs farther upstream than during the wet season, causing the flocculation of clays to occur in the innermost inner estuary. If the current model of the shifting of the turbidity maximum is largely correct, the interpretation would imply a seaward or landward shift of approximately 10-15 kilometers, between winter and summer seasons, respectively. Given the microtidal to mesotidal nature of the tidal range, this is to be expected. The salt intrusion limit has been observed to shift seaward by tens of kilometers during episodic periods of high fluvial discharge in the micro-tidal Hawkesbury River estuary (Hughes et al., 1998). Correspondingly, mud deposition in inner estuary deposits found inside Tillamook Bay is interpreted to occur during the wet, winter season, when the turbidity maximum shifts bayward.

As observed in bar-margin deposits in Zone 3, interlayered mud and sand occurs as inclined heterolithic stratification. In the examples studied, burrows were observed dominantly in the sand layers, with burrows extending into the muddy portions, and in some cases found fully within the muddy layers. This, combined with the structure-less texture of muddy layers and

rippled sand layers, led to the interpretation that mud layers and muddy sand layers, largely devoid of bioturbation, are sourced, or deposited, due to the flocculation of clays in the wet winter season. The high fluvial freshwater discharge advances farther downstream into the bay than during the dry season, and as a result, mixing of marine water and freshwater occurs in the area of tidal flats and tidal bars within the bay.

Discharge of high concentrations of suspended sediment, coupled with the action of tidal and wave currents, results in clay being reworked and distributed over a larger areal extent within the bay, as opposed to being areally-restricted to the fluvial-tidal channels, as observed in the fluvial-tidal transition zone. This is observed mainly in the center of the sand bar (Zone 3) studied, where muddy sediments dominated the bar surface, often in the form of mud hummocks, formed around current-baffling eelgrass concentrations. Corresponding to the high mud concentrations in the center of Zone 3 was the high invertebrate burrow concentration and diversity. Several factors likely affect the distribution of invertebrates in this zone: relatively low sedimentation rate; reduced total current energy due to the presence of eel grass; and high concentrations of easily decomposable organic carbon (Type II kerogen). Contrasting with the mouth of the Kilchis River (Zone 2) as an example, a higher sedimentation rate and higher current energy result in low to medium bioturbation intensity. Burrows are mostly those of *Neotrypaea californiensis*, and are akin to *Thalassinoides* and *Skolithos* traces. Higher concentrations of total organic carbon are likely introduced as plant fragments derived from forests in the hilly and mountainous terrain to the east. Organic carbon, derived from marine phytoplankton, is likely present at lower concentrations. The concentration and diversity of burrowing invertebrates is highest on exposed tidal flats and tidal bars of Zone 3, where tidal and wave currents are able to distribute marine-derived organic carbon, to be used as a food resource by organisms. The diversity of invertebrates utilizing food resources, and favorable environmental conditions, gives rise to a range of

burrow morphologies, mostly vertical to sub-vertical burrows ranging in diameter from millimeter size to centimeter-size. The most common burrows observed are akin to *Skolithos*, *Arenicolites*, *Siphonichnus*, *Thalassinoides*, and *Planolites*. Other burrows observed are akin to *Cylindrichnus*-, *Palaeophycus*-, *Polykladichnus*-, and *Psilonichnus*-, with one occurrence of a possible *Teichichnus*-like trace.

Vibracores show little to no record of bioturbation, likely due to a lack of differential compaction. However, interbeds and interlaminae of sand and mud can be observed in vibracores of the inner estuary. Where sand layers are observed successively, grain size variations and bedding contacts delineate the largely thin, centimeter- to decimeter-scale beds. Heterolithic and inclined heterolithic stratification is common, though given the range in depositional environments, as well as possible bed stacking geometries, the terms may be too general and not descriptive on their own. If the reported sedimentation rates of 20-40 centimeters/century (Glenn, 1978) are correct, the deepest vibracores, at approximately two meters on average, show a record dating back at most 1000 years, with the assumption of erosional episodes also occurring. Regardless of the actual sedimentation rate, it is very likely that beds are deposited during rapid, one-time events. Erosion results in the reduction of sediment packages, allowing for more deposition during subsequent events.

Sedimentation rates have also been interpreted to vary seasonally, with the aid of microbially-induced sedimentary structures (Appendix C). In the inner estuary, as well as the middle estuary, cyanobacterial activity results in the creation of microbial mats, as well as wrinkle marks on intertidal sediments. The biological activity of cyanobacteria causes the natural binding of sediment grains, and therefore various degrees of sediment cohesiveness. Forces acting on cohesive sediment result in the formation of structures such as wrinkle marks and polygonal desiccation cracks. For such structures to form, a period of non-deposition, or low deposition must occur for a sufficiently long time, on the order of weeks to months.

Deposition in the middle estuary, as well as the outer estuary, occurs under the influence of waves and tidal currents. Sediment mineralogy, dominated by marine-derived quartz grains, contrasts with the lithic rock fragments of the fluvially-derived sediment. The presence of low-relief, high wavelength dunes, and higher-relief, lower-wavelength dunes in the middle and outer estuary, respectively, is interpreted to be the result of increasing total wave and tidal current energy. Wave action in the outer estuary sand bar is the highest observed within Tillamook Bay, and this is reflected in the well-developed dunes, as well as the very good sorting character of the sediment. Bioturbation, as observed, was absent to medium in intensity, and appeared dominantly in the form of *Skolithos*-, *Siphonichnus*-, and *Thalassinoides*-like burrows. Burrow diameters appeared to increase overall, when compared to those in the inner estuary, though small diameter (<5 millimeter) burrows were still observed. If any suspended sediment reaches the outer estuary, either from the south-eastern part of the bay, where four of the largest tributaries discharge sediment, or from the Miami River in north-east, much of this sediment is likely flushed out of the estuary by the strong tidal currents and large tidal prism. The action of the tidal prism, as well as wave action in the bay, has an effect on the size and lateral migration patterns of sand bars and tidal channels. As observed in aerial photos taken between 1971 and 2005 (Fig. 2-74, Part I and II), tidal channels are relatively stable, and, though lateral migration does occur, over time, the channels largely maintain their respective positions and widths.

Future work and model improvements

The current study discusses the sedimentological and neoichnological characteristics of Tillamook Bay, but much more remains to be examined in order to refine the sedimentological and neoichnological model, both in the areas examined in this thesis, as well as others. All data examined in this study

was collected from areally-extensive tidal flats and tidal bars. From an exploration and reservoir analogue point of view, these are ideal sites for modern studies, as they have the potential to improve models and aid in more efficient and economic hydrocarbon exploration strategies. However, studies of more areally-restricted environments and – depending on location within the estuary – possibly lower reservoir quality environments may help improve depositional model interpretations. Having an improved understanding of the facies and channel geometries, can not only improve the understanding of depositional mechanisms of other, laterally-adjacent environments, but may also provide a better idea of the locations within the estuary complex where such environments contain good, reservoir-quality facies.

A detailed vibracore study in tidal channels of Tillamook Bay would greatly benefit the understanding of the different parameters affecting deposition within the estuary. For example, the presence of fluid muds, the relative sand-mud proportions, and the possible occurrence of mud couplets in subtidal portions would support or refute the seasonal influence and tidal reworking of suspended particulate matter.

Closely-spaced (i.e. meter scale) vibracores, in both channel-parallel and channel-perpendicular orientations would improve the chances of correlation between individual sand or mud beds, which may help improve the accuracy of the depositional model.

The bayhead delta region appears to be highly-variable, as observed in sediments of Zone 2. A highly-detailed study, possibly involving vibracores taken at closely-spaced intervals in the multiple different environments, would greatly benefit the understanding of the parameters affecting sedimentation and bioturbation at the bayhead location within the estuary. This can have an effect on the understanding of how the location of the turbidity maximum shifts between the wet season and dry season, and thus how the turbidity maximum influences the settling of suspended-sediment landward and bayward of the bayhead delta region.

An interesting area that may provide valuable insight into the transition between inner, middle, and outer estuary characteristics is that of the Miami River, in the north-eastern part of the bay (Fig. 3-1). Having the lowest fluvial discharge of the five tributaries entering Tillamook Bay, Miami River is isolated from the inner estuary defined in this study. However, freshwater discharge does occur in the Miami River, and as a result, the area may act as a “micro” estuary found within the larger Tillamook Bay Estuary. Passive observations, from the Oregon Coast Highway crossing the Miami River, reveal possible muddy tidal flats in a sheltered embayment between the Garibaldi marina and the river mouth. This small area can provide easy access, and could be examined using closely-spaced vibracores to observe the changes, if any, between the inner to outer Miami River “micro” estuary zone.

If future studies are to be conducted during the winter season, this may provide an ideal time to measure salinities and perhaps suspended-sediment concentrations at different locations within the inner estuary. The types of sedimentary structures observed, as well as the surface texture and dominant grain size, can be expected to vary in some zones of the estuary, than those recorded in this study, in which case all were observed during periods of low fluvial discharge of the summer season. A neoichnological study may be more difficult to undertake, as it may be highly dependent on weather; heavy rain during the winter season can erase surface burrow openings, and the influx of rainwater into the exposed sediments at low tide may push invertebrate organisms deeper into the sediment, thus making it more difficult to accurately assess bioturbation.

BIBLIOGRAPHY

- Glenn, J.L.** (1978) Sediment sources and Holocene sedimentation history in Tillamook Bay, Oregon: Data and Preliminary Interpretations. Open-file report 78-680: United States Department of the Interior Geological Survey, Denver, Colorado.
- Hughes, M.G., Harris, P.T. and Hubble, T.C.T.** (1998) Dynamics of the turbidity maximum zone in a micro-tidal estuary: Hawkesbury River, Australia.

APPENDICES

Appendix A
Supplementary Figures

Appendix B
Sediment Logs

Appendix C
Microbially-Induced Sedimentary Structures (MISS): Examples
from Intertidal Flats of Tillamook Bay Estuary, Oregon

Appendix A
Supplementary Figures

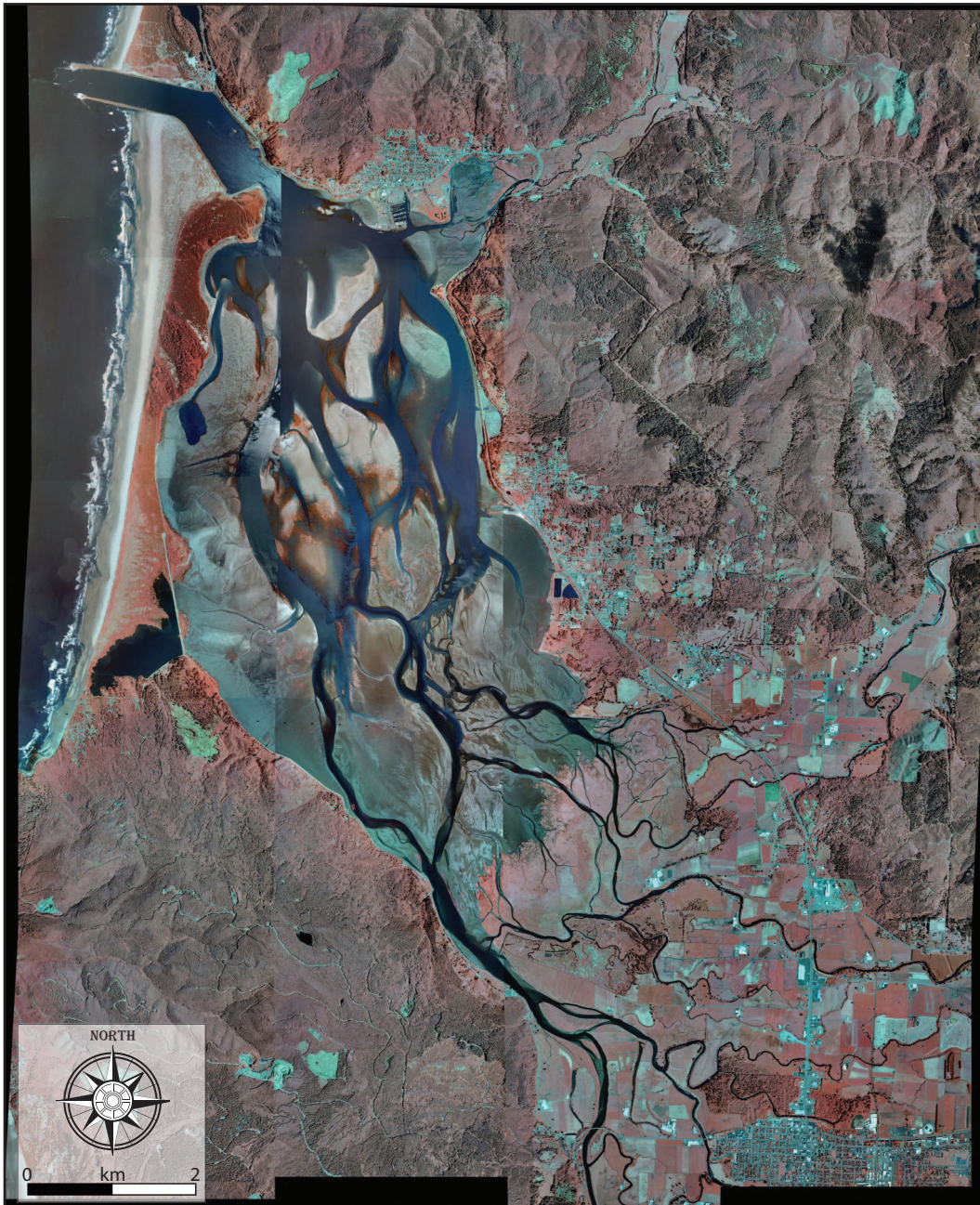


Figure A-1. Intertidal Color Infrared Aerial Mosaic of Tillamook Bay Estuary. Infrared aerial mosaic of Tillamook Bay, acquired at low tide in spring 2005. Images scanned from false-color infrared film negatives. Mosaic downloaded from Oregon Coastal Atlas, www.coastalatlantlas.net. Courtesy of Oregon Department of Land Conservation and Development (DLCD), U.S. Environmental Protection Agency (EPA), U.S. Department of Agriculture. Aerial photography by: Bergman Photographic Services, Inc., Portland Oregon. Digital Scanning of photo negatives by: David Smith and Associates, Inc., Portland, Oregon.



Figure A-2. Historical photos of Bayocean Peninsula. Top photograph: aerial view, looking north, of Bayocean Peninsula and Tillamook Bay; date unknown, but before 1952. Cape Meares Lighthouse, the trail leading to it, and the parking lot can be seen in the foreground, at the bottom of the image. Note the formation of what appears to be a flood-tidal and ebb-tidal delta to the east and west of Kincheloe Point (northern tip of the peninsula), respectively. **Bottom photograph:** view looking north-east towards the southern tip of Bayocean Peninsula. Photo taken approximately near the rocky point north of Cape Meares Lighthouse. Date also unknown, but before 1952. Note relatively low relief, as well as width (better observed in the top photo) of Quaternary dunes in the southern portion of the peninsula. Storm waves and large tides would later result in the breaching of those dunes in 1952, resulting in the formation of an ephemeral tidal inlet. Both photographs courtesy of Tillamook County Pioneer Museum, used by permission.

Figure A-3. Sediment and trace views, salt marsh-adjacent flats, Zone 2. (A and A') Cross-sectional view of muddy sand (dark beige-green colored layer in A') and sand layers (lighter beige colored layer in A'), separated by a layer rich in organic matter (grey-colored layer in A'). (B and B') Close up photo and drawing of the dominantly straight vertical and U-shaped, *Skolithos*-like (Sk) and *Arenicolites*-like (Ar) burrows, respectively.

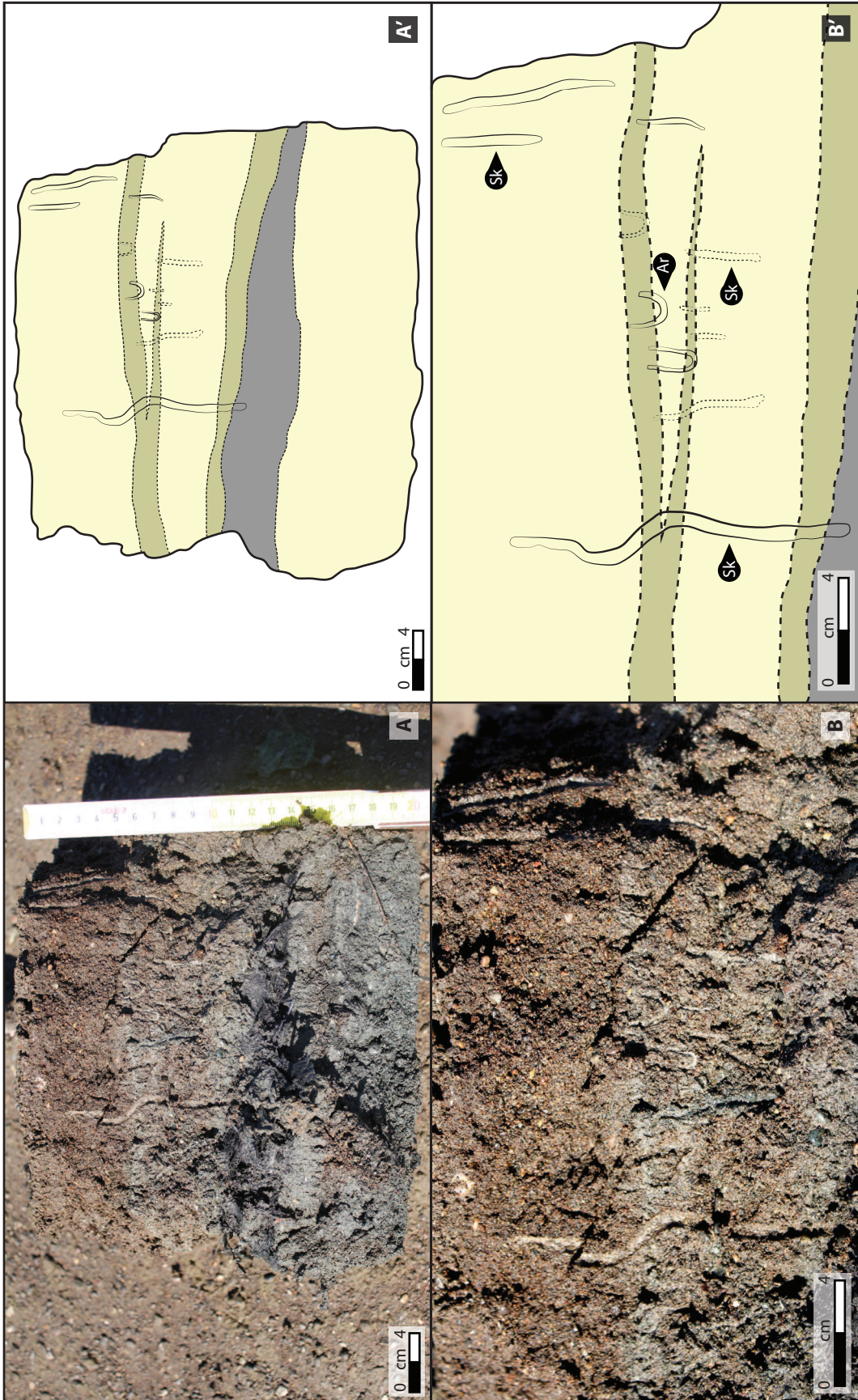
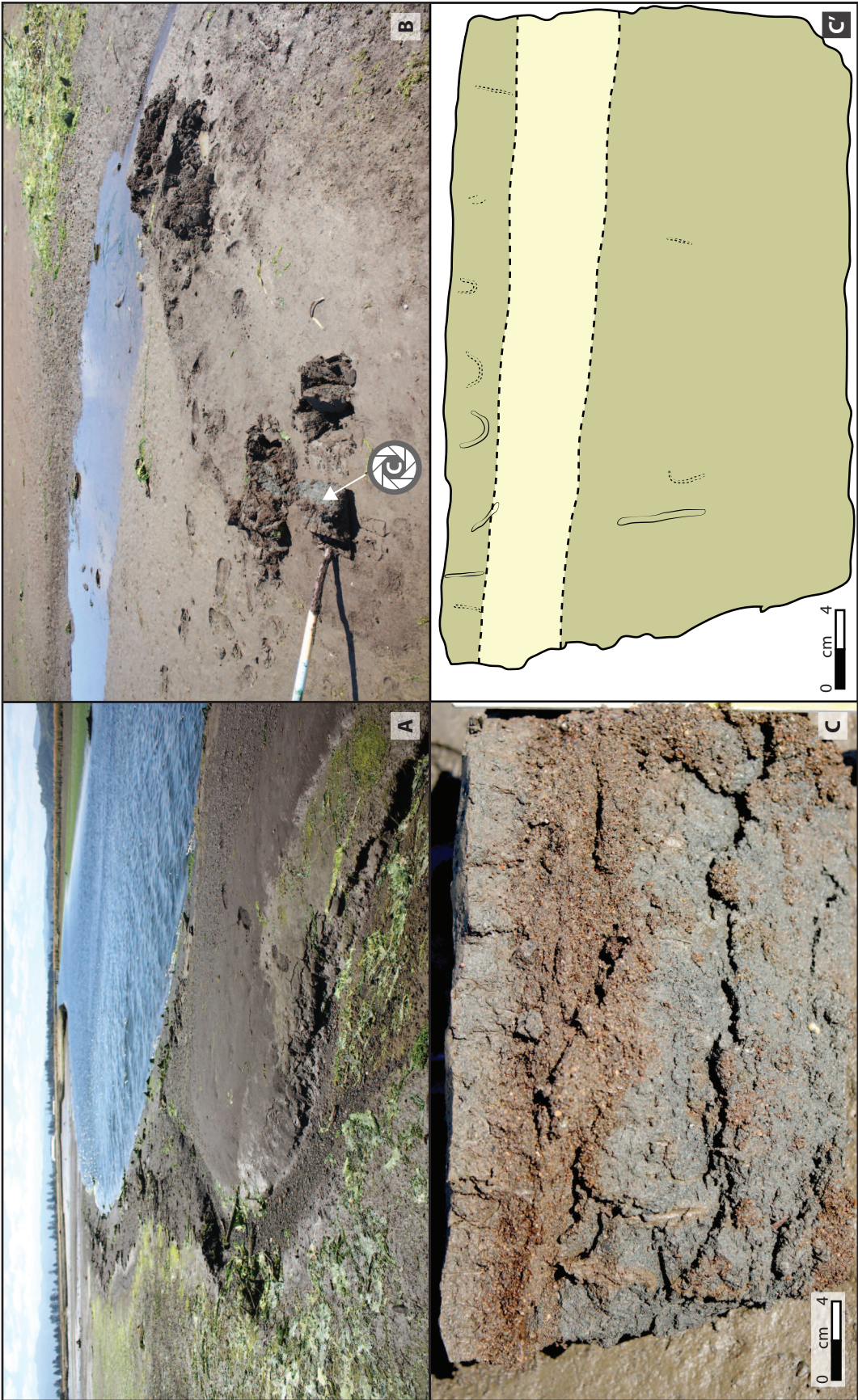


Figure A-4. Creek morphology, sedimentary structures and traces at channel margin, Zone 2. (A) Incision of small creek in coarse-grained and gravel-rich sediment near the cut-bank of the Kilchis River; view to the south-east. (B) Muddy medium-grained sand near small, bank-adjacent creek. (C and C') Cross-sectional view of muddy sand and cleaner sand layers, showing presence of small, *Arenicolites*-like and *Skolithos* - like burrows in the muddy sand layers.



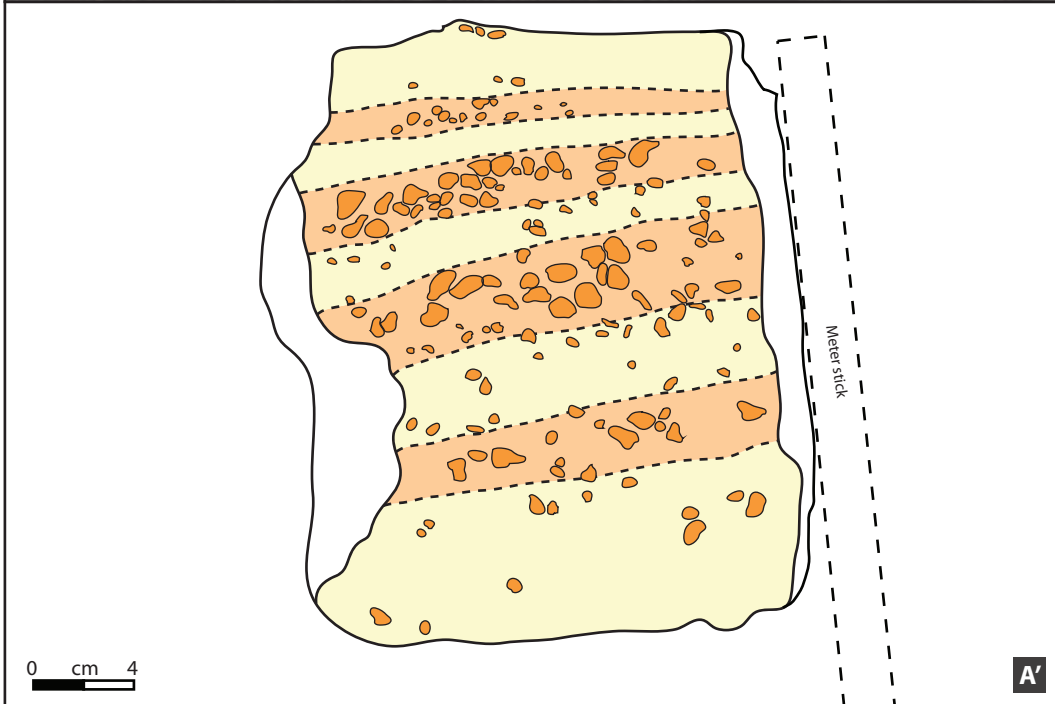


Figure A-5. Pebble-rich layers, Zone 2. (A and A') Photo and drawing of interbedded sand (beige color in A') and pebble-rich (orange color in A') layers. Note that pebble sized clasts also occur sporadically within the sand layers.

Figure A-6. Sub-surface sedimentary features and traces, channel-margin sediments, Zone 2. (A and A', B and B') Cross-sectional views of two samples displaying dominantly muddy sand (darker beige-green colored layer in A' and B') with a surficial, approximately 2cm thick, sandy layer (lighter beige colored layer in A' and B'). Burrows are commonly *Arenicolites*-like (Ar) and *Skolithos*-like (Sk) in appearance. Possible *Palaeophycus*-like (Pa?) burrows are also observed. A wood clast (wd) is noted in A'. Note that multiple burrows display some degree of oxidized, orange colored, lining in both samples.

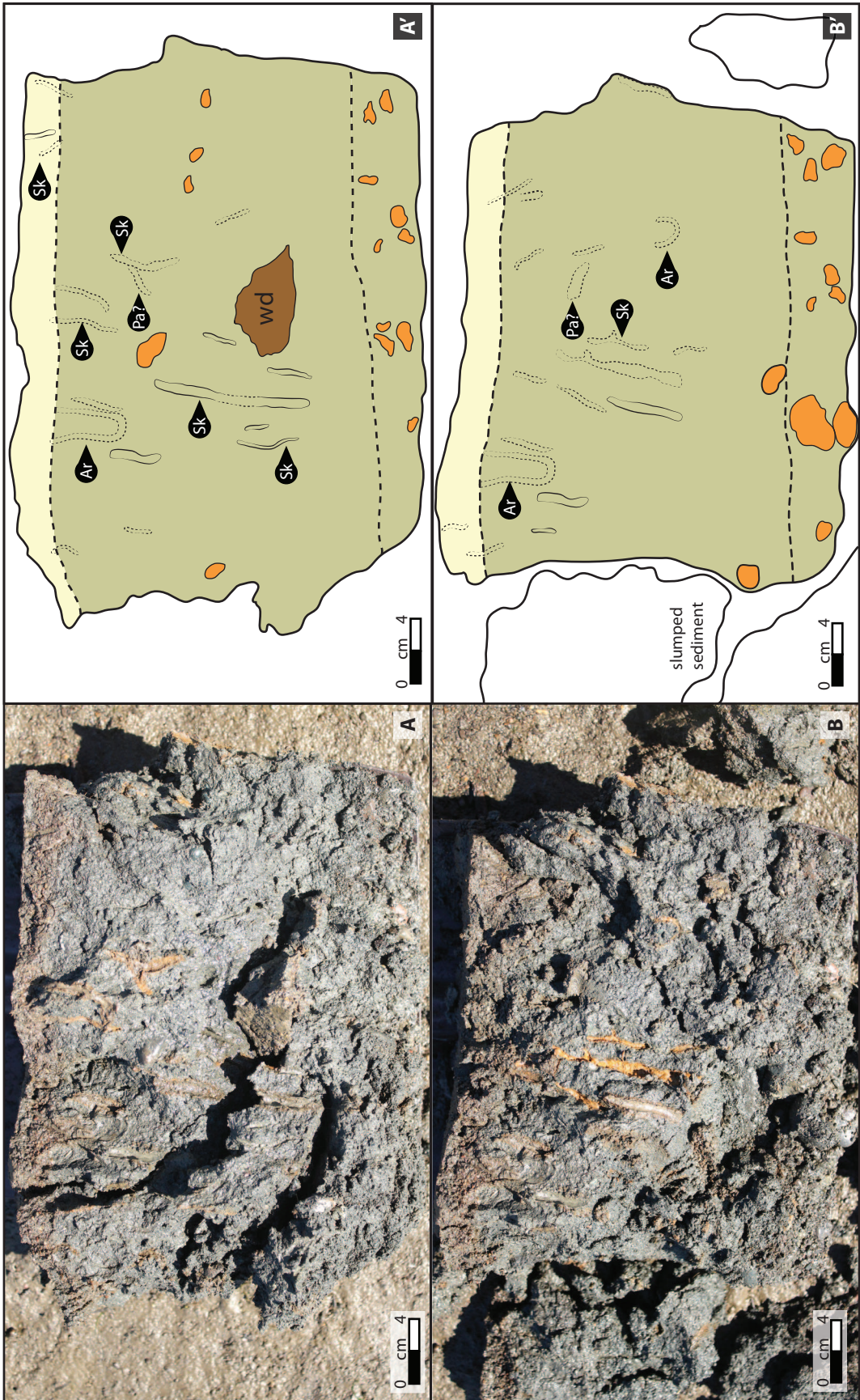


Figure A-7. Sub-surface sedimentary features and traces, muddy sand channel margin, Zone 2. (A and A') Cross-sectional view of muddy sand (darker beige-green colored layer in A') and sand layers (lighter beige colored layer in A'), with *Arenicolites*-like (Ar) and *Skolithos*-like (Sk) traces commonly associated with the muddy sand layers. (B and B') Close-up photo and drawing of *Skolithos*-like (Sk) trace observed in A with a semi-exposed *Nephtys* sp. worm present along the trace.

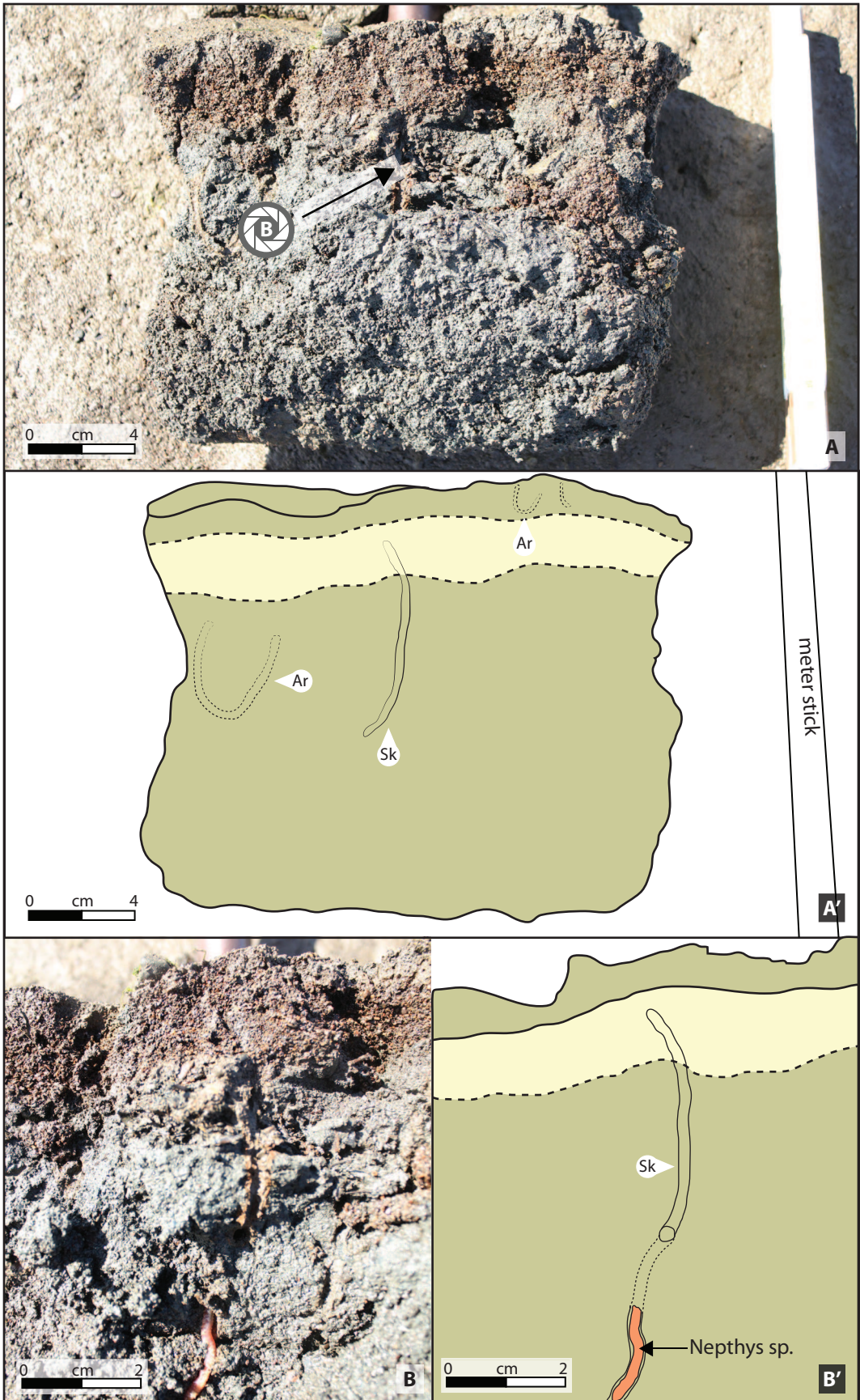
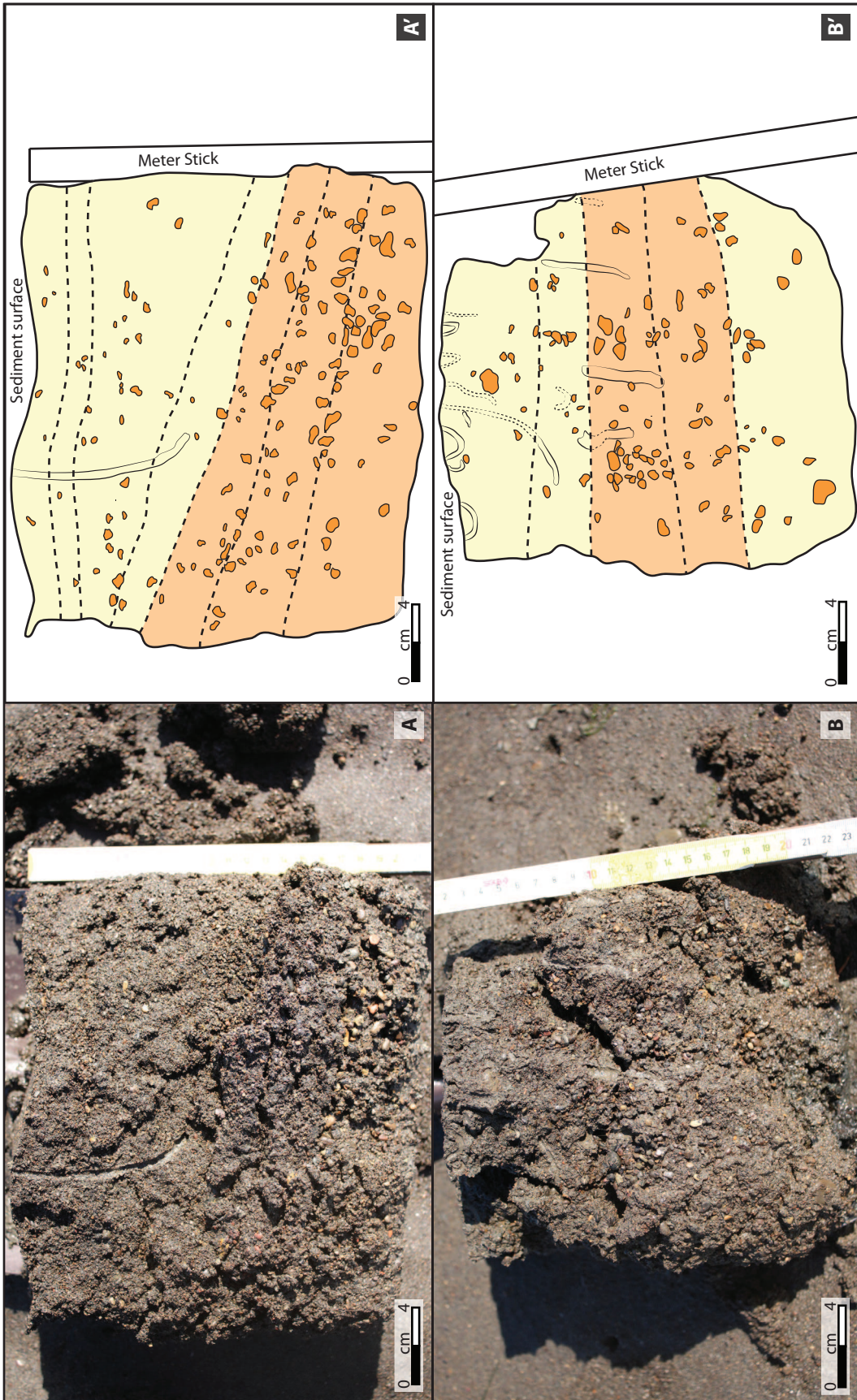
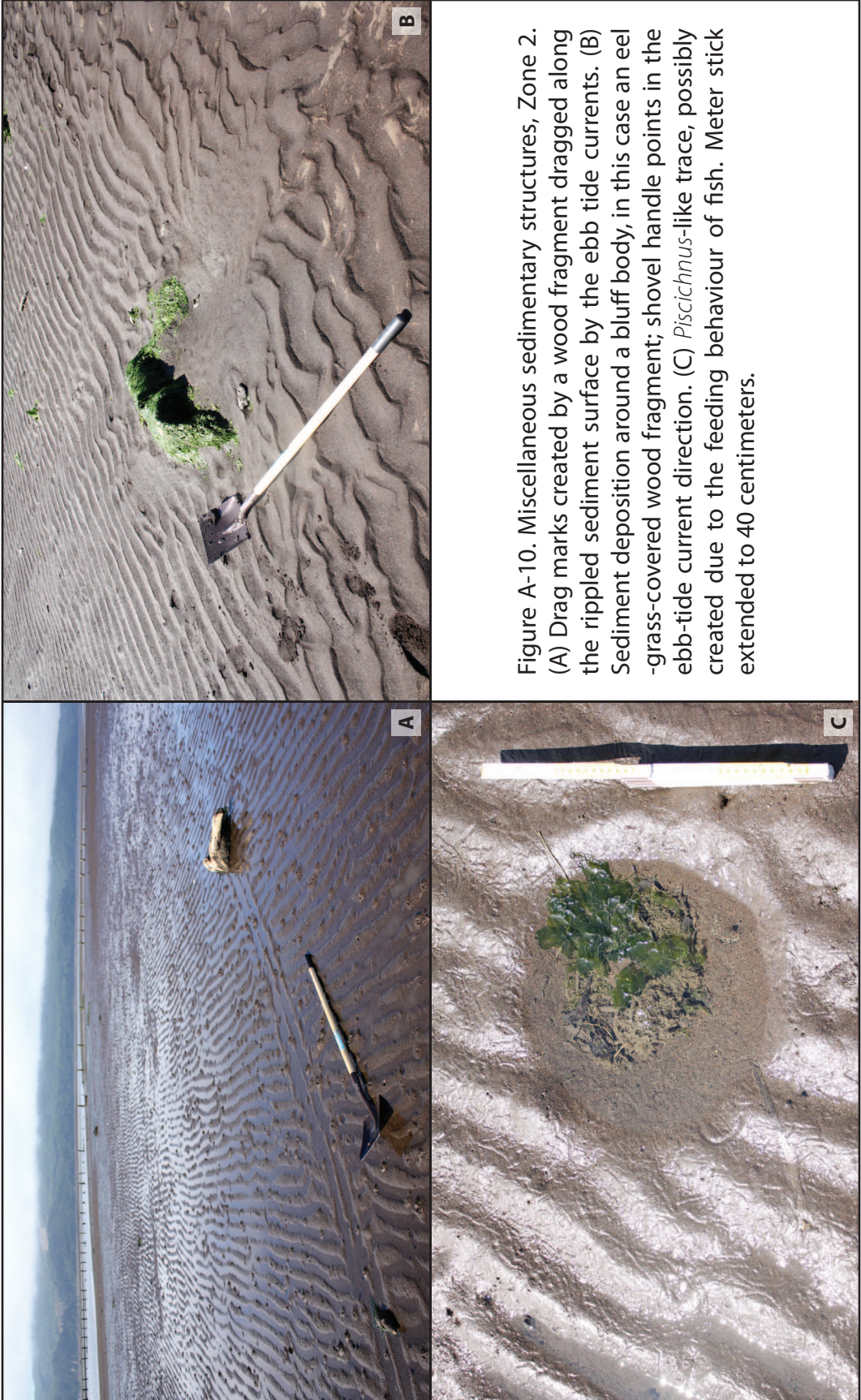




Figure A-8. Surface texture and tidal creek facies, Zone 2. (A) Small tidal creek that aids in draining the muddy sand flats of sub-zone 5. (B) Close up view of tidal creek in (A) where a sporadic coarser grained lag is observed. Ruler for scale is 24 cm long.

Figure A-9. Traces in pebble-rich sand, sub-environment 2, Zone 2. (A and A') Cross-sectional view of planar to slightly inclined sand (lighter beige colored layer in A') and pebbly sand (orange colored layer in A') sub-surface layers with relatively large unlined, vertical to sub-vertical, *Skolithos*-like trace observed. (B and B') Cross-sectional view of planar sand (lighter beige colored layer in B') and pebbly sand (orange colored layer in B') sub-surface layers with unlined vertical to sub-vertical *Skolithos*-like and U-shaped *Arenicolites*-like burrows observed.





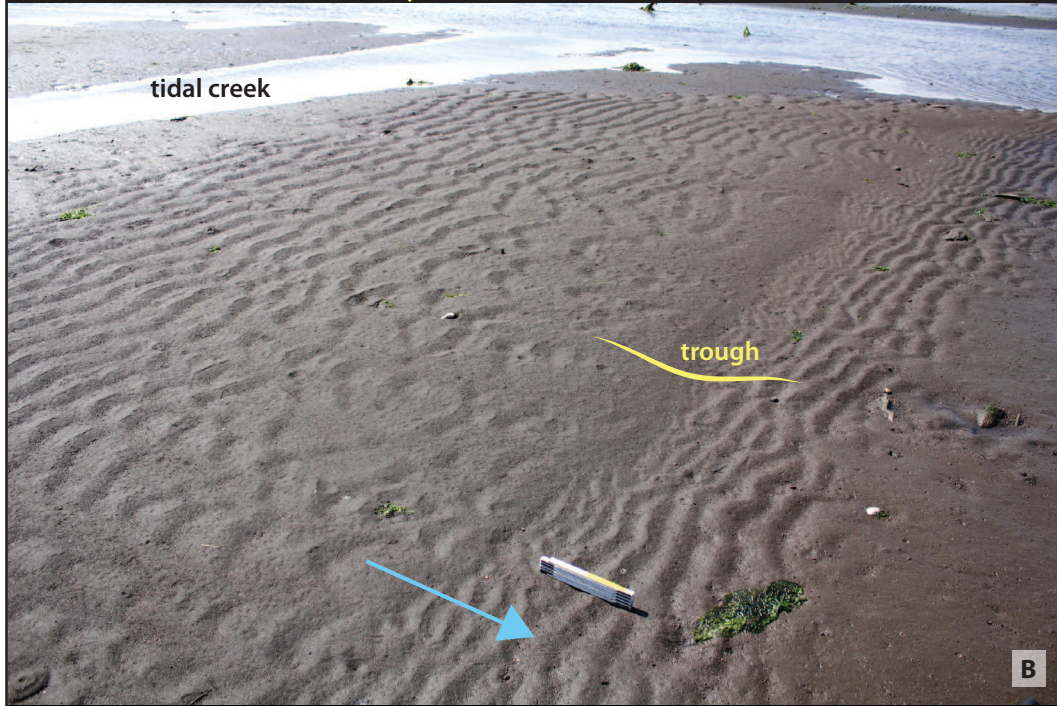
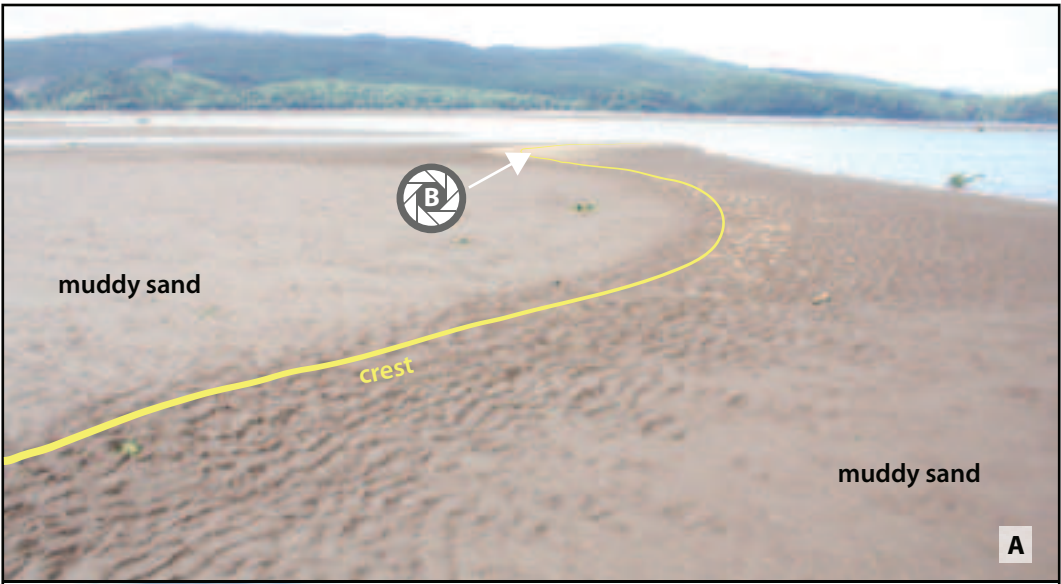


Figure A-11. Sedimentary features indicative of changing flow conditions. (A) View looking north-east along the crest of a low-relief dune. Note transverse ripples superimposed on the stoss side of the dune, and their transition past the crest into linguoid ripples superimposed on the lee side; ebb-current direction shown by the blue arrow. (B) Gently-sloping surface, containing dominantly transverse ripples near the tidal creek seen in the background, to poorly-developed linguoid ripples towards the lower side leading to a trough. Flow velocity of the ebb current (shown by the blue arrow) is interpreted to increase downslope, only to decrease again once it reaches a sloping-up surface; the velocity reduction is sufficient to allow formation of transverse ripples. Note sharp termination of ripples into a muddy sand flat at the right of the photo.

Figure A-12. Low-relief dune, Zone 2. (A) View of the curved crest of a low-relief dune. Note the ripples superimposed on the lee dune surface, and the gradual transition of this surface into a flat-lying, muddy sand area. Another muddy sand area exists upstream (from the perspective of ebb-tide currents (indicated by the blue arrow) of the dune crest. (B and C) Views close to the highest-relief part of the dune. Note the dried sediment (appearing lighter-colored) forming the top of the dune, as well as the more elongate linguoid ripples superimposed on the dune top. The stoss and lee sides contain distinctly less elongate ripples, pointing to a likely change in current energies between the dune crest and lee and stoss sides.



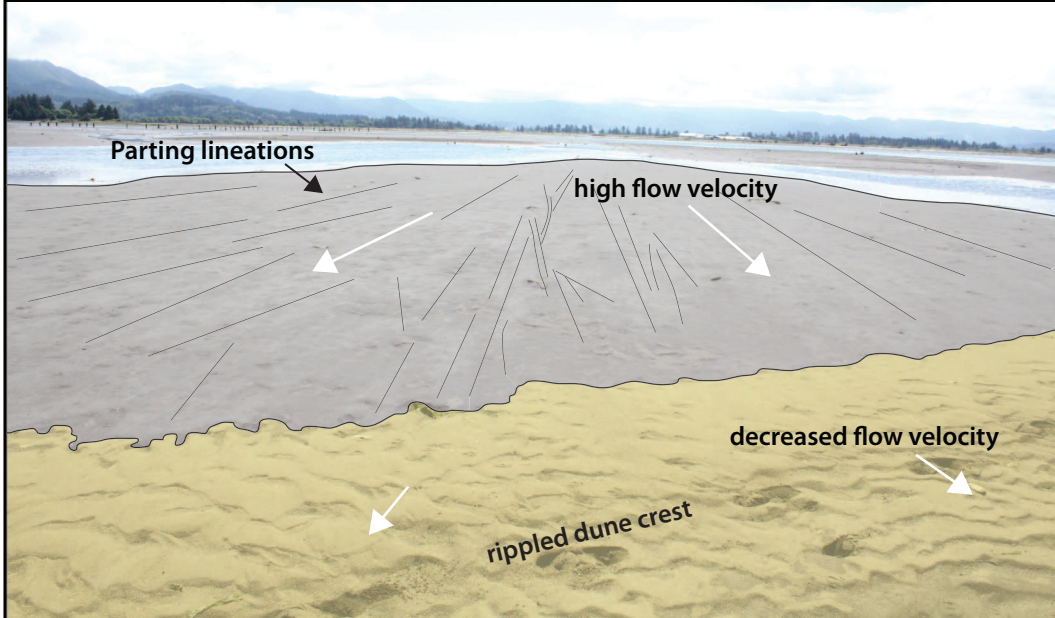


Figure A-13. Parting lineations, Zone 2. Photograph and trace drawing of an area containing abundant parting lineations, that sharply transition into the stoss side of a rippled dune. The parting lineations, shown as thin black lines, occur in an area interpreted to experience higher-flow velocities (indicated by longer white arrows). A decrease in flow velocity occurs at the encounter with the dune stoss side, where sediment is able to settle and ripples begin to form.

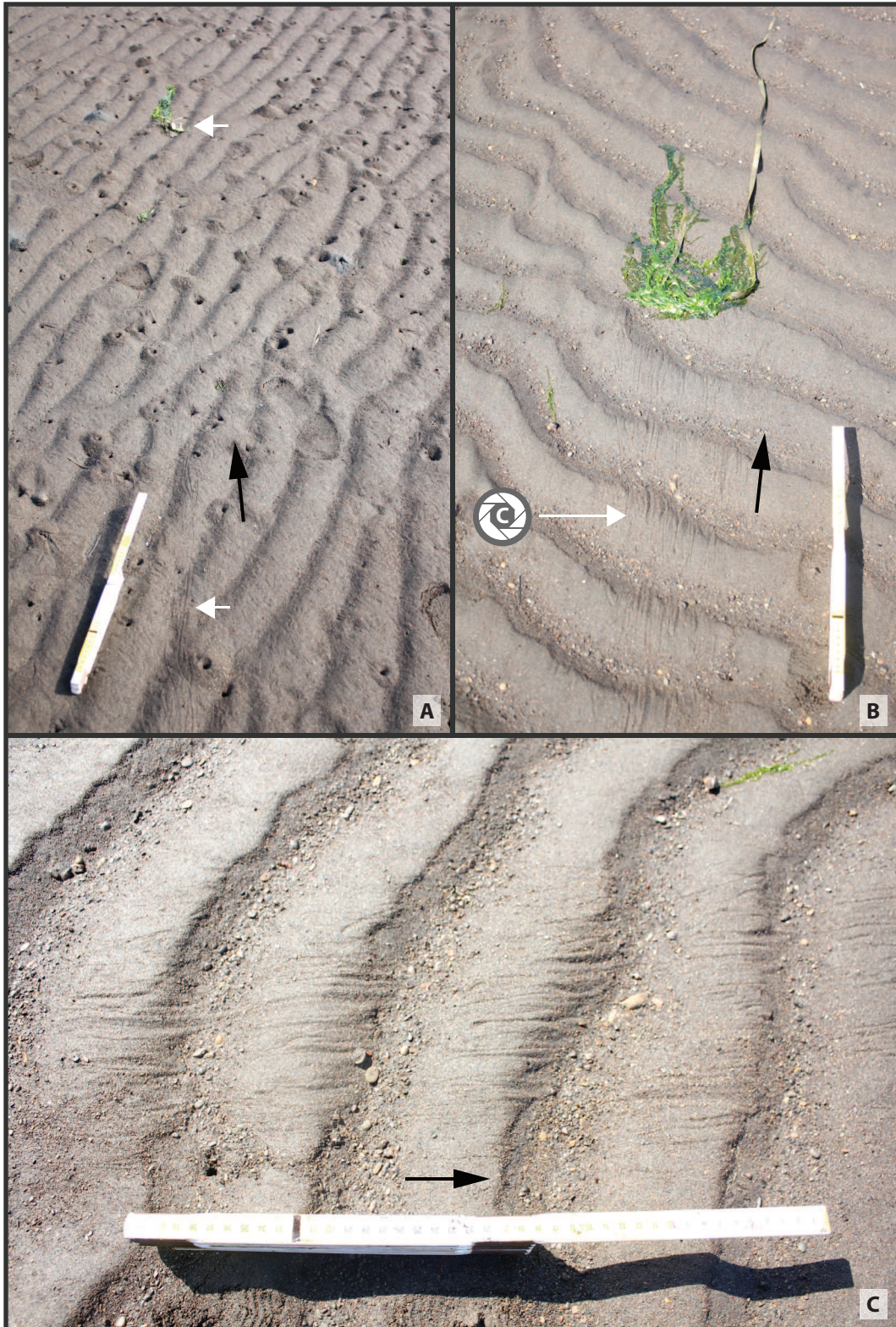


Figure A-14. Eel grass-generated drag marks, Zone 2. (A,B, and C) Various views of the drag marks created by eel-grass being moved under the action of ebb tidal currents. White arrows in (A) point to the drag marks and the eel-grass in the background. Black arrows indicate ebb-tide direction. Meter stick extended to 40 centimeters in all photographs.

Figure A-15. Low-relief dune features, Zone 2. (A) View perpendicular to a dune crest, showing the oblique orientation of ripples on the sediment in front of the dune. Tidal creek margin seen in the lower left hand corner. (B) Close-up view of the lee side of the dune, showing the axis of rotation of ripples. Due to the influence of tidal currents that flow around the protruding sediment flows on the dune lee side, the ripples appear to curve, as shown in this example. Ebb tidal current direction is from left to right. (C) View parallel to the dune crest, showing dune front sediment flows, with superimposed ripples. Note that ripples are oriented largely parallel to the dune crest, as opposed to being curved as near the tidal creek. Ebb tidal current flow is indicated by the blue arrow.

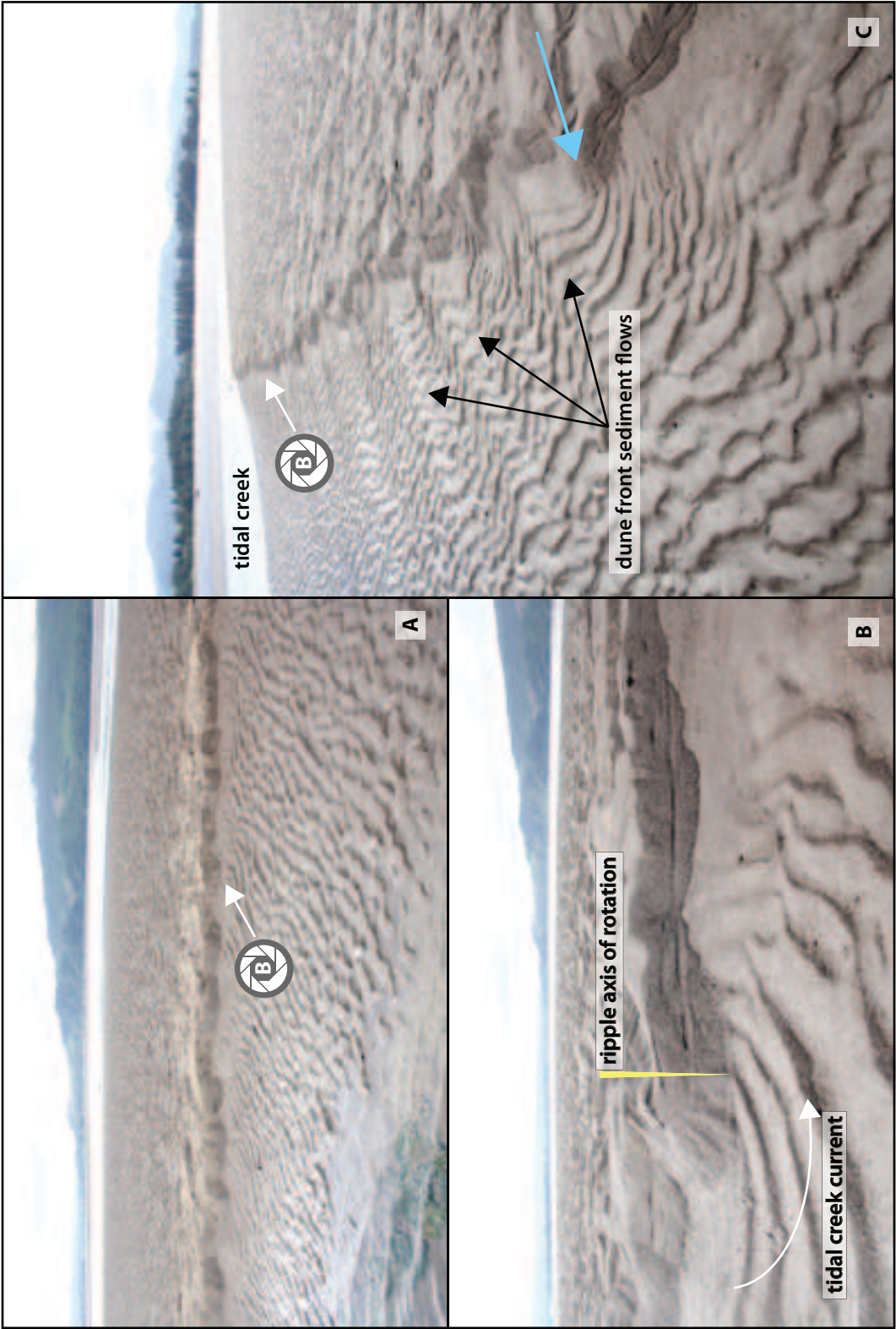


Figure A-16. Low-relief dune features, Zone 2 (general view); (Next page). Photos of the dune shown in figure A-15, but taken at a separate time. (A and B) Views of the vertical relief of the dune, showing a smaller relief towards the edge of the dune, and a higher relief of approximately 35-40 centimeters at the highest point at its crest. (B and C) Views of the lee side of the dune, indicating the angle or repose of approximately 30°, and the presence of fecal pellets accumulating at the base of the lee slope.

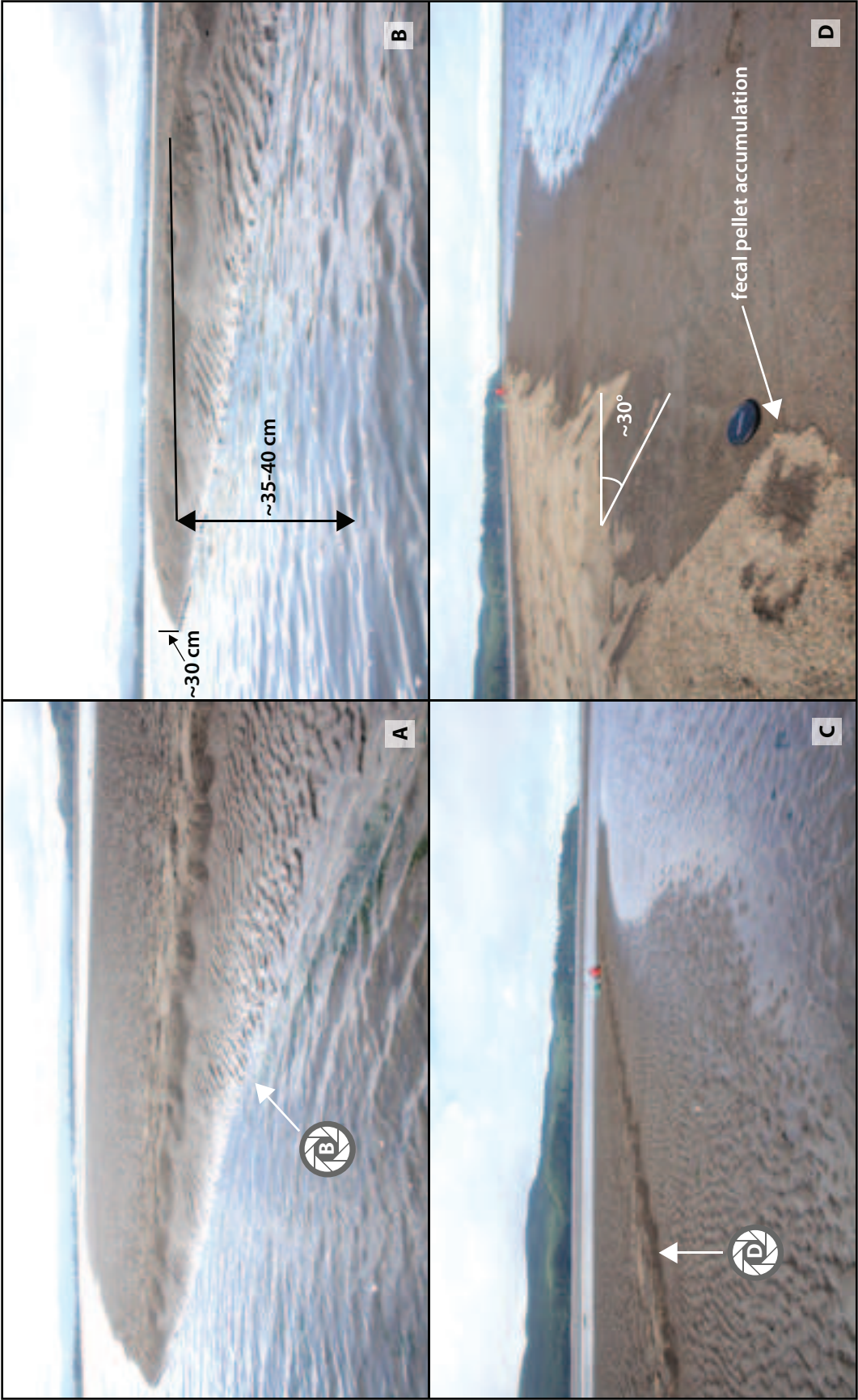
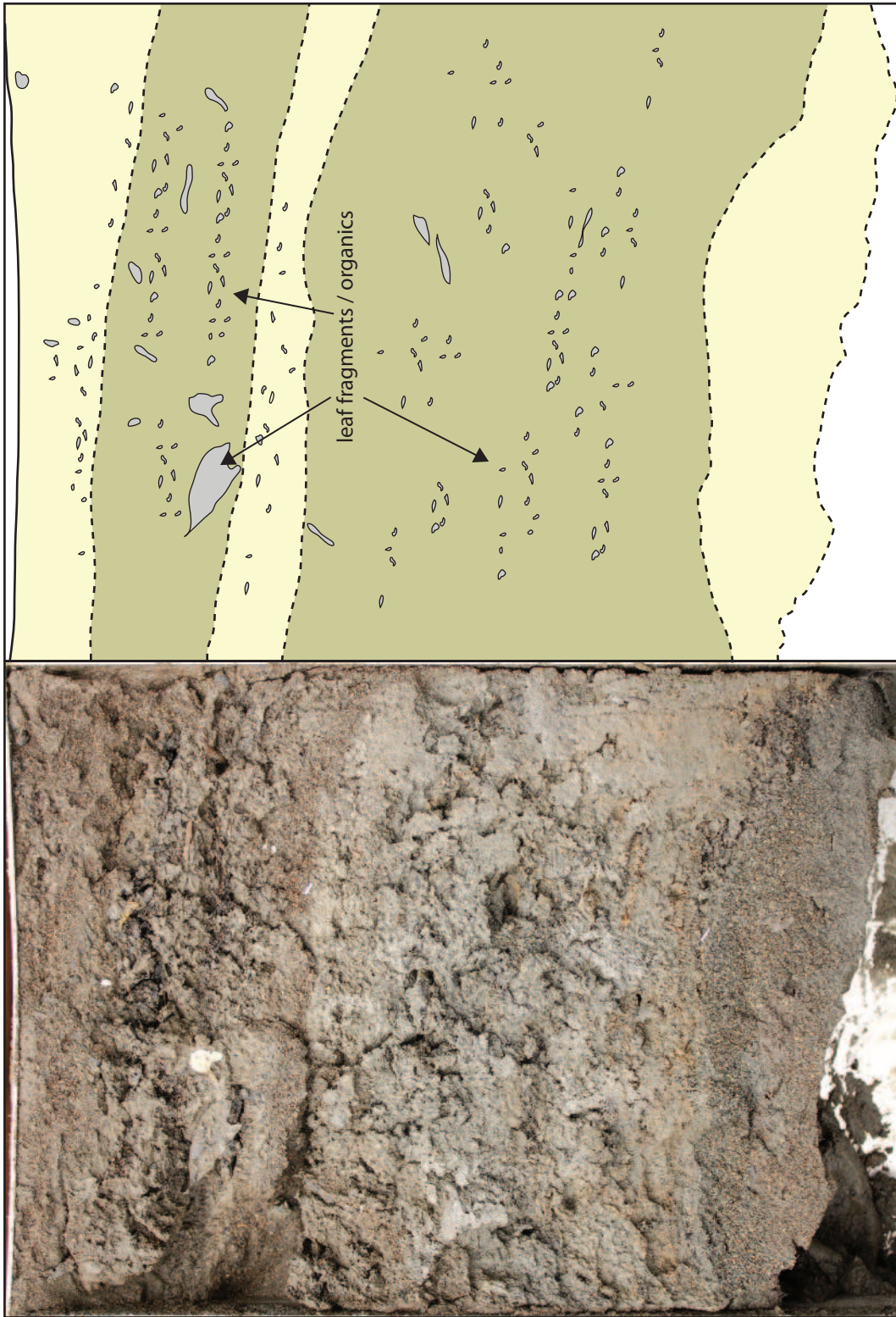


Figure A-17. Sub-surface sedimentary features observed in tidal creek facies Zone 3. Photo (left) and drawing (right) showing cross-sectional view of interbedded sand (beige colored layer in drawing) and muddy sand (darker beige-green colored layer in drawing) layers with organic debris. The photo and drawing are each 18cm across.



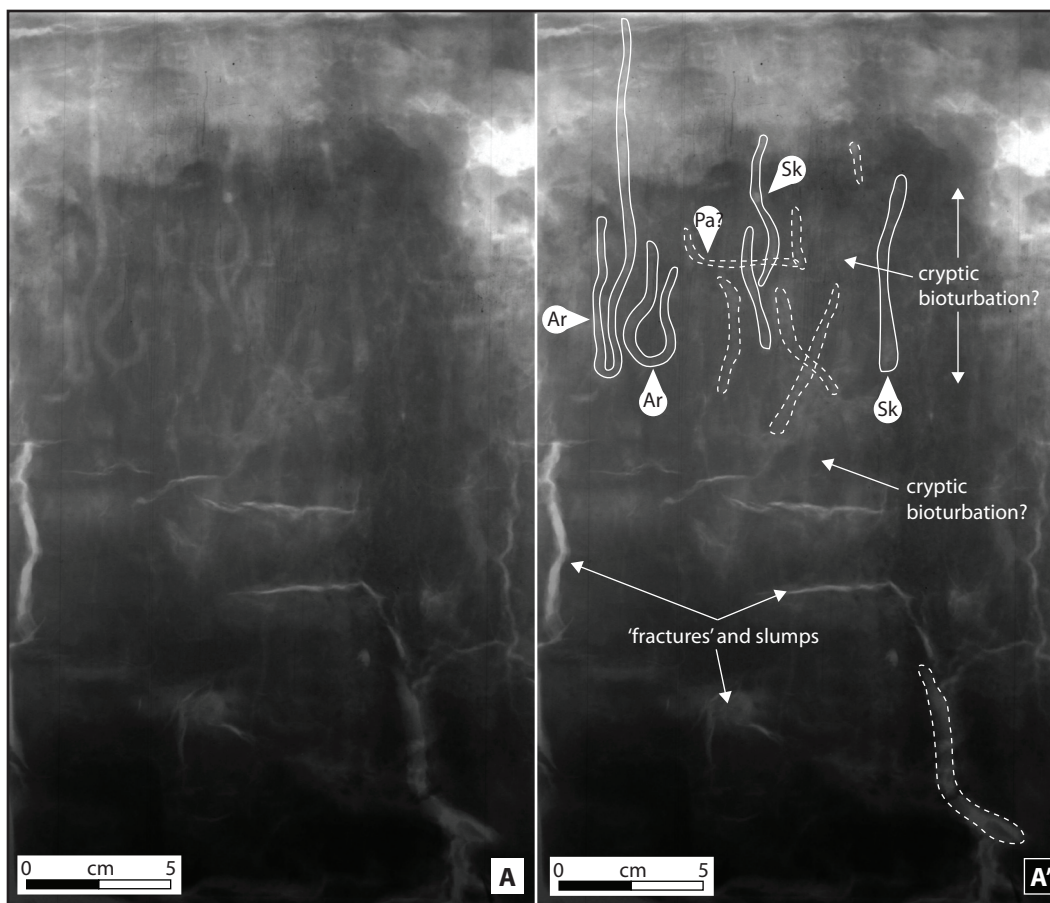


Figure A-18. X-ray image of boxcored tidal creek sediments, Zone 3. (A) Raw X-ray image of boxcore sediment with traces and sediment fractures or slumps appearing in the lighter colored areas of the image. (A') Interpreted X-ray image where *Arenicolites*-like (Ar) and *Skolithos*-like (Sk) burrows were observed with possible *Palaeophycus*-like (Pa) burrows and possible cryptic bioturbation.

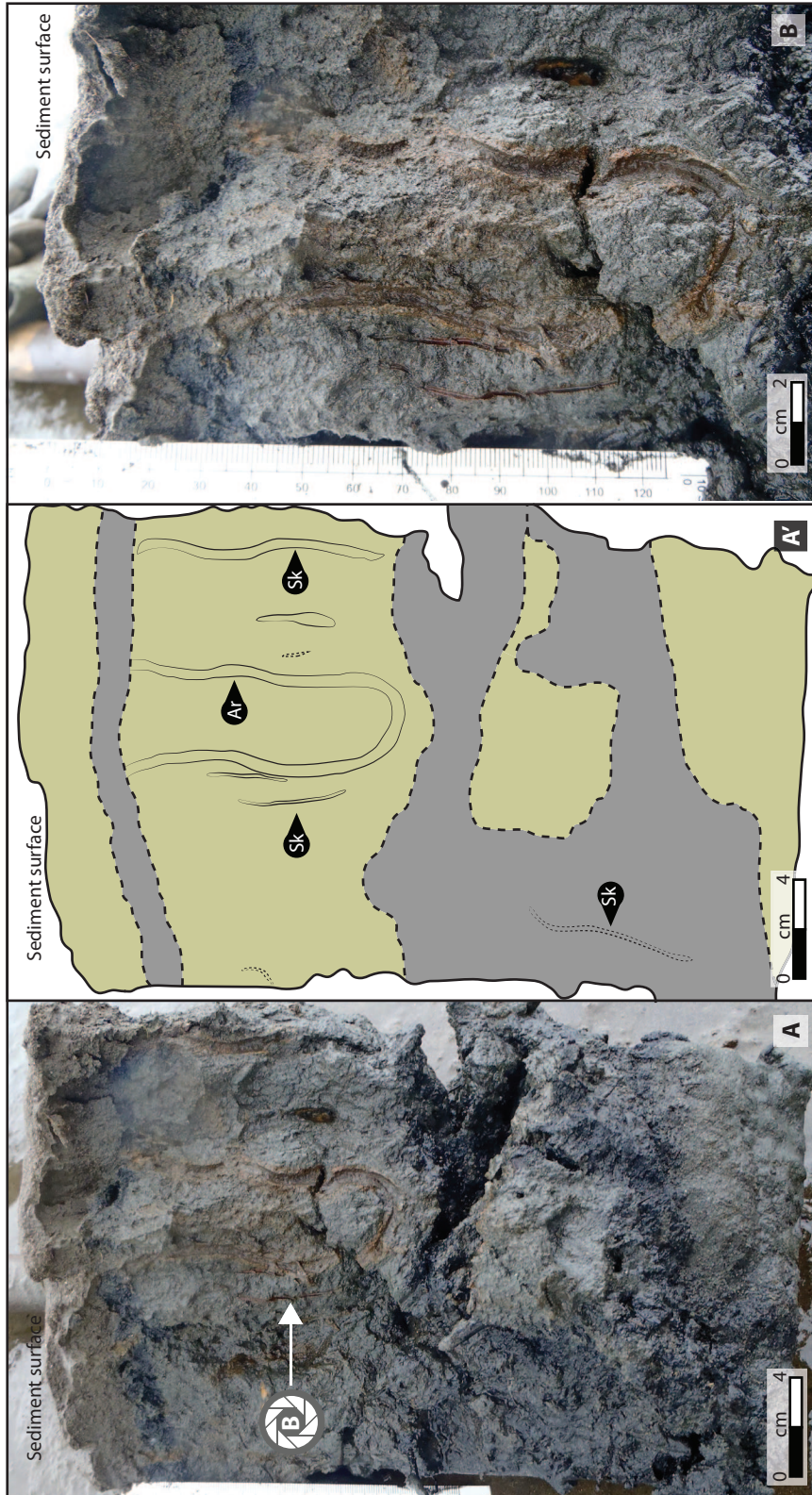


Figure A-19. Sub-surface trace features in muddy sand and organic rich mud, Zone 3. (A and A') Cross-sectional photo (A) and drawing (A') of mixed muddy sand (darker beige-green colored layers in A) and organic rich mud (grey colored layer in A') displaying slightly lined *Skolithos*-like (Sk), and *Arenicolites*-like (Ar) burrows. (B) Close up cross-sectional view of relatively large, slightly lined *Arenicolites*-like burrow with adjacent smaller, lined *Skolithos*-like burrows.

Figure A-20. Sub-surface trace features in muddy sand, Zone 3. (A and A') Cross-sectional photo (A) and drawing (A') of muddy sand displaying *Skolithos*-like (Sk), *Thalassinoides*-like (Th) and possible *Palaeophycus*-like (Pa) burrows. (B) Close up cross-sectional view of *Skolithos*-like (Sk) and *Thalassinoides*-like (Th) traces with *Nereis* sp. worm in a *Palaeophycus*-like (Pa) trace.

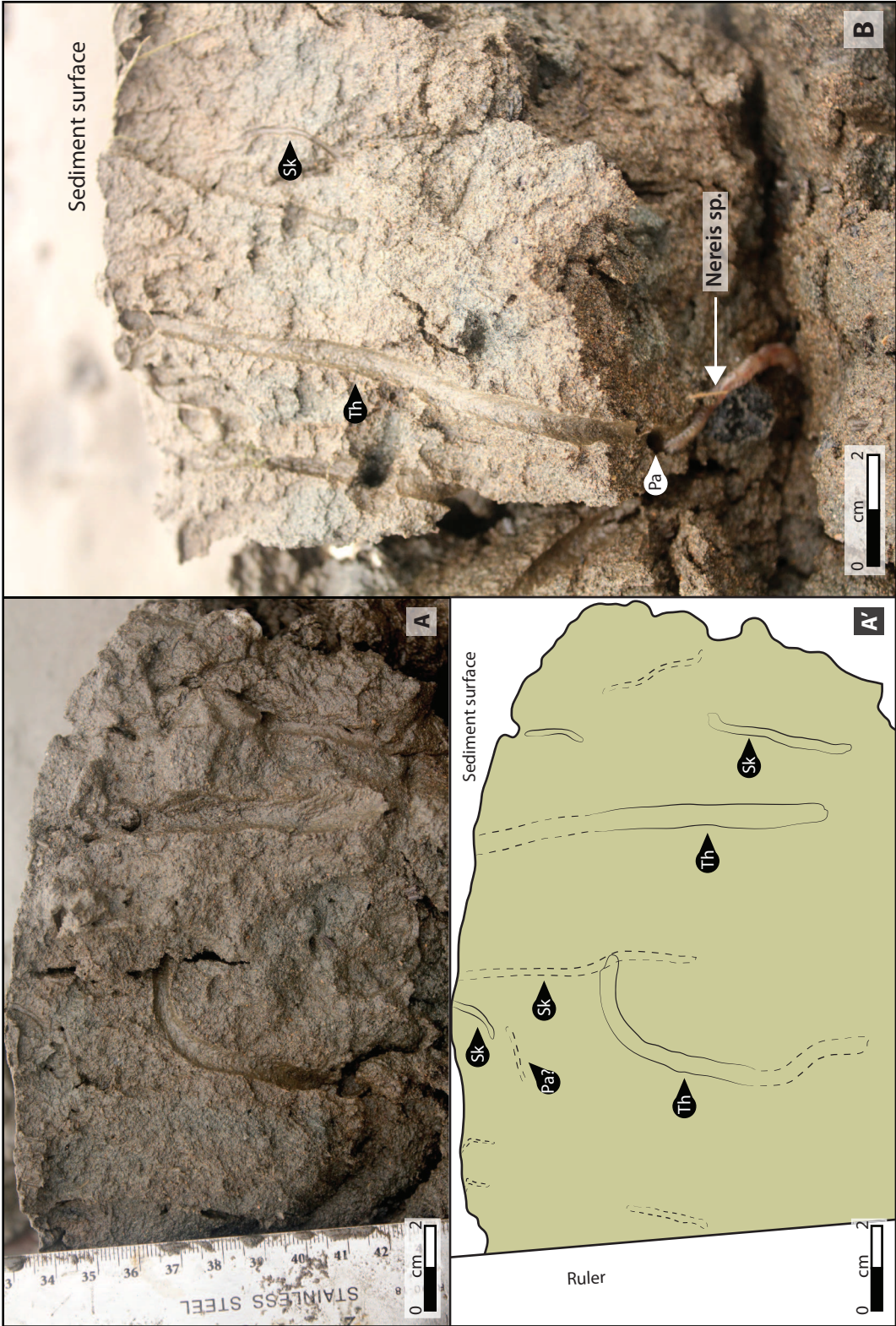


Figure A-21. Sedimentary features and traces observed in muddy central bar sediments, Zone 3. (A) Overview of tidal flat displaying a relatively planar muddy sand surface marked by multiple burrow openings and patches of macroalgae and eelgrass. Shovel for scale is 1m in length. (B) Close up view of large (>1cm in diameter) burrow openings and small (<1cm in diameter) burrow openings. The large burrow openings in this photo are likely the result of bivalve siphons. (C) Unlined to faintly lined *Arenicolites*-like (Ar) burrow observed in the subsurface. Note that other small indeterminate traces are also present, with a large wood clast also observed, as seen near the bottom of the photo.

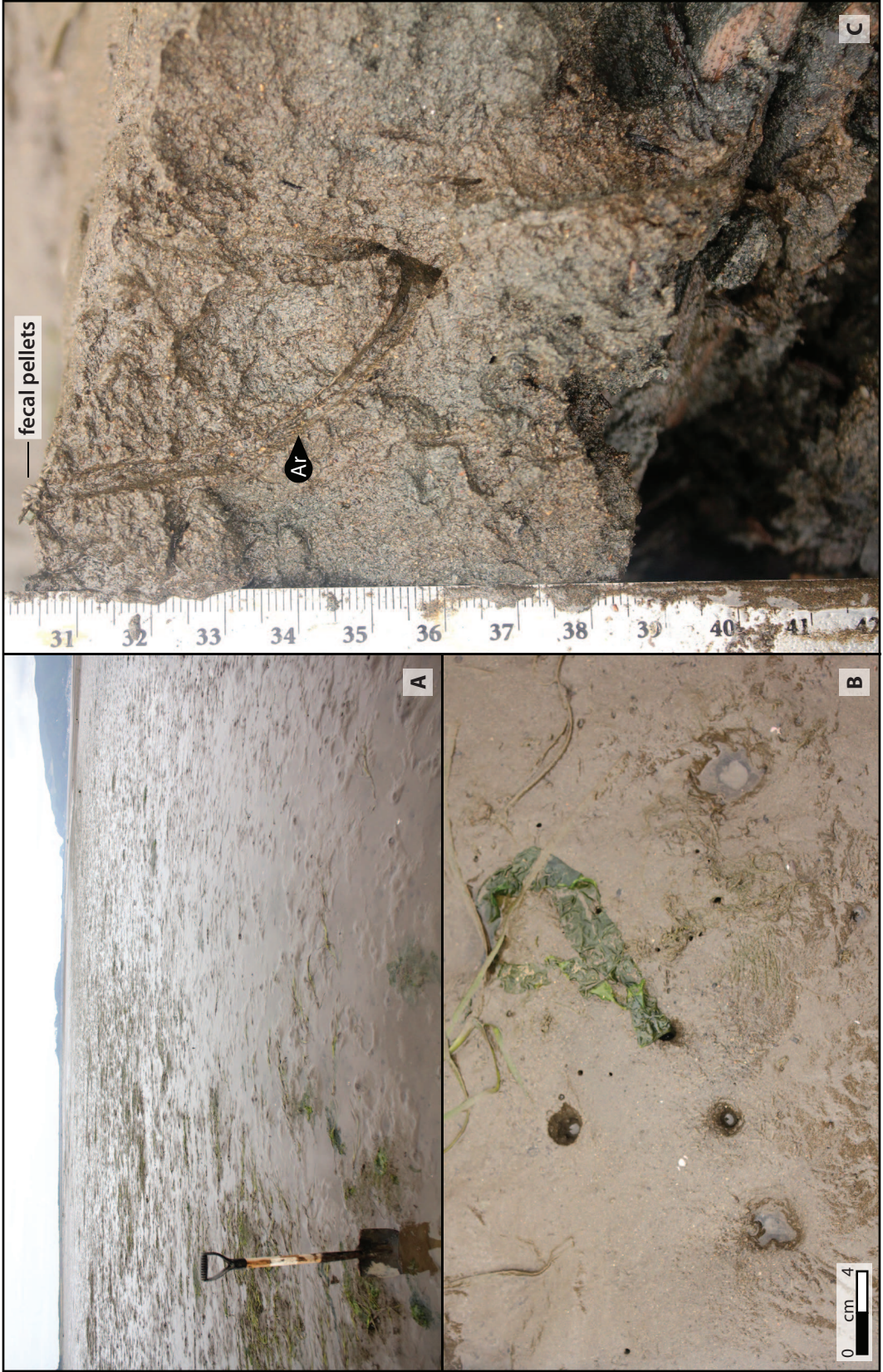
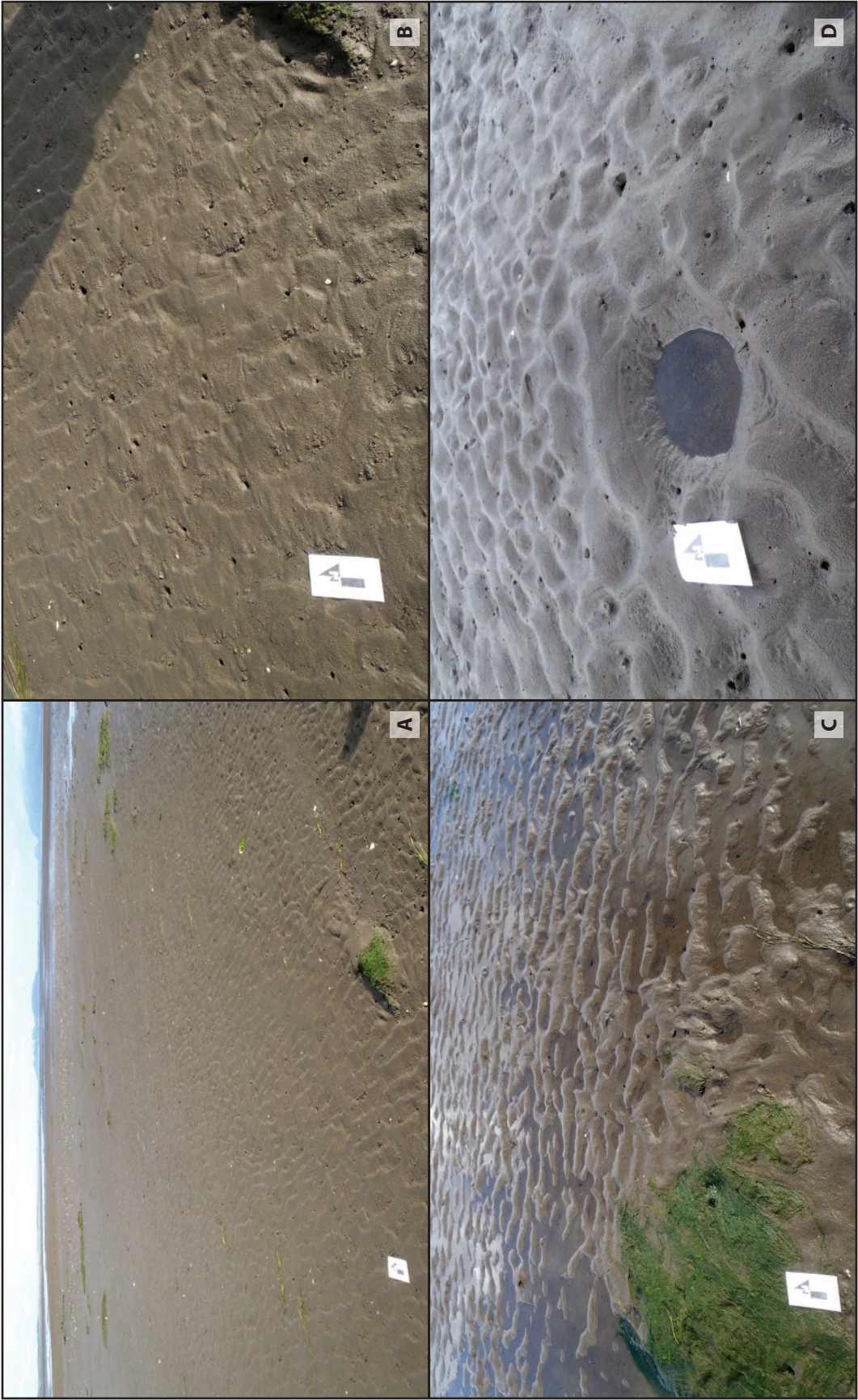


Figure A-22. Surface texture and traces, distal Zone 3. Scale card in photos is 15cm long. (A) Over-view of sediment displaying dominantly current generated, sinuous crested ripples. (B) Close up view of ripples seen in A. (C) Combined flow (wave and current generated) ripples and mound stabilized by macroalgae. (D) *Piscichnus*-like trace potentially created by feeding fish.



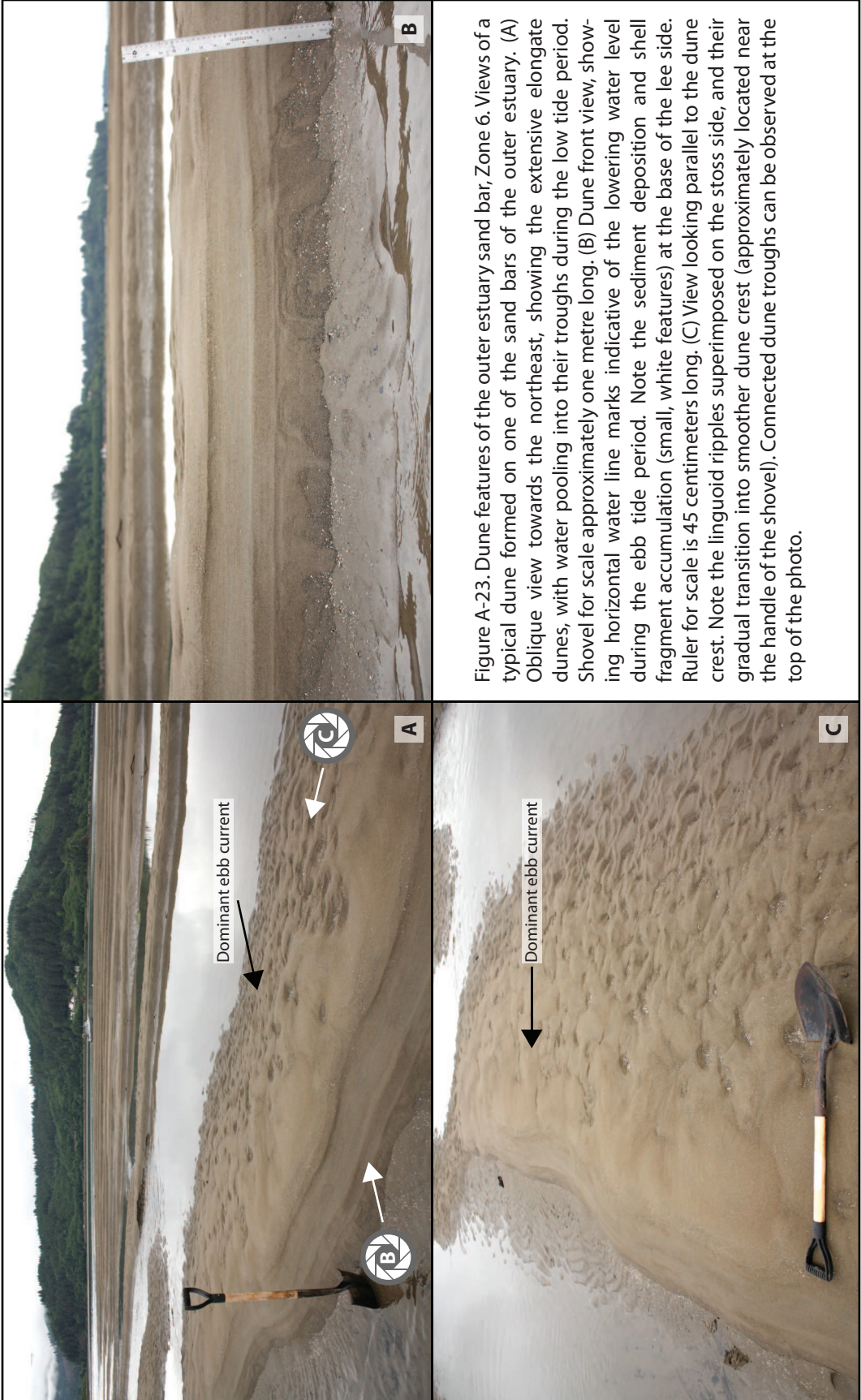
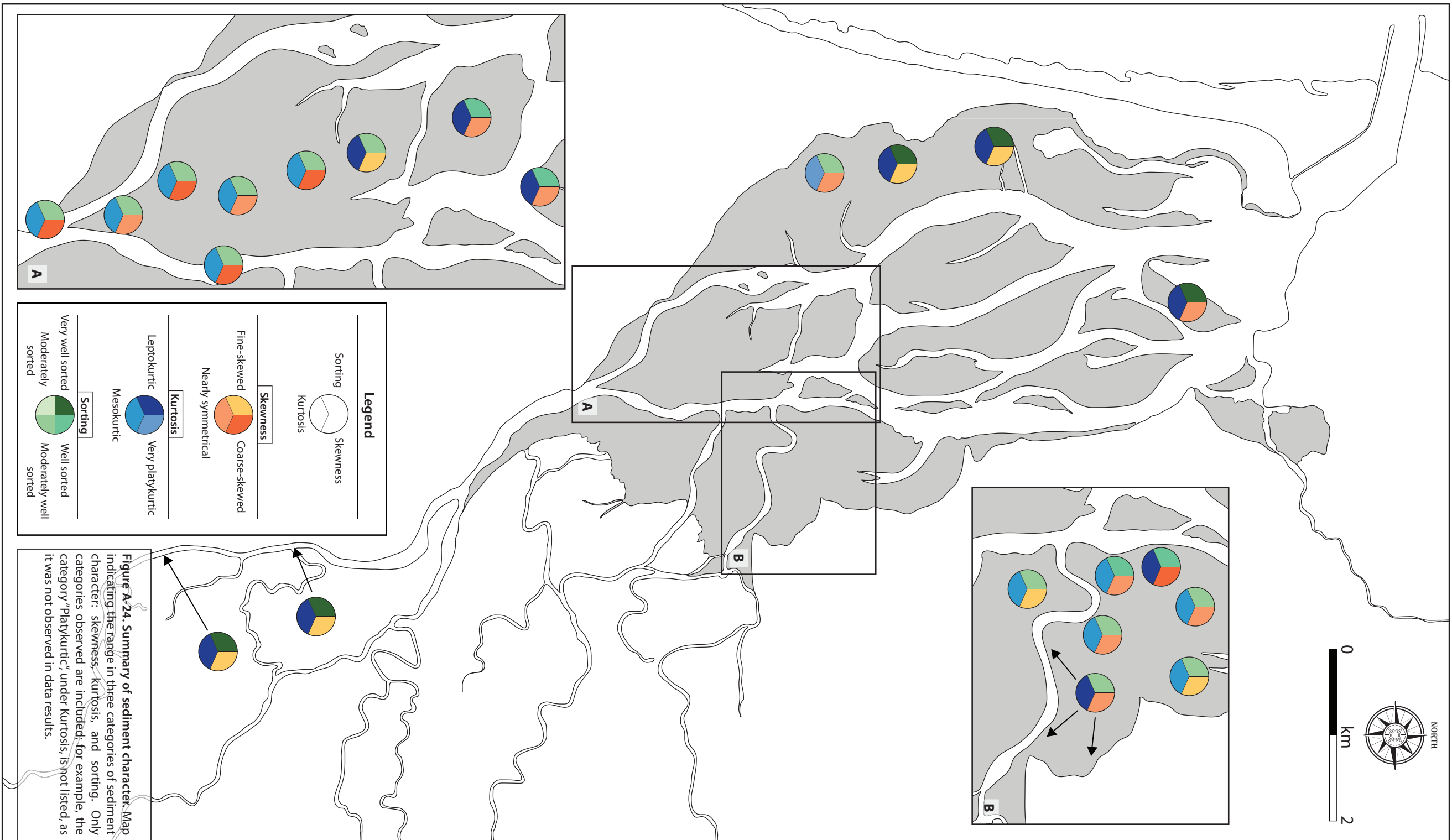
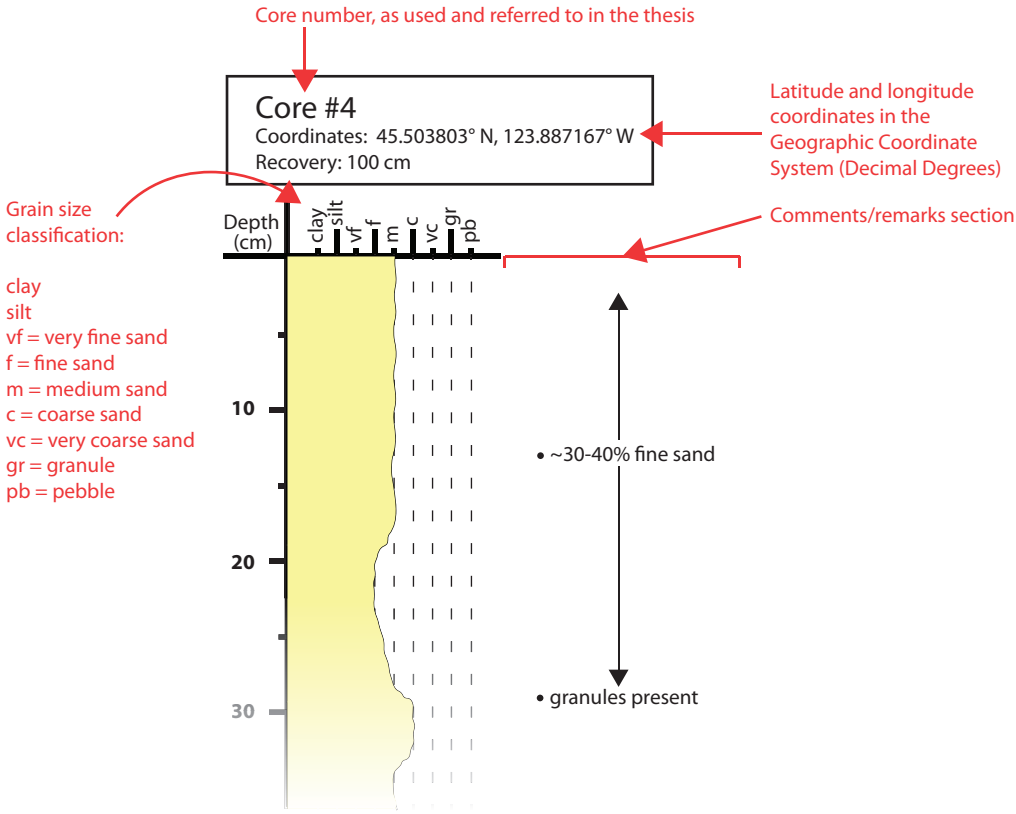


Figure A-23. Dune features of the outer estuary sand bar, Zone 6. Views of a typical dune formed on one of the sand bars of the outer estuary. (A) Oblique view towards the northeast, showing the extensive elongate dunes, with water pooling into their troughs during the low tide period. Shovel for scale approximately one metre long. (B) Dune front view, showing horizontal water line marks indicative of the lowering water level during the ebb tide period. Note the sediment deposition and shell fragment accumulation (small, white features) at the base of the lee side. Ruler for scale is 45 centimeters long. (C) View looking parallel to the dune crest. Note the linguoid ripples superimposed on the stoss side, and their gradual transition into smoother dune crest (approximately located near the handle of the shovel). Connected dune troughs can be observed at the top of the photo.



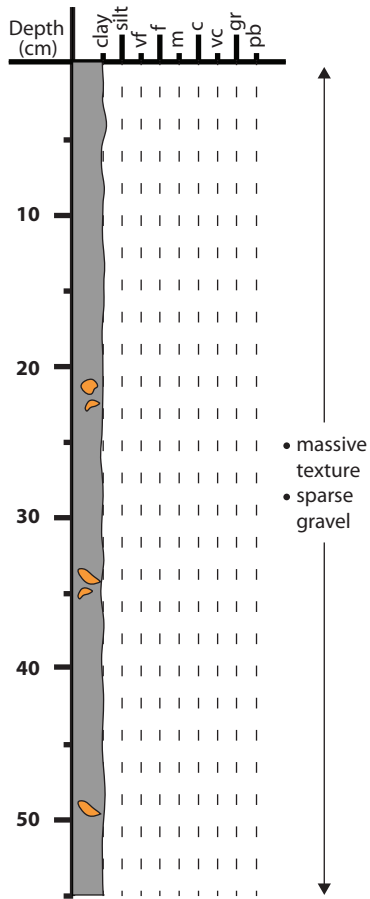
Appendix B Sediment Logs

Appendix B contains the complete sediment logs (including comments and remarks) of the 32 cores examined in this study. An explanation of the log set-up is provided below. For a map showing the location of each core, refer to Figure 1-9, Chapter 1.



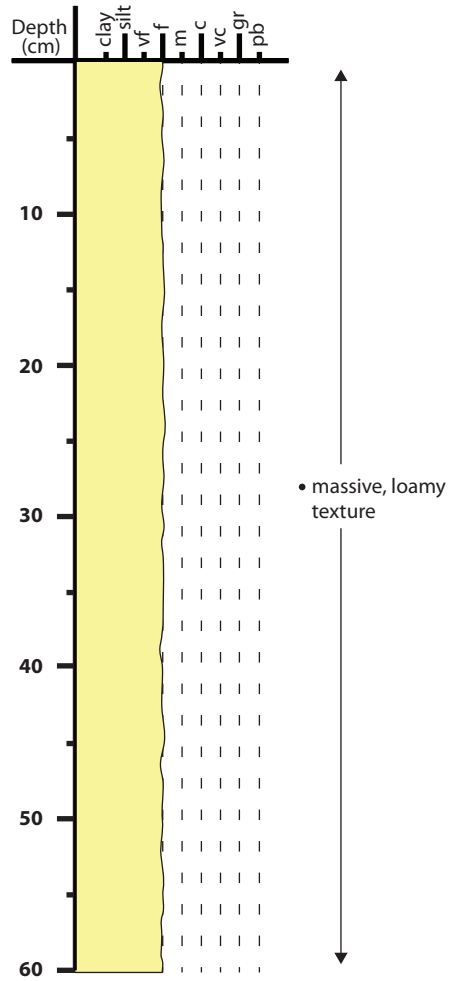
Core #1

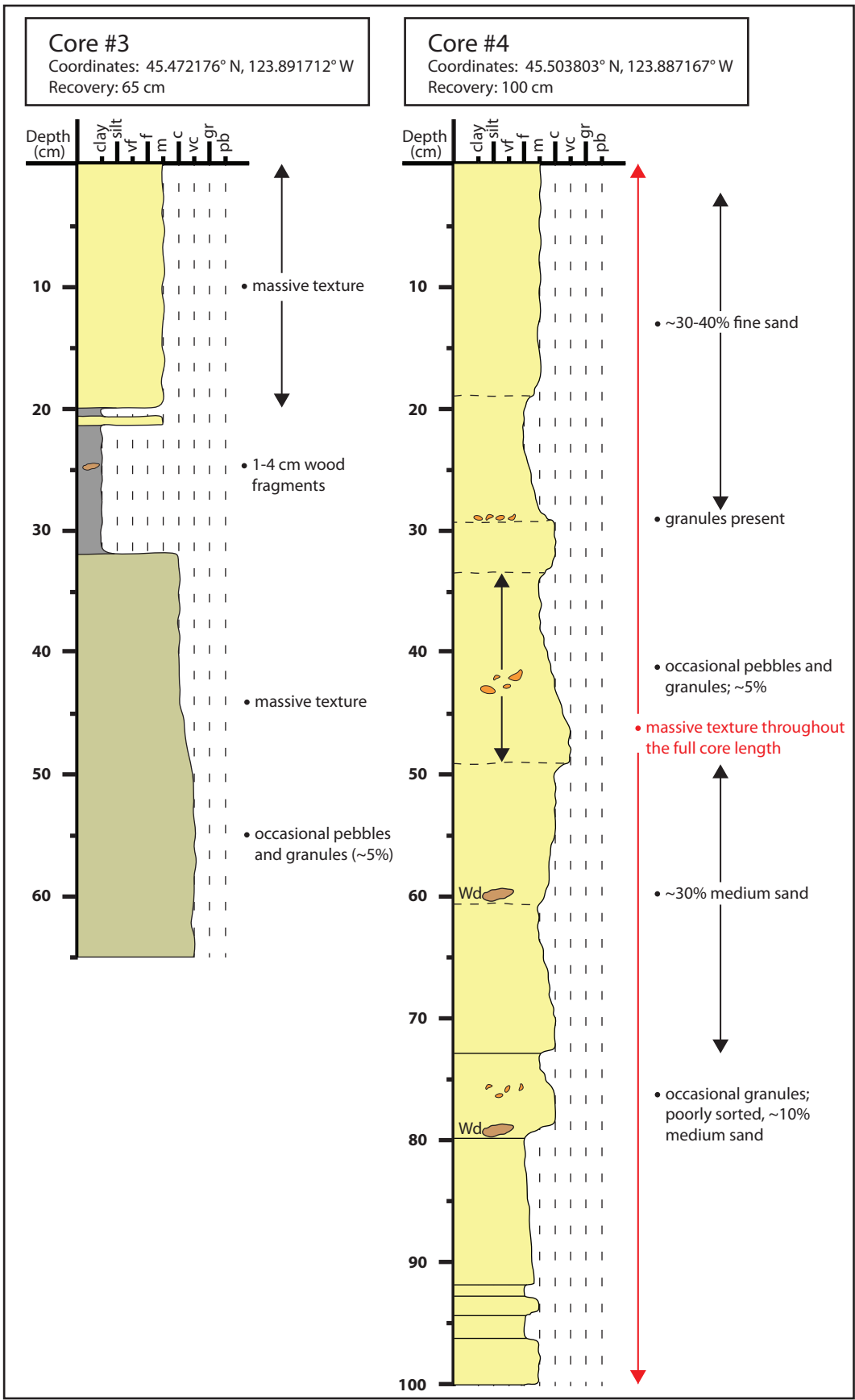
Coordinates: 45.430240° N, 123.844950° W
Recovery: 55 cm



Core #2

Coordinates: 45.453048° N, 123.877763° W
Recovery: 60 cm

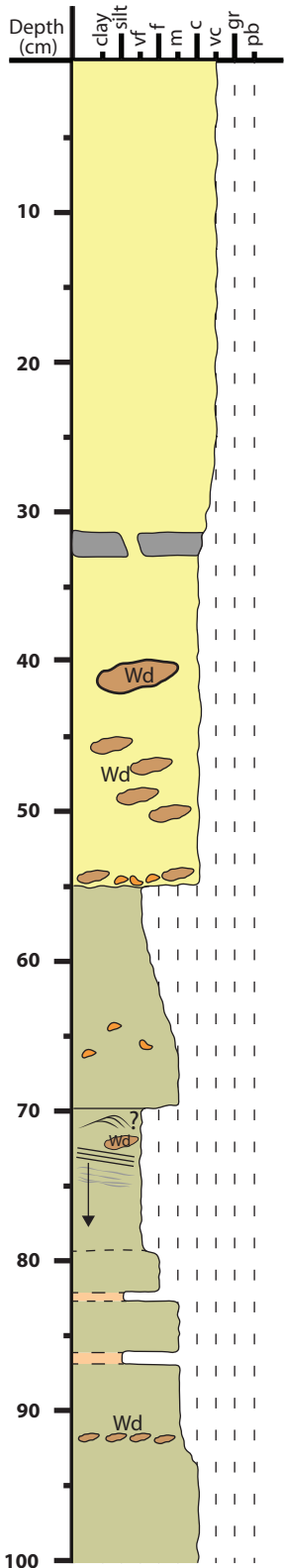




Core #5

Coordinates: 45.503240° N, 123.892710° W

Recovery: 120 cm



- moderately sorted; ~30-40% coarse, medium and fine sand
- massive texture

- slightly inclined, vertical sand-infilled structure; possible burrow or mud rip-up clasts contained within the sand layer

- abundant wood fragments; ~20-25% v. coarse sand and granules

- wood fragments and granule lag, ~4 cm thick; erosional contact
- ~20%

- increasing clay content <5%
- ~10-15% v. coarse sand and granules; occasional pebbles

- light brown layer, clay-rich, abundant wood

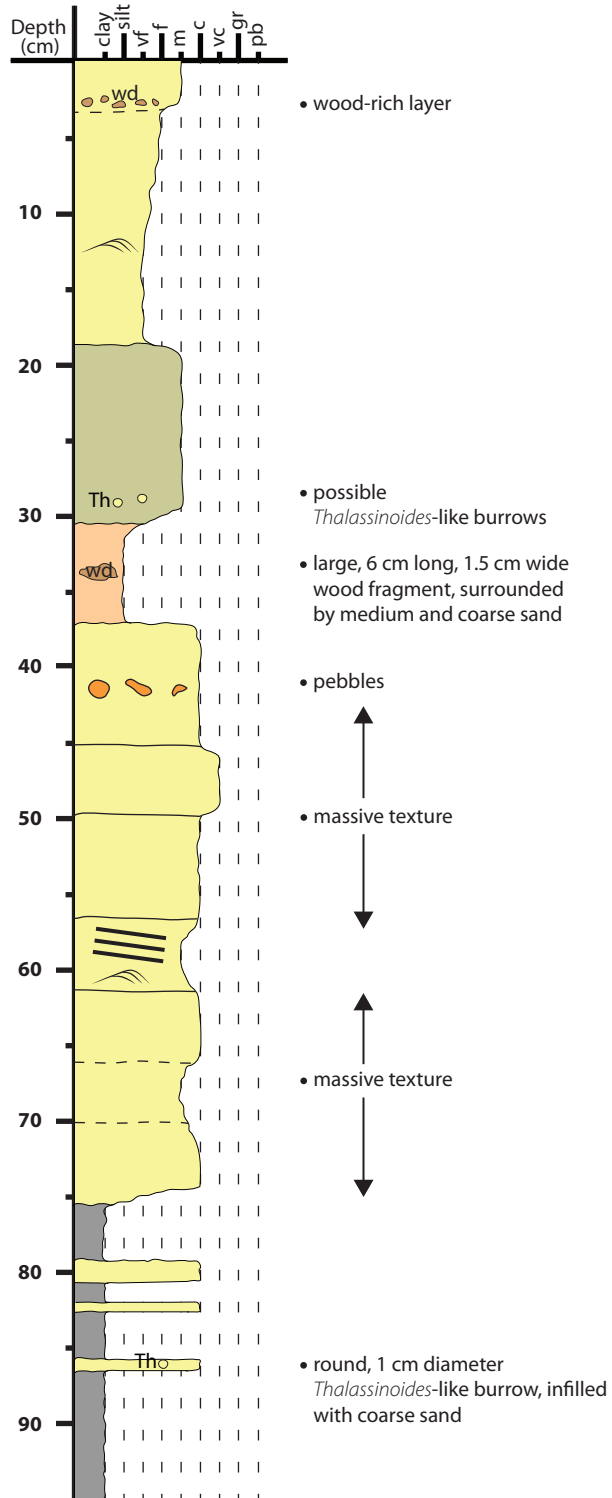
- contacts appear gradual, not clearly defined

- massive texture

- ~30% v. coarse sand
- massive texture

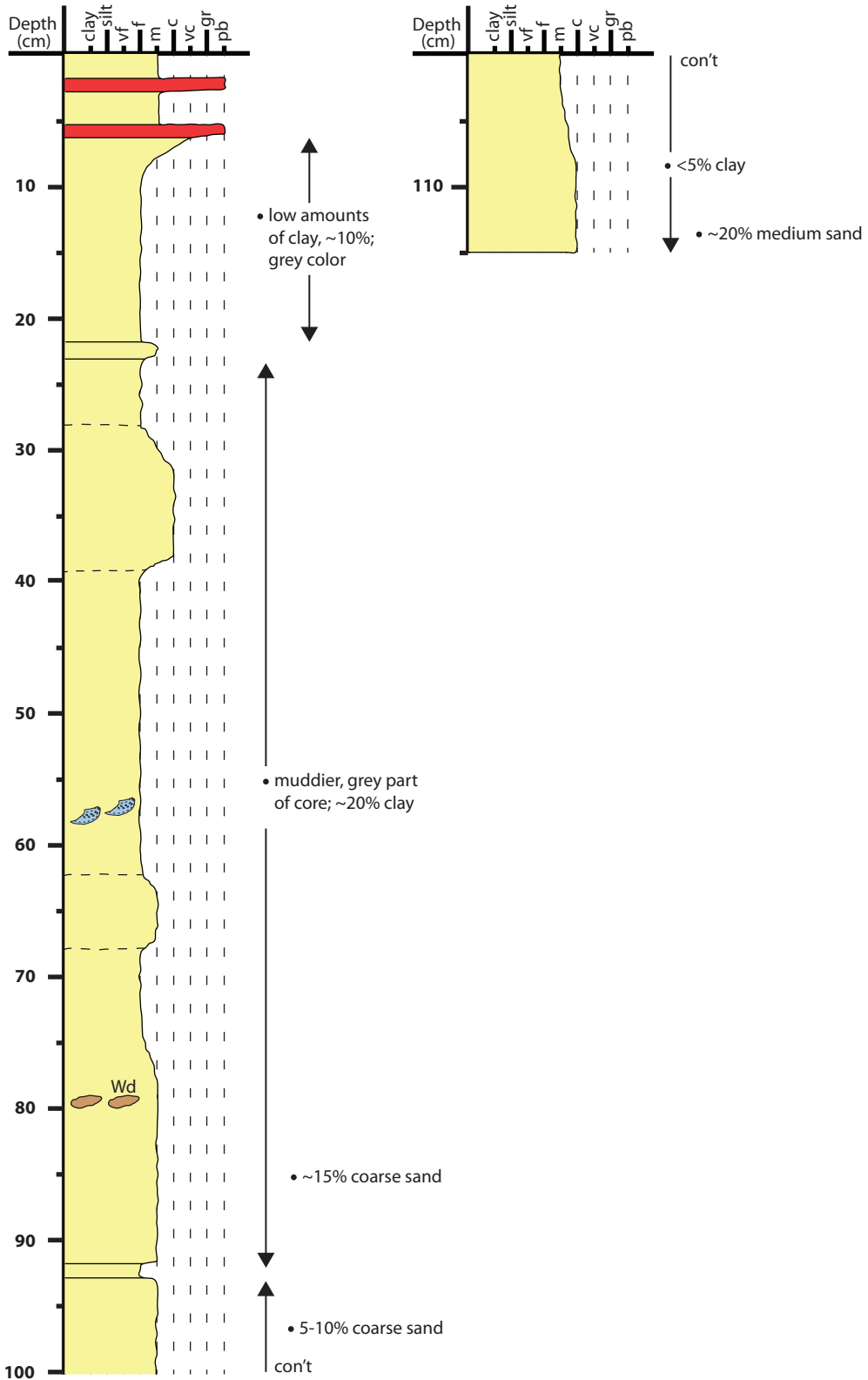
Core #6

Coordinates: 45.504510° N, 123.897530° W
Recovery: 95 cm



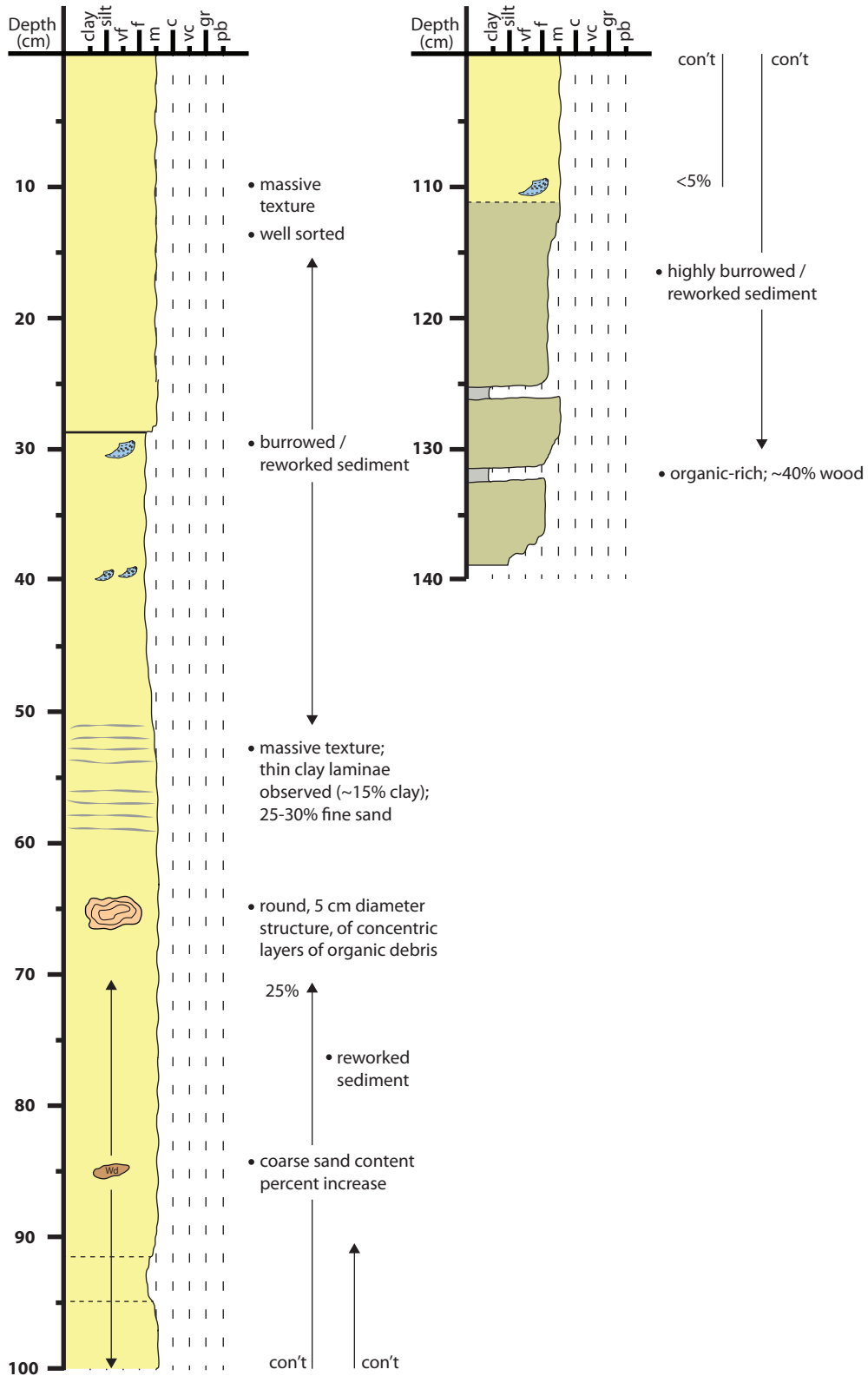
Core #7

Coordinates: 45.499590° N, 123.898200° W
Recovery: 115 cm



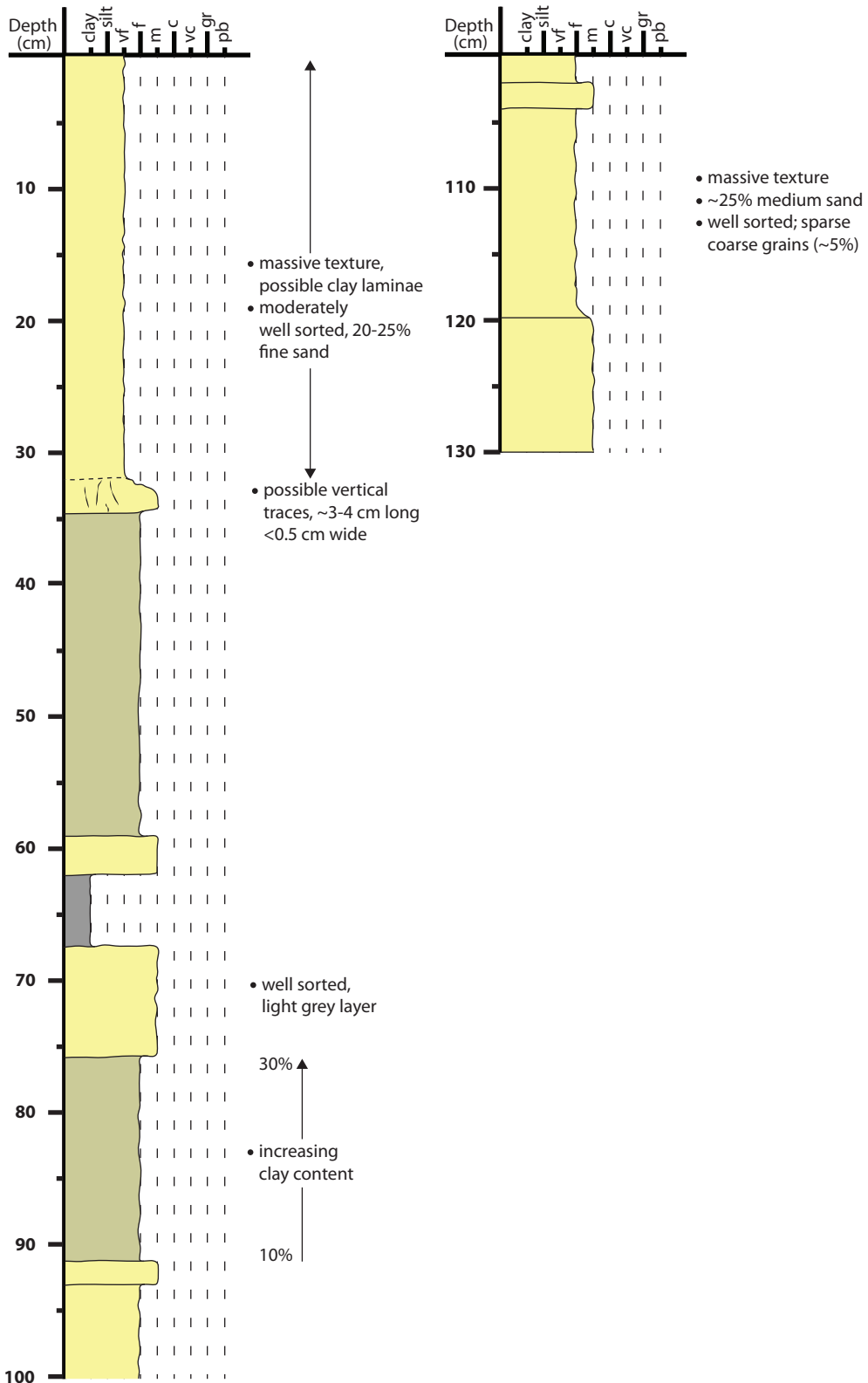
Core #8

Coordinates: 45.487110° N, 123.904549° W
 Recovery: 137 cm

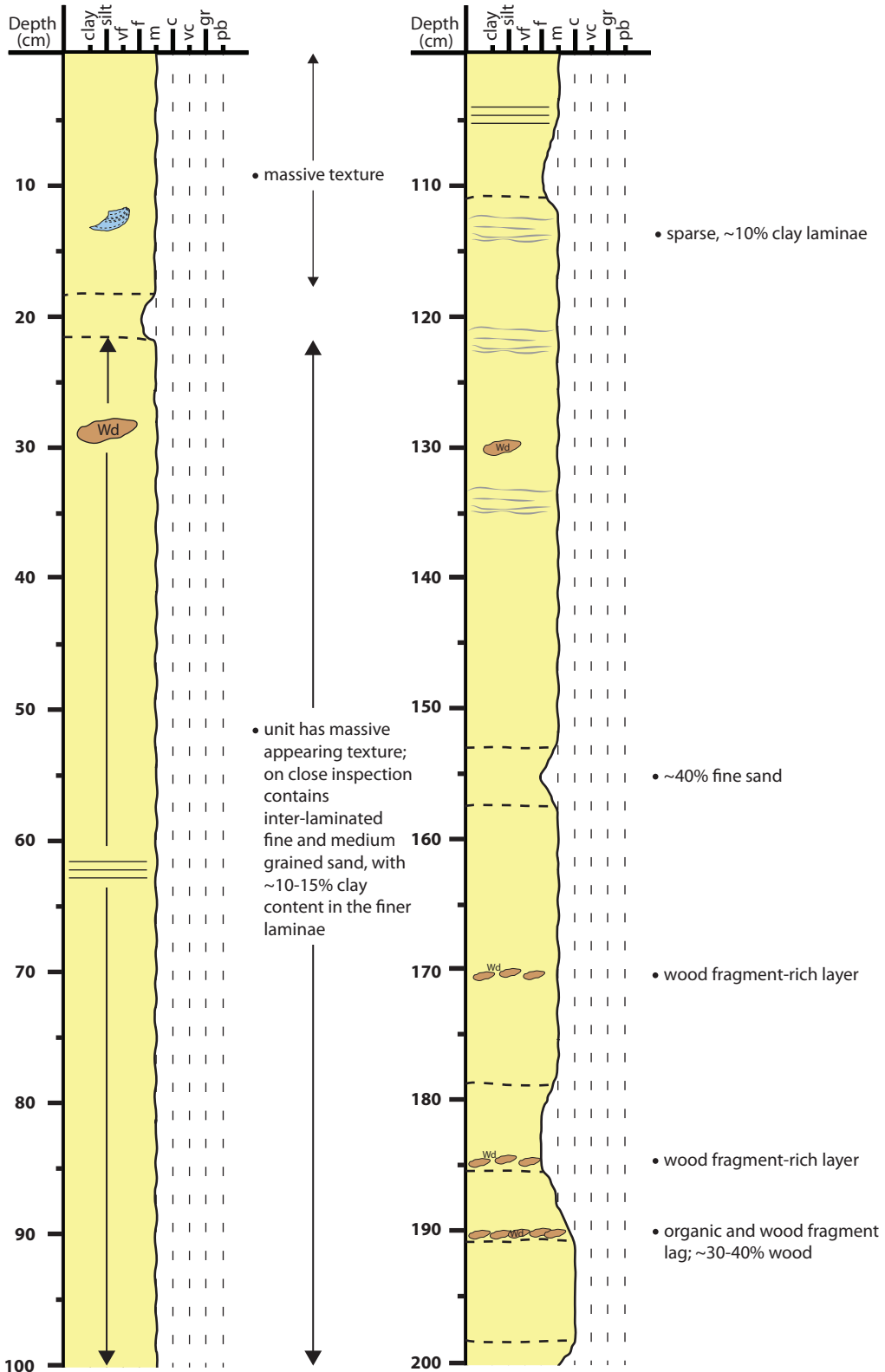


Core #9

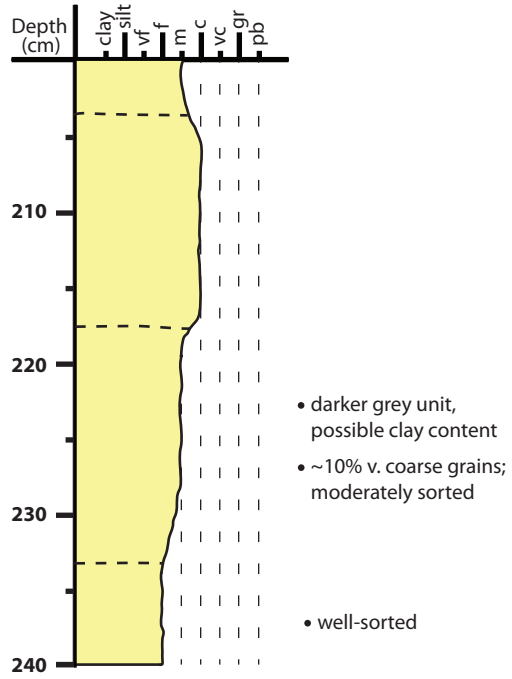
Coordinates: 45.490176° N, 123.909621° W
Recovery: 130 cm

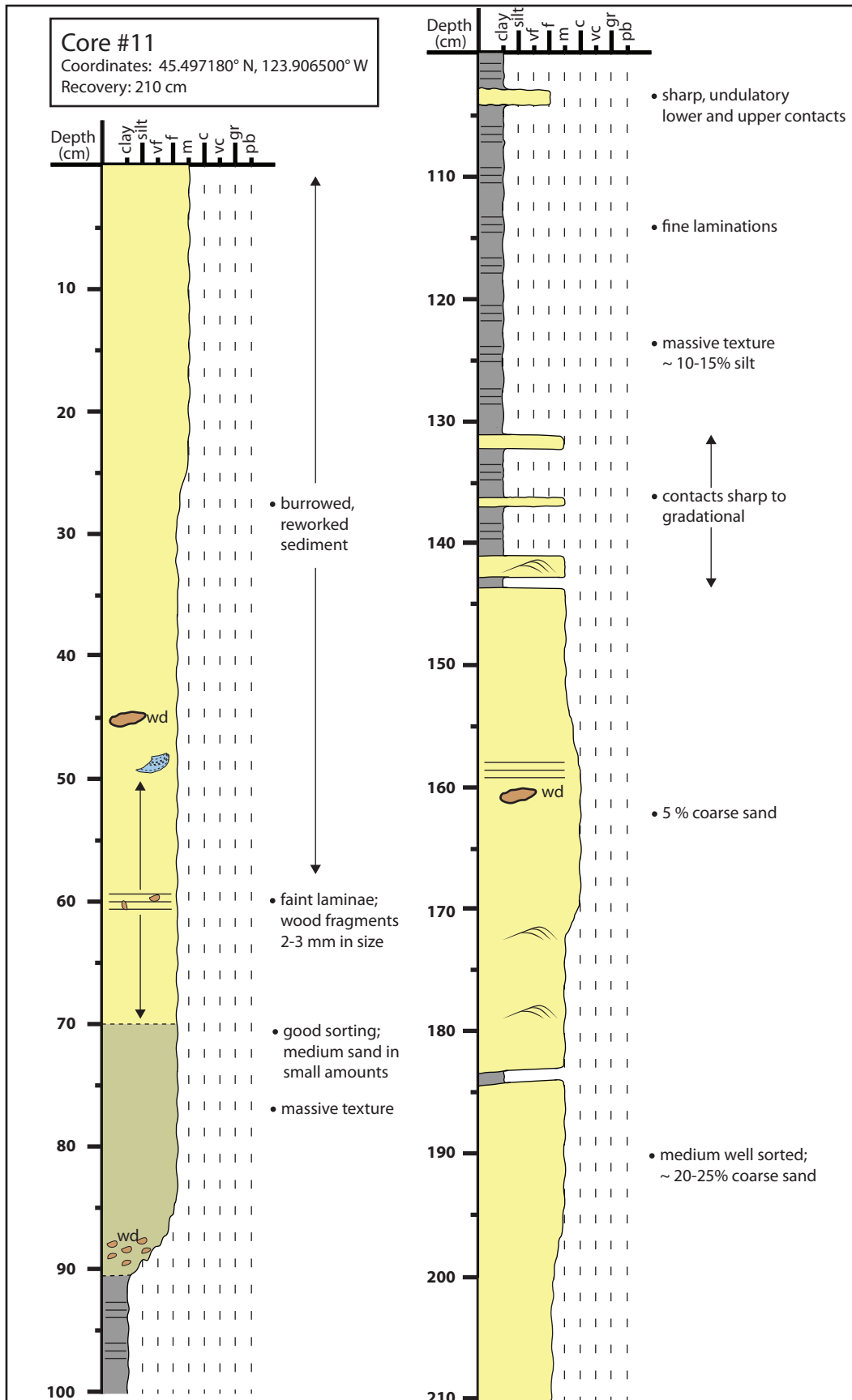


Core #10 (page 1 of 2)
 Coordinates: 45.494450° N, 123.909930° W
 Recovery: 240 cm



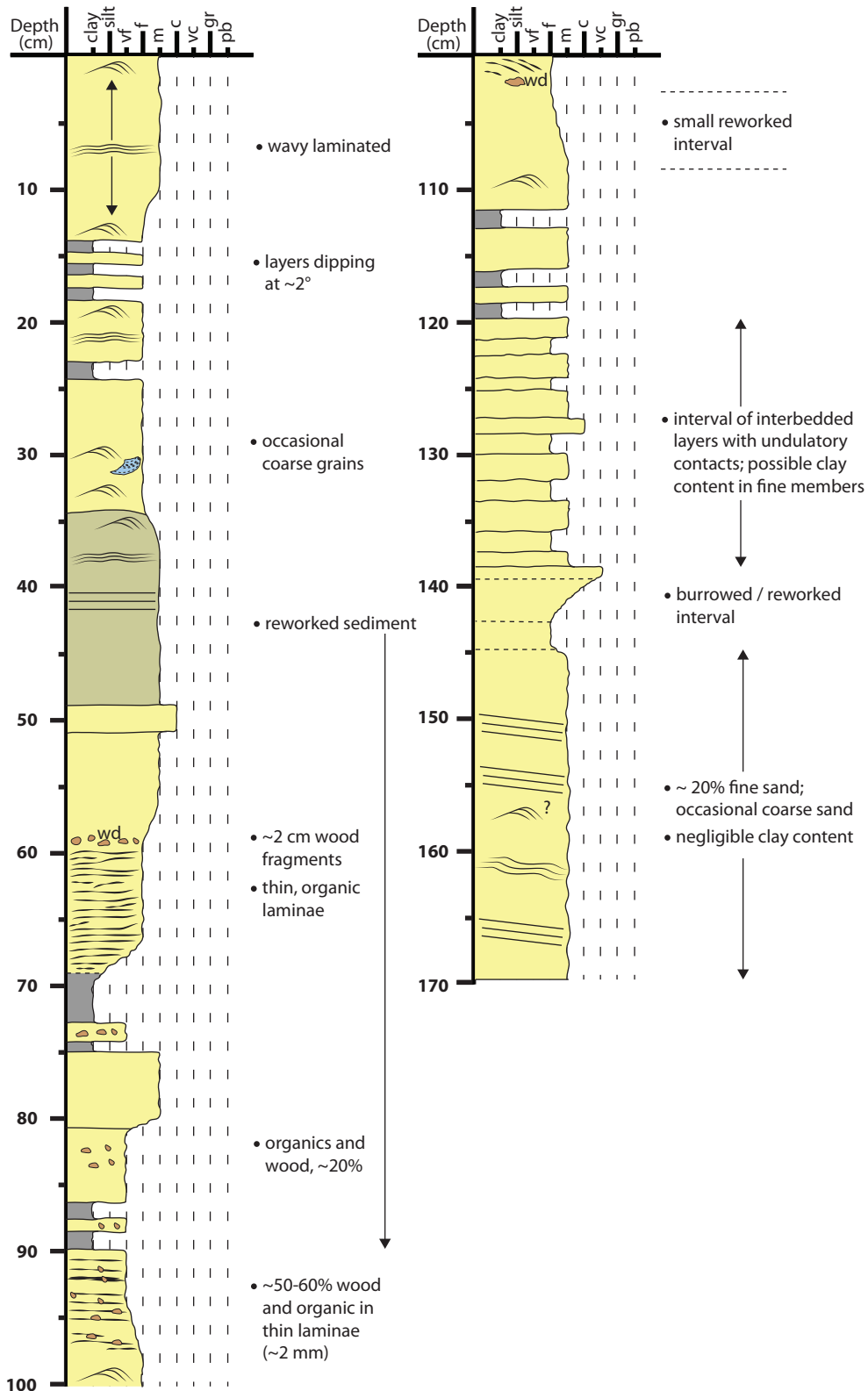
Core #10 (page 2 of 2)
Coordinates: 45.494450° N, 123.909930° W
Recovery: 240 cm





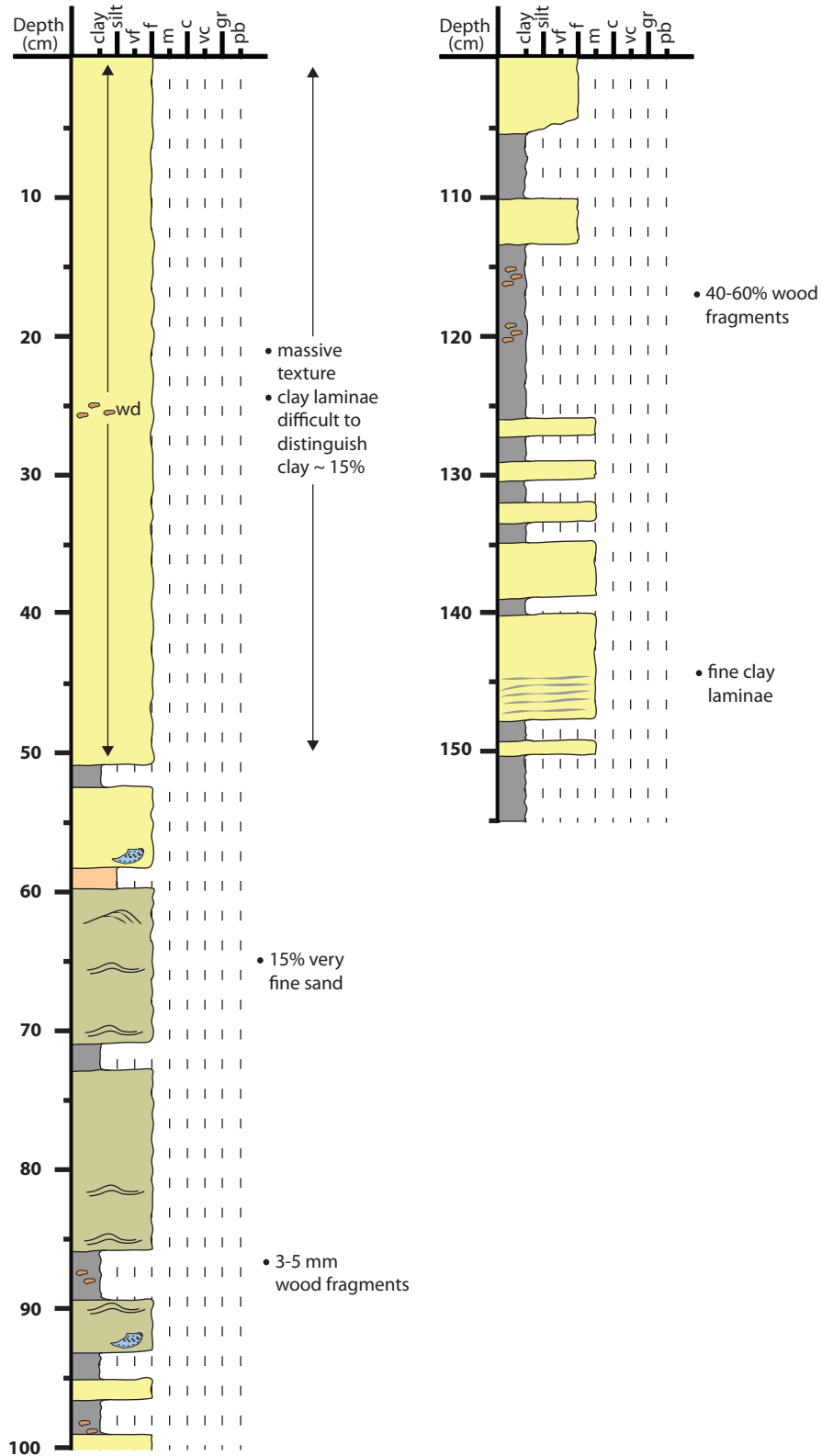
Core #12

Coordinates: 45.499550° N, -123.903690° W
 Recovery: 170 cm



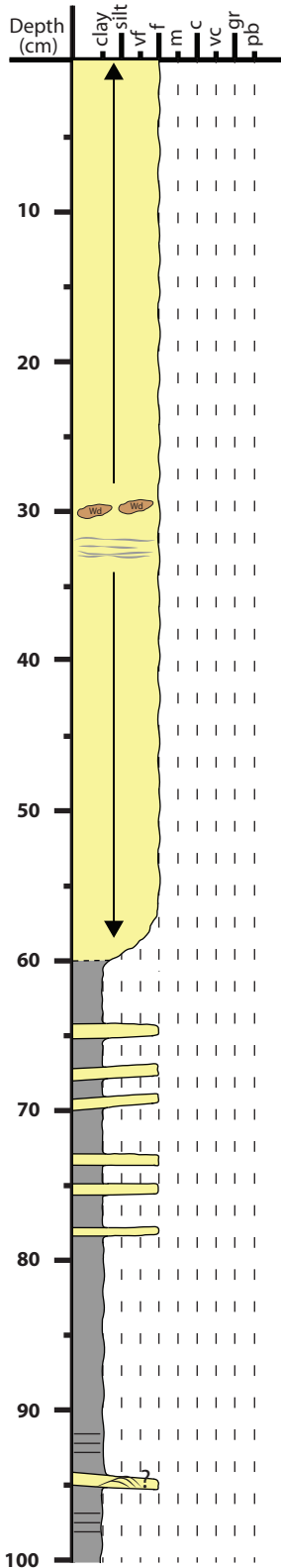
Core #13

Coordinates: 45.498150° N, 123.912390° W
Recovery: 155 cm

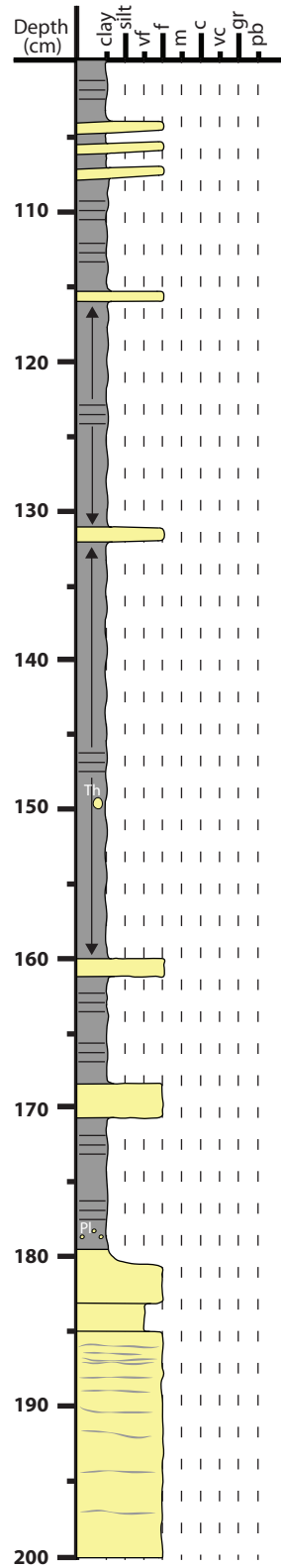


Core #14

Coordinates: 45.501820° N, 123.911220° W
Recovery: 200 cm



- 2-3 mm wood fragments common
- faint clay laminae ~1mm thick (~15-20%)
- highly-reworked interval; sed. structures obliterated



- layer with abundant wood fragments

- massive-appearing texture; contains ~15-20% fine sand
- possible round *Thalassinoides*-like sand-infilled burrow, 1 cm diameter

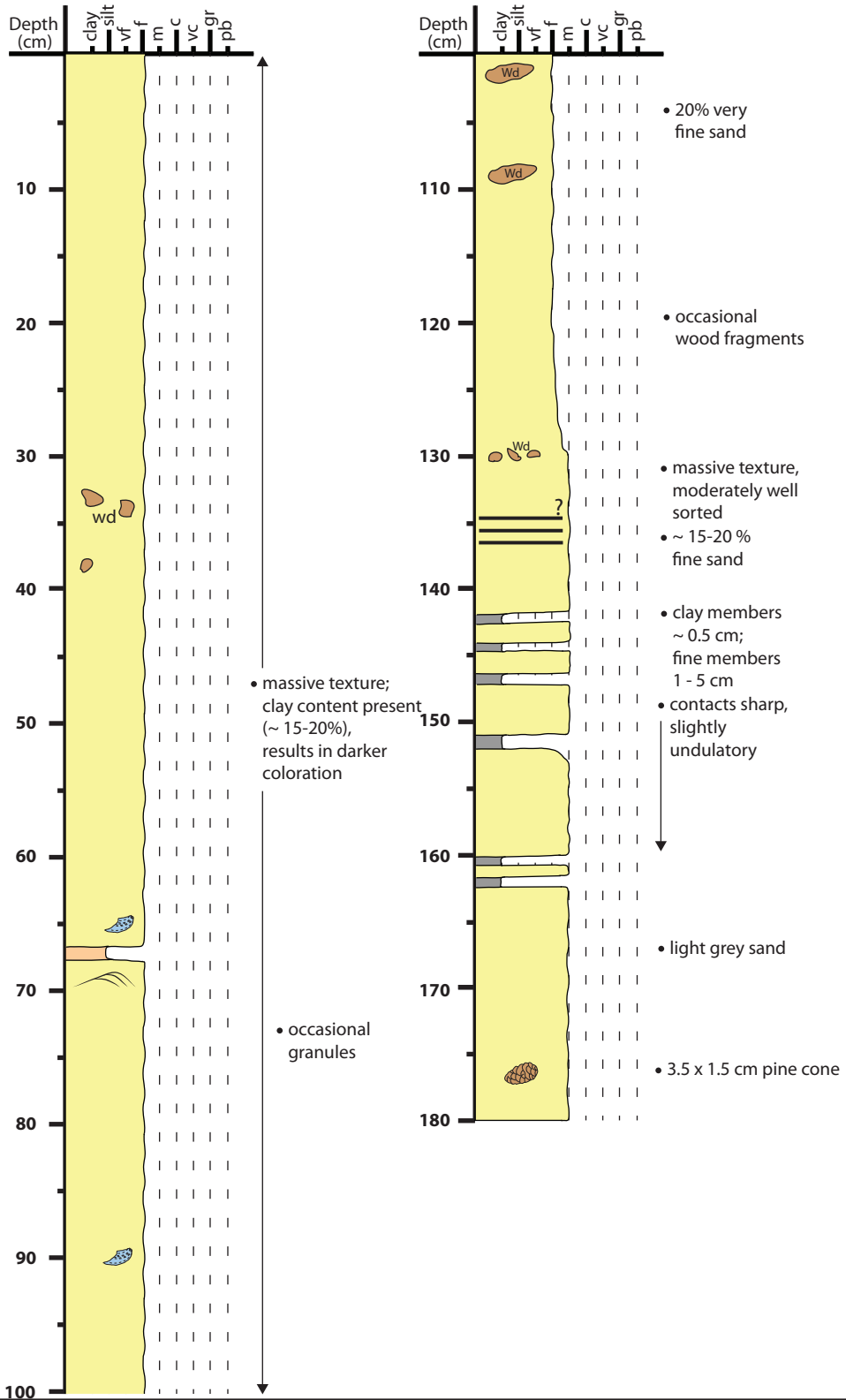
- massive-appearing texture; contains ~15-20% fine sand
- several *Planolites*-like burrows

- thin, 1-2 mm, clay laminae; increasing clay content

~15-20%

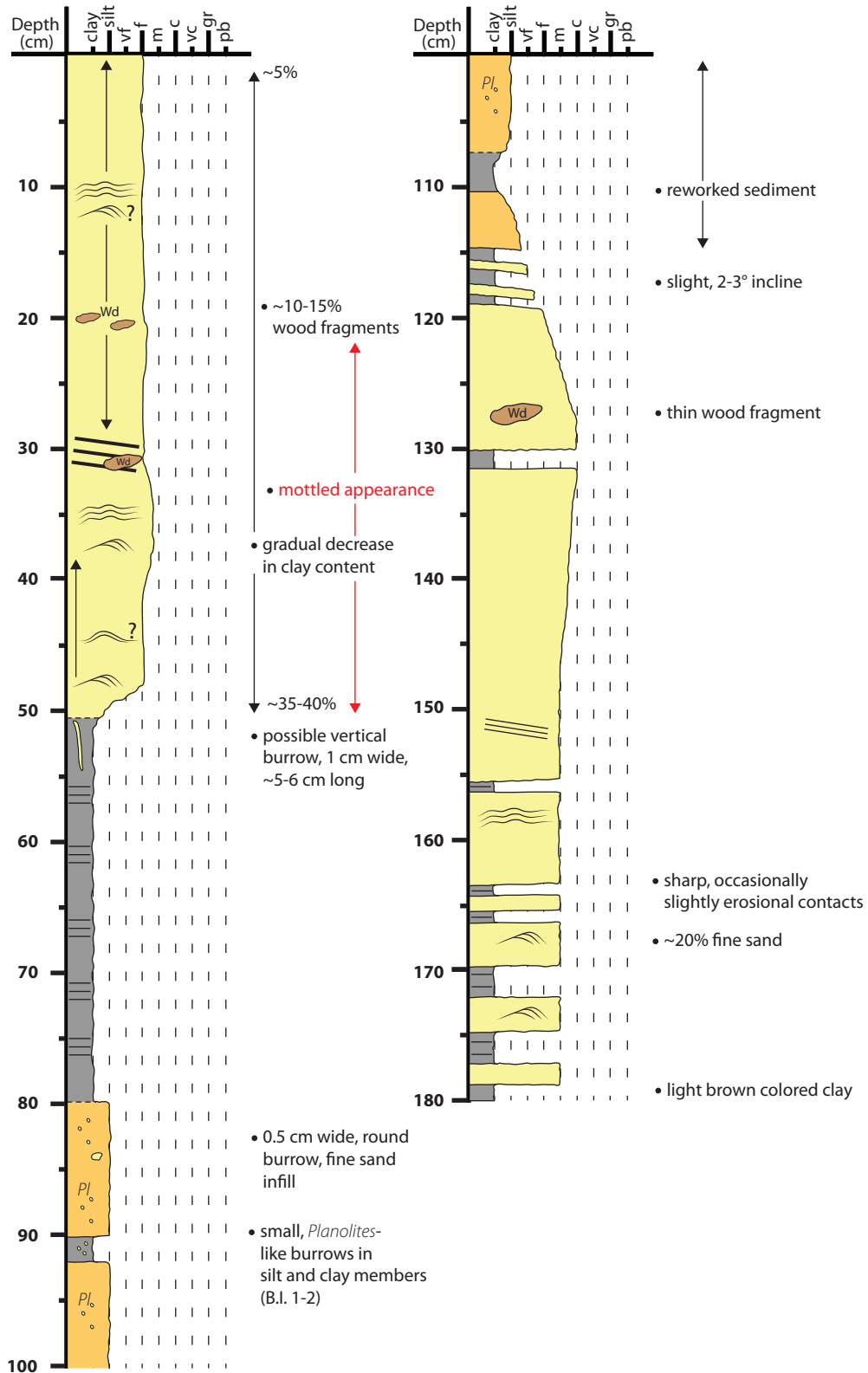
Core #15

Coordinates: 45.508450° N, 123.913600° W
 Recovery: 180 cm



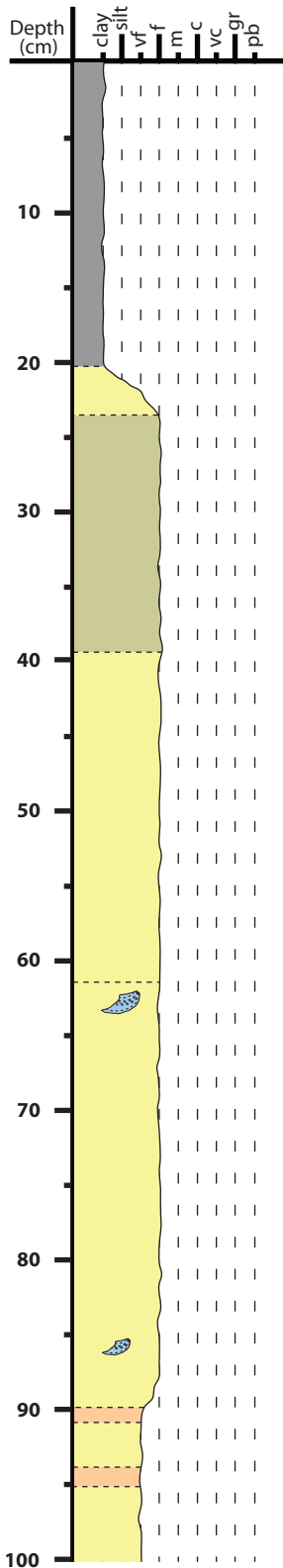
Core #16

Coordinates: 45.513420° N, 123.911470° W
 Recovery: 180 cm



Core #17

Coordinates: 45.506059° N, 123.938482° W
 Recovery: 170 cm



- massive texture, some fine laminae observed

- ~20-30% clay

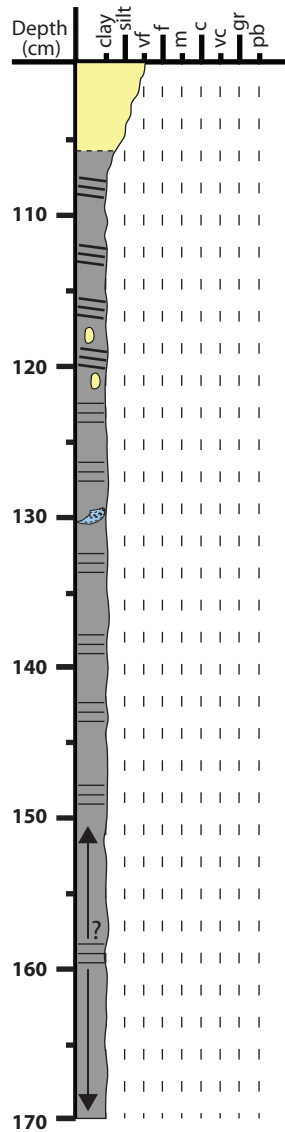
- ~20-30% clay

- appears finely laminated

- light grey color, silty

- light brown color, silty

con't



con't

- low angle bedding

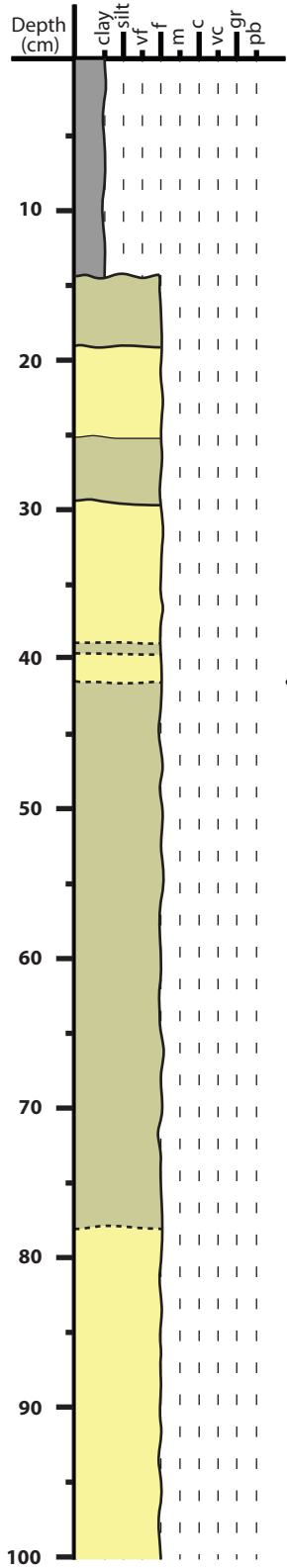
- possible round, sand-filled burrows, ~1 cm diameter

- finely laminated

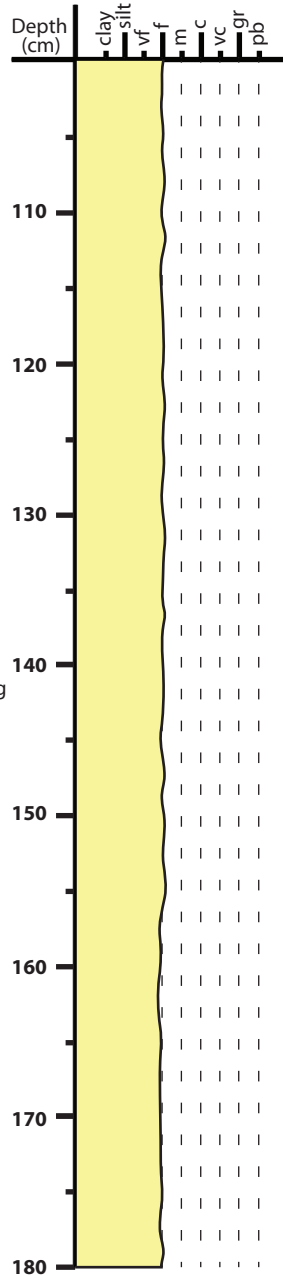
- massive-appearing texture; some faintly observable laminae

Core #18

Coordinates: 45.506788° N, 123.936791° W
Recovery: 180 cm

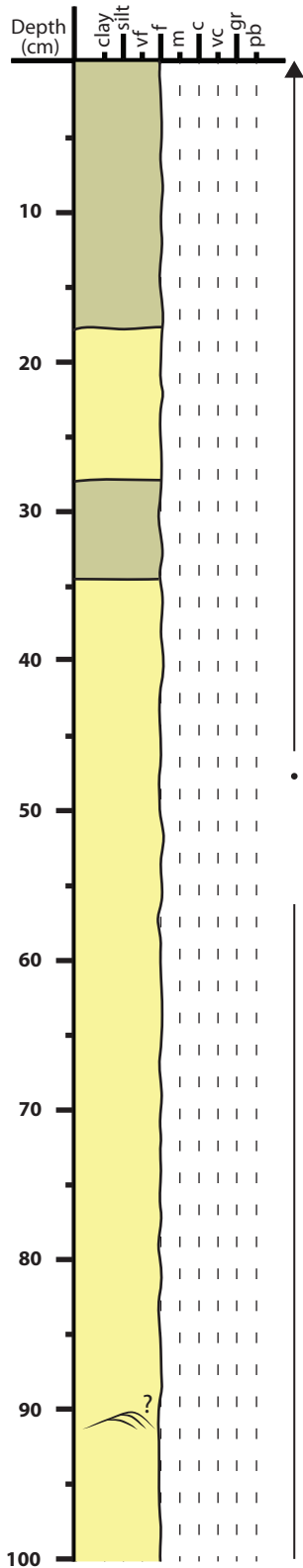


• massive-appearing texture; some bed contacts observed in upper part



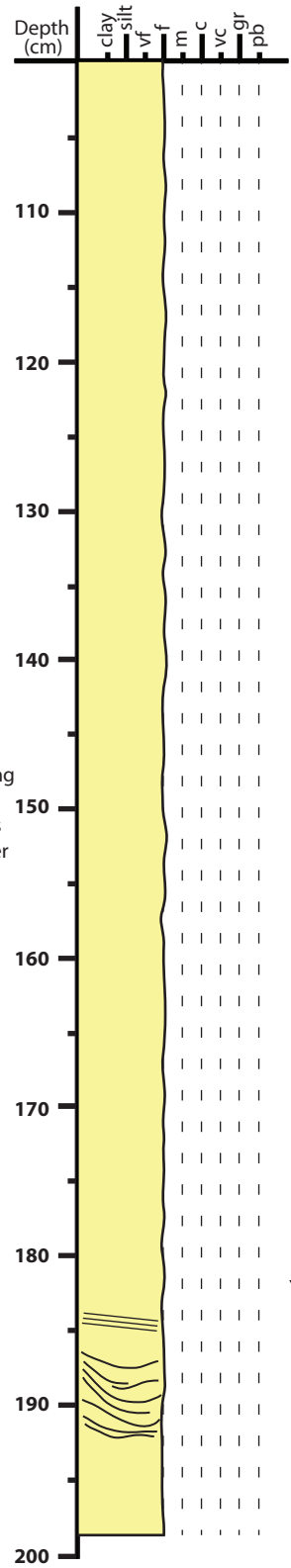
Core #19

Coordinates: 45.507601° N, 123.935281° W
Recovery: 198 cm



• massive-appearing texture; few bedding contacts observed in upper part

con't



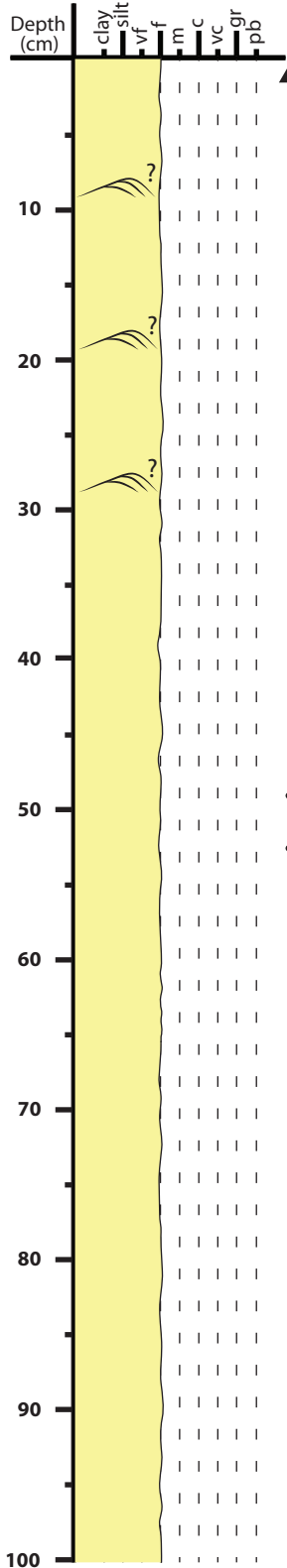
con't

• possible soft sediment deformation

Core #20

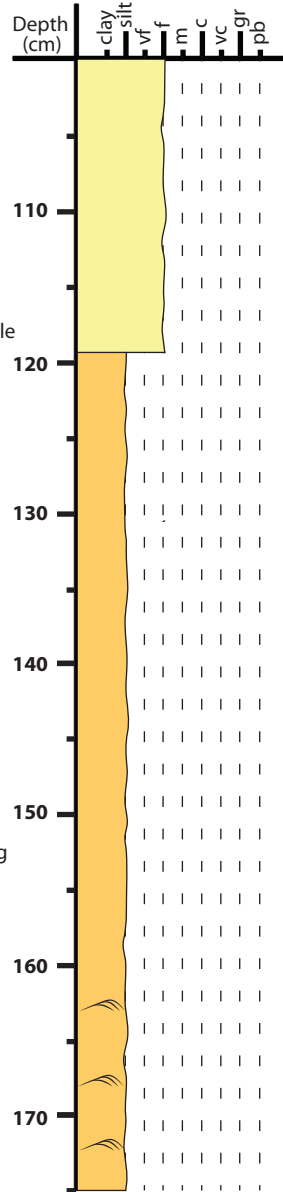
Coordinates: 45.515105° N, 123.940199° W

Recovery: 175 cm



• faintly observable ripples

• clean, very well sorted;
• massive-appearing texture

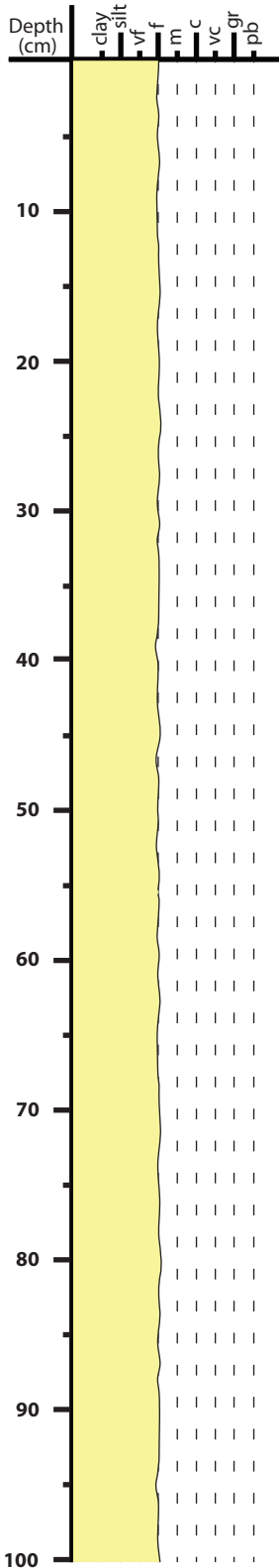


con't

• massive-appearing texture; ~10-15% fine sand

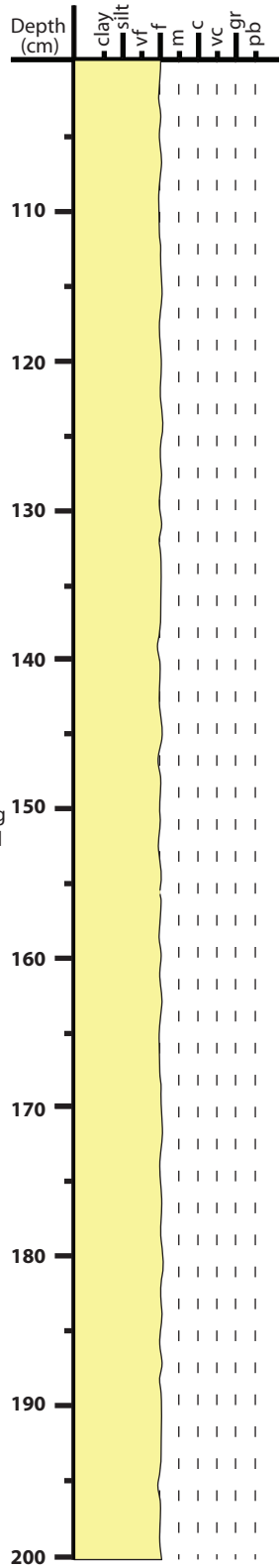
Core #21

Coordinates: 45.515165° N, 123.935691° W
Recovery: 200 cm

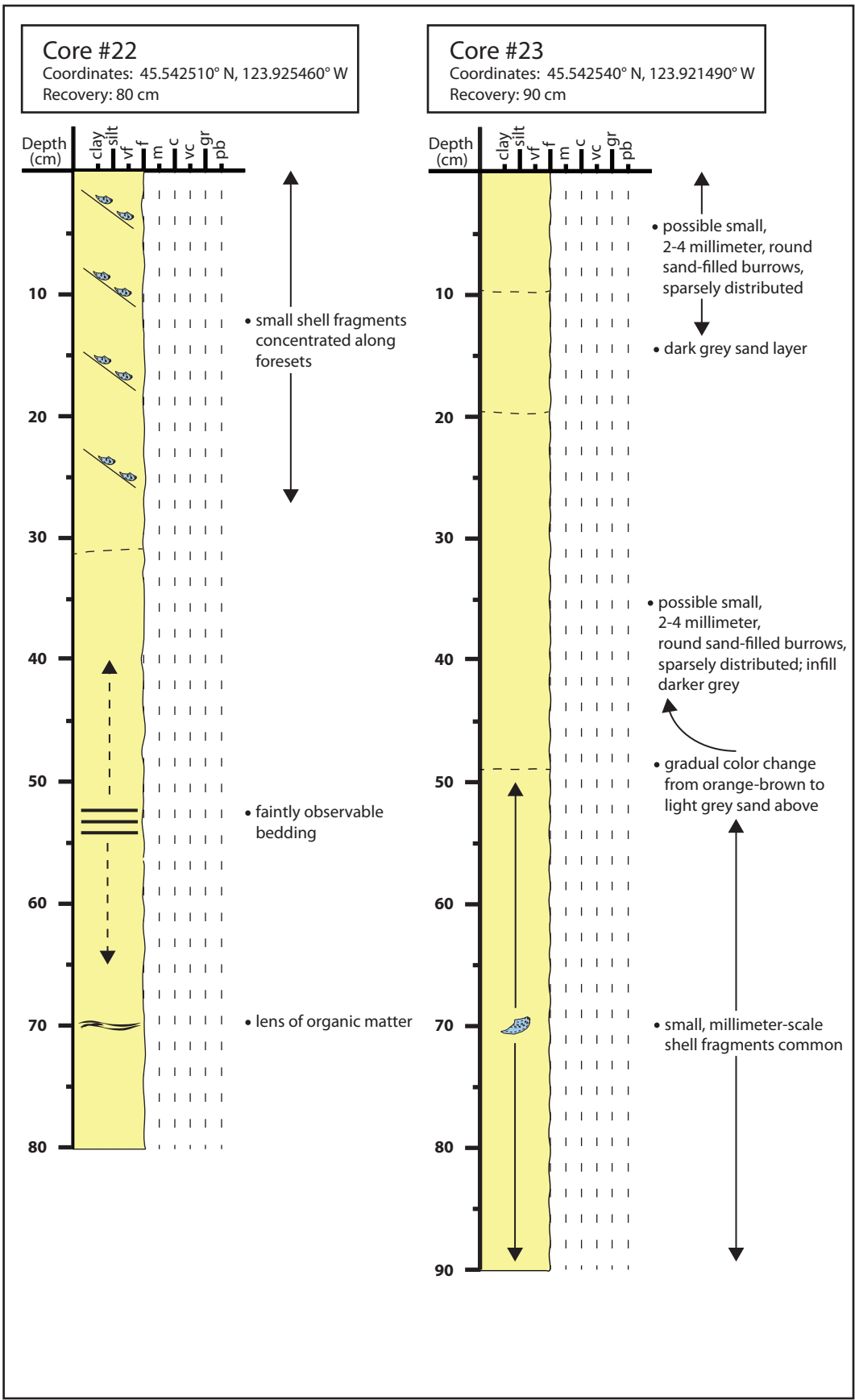


• massive-appearing texture; clean, well sorted sand

con't

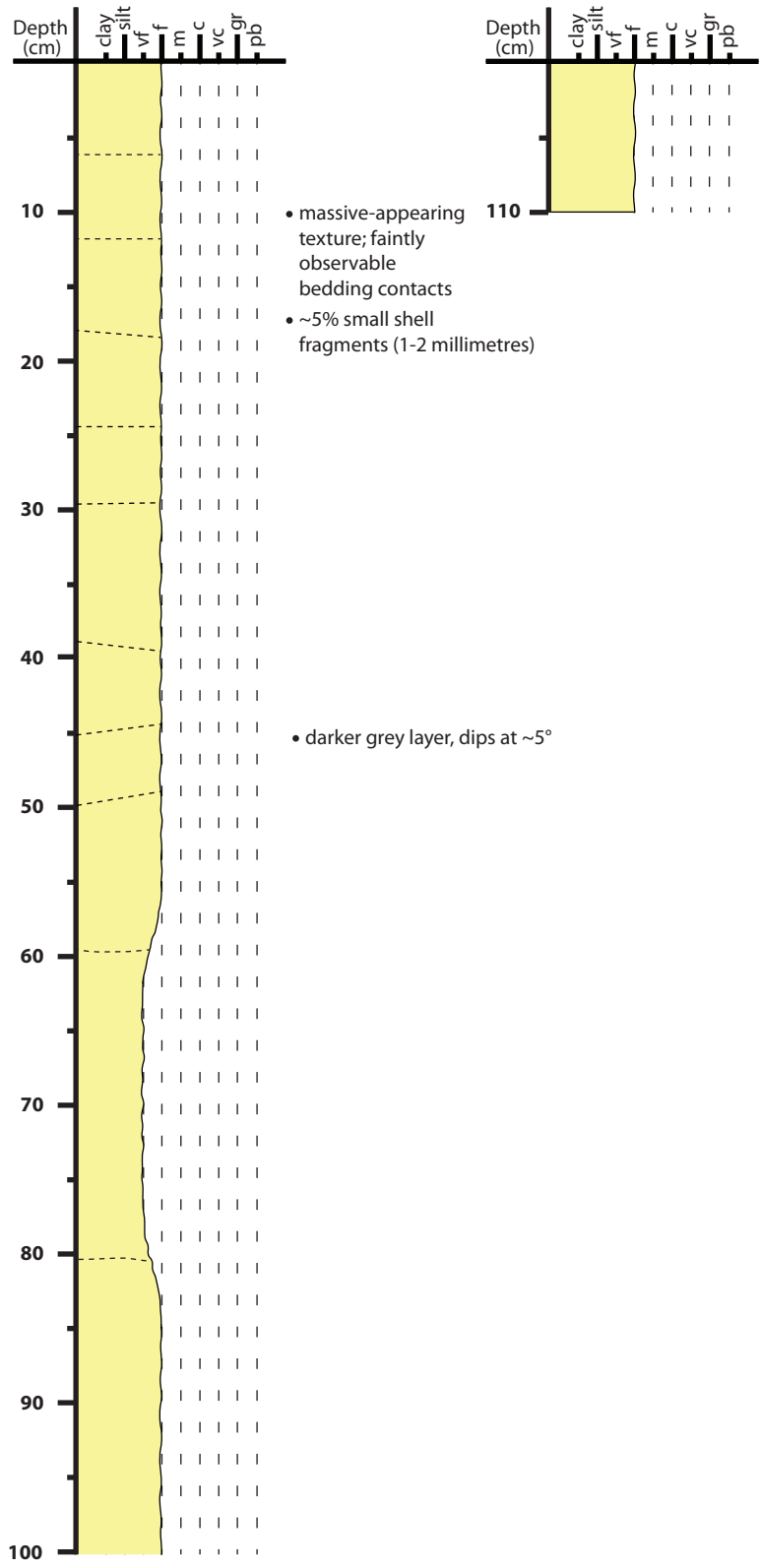


con't



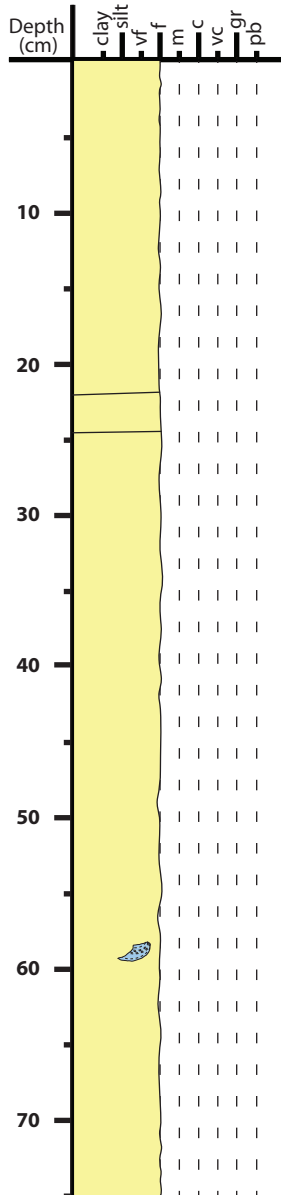
Core #24

Coordinates: 45.545280° N, 123.922870° W
Recovery: 110 cm



Core #25

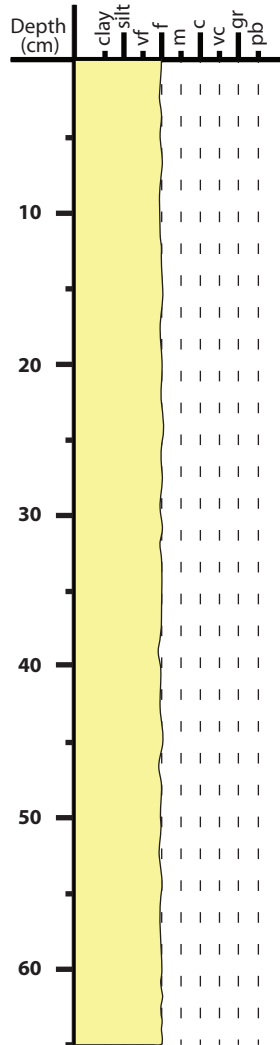
Coordinates: 45.544880° N, 123.921490° W
Recovery: 75 cm



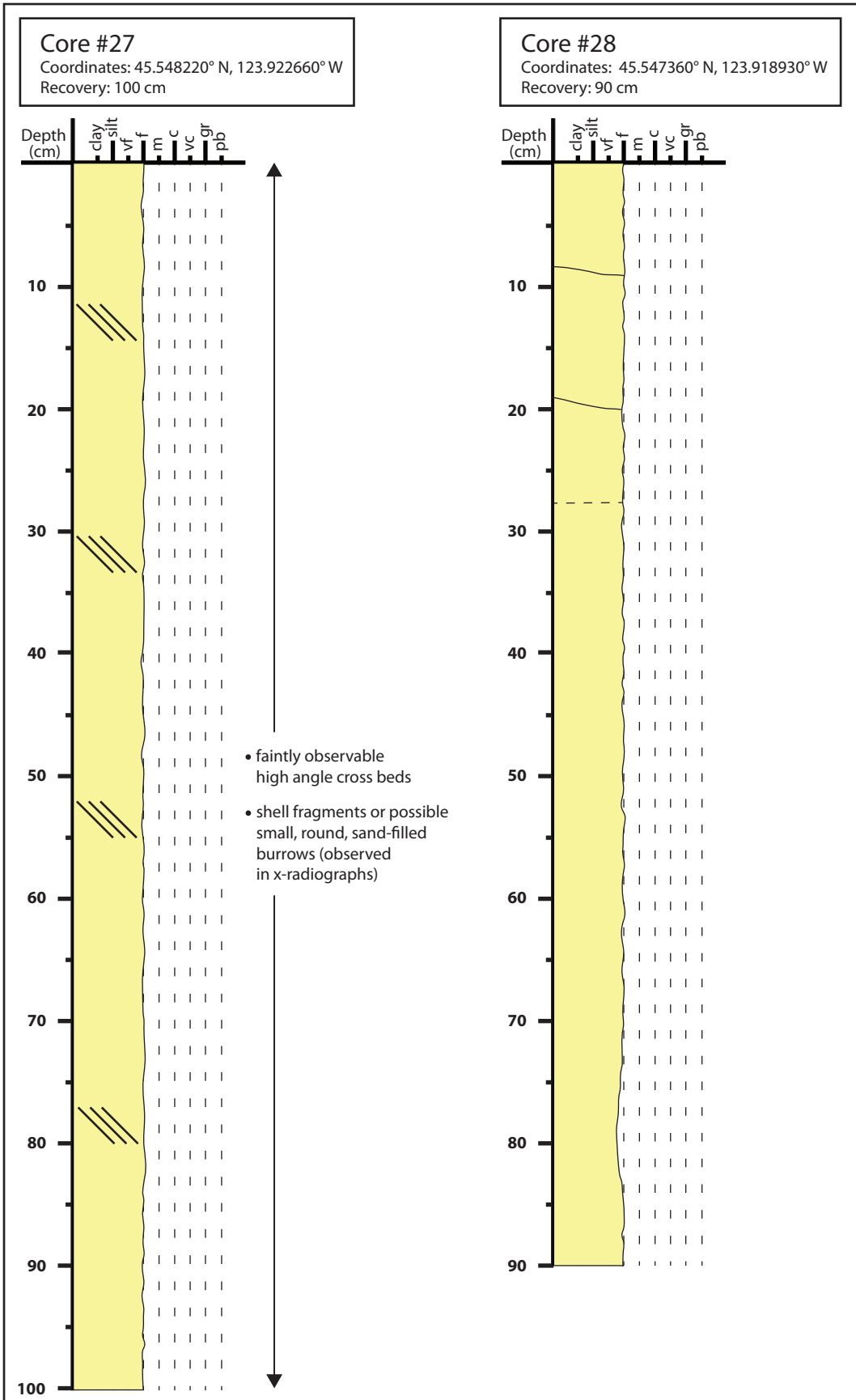
• light grey sand

Core #26

Coordinates: 45.545290° N, 123.919140° W
Recovery: 65 cm



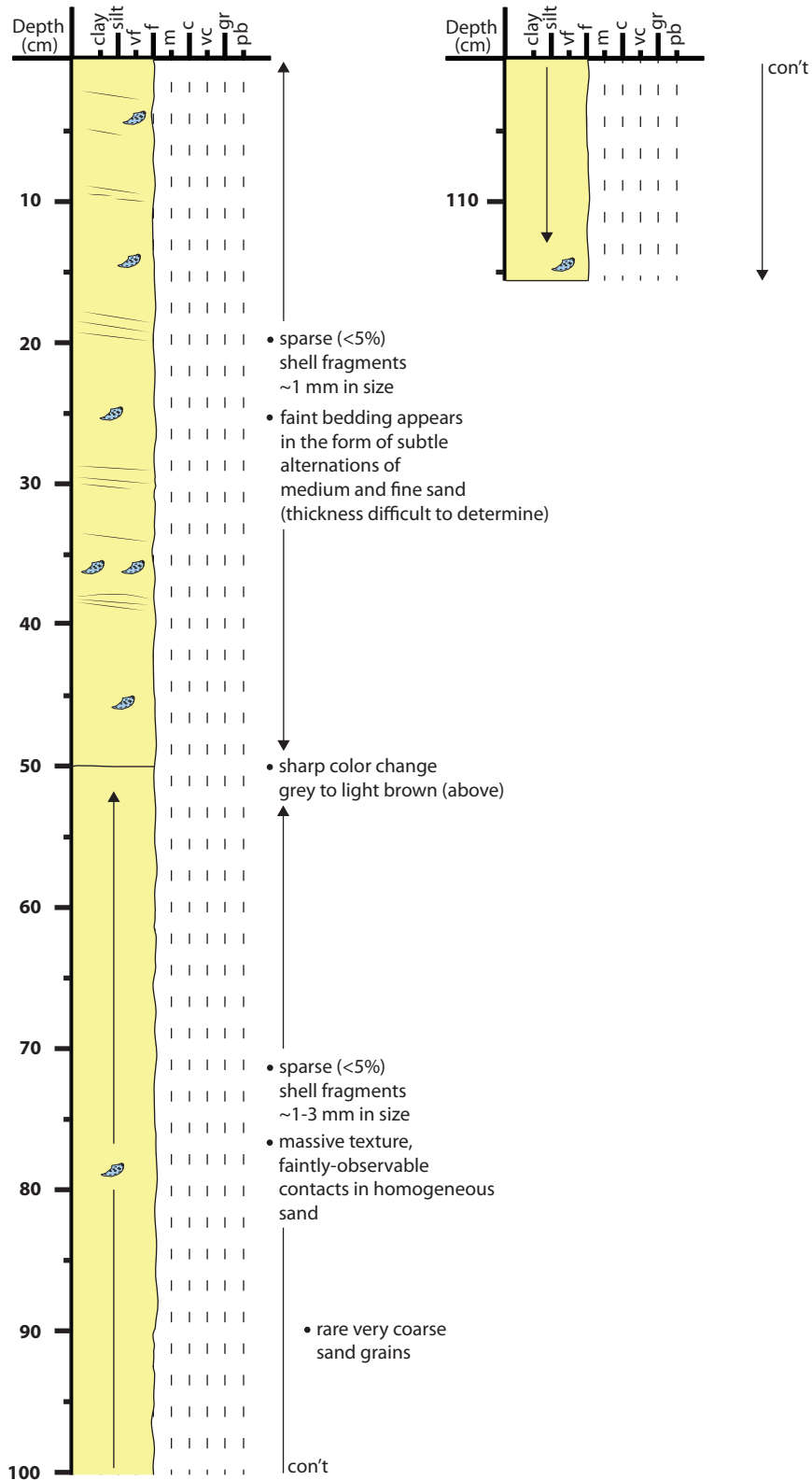
- massive texture; no sedimentary structures observed
- small, millimeter-scale shell fragments sparsely distributed

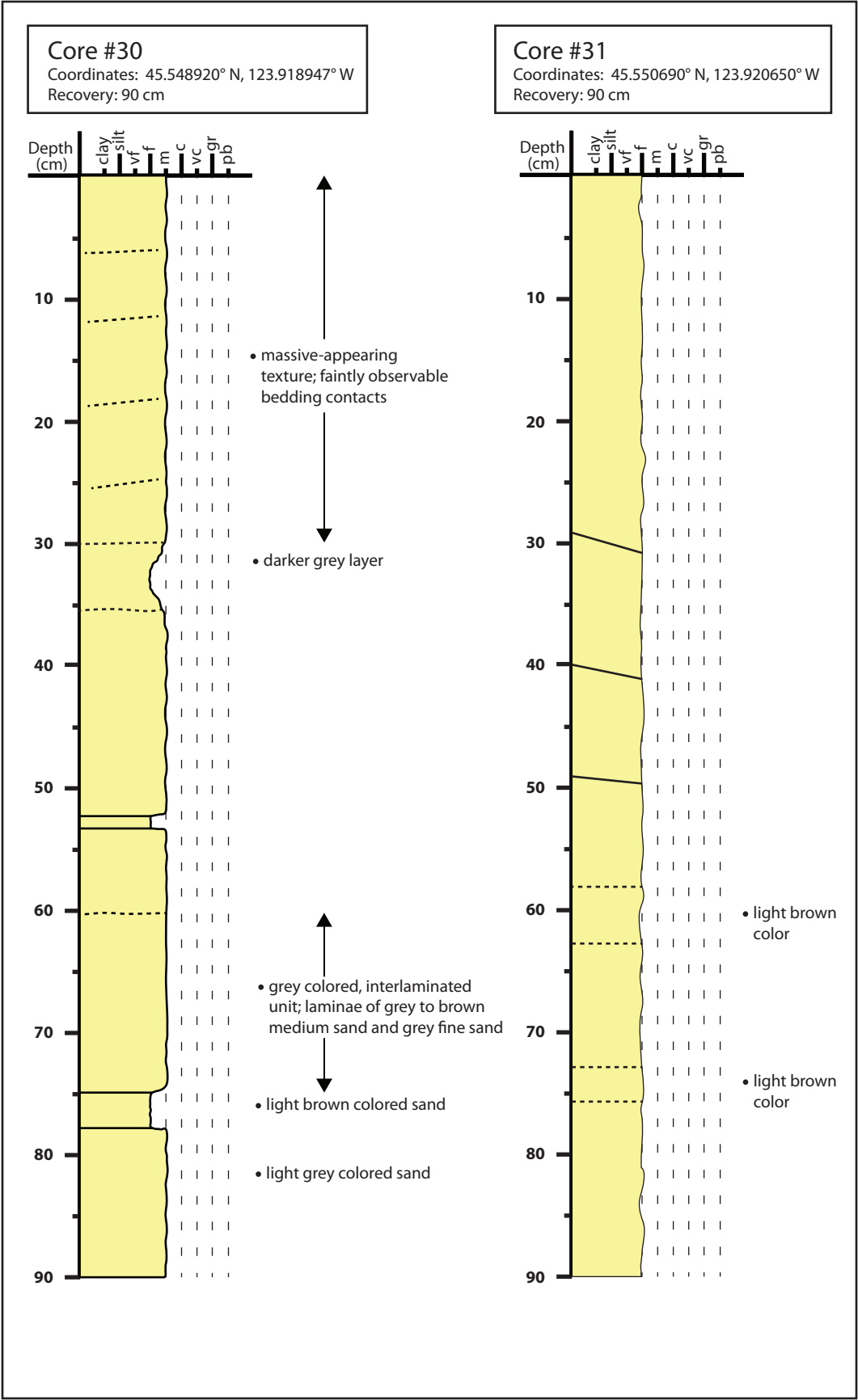


Core #29

Coordinates: 45.548460° N, 123.918370° W

Recovery: 116 cm

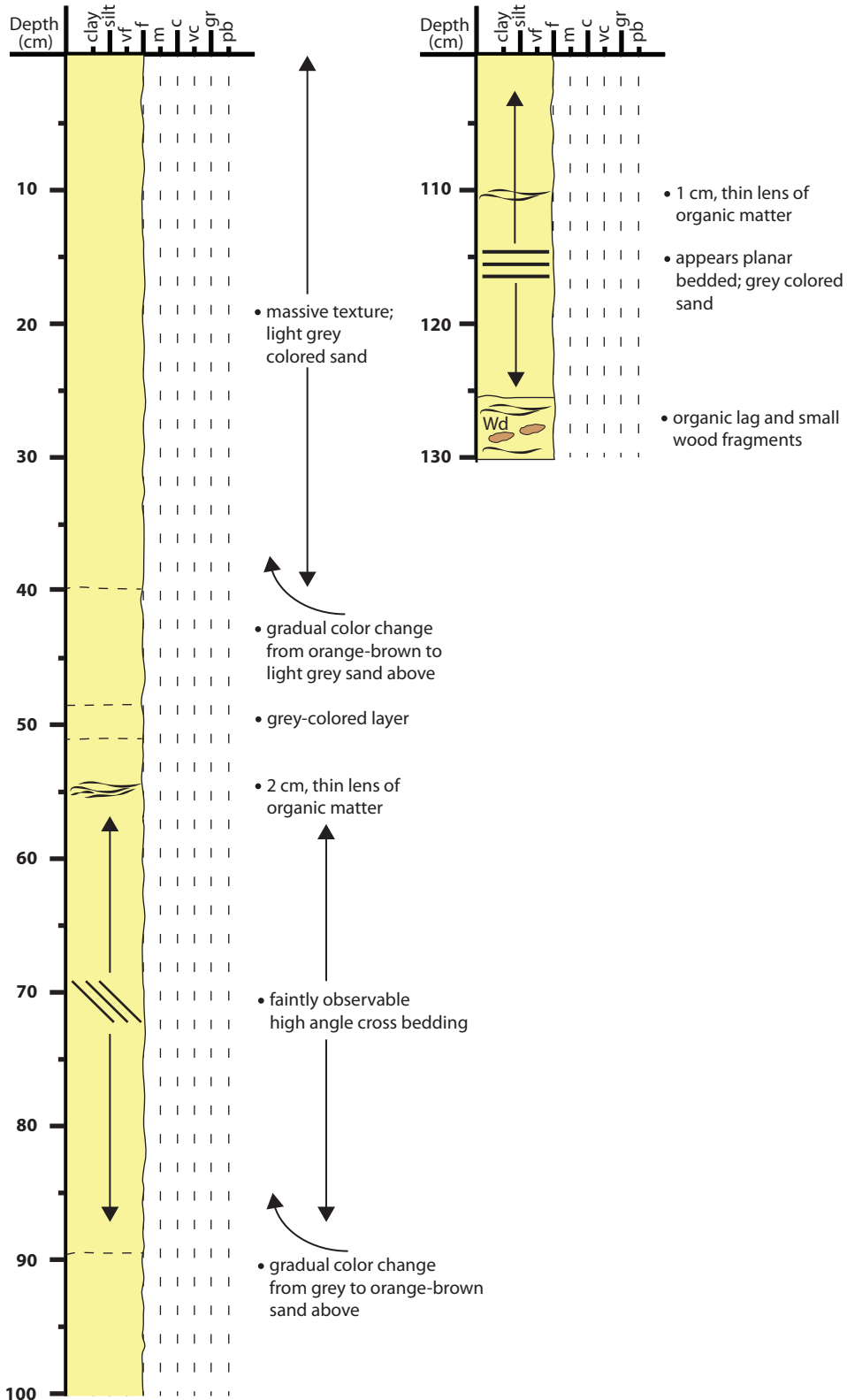




Core #32

Coordinates: 45.551620° N, 123.917440° W

Recovery: 130 cm



APPENDIX C

MICROBIALLY-INDUCED SEDIMENTARY STRUCTURES (MISS); EXAMPLES FROM INTERTIDAL FLATS OF TILLAMOOK BAY ESTUARY, OREGON

INTRODUCTION

The presence of epibenthic bacteria, cyanobacteria, and diatoms, results in the development of microbial mats in modern shallow-marine settings (Cuadrado et al., 2011). Their development begins with the formation of thin microbial films on the surface of siliciclastic sediment (Gerdes et al., 2000). Unlike organic films formed on rocks or in stromatolites, the organic film on soft sediment may fill pore spaces between sand grains, resulting in a leathery coating in the upper few millimetres of sediment (Seilacher, 1999). Microbial mats, and sedimentary structures implicated in their development, have been described extensively in the literature, particularly from Proterozoic, and more recently Lower Triassic, successions (Pruss et al., 2005). Microbial mats were likely important in the evolution of marine metazoans. Seilacher (1999) distinguished four lifestyles of Ediacaran organisms that used biomats as a food source: mat encrusters, mat scratchers, mat stickers, and undermat miners. These organisms may have also used the biomats as “oxygen masks” during a time of poor ocean water oxygenation (Seilacher, 1999).

Numerous structures, associated with microbial biofilms or mats, have been grouped together in the category of “microbially induced sedimentary structures” (MISS, *sensu* Noffke et al., 2001). These commonly include wrinkle structures, shrinkage cracks and pustules among others. Wrinkle marks and the similar *Kinneyia* ripples are believed to be related to microbial mats, although their exact mechanism of formation is not well understood (Bouougri and Porada, 2002). *Kinneyia* ripples, compared to wrinkle marks, have more linear and parallel crests, whereas the latter exhibit more chaotic distributions, and may form on the surface of microbial mats (Bouougri and Porada, 2002). Shrinkage of water-saturated organic material (such as microbial mats) due to

dewatering, can result in the formation of cracks of varying types, some of which can become infilled with sand (Bouougri and Porada, 2002). Wrinkle marks, and an areally-restricted microbial mat exhibiting erosional pockets and remnants, as well as polygonal cracks, are observed in two study locations at Tillamook Bay on the coast of Oregon. These structures are described herein and their significance in the development, preservation and alteration of sedimentary structures at Tillamook Bay intertidal flats is discussed.

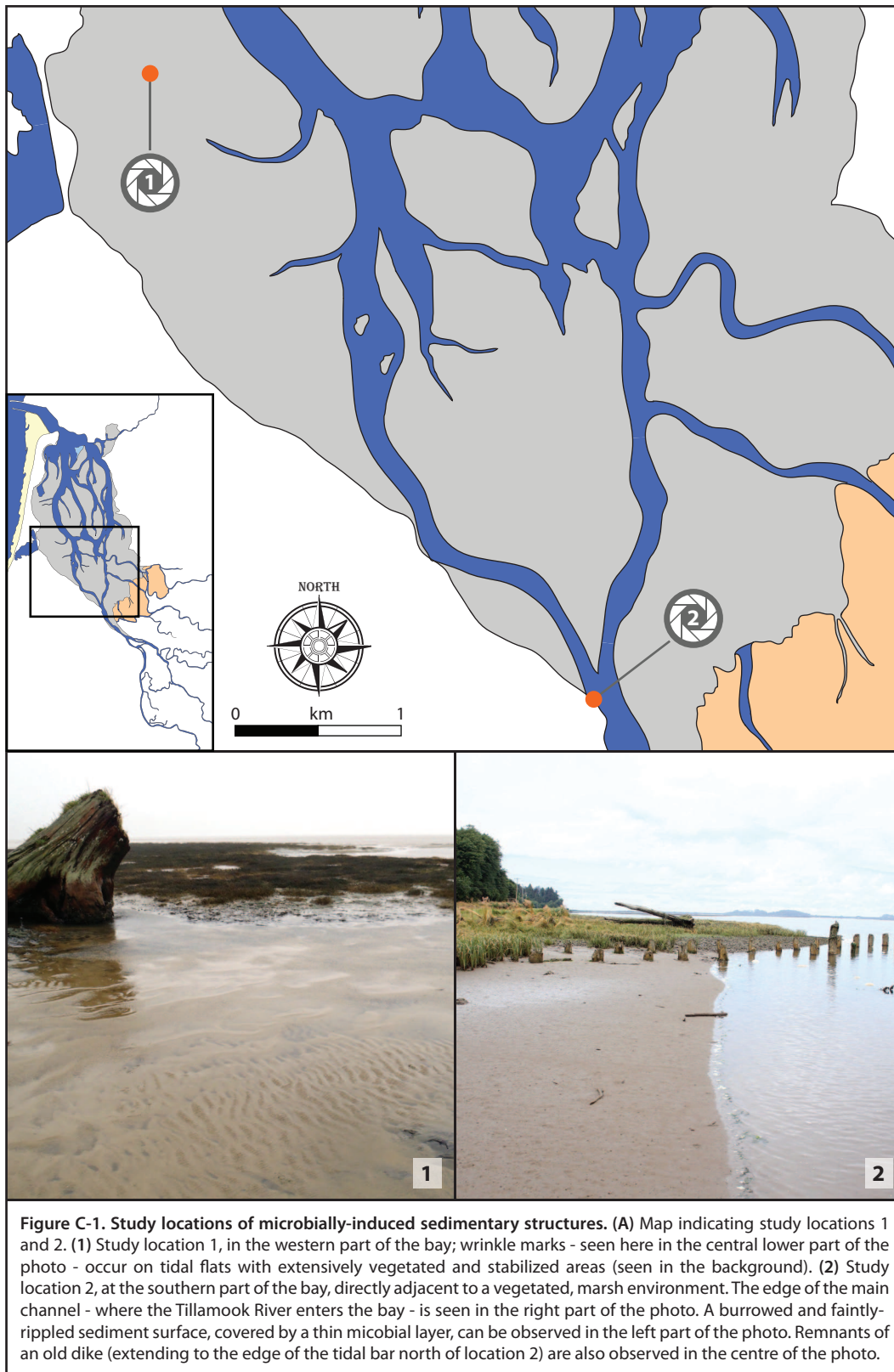
STUDY LOCATIONS

Wrinkle marks and microbial mat features are observed and assessed at two localities at Tillamook Bay (Fig. C-1). These microbially-induced sedimentary structures are relatively well developed and preserved, allowing for detailed description. A third location, on the western shore-attached tidal flats near Bayocean Peninsula, containing a well-developed burrowed microbial mat, is briefly discussed.

1. Location one, on the western side of Tillamook Bay, occurs in close proximity to the Bayocean Peninsula. Wrinkle structures at this locality are observed on sand-dominated, shore-attached tidal flats in the western part of the bay.
2. Location two, on the southwestern side of Tillamook Bay is located directly south of the flood-oriented tip of the inner estuary tidal bar, across the tidal channel separating the tidal bar and zone of the microbial mat.

METHODOLOGY

At location one, on the western margin of the bay, wrinkle marks are photographed and described in detail, as observed from oblique, as well as straight angles. Sediment comprising crests of the low-amplitude wrinkle



marks is carefully sampled using a thin-bladed knife and placed in individual sample bags. Each bag is labelled with a corresponding sample location, for a total of 15 samples, three from each of the five sample locations. In the university lab, grain size analysis, as well as total organic carbon (TOC) analysis, is performed on all 15 samples according to steps as described in Folk (1974) and Heiri et al. (2001), respectively.

At location two, where the microbial mat and related structures are observed, photographs and descriptions were recorded of the surface sediment texture, as well as of cross-sectional samples removed from small trenches dug into the sediment. A short, 30-centimeter long core is also sampled at this location and subsequently cut longitudinally and photographed in detail. Sediment is also sampled at a depth of 15 centimeters, and placed in individually marked sample bags. As for location one, grain size analyses and total organic carbon (TOC) analyses were performed on sediment samples.

DESCRIPTIONS AND RESULTS

Location 1: Wrinkle marks superimposed on current ripples.

On the western side of the bay, in the well-sorted, relatively clean sand of the shore-attached tidal flats, wrinkle structures are observed, primarily superimposed on low-relief current ripples. In the vicinity of sediment containing wrinkle marks, moderately vegetated sand, with green algae growing on them, formed algal mats of higher relief than the surrounding flat (Fig. C-2 A,B,C,D). The wrinkle marks have a moderately irregular, elongate, straight to slightly sinuous morphology and wavelengths between crests 1 centimeter wide on average, with millimeter-scale amplitude measured via cross-sectional views (Fig. C-3 A,B,C,D; Fig. C-4 109 A,A'). The marks are observed to form dominantly at an oblique to perpendicular orientation

Figure C-2. Algal mats and wrinkle marks, western margin of Tillamook Bay. (A) General view of the edge of an algal mat. Rippled sediment, containing wrinkle marks, can be seen at the center left part of the photo. This is shown in detail in figure C-3. (B and C) Top view of the algal mat and the erosional pockets formed on its surface. Wrinkle marks can be observed at the bottom of photo (B), near the digital scale. Note also the irregular, wrinkled surface of the algal mat. Foot for scale in (C) is approximately 10 centimeters across. (D) Close up view of the wrinkled surface of the algal mat, covered in a thin, millimeter-scale layer of water.

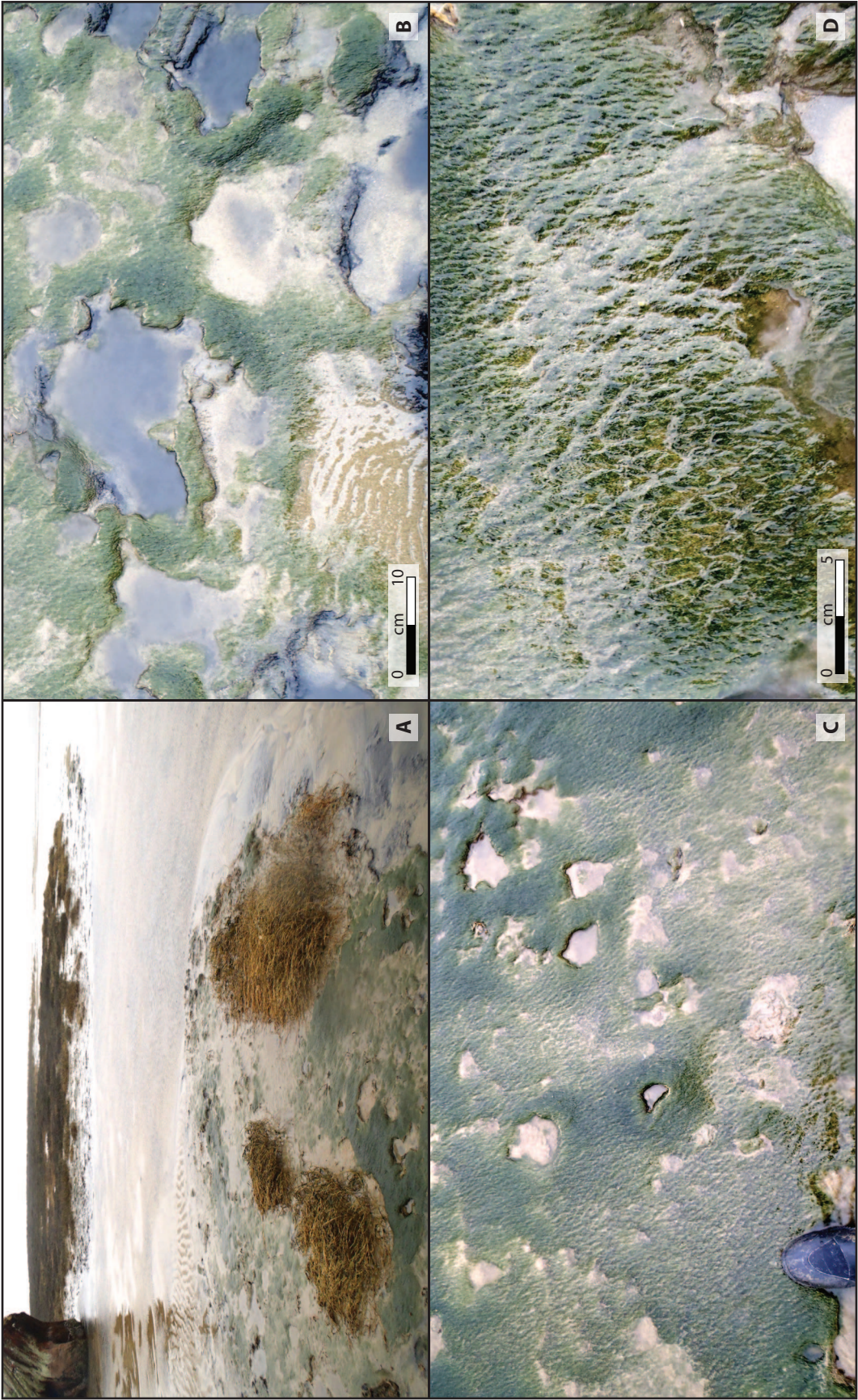


Figure C-3. Wrinkle marks on rippled sediment, western margin of Tillamook Bay. (A) General view of sediment surface, with wrinkle marks superimposed on ripple crests. Tree trunk in the background approximately two meters high. Note highly-vegetated tidal flat north of the tree trunk. **(B)** View to the north, showing an extensive algal mat (with numerous erosional pockets on its surface) and rippled, wrinkle mark-containing sediment in the foreground. **(C)** Sampling of ripple crests exhibiting wrinkle marks. Note transition towards the algal mat to the right. **(D)** Slightly oblique view of wrinkle marks forming on transverse, low-relief ripples at the edge of an algal mat. Digital scale applies to the foreground area.

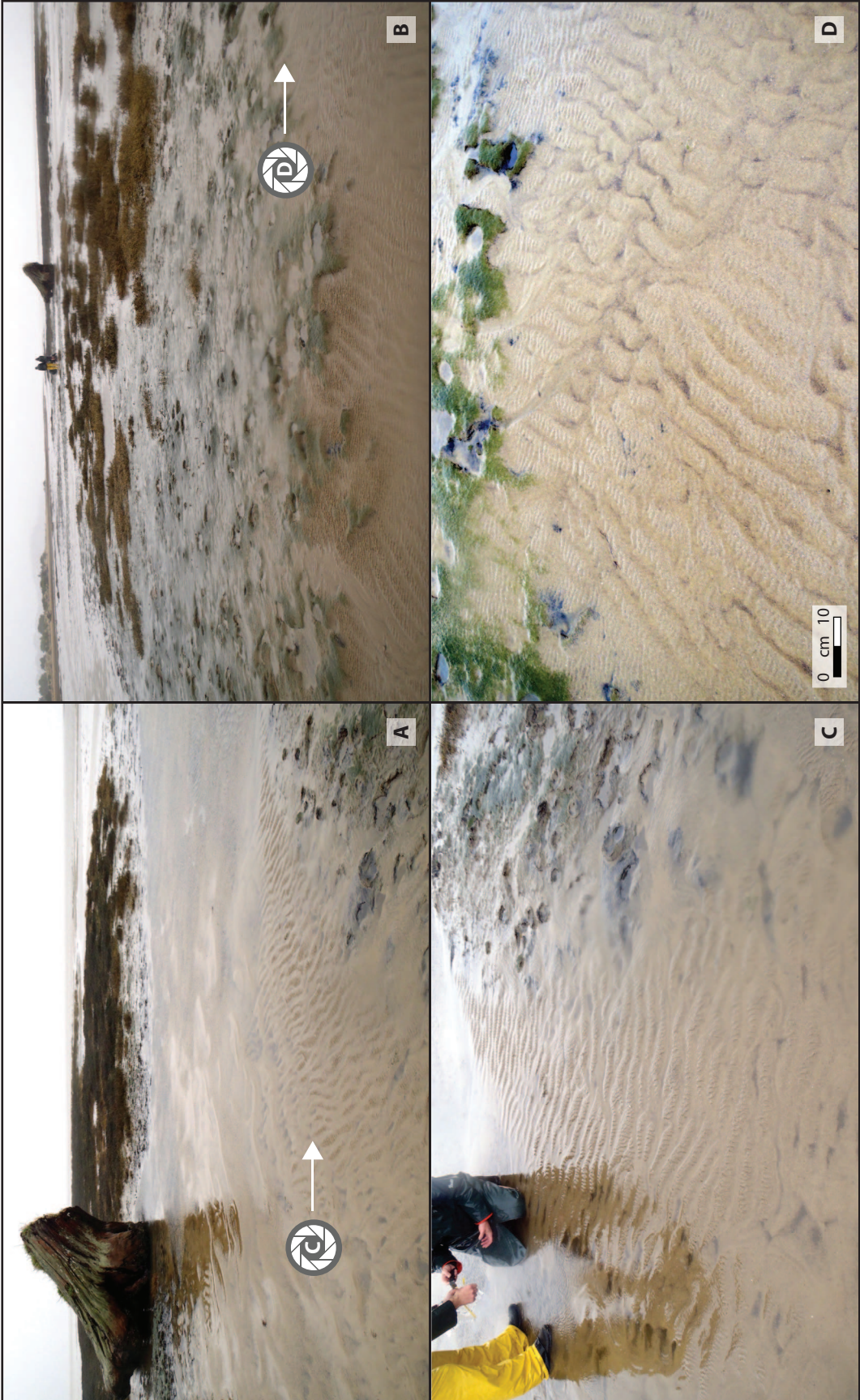




Figure C-4. Wrinkle mark morphology. (A and A') Close-up photograph and trace drawing of wrinkle marks observed on low-relief ripples. A thin layer of water covers the troughs of ripples seen in the photograph. Ripple crests are outlined in the grey color, while the rest of the sediment is outlined in the light yellow. Wrinkle marks, or the approximate areas they cover, are outlined in purple brown. Note the perpendicular to oblique orientation of the wrinkle marks, with respect to the longitudinal orientation of the straight to sinuous ripple crests.

respective to ripple crest orientations. The concentrations of wrinkle marks vary widely, from several, hardly distinguishable marks per square meter, to tens of well-developed marks per square meter.

In order to analyze the total organic carbon (TOC) content of the sediment exhibiting wrinkle marks, five stations were chosen, each with three sampling sites, containing poorly-developed wrinkle marks, moderately-developed wrinkle marks, and well-developed wrinkle marks. The results of the total organic carbon analyses are listed in Table C-1.

Sample	TOC %
1a	0.21
1b	0.27
1c	1.10
2a	0.14
2b	0.20
2c	0.63
3a	0.15
3b	0.15
3c	0.36
4a	0.20
4b	0.21
4c	0.75
5a	0.24
5b	0.26
5c	1.00

Table C-1. Total Organic Carbon (TOC) percent values from sediment containing wrinkle marks.

Averaged results from total organic carbon (TOC) analyses, from five stations (numbered 1 through 5), each consisting of three samples: **(a)** poorly-developed to absent wrinkle marks; **(b)** moderately-developed wrinkle marks; and **(c)** well-developed wrinkle marks.

An increase in total organic carbon percent values is observed between successive samples at each of the five locations. The total organic carbon (TOC) percent values between sample types (a) poorly-developed and (b) moderately-developed wrinkle marks at each station show little to no difference. Station 3 shows the smallest TOC percent increase overall between (a) poorly-developed, (b) moderately-developed and (c) well-developed wrinkle marks. All other stations show more consistent TOC percent changes, with the results of Station 2a displaying the lowest overall TOC percent value. In all cases, the samples from locations with (c) well-developed wrinkle marks exhibited significantly higher TOC percentages than those from locations with no or (a) poorly developed wrinkle marks.

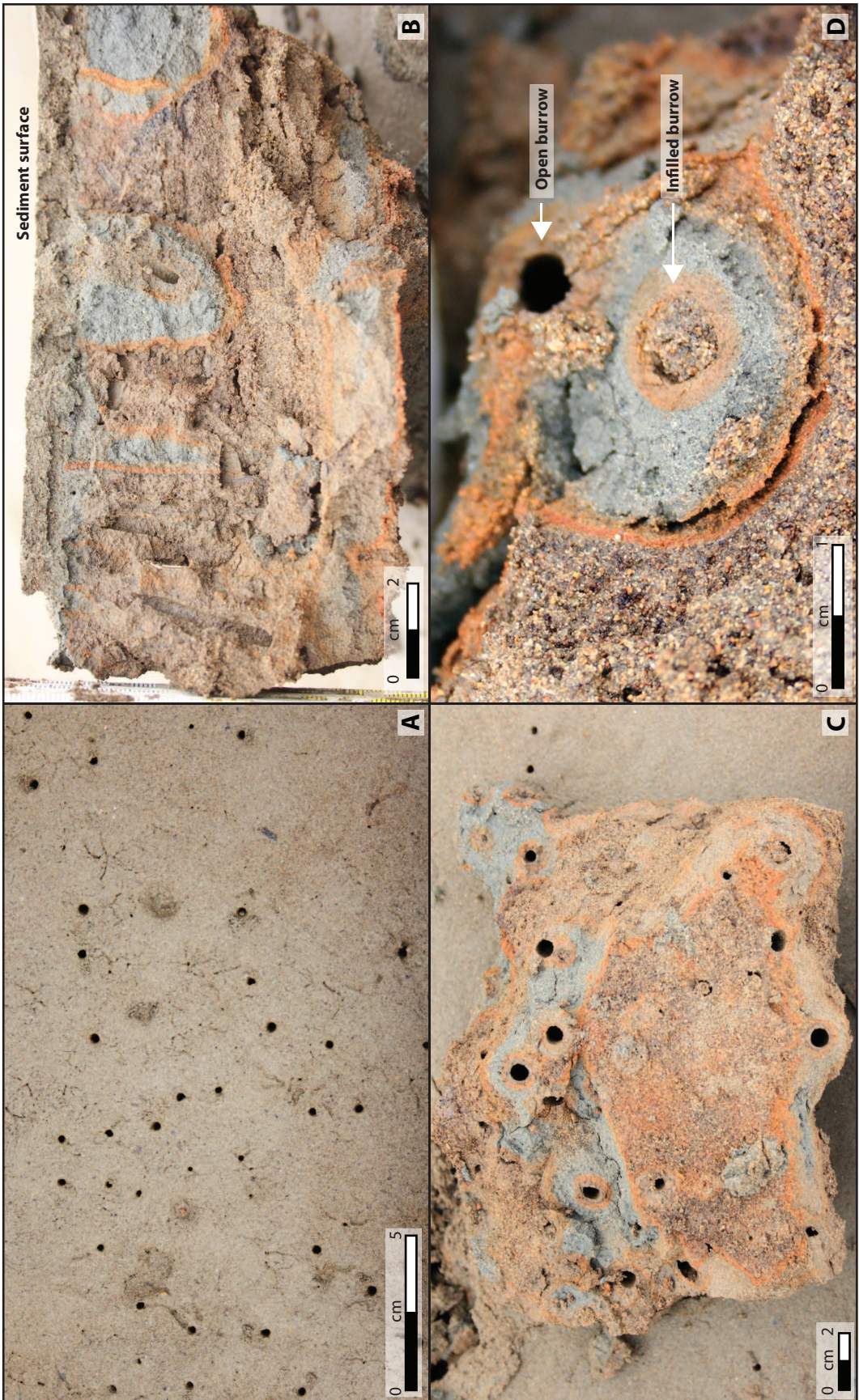
Location 2: Burrowed microbial mat

A second occurrence of microbially-induced sedimentary structures is observed on an areally-restricted intertidal flat in the south-western part of the bay (Fig. C-5 A,B,C). Directly adjacent to a main fluvial-tidal channel, near the mouth of the Tillamook River, the intertidal flat is heavily vegetated in parts, and extends landward to Bayocean Road nearby. Location 2 occurs in a quiescent, relatively sheltered setting in comparison with Location 1. A thin, burrowed, microbial mat covers the exposed (i.e. non-vegetated) intertidal zone. The dominant sedimentary structures observed on the surface of the microbial mat are medium-scale polygonal desiccation fractures, as well as erosional pits and remnants. Sediment, both at the surface and below the surface, is cohesive, allowing for excellent preservation of distinct sediment layers, observed in cross-sectional views of samples removed with a shovel. Burrows observed on the surface (Fig. C-6 A), consist of simple, vertical to sub-vertical, shafts (i.e. similar to the ichnogenus *Skolithos*), with diameters of approximately 5 to 7 millimeters. Organic detritus, in the form of wood and plant material, is abundant within the upper 5-10cm of the sediment surface.

Figure C-5. View of the microbial mat, southern part of Tillamook Bay. General view of the area located south of the inner estuary sand bar, or zone 3. (A) View to the southeast, along the vegetated edge of the bay, and the Tillamook River channel. The irregular microbial mat surface, with erosional pockets and remnants, can be observed. (B) Closer view of the mat surface, with well-developed polygonal shrinkage cracks seen on the surface. Meter-stick for scale is 20 centimeters long. (C) View to the northwest, showing better-developed erosional pockets and remnants on the mat surface. Remaining pillars from an old dike can be seen in the background.



Figure C-6. Various views of burrow morphologies from a burrowed microbial mat. (A) Top view of the burrowed mat. (B) Side view of a sample of sediment from a small trench. Note the oxidized nature of the sediment in the vicinity of burrows. Burrow morphologies are vertical to subvertical and approximately 0.5 centimeters in diameter, making them similar to Skolithos-like burrows. The top centimeter below the surface is that of the youngest microbial mat layer. (C) Bottom view of vertical burrows. Note iron oxidation forming in the immediate vicinity of burrows. Also note the bottom half of the sample (i.e. the part seen in the bottom half of the photo), which shows more extensive iron oxidation, as well several sand-infilled burrows. (D) Close-up view of an open burrow and sand-infilled burrow.



Iron oxidation is observed as two distinct orange colored halo bands surrounding the burrows (Figure C-6 B,C,D). The burrows are numerous (4-6 burrows / 5 cm²) and open to the surface. More extensive zones of iron oxidation are observed to form around sand-infilled, abandoned or unoccupied burrows (Figure C-6 C,D). Although prevalent throughout sediment layers, iron oxidation is intermittently distributed. It is commonly associated with burrows, however in some cases it occurred with no indication of biogenic structures present, and commonly terminates abruptly, both vertically as well as horizontally within a layer.

Organic-rich layers, appearing dark grey in color, and containing visible fragments of plant material, are common in the area of the tidal flat, and are locally iron oxidized (Figure C-7 A,B,C). An oily sheen-like discoloration of the sediment occurs sporadically within layers of otherwise clean sand, always in close proximity to organic-rich layers (Figure C-7 A,B,C).

In boxcores retrieved from this location iron oxidation is inherent as thin, elongate zones, usually at a depth of approximately 20 centimeters below the surface (Fig. C-8 A,A'; Fig. C-9 Part I A,A', Fig. C-9 Part II A,B). Red-brown nodules, averaging 2-3 millimeters in diameter, are also observed distributed largely around thin, iron-oxidized zones. Layering of sediment, as observed in cross-sectional views, consist of light to dark grey sand, light yellow sand, and orange to brown sand. Roots are common to abundant, particularly in areas adjacent to the marsh, and are also observed in boxcores, associated with possible siderite nodules. Low amplitude (0.5-1.0 cm) ripple are commonly observed. In one instance, a higher-relief sand-dominated ripple, with an amplitude of several centimeters, was also observed. Small current ripples, low-angle laminae, and possible soft sediment deformation is observed in boxcored samples.

Figure C-7 Sedimentary features under the modern microbial mat surface. (A) Cross-sectional view of a sample (seen on a shovel) dug into a small trench. Note iron oxidation, presence of muddy, organic-rich layers, and well-developed ripple cross-laminae. (B) Close-up view of the current-rippled sand seen in (A), as well as the organic-rich, iron oxidized layers. Note the varying thickness of layers overlying the rippled sediment. (C) Oily sheen-like texture on a sample with thin, organic-rich layers. This texture is commonly observed in the sediments below the microbial mat. Way up for the sample is indicated on the photo.

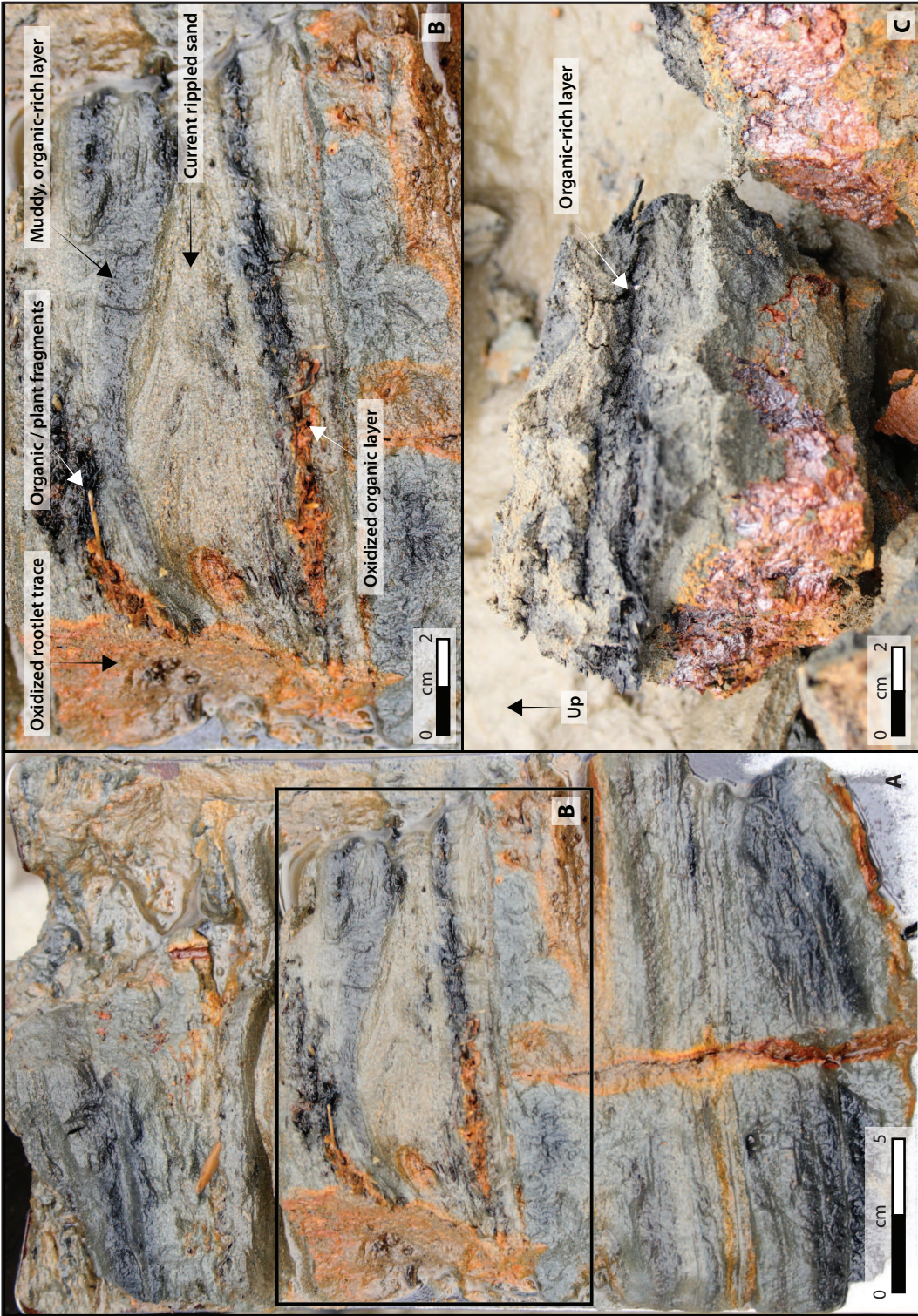


Figure C-8. Sedimentary and biogenic structures present under a microbial mat. (A and A') Photograph and trace drawing of sediment retrieved with a boxcore. Note the vertical nature of *Skolithos*-like burrows, as well as the preferential oxidation of burrow structures and rippled sand layers. Some round, oxidized features may be possible *Planolites*-like burrows. Possible micro-faulting of sediment, indicated by a question mark in the bottom half of the photo.



Figure-specific legend:

- Oxidized burrows/root traces
- Heavily-oxidized sand layer
- Lightly-oxidized sand layer
- Unoxidized sand layer
- Anoxic sand layer
- Internal layer structure
- Ripple foresets

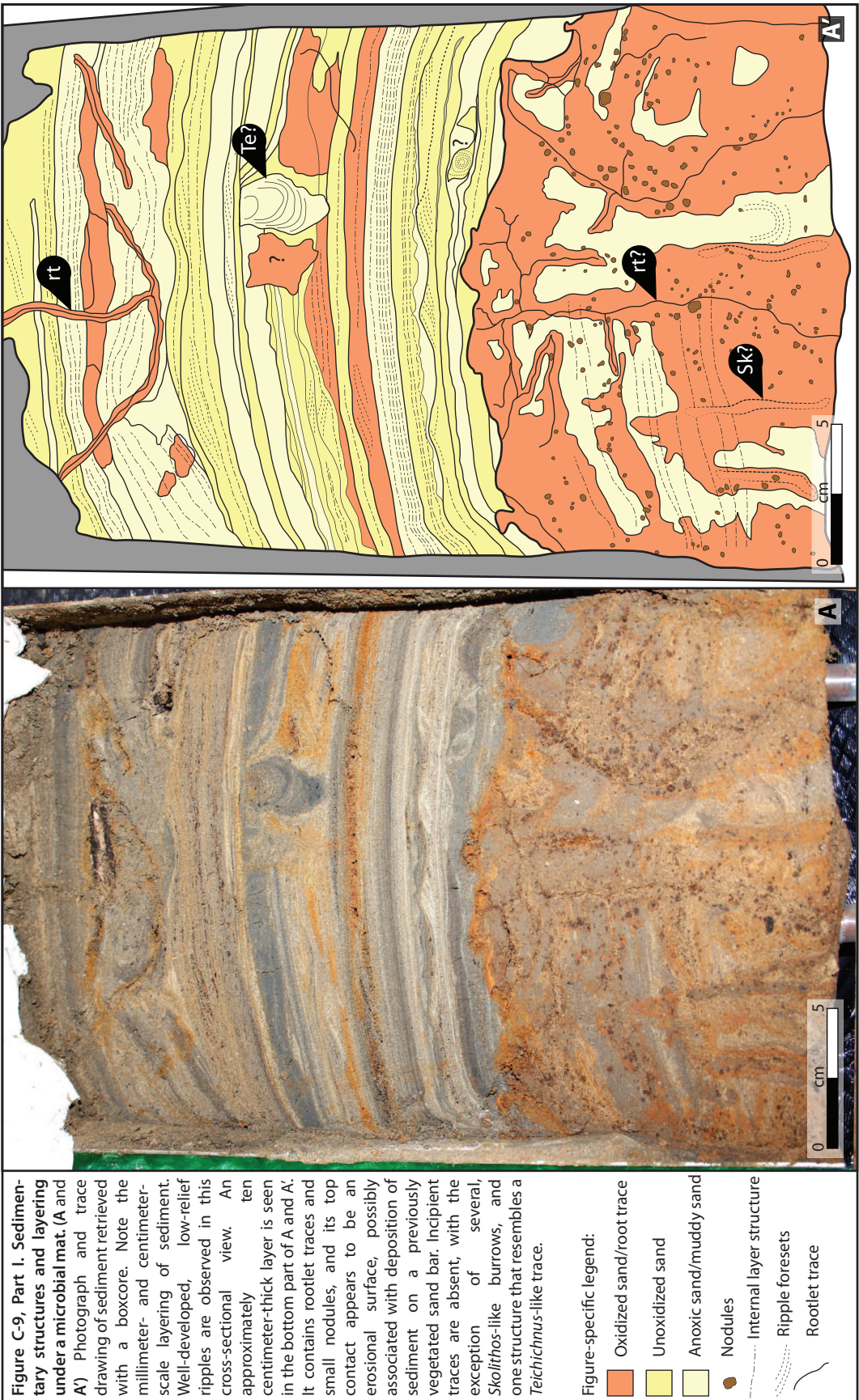
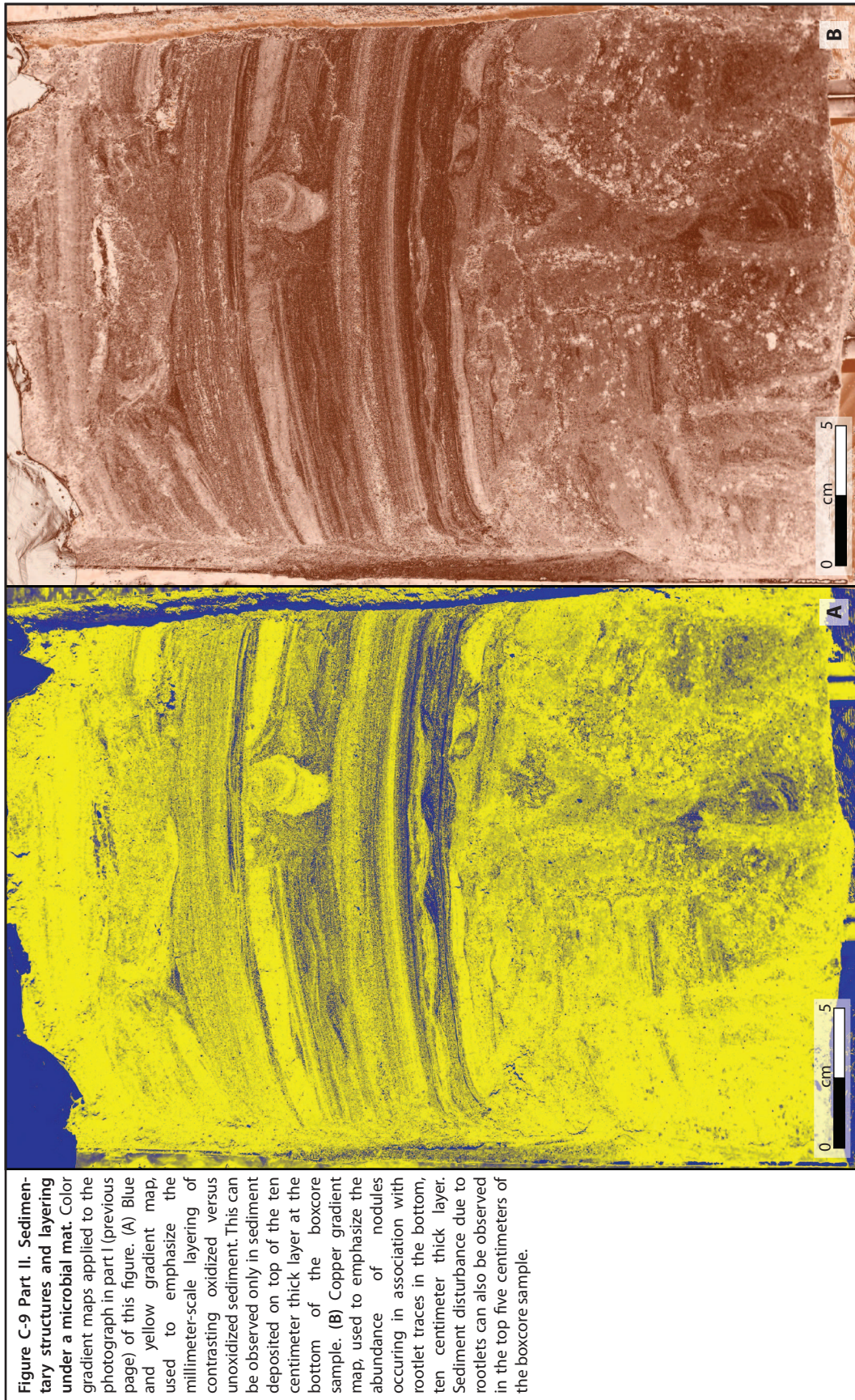


Figure C-9, Part I. Sedimentary structures and layering under a microbial mat. (A and A') Photograph and trace drawing of sediment retrieved with a boxcore. Note the millimeter- and centimeter-scale layering of sediment. Well-developed, low-relief ripples are observed in this cross-sectional view. An approximately ten centimeter-thick layer is seen in the bottom part of A and A'. It contains rootlet traces and small nodules, and its top contact appears to be an erosional surface, possibly associated with deposition of sediment on a previously vegetated sand bar. Incipient traces are absent, with the exception of several, *Skolithos*-like burrows, and one structure that resembles a *Teichichnus*-like trace.

Figure-specific legend:

- Oxidized sand/root trace
- Unoxidized sand
- Anoxic sand/muddy sand
- Nodules
- Internal layer structure
- Ripple foresets
- Rootlet trace



INTERPRETATIONS AND DISCUSSION

Microbial mats are not as easily distinguishable in siliciclastic rocks as they are in carbonate rocks, but have nevertheless been mentioned from multiple ancient examples. Structures associated with microbial mats include wrinkle structures, diastasis cracks, gas domes, palimpsest ripples, and multi-directional ripple marks (Banerjee and Jeevankumar, 2005). The term “wrinkle structure” may refer to a variety of structures, such as *Runzelmarken* and the similar *Kinneyia* ripples described by from the Äleklinta sequence in Sweden (Martinsson, 1965; Gedda, 1993; Gingras, 2002). Wrinkle structures have been described from terrestrial to marine, including subtidal settings (Banerjee and Jeevankumar, 2005). Gedda (1993) described micro-ripples formed in a silty, millimetre-scale layer deposited on underlying macro-ripples.

The structures observed and described herein closely resemble wrinkle marks, or *Runzelmarken*, and are thus discussed in the context of microbially-induced sedimentary structures and geomicrobiology. The microbial mat observed at location two, can also be interpreted in this way, as similar processes affect the stabilization and cohesiveness of sediment that later results in similar structures being formed.

Runzelmarken

First described by Häntzschel and Reineck (1968), *Runzelmarken*, or wrinkle marks, are low-relief, chaotically-distributed ripple-like structures. Due to their chaotic distribution, and parallel to sinuous nature, the sediment surface on which they form appears wrinkled (Reineck and Singh, 1973). Wrinkle marks have been shown to form on partly cohesive sediment surfaces, under a thin (less than one centimeter) film of water, and under the action of strong winds blowing over the water (Reineck, 1969). Even though Reineck (1969) mentions that structures resembling *Runzelmarken* have also been

described from deep-water flysch sediments, his main interpretation of wind-induced structures has remained the most widely accepted, with the latter interpretation rarely discussed (Gingras, 2002).

As noted by Gingras (2002), *Runzelmarken* are most appropriately considered to be structures produced due to shear stress exerted on the cohesive or semi-cohesive sediment surface. Although water can act as a binding agent, microbial stabilization is another effective mechanism by which sediment cohesion can be created (Gingras, 2002). With that in mind, there are also multiple different ways to strain the upper portion of the sediment surface, including the effect of hydraulic currents and sediment creep down foresets. Seilacher (1999, p. 88) stated that wrinkle marks reflected “the shearing of a mucus-bound veneer by tractional currents”. Although *Runzelmarken* occur commonly in the rock record, they are often misinterpreted as definitive evidence of intertidal deposition, which may not always be the case. As Gingras (2002) suggested, using other sedimentary descriptions is crucial in assigning a subtidal versus intertidal origin to those structures.

The position of Noffke et al. (2001) on the interpretation of biogenically-induced structures and those induced by leveling is not clear, from the standpoint of leveling by organic mats and the influence of penecontemporaneous events (Gingras, 2002). The ‘wrinkle structures’ described by Noffke et al. (2001) resemble *Runzelmarken*, but, as discussed in Gingras (2002), the structures lack the sinuous, parallel ripple crests associated with the latter, and are likely more closely related to biogenically-induced structures. Noffke et al. (2001) are correct in pointing out that the structures they describe as being biogenically-induced, occur on scales of centimeters and decimeters, in the case of palimpsest ripple marks and erosional remnants and pockets, respectively. However, their allocation of the term ‘wrinkle marks’ in the category of structures induced by leveling, is neither clearly defined nor supported. In their response to Gingras (2002), Noffke et al. (2002) noted that shear stresses acting on biofilm-covered sediment surfaces, would induce a

“thixotropic” behaviour of sediment, and result in similarly-appearing wrinkle structures. Their interpretation, therefore, concludes that deformation and/or erosion due to shear stresses occurs post-biofilm leveling.

Runzelmarken, as initially described, are not synonymous with adhesion ripples (Gingras, 2002), which form on high-moisture substrates, where wind-blown sand comes in contact with a damp surface, as observed by Chakraborty and Chakraborty (2001). Their observations conclude that on substrates with more than 80% pore water saturation, adhesion ripples are formed, whereas in cases of lower moisture content, but higher wind velocities, adhesion planar lamination occurs.

Seven distinct types of wrinkle structures have been described from mud-free sandstones from an offshore setting, based on criteria such as relief, geometry, lateral continuity and asymmetry (Banerjee and Jeevankumar, 2005). The structures were observed in sandstone beds, beds of shale, and heterolithic storm-deposited facies; their preservation has been attributed to the low-energy, offshore setting, where slow deposition of clay particles in oxygen-depleted, deep conditions, allowed fine-scale, ultramicroscopic, microbial mat growth (Banerjee and Jeevankumar, 2005). The wrinkle structures were subsequently capped by impermeable mud layers that allowed for good preservation. Although it has been noted that a higher occurrence of organic mats occurs in modern shore zones, their preservation is reduced due to correspondingly higher erosion rates. Similarly, the distribution of such structures in outcrop exposures of the Koldaha shale are restricted (Banerjee and Jeevankumar, 2005).

While wrinkle marks may potentially form under the influence of strong winds (if the sediment surface is semi-cohesive and overlain by a thin film of water), wind-induced structures tend to form on decimeter scales, and have distinctly different morphologies from the chaotic, millimeter-scale ripples often associated with, for example, *Runzelmarken*. Bouougri and Porada (2012) observed and described modern, wind-induced, structures associated with

microbial mat deformation, on tidal flats and sabkhas of south-eastern Tunisia. Although they resemble wrinkle structures in some cases, the structures described by Bouougri and Porada (2012) are named “mat deformation structures”, and are part of the larger group of mat related structures (MRS). Dominant physical factors acting on microbial mats forming on siliciclastic marginal-marine settings include wind and wave- or tide-related tractional currents. Structures developed under the influence of these factors include wrinkles, bulges (from gas accumulations under the surface of the mats), and folds (Bouougri and Porada, 2012). The multitude of structures observed to form under the influence of strong wind currents, as described by Bouougri and Porada (2012), are tears, folds and buckles, folds, flipped-over edges, roll-ups, and mat fragments and chips. Many of those structures start to form when an initial dewatering and shrinkage of the mats occurs, thus creating paths of resistance (albeit small) where the strong wind currents may act upon and initiate the formation of mat-deformation structures.

Runzelmarken are not often mentioned in the literature, as most authors refer to similar structures as simply “wrinkle structures”, and in some cases (e.g. Noffke et al., 2002; Bottjer and Hagadorn, 2007) they assign *Runzelmarken* to the broad category of wrinkle structures. However, Carmona et al. (2012) do not mention *Runzelmarken* in the category of “wrinkle structures”. They instead note the interpretation of “wrinkle structures, also called elephant skin and *Kinneyia* structures” (Carmona et al., 2012). Although it is true that elephant skin structures and *Kinneyia*-type ripples are types of wrinkle structures, the terms are not synonymous and should not be used interchangeably.

Cyanobacterial activity, and related microbial structures, have been less documented from siliciclastic environments than from their carbonate counterparts (Cuadrado and Pizani, 2007), and thus have been assigned in literature to the category of “microbially-induced sedimentary structures” (MISS, *sensu* Noffke et al., 2001). Such structures are important to understand, and in the context of Tillamook Bay, cyanobacterial activity on rippled intertidal

flats likely results in biostabilization of sediment and formation of *Runzelmarken* structures.

Microbial Mats and Biostabilization

High-energy currents may erode parts of cohesive mats, creating two types of erosional marks, namely “erosional pockets” (Reineck, 1979), left as decimeter-sized depressions, and “erosional remnants”, left as residual biolaminated buildups (Noffke, 1999; Bouougri and Porada, 2002). Wrinkle structures may develop on the surface of erosional remnants, while microbial mat chips, eroded from the mat at the location of erosional pockets, may be transported by currents and redeposited on the microbial mat, or on uncolonized sediment surfaces (Bouougri and Porada, 2002). Among commonly observed mat-related structures, such as polygonal cracks with upturned margins, are *teepee* structures, which, as the name implies, exhibit updomed laminae with sharp upturned edges (Carmona et al., 2012). These teepee structures are interpreted to form in supratidal flat settings, and sometimes associated with soft-sediment deformation (Carmona et al., 2012). Different interpretations exist for the formation of wrinkle structures, as being formed either on the surface of microbial mats, or underneath microbial mats (Carmona et al., 2012).

It has been observed that thin, 1 - 10 mm thick brownish to greenish films formed by microorganisms on siliciclastic tidal flats on the coast of Argentina are sometimes developed into microbial mats, mainly in the upper intertidal zone and lower supratidal flats (Cuadrado et al., 2011). Structures observed are similar to those observed at Tillamook Bay, were erosional pockets, which, as noted, can sometimes be produced by human footprints, and preserved for several months (Cuadrado and Pizani, 2007). Polygonal diastasis cracks have also been observed by in the upper supratidal, where desiccation and shrinkage are common (Cuadrado et al., 2011).

Over a period of several months, Cuadrado et al. (2011) examined changes in sediment biostabilization in the intertidal-lower supratidal zone, and observed that the mats developed within the sediment, causing an initial smoothing of the pre-existing ripples surface. Increased biostabilization and smoothing of ripples takes place during periods of low sedimentation and low erosion (Cuadrado et al., 2011). The action of storm waves did not appear to increase erosion of the biostabilized ripples that appear to have erosion thresholds 3 to 5 times higher than sediments that do not contain endobenthic microbial mats (Cuadrado et al., 2011). This is supported by recent flume experiments in which it was observed that microbial binding more than doubled the threshold velocity needed to entrain sand in unidirectional currents (Hagadorn and McDowell, 2012). In the case of epibenthic microbial mats forming on tidal flats, Cuadrado et al. (2011) observed the occurrence of polygonal desiccation cracks, as well as numerous erosional pockets, many of which were recolonized shortly after erosional storm events.

Erosional pockets and remnants, polygonal cracks, flipped-over mats and gas domes have been observed on supratidal flats of Puerto Rosales, along with flood-oriented ripple marks in erosional pockets. Established microbial mats can withstand strong storm currents, but cannot form under high-energy conditions, though strong currents and waves often produce lags of microbial mat chips, which can have a newer microbial mat overgrowth layer (Cuadrado et al., 2013). Upper intertidal to supratidal settings include areas protected by grasses, allowing for biostabilization of sediment via microbial mats. In addition to the calm, low-energy setting, fine grained, quartz-rich sand grains allow light penetration in the upper few millimeters of sediment, thus promoting cyanobacterial photosynthesis (Cuadrado et al., 2013). Vertical sections of sediment, have been shown to contain biolaminates of microbial mats, deposited during quiescent conditions, interbedded with layers of rippled sand that were deposited during higher energy conditions (i.e. storms). Large grain sizes that occur at the base of these microsequences are deposited during

storm events; the layers fine upwards into microbial mats that, in turn, are subsequently covered by newly-deposited sediment (Cuadrado et al., 2013). Biolaminites contrast with tidal rhythmites, which are deposited due to varying, cyclic energy conditions (Cuadrado et al., 2013).

Three stages (or types) of microbial mats have been identified, reflecting increasing stabilization and layering: stage 1, pioneer association; stage 2, higher maturity; and stage 3, climax community (Gerdes and Klenke, 2007). Previous experiments have illustrated that the time required for the re-establishment of each microbial mat stage varies from two days in stage 1, then five to six weeks in stage 2, and up to three to four months in stage 3 (Gerdes and Klenke, 2007). Microbial mat growth is strongly dependent on sedimentation rates (termed "ecologic time" by Gerdes and Klenke, 2007). As current energies and sedimentation rates are typically higher in the intertidal and decrease into the supratidal, the development stages of microbial mats can be inferred to reflect the setting in which they developed. As a result, mat types 1, 2, and 3, have been assigned to the ranges of medial to upper intertidal, mean high water level to lower supratidal, and supratidal zone, respectively (Gerdes and Klenke, 2007).

In their experiments, Gerdes and Klenke (2007) illustrated that the most common biogenic structures they observed were biolaminates (mat-stratified and stabilized layers) and biogenic bedding (interbedded mat layers and millimeter-scale siliciclastic units). Millimeter-scale bedding with sandy interlayers occurs dominantly in type 1 and 2 mats. Thick organic laminae with sandy interlayers occur in the lower supratidal range of type 2 mats, as well as type 3 mats (Gerdes and Klenke, 2007). Bioturbation is frequent in type 1 and 2 mats, and rare in type 3 mats. Gerdes and Klenke (2007) commonly observed laminated sand or ripple-bedded sand between sub-recent mat layers, many of which followed ripple morphology. Reactivation surfaces and megaripple bedding were also observed and interpreted as higher energy deposition (Gerdes and Klenke, 2007).

Iron oxide horizons were noted in vertical sections through type 2 and 3 mats in microsequences (or micro-scale laminae) occurring on bulging biolaminites that follow ripple morphology (Gerdes and Klenke, 2007). Stal (1994) attributed the presence of such horizons to *Microcoleus chthonoplastes*, a type of cyanobacteria that binds iron to polysaccharide sheaths and reduces it in the process. This process contributes to microbial mat preservation as the ferrous iron reacts with oxygen, reducing the oxygen partial pressure in the vicinity of the cyanobacteria cell, thereby aiding in CO₂ fixation and limiting photorespiration (Stal, 1994). Ferric hydroxide, on the other hand, when present below a thick mat, acts in protecting the mat from seepage of sulphide from the underlying anoxic layer, while at the same time preventing the diffusion of oxygen deeper into the sediment, where anaerobic microbial activity occurs (Stal, 1994).

Microbial Mat Geochemistry

Microorganisms convert organic carbon to CO₂ and CH₄ at temperatures lower than 100°C. In a series of redox reactions, highly energetic oxidants are consumed near the surface, and more energetically-poor oxidants are consumed deeper in the sediment (Konhauser et al., 2011a). At the sediment surface, aerobic respiration is the first reaction that occurs, which results in organic matter being oxidized. It is important to note that much of the particulate organic carbon (POC, as described by Konhauser et al., 2011a) in coastal settings may be more difficult to decompose, due to it being land-derived and consisting of plant material (Konhauser et al., 2011a). As a result, high total organic carbon (TOC) concentrations in estuarine settings, as observed at Tillamook Bay, may not necessarily correlate with biologic activity and burrowing density.

In coastal settings, high deposition rates during periods of high fluvial discharge may restrict the diffusion of oxygen deep into the sediment, and as a

result, the oxic zone may be relatively shallow (Konhauser et al., 2011a). However, the activity of burrowing organisms allows water to circulate deeper into the sediments, by way of burrow networks, in a process known as bioirrigation (Gingras and Konhauser, 2011; Konhauser et al., 2011a). Microbial mats can provide areas available to be colonized by burrowers in search of oxygen-rich sediments. Undermat lifestyles of organisms may occur when enough food resources, as well as oxygen, are widely available. Burrowing animals are able to then exploit modern biomats and oxygen resources available under the mats (Gingras et al., 2011). This may explain the medium to high density of vertical burrows observed on the surface of the microbial mat at Location 2. Similar high burrow densities are also observed on shore-attached tidal flats on the western margin of Tillamook Bay. Although in early stages of development, the microbial mat is highly burrowed (Fig. C-10 A,B,C). The burrows end abruptly at the edge of the mat, indicating a rapid change in conditions suitable for the burrowing organism. It is likely that food resources, as well as the availability of oxygen under the microbial mat, are higher than in the surrounding sediment, thus influencing preferential burrowing of the microbial mat.

Similar to bioirrigation, organic-rich linings on burrow walls result in concentrated zones of organic material, in the form of agglutinated, fecal, or primary organic material (Gingras and Konhauser, 2011). The location of organic material may extend centimeters to decimeters into the sediment, thus providing bacterial species with substrata containing the necessary elements required for microbial respiration (Gingras and Konhauser, 2011). An increase in water depth and distance from land results in reduced concentrations of total organic carbon and nutrients, and corresponding low accumulations of organic matter in settings such as the deep sea.

Another model for ferric hydroxide precipitation, is that of Fe(II) diffusion upwards from the Fe(III) and sulfate reduction boundary into the sediment, where it is reoxidized (Konhauser et al., 2011b). It is important to



Figure C-10. Eroded and preferentially-burrowed microbial mat. (A) General view of the microbial mat in the western part of the bay, directly adjacent to Bayocean Peninsula; the edge of the bay is present several meters to the left, outside the view of the photo. Note the presence of remnant ripples (black arrows), as well as the presence of erosional pockets and an oyster shell mould. Crests of high-wavelength dunes can be seen in the background, leading to the forested dunes at the top of the photo. (B) and (C). Close-up views of the edge of the burrowed microbial mat. Note the high density of burrows in the area of the well-developed mat, and the sharp drop in burrow density at the edge of the mat, where the weakly-developed ripples are observed. This may indicate the opportunistic behaviour of the burrowers (unknown) in relation to increased oxygen concentrations beneath the microbial mat. Oyster shells are seen near the knife used for scale.

note that the availability of HCO_3^- in suboxic and anoxic pore waters, combined with the high reactivity of ferrous iron, may cause precipitation of ferrous iron as siderite (Konhauser et al., 2011b). However, when sulfate reduction results in significant quantities of HS^- being produced (i.e. higher than Fe(II) concentrations), the anion's reactivity with ferrous iron may result in the formation of pyrite instead of siderite (Konhauser et al., 2011b).

Siderite formation in brackish water is less common than in freshwater, but nevertheless the process occurs where Fe(III) reduction rates exceed those of sulfate reduction (Curtis, 1995). The presence of organic matter in brackish-water settings, when combined with lower amounts of sulfate, allow the precipitation of siderite (Adams et al., 2006). Similarly, rootlets present in sediment may act as electron donors for Fe(III)-reducing bacteria. While lignin, waxes, and resins are difficult to degrade by such bacteria, their natural decomposition over time allows fungi and certain other bacteria (e.g. actinomycetes) to degrade lignin. As a result, Fe(III)-reducing bacteria can use by-products (such as cellulose) from this degradation as sources of organic matter (Adams et al., 2006). If organic matter concentrations are too low for the needs of sulfate-reducing bacteria, the precipitation of iron carbonates (i.e. siderite) is favoured over that of iron sulfides.

Seasonal Controls

A possible *Teichichnus*-like trace, observed at Location 2, south of the inner estuary sand bar, is possibly produced by a polychaete worm (Fig. C-9 Part 1 A,A'). Though only observed in one instance, and in one part of the estuary, *Teichichnus*-like traces have been described from various parts of estuarine settings, sometimes as monospecific assemblages with common syneresis cracks in estuary-bay tidal deposits, in lagoonal deposits, in estuary-mouth facies, and channel margins (Buatois et al., 2005). Whether as

monospecific assemblages, or associated with *Planolites*, *Teichichnus* are common in restricted heterolithic facies.

Cyanobacterial mats, resulting in binding of sediment and formation of desiccation cracks, have been observed at Boundary Bay, British Columbia, in wave-rippled fine-grained sand (Dashtgard, 2011). In a similar fashion, it is believed that the presence of desiccation cracks in the intertidal zone of Tillamook Bay is related to the presence of cyanobacteria, as the sediment surface is visibly bound and slightly cohesive. Similar structures, resembling the medium-sized polygons of Location 2, have been observed in modern siliciclastic biolaminates on the Tunisian Mediterranean Coast, as well as in ancient outcrop examples of the Schwarzrand Group in Namibia, and Tizi n-Taghatine Group in Morocco (Bouougri and Porada, 2011).

A period of non-deposition of sediment is required for the formation of siliciclastic biolaminates, during which time microbial action results in the rather rapid (sometimes on the order of days) establishment of a microbial mat on an existing sediment surface (Bouougri and Porada, 2011). As such, the location of microbial mats in a quiescent area, close to a salt marsh, adjacent to a major tidal channel, provides ideal conditions for the colonization of sediment surfaces by microbes and the subsequent vertical accretion of mats. Low discharge conditions during summer months may provide a sufficiently-long time frame of no or little sediment deposition. Higher discharge during winter months results in more sediment being deposited on top of the microbial mats. Though microbial mats may form rather quickly, it has been noted that a long period of non-deposition – on the order of several months – may be required for the preservation of the mats (Gerdes and Klenke, 2007). The dry season months, during which discharge from the Tillamook River and Wilson River are low, is likely the time period that allows microbial mat formation at Location 2. The cyclicity of dry versus wet seasons results in the continued burial and re-establishment of mats over time (Fig. C-8 A,A'; Fig. C-9 Part I A,A'). Due to the proximity of Location 2 to the main tidal channel, it is

likely that sedimentation of rippled sand units may occur during the dry season as well. This may be a plausible explanation if storms associated with high rainfall amounts and / or high ocean storm swells result in increased erosion of bedrock in the drainage basins (and therefore increased suspended sediment concentrations), or the transport and reworking of marine sediment into the bay, respectively.

Bibliography

- Adams, L.K., MacQuaker, J.H.S. and Marshall, J.D.** (2006) Iron(III)-reduction in a low-organic-carbon brackish-marine system. *Journal of Sedimentary Research*, v. 76, p. 919-925.
- Banerjee, S. and Jeevankumar, S.** (2005) Microbially originated wrinkle structures on sandstone and their stratigraphic context: Palaeoproterozoic Koldaha Shale, central India. *Sedimentary Geology*, v. 176, p. 211-224.
- Bottjer, D. J. and Hagadorn, J. W.** (2007) Mat growth features: *In* Schieber, J., Bose, P. K., Erickson, P. G., Banerjee, S., Sarkar, S., Altermann, W., and Catuneanu, O., eds., *Atlas of microbial mat features preserved within the siliciclastic rock record*: Elsevier, Amsterdam, p. 53-71.
- Bouougri, E.H., and Porada, H.** (2002) Mat-related sedimentary structures in Neoproterozoic peritidal passive margin deposits of the West African Craton (Anti-Atlas, Morocco). *Sedimentary Geology*, v. 153, p. 85-106.
- Bouougri, E.H., and Porada, H.** (2011) Biolaminated Siliciclastic Deposits. *In* Reitner, J.; Quéric, N.-V., and Arp, G., eds., *Lecture Notes in Earth Sciences: Advances in Stromatolite Geobiology*: Springer, Berlin, p. 487-504.
- Bouougri, E.H., and Porada, H.** (2012) Wind-induced mat deformation structures in recent tidal flats and sabkhas of SE-Tunisia and their significance for environmental interpretation of fossil structures. *Sedimentary Geology*, v. 263-264, p.56-66
- Buatois, L.A., Gingras, M.K., MacEachern, J., Mángano, M.G., Zonneveld, JP, Pemberton, S.G., Netto, R.G. and Martin, A.** (2005) Colonization of Brackish-Water Systems through Time: Evidence from the Trace-Fossil Record. *Palaios*, v. 20, p. 321-347.
- Carmona, N.B., Ponce, J.J., Wetzel, A., Bournod, C.N. and Cuadrado, D.G.** (2012) Microbially induced sedimentary structures in Neogene tidal flats from Argentina: Paleoenvironmental, stratigraphic and taphonomic implications. *Palaeogeography, Palaeoclimatology, Palaeoecology*, v. 353-355, p. 1-9.
- Chackraborty, T. and Chackraborty, C.** (2001) Eolian-aqueous interactions in the development of a Proterozoic sand sheet: Shikaoda Formation, Hosangabad, India. *Journal of Sedimentary Research*, v. 71, no. 1, p. 107-117.
- Cuadrado, D.G., Bournod, C.N., Pan, J. and Carmona, N.B.** (2013) Microbially-induced sedimentary structures (MISS) as record of storm action in supratidal modern estuarine setting. *Sedimentary Geology*, v. 296, p. 1-8.
- Cuadrado, D.G. and Pizani, N.V.** (2007) Identification of microbially-induced sedimentary structures over a tidal flat. *Latin American Journal of Sedimentology and Basin Analysis*, v. 14, no. 2, p. 105-116.
- Cuadrado, D.G., Carmona, N.B., and Bournod, C.** (2011) Biostabilization of sediments by microbial mats in a temperate siliciclastic tidal flat, Bahía Blanca estuary (Argentina). *Sedimentary Geology*, v. 237, p. 95-101.

- Cuadrado, D.G., Carmona, N.B., and Bournod, C.** (2012) Mineral precipitation on modern siliciclastic tidal flats colonized by microbial mats. *Sedimentary Geology*, v. 271-272, p. 58-66.
- Curtis, C.D.** (1995) Post-depositional evolution of mudstones 1: Early days and parental influences: *Geological Society of London, Journal*, v. 152, p. 577–586.
- Dashtgard, S.E.** (2011) Linking invertebrate burrow distributions (neochronology) to physicochemical stresses on a sandy tidal flat: implications for the rock record. *Sedimentology*, v. 58, p. 1303-1325.
- Folk, R.L.** (1974) *Petrology of Sedimentary Rocks*. Hemphill Publishing Company, Austin, Texas. 184 pp.
- Gedda, B.** (1993) Trace fossils and palaeoenvironments in the Middle Cambrian at Äleklinta, Öland, Sweden. *Examensarbeten i geologi vid Lunds Universitet*., no. 49, p. 1-11.
- Gerdes, G. and Klenke, T.** (2003) Geologische Bedeutung ökologischer Zeiträume in biogener Schichtung (Mikrobenmatten, potentielle Stromatolithe). *Mitteilung der Gesellschaft für Geologie und Bergbaustudien Österr.*, v. 46, p. 35-49.
- Gerdes, G. and Klenke, T.** (2007) States of biogenic bedding as records of the interplay of ecologic time and environment (a case study of modern siliciclastic sediments, Mellum Island, southern North Sea). *Senckenbergiana Maritima*, v. 37, no. 2, p. 129-144.
- Gerdes, G., Klenke, T. and Noffke, N.** (2000) Microbial signatures in peritidal siliciclastic sediments: a catalogue. *Sedimentology*, v. 47, p. 279-308.
- Gingras, M.K.** (2002) Microbially induced sedimentary structures – a new category within the classification of primary sedimentary structures – Discussion. *Journal of Sedimentary Research*, v. 72, no. 4, p. 587-588.
- Gingras, M.K. and Konhauser, K.O.** (2011) Ichnology. *In: Reitner, L. and Thiel, V. (Eds): Encyclopedia of Geobiology*. Springer, Berlin, p. 481- 482.
- Gingras, M.K., Hagadorn, J.W., Seilcaher, A., Lalonde, S.V., Pecoits, E., Petrash, D. and Konhauser, K.O.** (2011) Possible evolution of mobile animals in association with microbial mats. *Nature Geoscience*, v. 4, p. 372-375.
- Hagadorn, J.W. and McDowell, C.** (2012) Microbial influence on erosion, grain transport and bedform genesis in sandy substrates under unidirectional flow. *Sedimentology*, v. 59, p. 795-808.
- Häntzschel, W. and Reineck, H.E.** (1968) Faziesuntersuchungen im Hettangium von Helmstedt (Niedersachsen). *Mitteilungen aus dem Geologischen Staatsinstitut in Hamburg*, v. 37, p. 5–39.
- Heiri, O., Lotter, A.F. and Lemcke, G.** (2001) Loss on ignition as a method for estimating organic and carbonate content in sediments: reproducibility and comparability of results: *Journal of Paleolimnology*, v. 25, p. 101-110.

- Konhauser, K.O., Gingras, M.K. and Kappler, A.** (2011a) Diagenesis – Biologically Controlled. *In: Reitner, J. and Thiel, V. (Eds): Encyclopedia of Geobiology.* Springer, Berlin, p. 777-784.
- Konhauser, K.O., Kappler, A.K. and Roden, E.E.** (2011b) The microbial role in iron redox and biomineralization reactions. *Elements*, v. 7, p. 89-93.
- Martinsson, A.** (1965) Aspects of a middle Cambrian thanatotope on Öhlund. *Geologiska Foereningen i Stockholm Foerhandlingar*, v. 87, p. 181-230.
- Noffke, N.** (1999) Erosional remnants and pockets evolving from biotic-physical interactions in a Recent lower supratidal environment. *Sedimentary Geology*, v. 123, p. 175-181.
- Noffke, N., Gerdes, G., Klenke, T. and Krumbein W.E.** (2001) Microbially-induced sedimentary structures – a new category within the classification of primary sedimentary structures. *Journal of Sedimentary Research*, v. 71, no. 5, p. 649-656.
- Noffke, N., Gerdes, G., Klenke, T. and Krumbein W.E.** (2002) Microbially induced sedimentary structures – a new category within the classification of primary sedimentary structures - Reply. *Journal of Sedimentary Research*, v. 72, no. 4, p. 589-590.
- Pruss, S.B., Corsetti, F.A. and Bottjer, D.J.** (2005) The unusual sedimentary rock record of the Early Triassic: A case study from the southwestern United States. *Palaeogeography, Palaeoclimatology, Palaeoecology*, v. 222, p. 33–52.
- Reineck, H.E.** (1969) Die Entstehung von Runzelmarken. *Senckenbergiana Maritima*, v. 1, p. 237–247.
- Reineck, H.E.** (1979) Rezente und fossile Algenmatten und Wurzelhorizonte. *Natur und Museum*, v. 109, p. 290-296.
- Reineck, H.E. and Singh, I.B.** (1973) *Depositional Sedimentary Environments.* Springer-Verlag, Berlin, Heidelberg, New York, 439 pp.
- Seilacher, A.** (1999) Biomat-related Lifestyles in the Precambrian. *Palaios*, v. 14, p. 86-93.
- Stal, L.J.** (1994) Microbial mats: ecophysiological interactions related to biogenic sediment stabilization. *In Krumbein, W.E., Paterson, D.M. and Stal, L.J. (Eds.): Biostabilization of Sediments.* Bibliotheks und Informationssystem der Carl von Ossietzky, Universität Oldenburg, p. 41-53.